Unité mixte Inserm-UdS 682
De l'homéostasie tissulaire
au cancer et à l'inflammation
Directrice: Michèle KEDINGER
http://u682-inserm.u-strasbg.fr

Thèse présentée pour obtenir le grade de Docteur
de l'Université de Strasbourg

Discipline : Aspects Moléculaires et Cellulaires de la Biologie

Par Isabelle GASSER

Développement d'un modèle murin pour cibler et comprendre le rôle de la Ténascine-C dans la progression tumorale

Soutenue publiquement le 30 Septembre 2011

Membres du jury

Directeur de thèse	Dr Gertraud OREND	INSERM 682 - Strasbourg
Examinateur	Pr Jean-Emmanuel KURTZ	CHU Hautepierre - Strasbourg
Rapporteur externe	Dr Ruth CHIQUET- EHRISMANN	Friedrich Miescher Institute - Basel - Suisse
Rapporteur externe	Dr Véronique ORIAN- ROUSSEAU	Karlsruhe Institute of Technology - Allemagne

Summary

In my project, I studied several aspects of the composition and organization of the tumor microenvironment. My objectives were to understand how the Tenascin-C (TNC) matrix is organized in human cancers and in murine cancer models to improve our knowledge about the role of TNC in tumorigenesis. My work has contributed to the understanding of how TNC is enhancing angiogenesis and tumor progression. In particular I had shown that DKK1 is important in tumor angiogenesis since TNC repressed the Wnt inhibitor DKK1 and overexpression of DKK1 blocked tumor angiogenesis in a xenograft model. In several *in vivo* models*,* I observed that TNC is organized into conduit structures together with other extracellular matrix molecules. These conduits form a continuum with blood vessels and are in close vicinity to carcinoma associated fibroblasts and activated macrophages and thus might serve as guiding cue for these cells in addition to endothelial and cancer cells. The TNC matrix conduits might also present microenvironmental niches that may be involved in resistance to anti-angiogenic drugs. To address this latter possibility I had established an orthotopic xenograft mouse model with human colorectal carcinoma cells that is sensitive to Bevacizumab and that recapitulates important features of human colorectal carcinoma. Upon Bevacizumab treatment a strong increase in liver metastasis was observed. The underlying mechanisms need to be addressed in the future.

Résumé

Mon projet s'est attaché à étudier différents aspects de la composition et de l'organisation de l'environnement tumoral. L'objectif de mon travail a été de comprendre comment la Ténascine-C (TNC) est organisée dans les cancers humains et dans des modèles de cancers murins, afin d'améliorer nos connaissances sur le rôle de la TNC dans la tumorigenèse. Mon travail a contribué à comprendre comment la TNC promeut l'angiogenèse et la progression tumorale. J'ai montré en particulier qu'en réprimant un inhibiteur de la voie Wnt, DKK1, qui en temps normal bloque l'angiogenèse, la TNC est capable d'influencer l'angiogenèse tumorale. Dans différents modèle *in vivo,* j'ai observé que la TNC était organisée en conduits avec d'autres molécules de la matrice extracellulaire. Ces structures forment un continuum avec les vaisseaux sanguins et sont intimement liées aux fibroblastes et aux macrophages associés au cancer. Elles pourraient servir au transport à distance de ces cellules en plus des cellules endotheliales et des cellules tumorales. Elles pourraient également être impliquées dans le présence de niches environnementales qui seraient impliquées dans les phénomènes de résistance aux drogues anti-angiogéniques. Pour pouvoir répondre à cette problématique à plus long terme, j'ai développé un modèle de greffe orthotopique de cellules coliques cancéreuses humaines chez la souris, qui est sensible au Bevacizumab et qui récapitule d'importantes caractéristiques du cancer colorectal humain. Suite au traitement de nombreuses métastases hépatiques ont été mises en évidence, les mécanismes sous-jacents restent à étudier.

Acknowledgments

First of all I would like to thank the members of my thesis committee, Professor Jean-Emmanuel Kurtz, Doctor Ruth Chiquet-Ehrismann and Doctor Véronique Orian-Rousseau to accept to evaluate my thesis work.

Je tiens également à remercier Monsieur Philippe Richert, Président du Conseil Régional, pour avoir mis à ma disposition l'amphithéâtre de la Maison de la Région, pour présenter mes travaux de recherche lors de ma soutenance.

Un grand merci à Madame Michèle Kedinger, directrice de l'Unité Inserm 682, pour m'avoir permis de réaliser ma thèse au sein de cette unité ; merci pour vos précieux conseils, votre soutien et votre grande disponibilité tout au long de ces quatre années.

Gertraud, I thank you so much to give me the opportunity to work in your team, for the interesting discussions and also for encouraging me and always pushing me to persevere and to go through even when I was ready to give up. I am also so grateful for having relied on me when I wanted to do "monitorat". Thank you for teaching me how to think positively.

Un grand merci à Patricia et Klaus-Peter Janssen d'avoir accepté de constituer mon jury de mi-parcours de thèse et de m'avoir livré vos précieux conseils.

Merci à toi, Olivier ; sans ton aide informatique, j'aurais jeté mon ordinateur plusieurs fois par la fenêtre… mon compte serait resté verrouillé à jamais, mes données se seraient évaporées dans la nature… mais avant tout merci d'avoir toujours trouvé un moment pour répondre à mes « petites » questions…

Falk, que dire sinon merci pour ces quatre années si riches. Merci d'avoir su si souvent me remonter le moral et me redonner confiance en moi. Merci pour ta franchise et ta gentillesse. Merci de m'avoir laissé gagner de temps en temps lors de nos matchs de squash. Et surtout, merci de m'avoir appris à utiliser un peu plus intelligemment mon ordinateur ! Heureusement que tes conseils étaient gratuits, sinon je serais aujourd'hui ruinée …

Mika, un immense merci, d'abord pour avoir pris soin de mes souris, pour tes incantations, tes formules magiques quand mes colonies étaient sur le point de disparaitre… mais surtout pour ta gentillesse, ta bonne humeur et tes bons plans. Merci pour ta sonnerie de portable qui a distrait pendant trois ans tout le bureau… ça va me manquer !

Je tiens à remercier très sincèrement Benoît et Thomas, sans qui ma fin de thèse aurait été un véritable enfer, pour leur aide et leurs précieux conseils lors de la rédaction du manuscrit.

Anja, thank you so much for your optimism, I was really happy to share the office with you.

Gracias a ti, Ines, por el sol y la musica que has comunicado en el laboratorio…

Manon, Thoueiba et Elmina, merci pour tous ces fous rires et cette ambiance si chaleureuse au labo… un petit clin d'œil aux deux dernières, sans qui les trajets en voiture auraient été bien tristes ; je n'ai qu'une chose à dire « Quel sens de l'orientation fantastique, les filles ! ».
Merci à vous pour tous ces apéros et ces soirées entre AMIS !

Une pensée également pour Florilène, Laura, Céline et Tristan qui ont égayé toutes les pauses de midi. Merci Céline de m'avoir initié aux joies du scrapbooking, bon vent à vous!

Christiane et Annick, mes bonnes fées, merci pour vos si bons conseils et vos petits trucs qui ont souvent fait la différence en histologie et en culture. Merci pour votre aide tout au long de ma thèse et cette ambiance si chaleureuse en labo d'histologie qui faisait qu'on s'y sentait un peu comme à la maison.

Une petite pensée pour ceux qui sont déjà partis, Caro, Martial et Marija…

Merci Dominique, Guy et Gérard pour vos conseils et votre esprit critique. Merci à la Bagnard Team; Nadège, Laurent, Alexia, Archana pour votre bonne humeur.

Un grand merci à Erwan, Dominique et Eric d'avoir toujours pris le temps de répondre à mes questions, merci pour vos recommandations concernant les xénogreffes et les aspects plus cliniques.

Isabelle et Léonor, merci à toutes les deux pour votre grande disponibilité et votre sourire.

Merci Michèle, Fanny et Pierre pour votre gentillesse et pour vous être si bien occupés de mes souris.

Un grand merci aux membres des autres équipes, Katia, Claire, Lylia, Isabelle Hinkel, Nadine, Marie, Elisabeth, Christophe, Patrick et Jean-François et Jean-Noël d'avoir toujours fait que l'ambiance soit agréable au sein de notre unité.

Un merci particulier à Isabelle Duluc qui a pris de son temps pour m'apprendre à faire les injections dans le caecum. Merci à Isabelle Gross et à Manuela pour les longues discussions sur l'immobilier à Strasbourg.

Je sors un peu du labo, pour dire un grand merci à l'équipe « OpenLab » de m'avoir initié aux joies de l'enseignement… Merci Laurence et Michel pour vos précieux conseils afin de rendre la science plus compréhensible et plus accessible aux lycéens. Un grand merci à Madame Catherine Florentz pour avoir partagé son expérience avec nous durant quelques séances. Merci à Fanny et à Pascal Mathelin pour leur aide. Merci Caro, Sara, Judith, Elise, Anne- Sophie, Aurélie, François et Denis pour les trajets en covoiturage, toujours si amusants…

Pour terminer, je m'éloigne maintenant du cadre professionnel, pour dire un grand merci à mes amis de toujours: Audrey, Joël, Gaëlle, Mathieu, Elodie et François qui ont su écouter avec beaucoup de patience mes (mes)aventures avec les souris tout au long de ma thèse, et surtout qui ont su me changer les idées quand les choses n'avançaient pas dans le bon sens.
Une petite pensée pour Anaïs qui a su me faire rire même quand le cœur n'y était pas trop, merci pour ces parties de squash endiablées…

Un petit clin d'œil à mes deux aventuriers du bout du monde, Marie et Xavier, qui m'ont permis de m'échapper du labo et de m'envoler vers des paysages merveilleux en un clic de souris.
Un merci tout particulier à Mélanie et JD pour ces soirées qui m'ont permis de décompresser et de tant de rire… merci Mélanie pour tes efforts de relecture…

Et pour finir, je tiens tout particulièrement à remercier ma famille de m'avoir soutenu depuis toujours, et surtout d'avoir été disponible pour écouter et réécouter l'avancée de mes travaux. Chacun de vous a contribué à sa manière à cette belle aventure. Vous avez été mon soutien, ma force et mon courage durant toutes ces années, je vous aime tous si fort…

Merci Maman, Papa d'avoir toujours cru en moi, merci pour ce que vous faites pour moi, sans vous rien de tout cela n'aurait été possible. Tu vois, Papa, j'ai finalement passé la deuxième année…

Merci Edmond d'avoir toujours été là pour m'écouter, merci pour ces longues discussions parfois presque philosophiques sur la vie, l'avenir... Tu m'as aidé à grandir et à avancer.

Merci Cécile pour l'intérêt que tu as toujours porté à mon travail.

Merci Rémy, Stéphane et Marie pour avoir su trouver les mots justes pour m'encourager.

Merci Josette pour les petits coups de téléphone qui redonnent du courage et surtout merci de toujours avoir pensé à me découper les coupures de presse concernant la recherche et le cancer…

Merci Jean-Marc de m'avoir parfois permis de prendre un peu du recul avec vos phrases parfois provocatrices…

Un merci très spécial à Wiwitchele qui m'a bien malgré lui rappelé pourquoi je voulais tant faire de la recherche… Merci aussi à toi de ne pas poser de questions, le jour de l'oral !

Et pour finir, merci à toi Jean, qui a supporté ma mauvaise humeur ces trois derniers mois, qui a été ma deuxième paire de mains cette dernière semaine. Merci de m'avoir aidé à relativiser, à prendre de l'assurance et d'avoir mis de la couleur dans mes journées quand je voyais tout en noir...merci de m'avoir permis de garder le sourire…

MY PhD thesis was supported by Inserm and REGION ALSACE.

« Ce sont les Grecs qui nous ont légué le plus beau mot de notre langue: le mot «enthousiasme» - du grec en theo, un Dieu intérieur »

Louis Pasteur

Table of contents

List of figures **4**
List of tables **6**
Abbreviations **7**
INTRODUCTION **9**
1. Tumorigenesis is a multi step process 9
1.1 Cancer cell initiation 9
1.2 Tumor angiogenesis 9
1.3 Metastatic dissemination of tumor cells 13
2. Tumor as an organ: the importance of the microenvironment in tumor progression 14
2.1 Tumor as an organ 14
2.2 Tumor microenvironment 15
2.2.1 Cancer-associated fibroblasts 16
2.2.2 Immune cells 17
2.2.3 Endothelial cells 18
2.2.4 Extracellular matrix molecules 18
2.3 The extracellular matrix molecule: Tenascin-C, a key player in tumorigenesis 19
2.3.1 Structure 19
2.3.2 Role of TNC in cancer 21
3. Mouse and human models to study the role of the tumor microenvironment in tumorigenesis 23
3.1 Murine Rip1Tag2 insulinoma model 23
3.2 Human colorectal cancer analysis 24
4. Different targets on the road of cancer therapy: cancer cells, tumor vasculature and the tumor microenvironment 26
5. Limits of anti-angiogenic therapies: the case of Bevacizumab 28
5.1 A general introduction to Bevacizumab and resistance to anti-angiogenic drugs 28
5.2 Human colorectal cancer and Bevacizumab treatment 29
6. The role of the tumor microenvironment in tumor resistance and recurrence after anti-angiogenic therapies 30
OBJECTIVES **31**
Objective 1: Characterization of the extracellular matrix and cellular components of the tumor microenvironment in a murine tumor model and in human cancer tissue 31
Objective 2: Development of a murine orthotopic xenograft model for investigating the role of tumor and host-derived TNC on tumor angiogenesis 31
Objective 3: Preliminary results: development of a murine orthotopic xenograft model for investigating the impact of an anti-angiogenic therapy on the microenvironment 32
MATERIAL AND METHODS **33**
1. In vitro experiments 33
1.1 Cell lines and culture conditions 33
1.2 Generation of cells for live imaging 33
1.3 Generation of cells with overexpression of DKK1 34
1.4 Generation of cells with knock down of TNC 35
1.5 Expression analysis by immunoblotting 35
2. Tumor material 36
2.1 Human colorectal carcinoma 36
2.2 Human insulinoma 36

3. Animals 36
3.1 RT2 and RT2/TNC insulinoma mice 36
3.2 Ras and APC mice 37
3.3 Immunodeficient mice 38
3.3.1 Nude mice 38
3.3.2 Rag2KO and Rag2KO/TNCKO mice 38
4. Heterotopic and orthotopic xenograft models 39
4.1 Heterotopic xenograft model 39
4.1.1 Cell injection 39
4.1.2 Injection of human tumor material 39
4.2 Orthotopic colon cancer xenograft model 39
5. Live imaging of tumorigenesis 40
6. Experimental design of the anti-angiogenic treatment 41
7. Analysis of tumor volume and tissue preparation 41
7.1 Tumor volume 41
7.2 Tissue preparation 42
7.2.1 Analysis of the vasculature 42
7.2.2 Tissue preparation 42
8. Analysis of protein expression by tissue staining 42
9. Tumor analysis: imaging and quantification 44
10. Analysis of candidate gene expression by qRT-PCR 45
11. Statistical analysis 46
12. Analysis of liver metastasis 46
RESULTS 47
Paper contributions 47
PART A: characterization of the extracellular matrix and cellular components of the tumor microenvironment in a murine tumor model and in human cancer tissue 48
1. Description of the neuroendocrine Rip1Tag2 model with ectopic TNC expression 48
1.1 Tumor progression 48
1.2 Tumor growth 49
1.3 Tumor angiogenesis 51
1.4 Vessel anatomy 52
1.5 Expression and organization of TNC and other ECM molecules 57
1.6 TNC and tumor associated cells 65
1.6.1 Potential impact of TNC on fibroblasts 65
1.6.2 Potential impact of TNC on macrophages 69
1.6.3 No impact of TNC on lymph endothelial cells 69
1.7 Potential link of TNC to DKK1 repression and tumor angiogenesis 72
2. Organization of TNC in the microenvironment of intestinal carcinomas 80
2.1 TNC expression and ECM organization 80
2.2 Establishment of an optimized staining protocol for tissue analysis 82
2.3 TNC expression in human colon cancer xenografts 84
2.4 Association of CAF with TNC in human colorectal carcinoma and in the murine tumor xenografts 87
3. Organization of TNC in the microenvironment of human insulinomas 88

PART B: development of a murine orthotopic xenograft model for investigating the role of tumor and host-derived TNC on tumor angiogenesis 93

1. Use of immune-compromised Rag2KO mice for tumor engrafting 93

2. Establishment of immune-compromised Rag2KO mice lacking TNC expression for tumor cell grafting..... 95

PART C: development of a murine orthotopic xenograft model for investigating the impact of an anti-angiogenic therapy on tenascin-C expression..... 101

1. Monitoring tumorigenesis by live imaging..... 101

2. Histological characterization 102

3. Effect of Bevacizumab on the tumor vasculature 106

4. Effect of Bevacizumab on liver metastasis 107

DISCUSSION 109

1. TNC effects on tumor cells – impact on proliferation, migration, invasion and dissemination 110

2. TNC effects on tumor associated cells – role in angiogenesis 111
2.1 TNC effects on tumor associated cells..... 111
2.2 Wnt/β-catenin pathway and angiogenesis 112
2.3 DKK1 and angiogenesis 113
2.4 Potential link between TNC and DKK1 114

3. Potential mechanism of TNC conduit formation and function 114

4. Murine model systems and their potential applications in addressing the role of TNC in cancer progression..... 120
4.1 Stochastic immune competent RT2 insulinoma model 120
4.2 Tumor xenografting into immune-compromised mice lacking TNC 121
4.3 Orthotopic tumor xenografting mouse model for testing anti-angiogenic treatment..... 123

CONCLUSIONS AND PERSPECTIVES 127

REFERENCES 130

ANNEX 140

page

Figure 1: The angiogenic switch 11
Figure 2: Characterization of normal and tumor vessels 12
Figure 3: Metastatic dissemination 14
Figure 4: The tumor microenvironment 15
Figure 5: The structure of tenascin family 20
Figure 6: TNC characterization and expression 22
Figure 7: Multi stage of tumorigenesis in the RT2 model system 24
Figure 8: Resistance modes of anti-angiogenic therapies 29
Figure 9: Surgical procedure for orthotopic injection into the caecum 40
Figure 10: NightOwl imaging of the caecum tumor from Rag2KO mice *in vivo* and ex vivo 40
Figure 11: In vivo fluorescence imaging: characterization of tumor growth in xenografted tumors in Rag2KO mice 41
Figure 12: Tumor characterization in tumors from 10 and 12 week old RT2 and RT2/TNC mice 49
Figure 13: Enhanced proliferation in the presence of TNC 50
Figure 14: Overexpressed TNC promotes tumor angiogenesis in RT2 insulinoma 51
Figure 15: Blood vessel characterization in RT2 and RT2/TNC tumors 52
Figure 16: Anatomy of blood vessels upon overexpression of TNC 53
Figure 17: Tumor associated pericyte coverage of vessels in RT2 and RT2/TNC Tumors 54
Figure 18: Vessel anatomy in RT2 and RT2/TNC tumors 56
Figure 19: Characterization of a conduit 57
Figure 20: Organization of TNC matrix conduits in tumors of 12 week old RT2 and RT2/TNC mice 59
Figure 21: Conduits: TNC and other ECM molecules 61
Figure 22: Characterization of TNC conduits in RT2 TNC tumors 63
Figure 23: Representation of vessel like and conduit like structures in RT2 tumor ... 64
Figure 24: Characterization of different populations of fibrosblasts in murine and human tumors 66
Figure 25: Quantification of CAF in RT2 and RT2/TNC tumors 68
Figure 26: Characterization of immune cells in RT2 and RT2/TNC tumors 70
Figure 27: Representation of two conduit systems: lymphatic vessels and ECM tracks in tumors of 12 week old RT2 and RT2/TNC mice 71
Figure 28: Impact of TNC on Wnt signalling and DKK1 expression in RT2 tumors ... 73
Figure 29: Engineering of KRIB cells overexpressing DKK1 74

Figure 30: Consequences of DKK1 overexpression in KRIB cells *in vitro* and *in vivo* 76
Figure 31: Characterization of KRIB:DKK1 and KRIB:WT tumor 77
Figure 32: Angiogenesis in the KRIB:EV and KRIB:DKK1 tumors 79
Figure 33: ECM organization in human CRC and corresponding liver metastasis 81
Figure 34: TNC antibody specificity 83
Figure 35: TNC expression in human and mouse tumors 84
Figure 36: Comparison of TNC expression patterns in human CRC and corresponding human xenografted tumor 85
Figure 37: Presence of mouse and human TNC in different xenografted tumors 86
Figure 38: Cellular and fibrillar similarities of the tumor microenvironment in xenografted tumor in comparison to human tissues 87
Figure 39: Histological characterization of normal and insulinoma tissue 88
Figure 40: Organization of ECM in human insulinomas 90
Figure 41: TNC expression in normal human pancreas and insulinoma 91
Figure 42: Consequences on tumor formation and ECM organization in a heterotopic grafting model with HEK293 cells overexpressing TNC 94
Figure 43: Histological and immunological characterization of the orthotopic xenografted SW480 tumors in the Rag2KO and Rag2KO/TNCKO mouse models 96
Figure 44: TNC expression in Rag2KO and Rag2KO/TNCKO SW480 orthotopic xenografted tumors 97
Figure 45: Characterization of the ECM and cellular tumor microenvironment in SW480 orthotopic xenografted tumors in a Rag2KO/TNCKO host 98
Figure 46: Characterization of SW480 shTNC cells 100
Figure 47: NightOwl pictures showing tumor growth in the xenografted nude mice 102
Figure 48: Histology of caecum xenografted tumors 103
Figure 49: Immunophenotypic characterization of stromal cells in human colorectal cancer cell line xenografts and human CRC 104
Figure 50: Immunostaning for the ECM molecule TNC in human CRC and in orthotopic xenografted tumors 105
Figure 51: Quantification of CD31 in Bevacizumab and vehicle treated mice 106
Figure 52: Metastasis analysis in Bevacizumab treated mice 107
Figure 53: Summary of TNC conduit formation 118

page

Table 1: Summary of engineered cell lines 34
Table 2: Description of conditions for utilization of TNC antibodies 44
Table 3: Summary table of the different primers used for qPCR analysis 45
Table 4: Summary table of grafting experiments in immunodeficient mice lacking TNC or expressing TNC..... 95
Table 5: Summary of grafting experiment and treatment 101
Table 6: Mice with liver metastasis in control mice and after Bevacizumab treatment..... 107
Table 7: Summary of models..... 126

APC	Adenomatous Polyposis Coli
AtTu	Attached Tumor cell
Bev	Bevacizumab
BM	Basement Membrane
CAF	Carcinoma associated fibroblast
CAM	Chorio Allantoic Membrane
CD31	Cluster of Differentiation 31
CD45	Cluster of Differentiation 45
cDNA	complementary Desoxyribonucleic Acid
c-FN	cellular Fibronectin
CIMP	CpG Island Methylator Phenotype
CIN	Chromosomal Instability
Coll	Collagen
CRC	Colorectal Cancer
DAPI	4’,6-diamidino-2-phenylindole
DKK1	Dickkopf 1
DMEM	Dulbecco’s Modified Eagle Medium
ECM	Extracellular Matrix
EDA/EDB	Extra Domain A/B
EGF	Epidermal Growth Factor
EGF-L	Epidermal Growth Factor-Like
EGFR	Epidermal Growth Factor Receptor
EMT	Epithelial Mesenchymal Transition
Er	Erythrocyte
EV	Empty Vector
FBS	Fetal Bovine Serum
FITC	Fluorescein Isothiocyanate
FN	Fibronectin
FN-EDA	Fibronectin-Extra Domain A
FN-EDB	Fibronectin-Extra Domain B
GAPDH	Glyceraldehyde 3-phosphate dehydrogenase
GBM	Glioblastome Multiforme
GF	Growth factor
H&E	Hematoxilin eosin
hCRC	human Colorectal Cancer
HEK293	Human Embryonic Kidney
HIF	Hypoxia Inducible Factor
hTNC	human Tenascin-C
Id2	Inhibitor of DNA binding 2
IF	Immunofluorescence
IgG	Immunoglobulin G
KO	Knockout

LM	Laminins
Lyve-1	Lymphatic vessel endothelial hyaluronan receptor-1
MET	Mesenchymal Epithelial Transition
MMP	Matrix Metalloproteinase
MOI	Multiplicity Of Infection
mRNA	messenger Ribonucleic Acid
NaCl	Sodium Chloride
OPN	Osteopontin
PBDG	Porphobilinogen deaminase
PBS	Phosphate Buffered Saline
PBS-T	Phosphate Buffered Saline- 0.01% Tween
PDGF	Platelet Derived Growth Factor
PFA	Paraformaldehyde
p-FN	plasma-Fibronectin
PH3	Phospho histone H3
qPCR	quantitative Polymerase Chain Reaction
qRT-PCR	quantitative Reverse Transcription-Polymerase Chain Reaction
Rag2	Recombination activating gene 2
RNA	Ribonucleic Acid
RT2	Rip1Tag2
S.E.M.	Standard error of the mean
SEM	Scanning Electron Microscopy
ShRNA	Small hairpin Ribonucleic Acid
Sox4	SRY-related HMG-box 4
SV40 Tag	Simian Virus 40 large T-antigen
TAM	Tumor Associated Macrophage
TEM	Transmission Electron Microscopy
TNC	Tenascin-C
TNR	Tenascin-R
TNW	Tenascin-W
TNX	Tenascin-X
TSP1	Thrombospondin 1
VEGF	Vascular Endothelial Growth Factor
VEGFA	Vascular Endothelial Growth Factor A
WB	Western Blot
WT	Wildtype
αSMA	α Smooth Muscle Actin

Introduction

INTRODUCTION

Cancer is recognized to be a major problem of health. It is a leading cause of death with about 8 million of new diagnoses each year worldwide (WHO, 2008). Within Europe there are 3.2 million new cases and 1.7 million deaths each year (Ferlay et al., 2007). In the following, crucial steps in cancer progression will be introduced. Next, the importance of the tumor microenvironment will be investigated. And finally, different targets on the road of cancer therapy will be addressed, with focus on the tumor microenvironment and anti-angiogenic therapeutics.

1. Tumorigenesis is a multi step process

1.1 Cancer cell initiation

Tumor initiation is a process in which normal cells are modified (epigenetic and genetic) so that they are able to form tumors. Tumor cells initiate malignancy and drive progression into cancer undergoing the six hallmarks of cancer (revisited by Hanahan and Weinberg, 2011). They consist in angiogenesis, proliferation, metastasis formation and resistance to cell death. First, for a tumor cell to become malignant the cell needs to accumulate a number of genetic alterations that provoke uncontrolled tumor proliferation. Moreover, cancer cells have developed multiple strategies in order to not enter an apoptotic program (Hanahan and Weinberg, 2011).

1.2 Tumor angiogenesis

Angiogenesis is the physiological process involving the growth of new blood vessels from pre-existing vessels (Penn, 2008) in growth and development, but also in wound healing. Different types of angiogenesis were described. During sprouting angiogenesis, angiogenic growth factors activate receptors on endothelial cells in pre-existing blood vessels. Activated endothelial cells then begin to remodel the basement membrane notably through secretion of proteases. Thereby, the endothelial cells can escape from the parental vessel and migrate into the surrounding matrix, expand and finally establish connections with the neighbouring vessels. Sprouting occurs at a rate of several millimeters per day, and

enables new vessels to grow across gaps in the vasculature (Adams and Eichmann, 2010). The second type of angiogenesis is intussusceptive angiogenesis (Kurz et al., 2003), also known as splitting angiogenesis. It was first observed in neonatal rats. In this type of vessel formation, the capillary wall extends into the lumen to split a single vessel in two. Intussusception is important because it is based on a reorganization of existing cells and allows an increase in the number of capillaries without a proliferation of endothelial cells. It plays a critical role during embryonic development (Burri et al., 2004).

Under normal conditions, angiogenesis is a highly regulated process leading to the establishment of a hierarchically organized and well-functioning vascular network. In contrast, tumor angiogenesis is aberrant and leads to the formation of disorganized, chaotic and poorly functional vascular networks. However, it is also a crucial step in the transition of tumors from a dormant to a malignant state. In the absence of sufficient vascularization most tumors cannot exceed 2 mm^3 in volume, and remain clinically silent. Tumors require new blood vessel formation for tumor growth and progression towards metastasis. Actually, quiescent endothelial cells are activated under low blood perfusion and hypoxic stress and enter into a biological program allowing them to build new blood vessels. Tumor angiogenesis is mainly initiated at an early step of tumor progression that was called the 'angiogenic switch' (Figure 1) (Hanahan and Folkman, 1996; Bergers and Benjamin, 2003). This switch depends on a balance of pro-angiogenic (such as vascular endothelial growth factor, VEGF) and anti-angiogenic factors. An imbalance towards more pro-angiogenic factors is thought to be essential for triggering the angiogenic switch (Bergers and Benjamin, 2003).

The majority of tumor-associated vessels is not only stimulated but also abnormal (Jain et al., 2001; Jain et al., 2005; Nagly et al., 2010). Sprouting and intussusceptive angiogenesis also occur during tumorigenesis, but new concepts of vessel formation in tumors were recently described (Carmeliet and Jain, 2011). For example, vasculogenesis, formation of blood vessels during embryogenesis, can be reactivated in tumors and attract bone marrow derived cells (Dome et al., 2007).

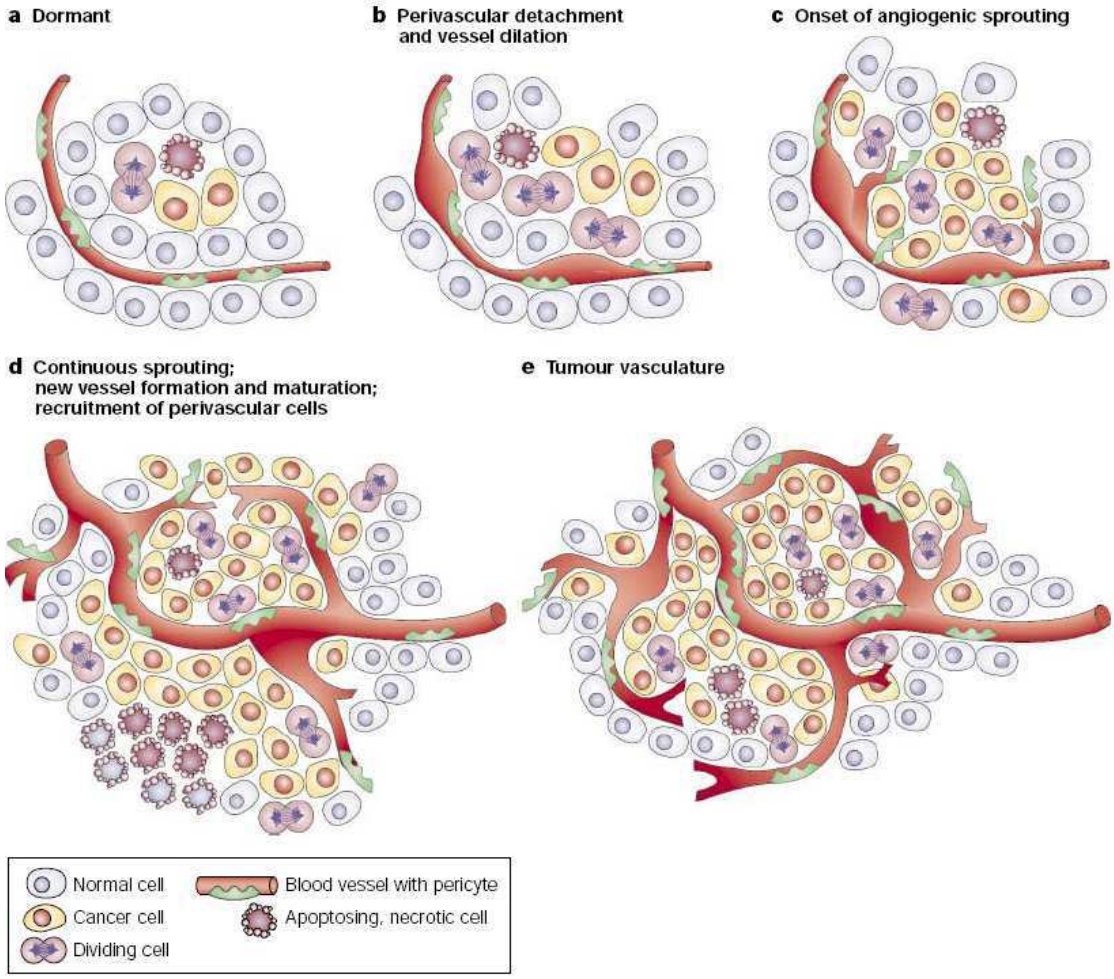

Figure 1: The angiogenic switch. It is a discrete step in tumor development that can occur at different stages in the tumor-progression pathway, depending on the nature of the tumor and its microenvironment. Most tumors start growing as avascular nodules (dormant) (**a**) until they reach a steady-state level of proliferating and apoptosing cells. The initiation of angiogenesis, or the 'angiogenic switch', has to occur to ensure exponential tumour growth. The switch begins with perivascular detachment and vessel dilation (**b**), followed by angiogenic sprouting (**c**), new vessel formation and maturation, and the recruitment of perivascular cells (**d**). Blood-vessel formation will continue as long as the tumour grows, and the blood vessels specifically feed hypoxic and necrotic areas of the tumour to provide it with essential nutrients and oxygen (**e**). **(Taken from Bergers and Benjamin, 2003)**

Carmeliet and Jain also described another atypical mechanism for blood vessel formation, which consisted of cancer cells that mimic endothelial cells. It is referred to as vasculogenic mimicry (Maniotis et al., 1999). They also described tumor vessels as tortuous and heterogenous. These atypical vascularisations in tumors might also affect cancer cells, thus if a tumor is not well vascularised, malignant cell clones that are resistant to hypoxia are selected. Hypoxia can also contribute to the activation of a genetic program allowing tumor cells to accomplish an epithelial to mesenchymal transition (Yoo, 2011) and consequently acquire invasive capacities to escape from hypoxic areas through leaky vessels (Jain et al.,

2005). Some abnormalities were also described on the vessel wall. Contrary to normal tissue, in which blood vessels interact with the sub-endothelial basement membrane (BM), which stabilize and permit interactions of endothelial cells with their microenvironment which include pericytes that provide direct support for endothelial cells (Figure 2) (Simon-Assmann et al., 2011; Diaz-Flores, 2009), in the majority of cancers, activated pericytes are immature and do not cover the whole endothelium (Raza et al., 2010; Baluk et al., 2003). All these processes might be responsible for tumor angiogenesis and promote tumor growth.

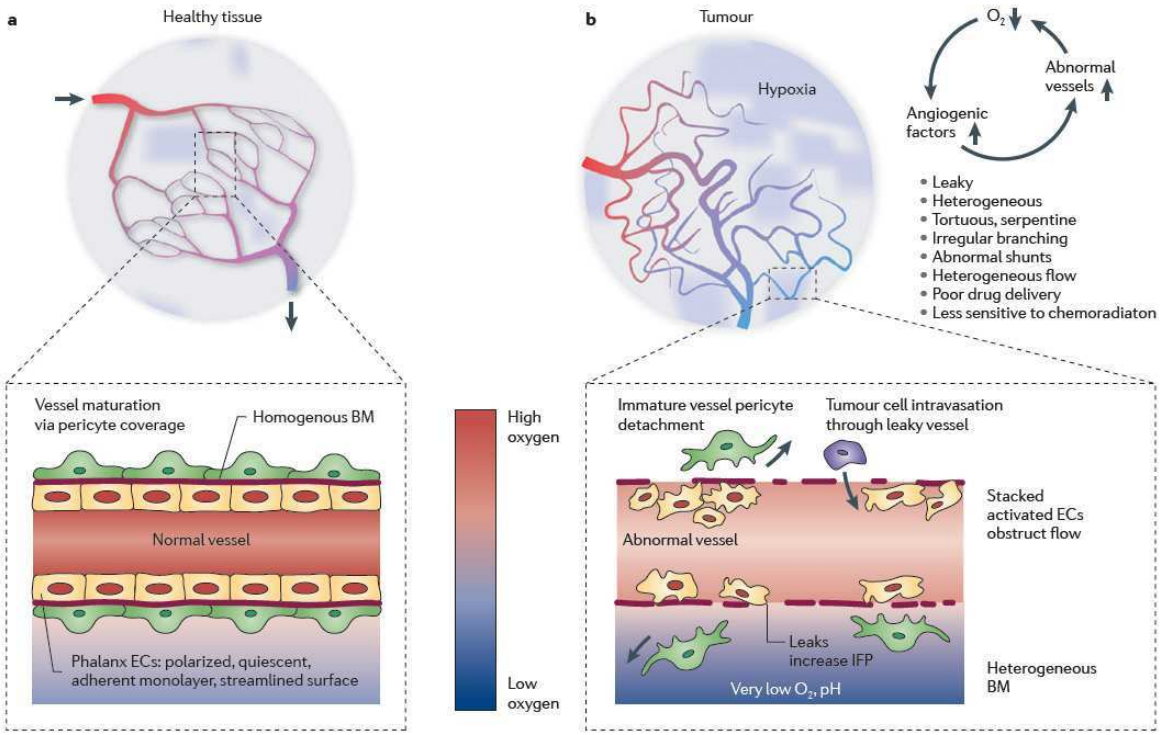

Figure 2: Characterization of normal and tumor vessels. **(a)**In healthy tissue, a regularly patterned and functioning vasculature is formed (upper panel), with a normal vessel wall and endothelium (lower panel). **(b)** In established tumors, the vasculature (upper panel), as well as the endothelium and vessel wall (lower panel) exhibit structural and functional abnormalities, leading to regions of severe hypoxia (represented by blue shading). BM, basement membrane; EC endothelial cell; IFP, interstitial fluid pressure. **(Taken from Carmeliet and Jain, 2011a)**

1.3 Metastatic dissemination of tumor cells

Metastasis remains the major cause of death of patients with cancer (Sporn, 2008). After degradation of the BM, tumor cells can invade the underlying tissue. Paracrine signals between tumor and stromal cells can then support the progression of aggressive tumors to an invasive stage leading to metastatic dissemination and colonization of distant organs.

Metastasis requires not only invasiveness but also such newly acquired traits as motility and adaptation to the new microenvironment. There are different steps in metastasis formation (Steeg, 2006) (Figure 3): first, invading cells must undergo an epithelial-to-mesenchymal transition (EMT) (Said and Williams, 2010). EMT relies on the loss of differentiated epithelial cell characteristics, such as loss of E-cadherin mediated intercellular adherent junctions, and acquirement of mesenchymal cell features such as cytoskeleton and extracellular matrix (ECM) receptor mediated motility and protease-mediated degradation of ECM (Figure 3) (Friedl et al., 2003). Tumor cells can then reach blood or lymphatic circulations through intravasation in abnormal tumor-associated vessels. Inversely, distant organ colonization rely on an inverse process called mesenchymal-to epithelial transition (MET) allowing tumor cells to adapt, survive and efficiently grow in a different tissue context.

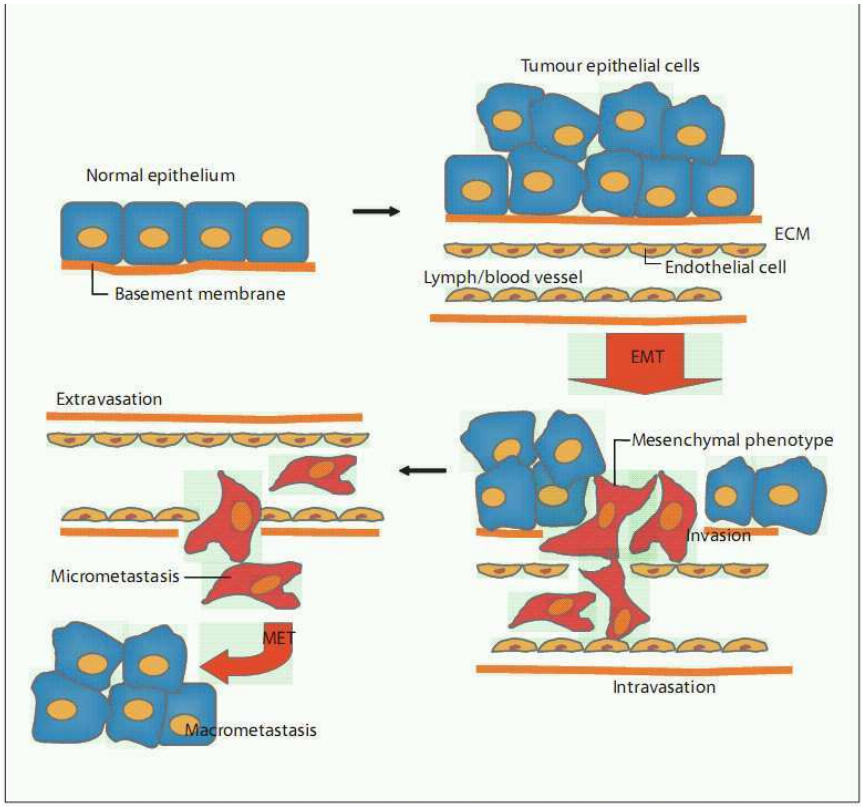

Figure 3: Metastatic dissemination. Schematic representation of epithelial cells undergoing EMT and MET. In EMT, the loss of epithelial differentiation and acquisition of mesenchymal phenotype endow the tumor cells with tumor migratory and invasive capabilities to invade the basement membranes and intravasate into circulation. The reverse process, MET, is implicated in secondary tumor growth where the mesenchymal-like cells re-adopt several epithelial properties to enable colonization at secondary sites. **(Taken from Said and Williams, 2010).**

2. Tumor as an organ: the importance of the microenvironment in tumor progression

2.1 Concept of the tumor as an organ

What is an organ? An organ is described as a collection of tissues assembled as a structural unit, which may serve a common function (Widmaier, 2007). Under normal conditions, tissues exchange information through cell-cell contacts, cytokines and growth factors (GF) and ECM interactions. An organ is composed of a main tissue (the parenchyma) and sporadic tissues (the stroma). For example, main tissue in the heart is the myocardium, while sporadic are the nerves, blood and connective tissue. In cancer, this concept remains valid: the interactions between cancer cells (the main tissue) and the tumor microenvironment (the sporadic tissue) create a context that promotes tumor growth and protect it from immune attacks (Bissell and Radisky, 2001). Bissell postulated that a functional association of cancer cells with the surrounding microenvironment forms a new "organ" undergoing continuous reorganization during malignant progression.

2.2 Tumor microenvironment

Similarly, the tumor microenvironment is known since a long time to play a central role in tumorigenesis (Bissell and Radisky, 2001), indeed, many "in situ" cancers never progress to an invasive stage, most likely due to host factors that prevent this development, a phenomenon termed "cancer without disease" (Folkman and Kalluri, 2004). This highlights the fact that a transformed cell per se is not sufficient to cause lethal cancer, but that manifestation of cancer requires a tumor microenvironment that is permissive to further tumor growth and metastasis. In addition to mutations in the cancer cells themselves, many changes occur in the microenvironment, the so called stroma, which may even precede the malignant transformation of epithelial cells leading to carcinomas, which present the majority of human cancers. The ECM of a tumorigenic tissue is very different from that of the normal tissue. The tumor stroma is composed of a fibrillar component and a cellular component such as carcinoma associated fibroblasts (CAF), immune cells and in particular tumor associated macrophages (TAM) and endothelial cells (Figure 4). The

secretion of multiple growth factors, i. e. vascular epidermal growth factor (VEGF), epidermal growth factor (EGF) and cytokines contribute to cell behaviour.

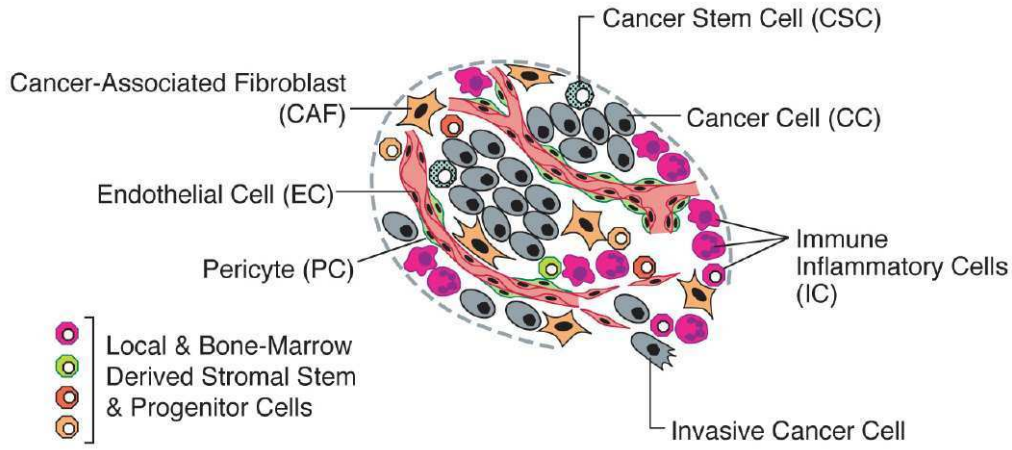

Figure 4: The tumor microenvironment. An assemblage of distinct cell types constitutes most solid tumors. Both the parenchyma and stroma of tumors contain distinct cell types and subtypes that collectively enable tumor growth and progression. Notably, the immune inflammatory cells present in tumors can include both tumor-promoting as well as tumor-killing subclasses. **(Taken from Hanahan and Weinberg, 2011)**

2.2.1 Cancer-associated fibroblasts

Under normal conditions, fibroblasts are the main cell type responsible for deposition of ECM (Rodemann and Muller, 1991; Tomasek et al., 2002) and also contribute to BM formation (Chang et al., 2002). Fibroblasts are involved in the wound healing process (Tomasek et al., 2002; Parsonage et al., 2005). Fibroblasts are described to invade lesions, secrete new ECM, which serve as scaffold for other cells and allows resorption of granulation tissue and restoration of physiological parameters of the tissue. Fibroblasts can be "activated" during wound healing, in fibrotic contexts and in tumor tissue, allowing the acquirement of a contractile phenotype (Tomasek et al., 2002; Parsonage et al., 2005).

Interestingly, at the tumor site a particular subpopulation of fibroblasts named CAF, peritumoral fibroblasts or reactive stromal fibroblasts remains persistently active within the tumor stroma (Barsky et al., 1984; Mueller and Fusenig, 2004). These cells were identified by their expression of α smooth muscle actin (αSMA), vimentin and FSP1 (MTS1/S100A4 reviewed by Kalluri, 2006; Tsukada et al., 1987; Ronnov-Jessen et al., 1996; Gabbiani,

2003). Although the mechanism of conversion of normal to CAF remains elusive, there have been studies illustrating that paracrine signals emitted by tumor cells contribute to their activation (Kalluri, 2006). CAF have been described to play important roles in key steps of tumorigenesis; they play a role in cancer initiation (Olumi et al., 1999; Bhowmick et al., 2004), progression (Orimo et al., 2005) and metastasis formation (Olaso et al., 1997). They are associated with all stages of tumor progression (Kalluri and Zeisberg 2006), and might constitute targets for anti-cancer therapy (Rettig et al., 1993; Zeisberg et al., 2003; Nakamura et al., 2005).

2.2.2 Immune cells

Tumors were coined by Dvorak in 1986 as a "wound that does not heal" (Dvorak, 1986). Indeed, inflammatory cells were shown to be important actors of tumor progression and, chronic inflammation is a hallmark of cancer (Coussens et al., 2002; de Visser et al., 2005). The tumor microenvironment can be infiltrated by numerous immune cells, including lymphocytes and natural killer (NK) cells that efficiently target tumor cells in early stages. Innate immunity can then exert deleterious effects and sustain tumor progression and contribute to stromal reactions.

Macrophages were shown to play an important role in that context and can represent up to 50% of the tumor mass (Nathan, 2006). They constitute a heterogeneous population and are often referred to as TAM. Blood monocytes can be subdivided in two macrophage subtypes that were named M1, that support microbicidal activity or alternatively activated (M2) macrophages that are not competent to eliminate pathogens (Goerdt and Orfanos 1999; Gordon and Taylor 2005; Pollard, 2009; Mege, 2011). It was demonstrated that M2 type TAM can exert pro-tumoral functions and mediate tumor cell survival, proliferation, and dissemination (Mantovani et al., 2002; Pollard et al., 2004; Talmadge et al., 2007). High levels of TAM are often correlated with a bad prognosis.

In addition to TAM, it was also reported that neutrophils might have a critical impact on the tumor microenvironment through the secretion of cytokines and chemokines, which

influence inflammatory cell recruitment (Pham et al., 2006). These cells secrete other products like reactive oxygen and proteinases (Gungor et al., 2006; Knaapen et al., 2006) which may induce tumor cell genomic instability, proliferation, angiogenesis and metastatic dissemination (Huh et al., 2010).

2.2.3 Endothelial cells

Normal vessels are defined by a monolayer of polarized cohesive endothelial cells. Tumor associated blood vessels are heterogenous and can exhibit abnormalities in terms of organization, structure and function. In a tumor endothelial cells loose their polarity, they detach from the BM and some of them die (Baluk et al., 2005; Ozawa et al., 2005; Mazzone et al., 2009). This phenomenon gives rise to "mosaic" vessels (Jain and Baxter, 1988) lined by tumor cell and endothelial cells, and explains that tumor cells are exposed to blood. Pericytes participate in these morphological features of the tumor vasculature (Hashizume et al., 2000; Hellstrom et al., 2001). Gaps between these cells contribute to tumor vessel leakiness and hemorrhages, enhance fluid pressure and limit perfusion (Jain et al., 2005; Pettersson et al., 2000).

2.2.4 Extracellular matrix molecules

The ECM molecules, surrounding tumor and stromal cells have both scaffolding and structural roles. For example, the ECM can be organized as a scaffold that embeds blood vessels. Many ECM molecules are usually highly overexpressed in malignant tumors compared to the normal tissues from which they derive.

Laminin (LM) is a part of the BM, which is found in all epithelium and endothelium and, it surrounds most of the muscle and nervous cells and adipocytes (Colognato et al., 2000; Ericksonet al., 2000; Simon-Assmann and Kedinger, 2000; Li et al., 2003). The BM has a structural role, but it plays also an important role in cell-cell interactions, thereby modulating proliferation, differentiation, and migration. Thus, LM family members play an

important role in certain pathologies such as cancer (De Arcangelis et al., 2001).

Fibronectins (FN) are classified into two groups: plasma FN (p-FN), a soluble form produced by hepatocytes that circulates in blood at high concentrations, and cellular FN (c-FN) produced in tissues where it is incorporated in fibrilllar matrix (van Obberghen-Schilling et al., 2011, Annex2). c-FN differs from p-FN by the presence of additional domains, including the highly conserved fibronectin type III "extra" domains B (EDB) and/or A (EDA). Fibronectin splice variants containing the EDB and EDA domains, often referred to as oncofetal variants, were described as the most specific markers of angiogenic blood vessels (Kaspar et al., 2006). FN-EDA is required for transduction of TGFβ to activate fibroblast into myofibroblasts and FN-EDB is associated with revascularization stuctures in many types of tumors (Kaczmarek et al., 1994 and Castellani, 2007). In addition, FN promotes adhesion and signalling through cell adhesion receptors, in particular integrins and provides a fibrillar scaffold for the assembly of other ECM proteins including TNC. It provides a platform for angiogenic signalling by increasing the bioavailability of soluble angiogenic factors, and cooperating with their transmembrane receptors (Hynes, 2007; Hynes, 2009; Miyamoto et al., 1996; Mosher et al., 1980).

2.3 The extracellular matrix molecule: Tenascin-C, a key player in tumorigenesis

2.3.1 Structure

Tenascins are a family of large multimeric ECM proteins. Vertebrates express four different members named Tenascin-C (TNC), -R (TNR), -X (TNX) and –W (TNW). They share common structural organization with an oligomerization domain followed by EGF-like repeats, fibronectin (FN) type III repeats and a fibrinogen globe (Figure 5).

TNC is one important factor of the tumor-specific microenvironment, it is comprised of 14.5 EGF-like repeats, of 30–50 amino acids, which contain six cysteine residues involved in intrachain disulfide bonds (Figure 6A). Up to 17 fibronectin type III domains (FNIII) are

present (about 90 amino acids) and are composed of 7 antiparallel β-strands arranged in two sheets (Figure 6A). TNC (Chiquet-Ehrismann et al., 1986) was first described in the early 1980 and was previously named glioma mesenchymal extracellular antigen (Bourdon et al., 1983) myotentidous antigen (Chiquet and Fambrough, 1984), cytoactin (Grumet et al., 1985) or J1 glycoprotein (Kruse et al.,1985). TNC, a hexameric protein (Figure 5B) is highly expressed during embryonic development, tissue repair and in pathological situations such as chronic inflammation and cancer (Jones and Jones, 2000).

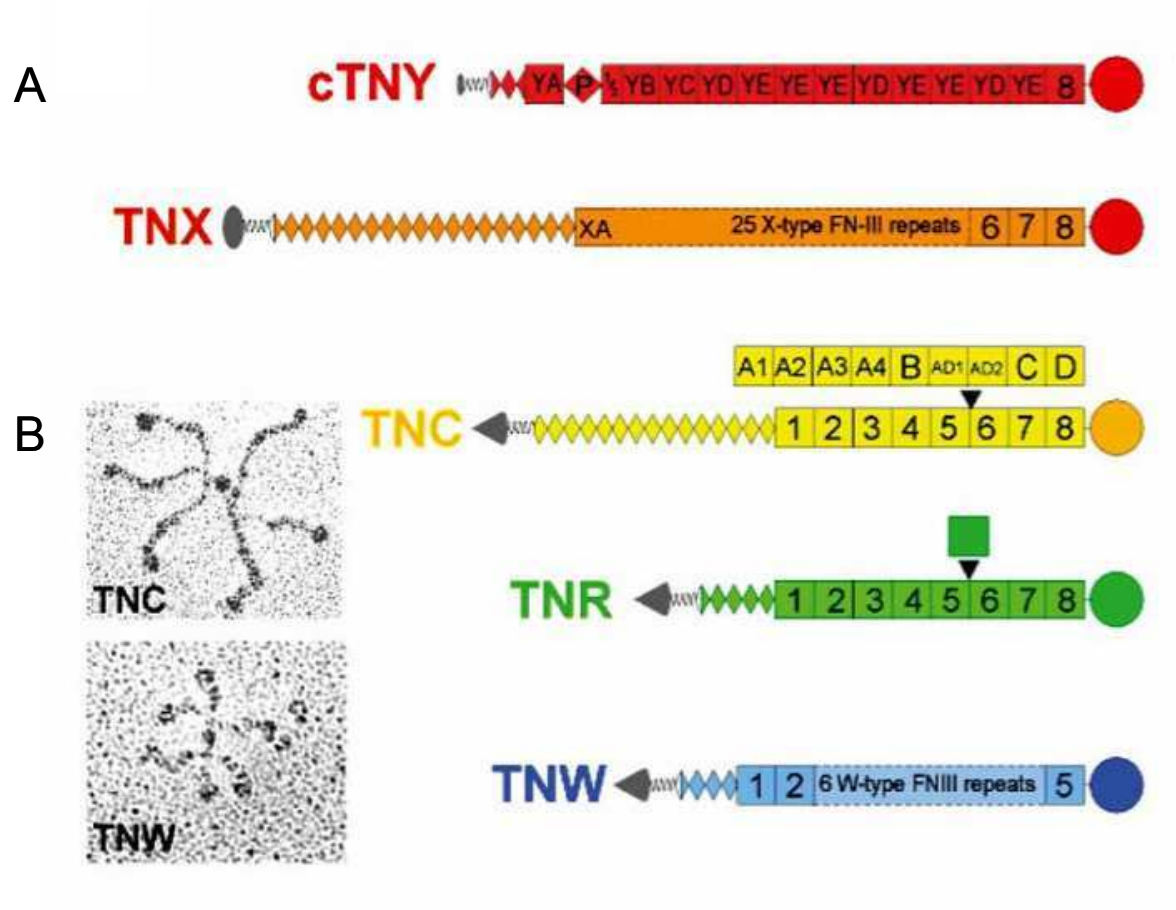

Figure 5: The structure of tenascin family (A). Structural representation of the five members of tenascin family. (**B)**. The appearance of purified TNC and TNW protein as a hexamer upon visualization with electron microscopy. heptad repeats (wavy line), EGF-like repeats (diamonds), fibronectin type III repeats (squares), fibrinogen globe (circle).

2.3.2 Role of TNC in cancer

TNC is highly expressed in most solid cancers and its high expression correlates with signs of bad prognosis for disease-free survival in patients with glioma, lung, breast, and colon cancer (Orend and Chiquet-Ehrismann, 2006) (Figure 6B and C). The full-length TNC is

expressed in pancreatic and prostate cancer (Katenkamp et al., 2004; Chen et al., 2009), and interestingly a novel isoform which is undetectable in normal tissue, is highly present in high grade gliomas (Carnemolla et al., 1999). Moreover, TNC was also shown to promote tumor growth and invasion in breast (Adams et al., 2002) and ovarian cancer (Wilson et al., 1999; Hancox et al., 2009). The source of TNC in most solid tumors such as breast or colon cancer, are CAF (Degen et al., 2007). In glioblastoma and melanoma, the cancer cells also secrete TNC (Herlyn et al., 1991; Natali et al., 1990).

TNC plays an important role in vascular remodelling in pathological situations including cancer (reviewed by Midwood et al., 2011; Midwood and Orend, 2009). TNC can interact with ECM and cells, it has been described to be implicated in inflammation (Betz et al., 1993; Filsell et al., 1999), in tissue remodelling, in wound contraction (Tamaeki, 2005), and in infection (Kaarteenako- Wiik et al., 2000, Paollysaka et al., 1993).
TNC is also playing an important role in tumor progression (Fukunago-Kalabis et al., 2010), and in metastasis formation (Oskarsson et al., 2011; Van Obberghen-Schilling et al., 2011, Annex2). Moreover, it has been shown that TNC attracted endothelial cells and played a role in generation of tumor derived endothelial cells (Pezzolo et al., 2011). TNC had also been described to select for proliferative endothelial cells (Alves et al., 2011). Some other studies associated TNC with angiogenesis (Jallo et al., 1997; Castellon et al., 2002; Paik et al., 2004).

TNC might also play a role in alternative programs of angiogenesis and formation of tubular structures, this will be discussed later. Thus, TNC was also described to be expressed in human colorectal cancer (CRC) as tube-like structures all over the tumor (Midwood and Orend, 2009). TNC has distinct effects on tumor cells and tumor associated cells found within the tumor stroma. A strong expression of TNC in cancer tissue suggests that this ECM molecule is involved in providing a permissive "tumor-bed" that promotes the survival and expansion of tumor cells and tumor associated cells and, thus may support progression into metastasing cancer.

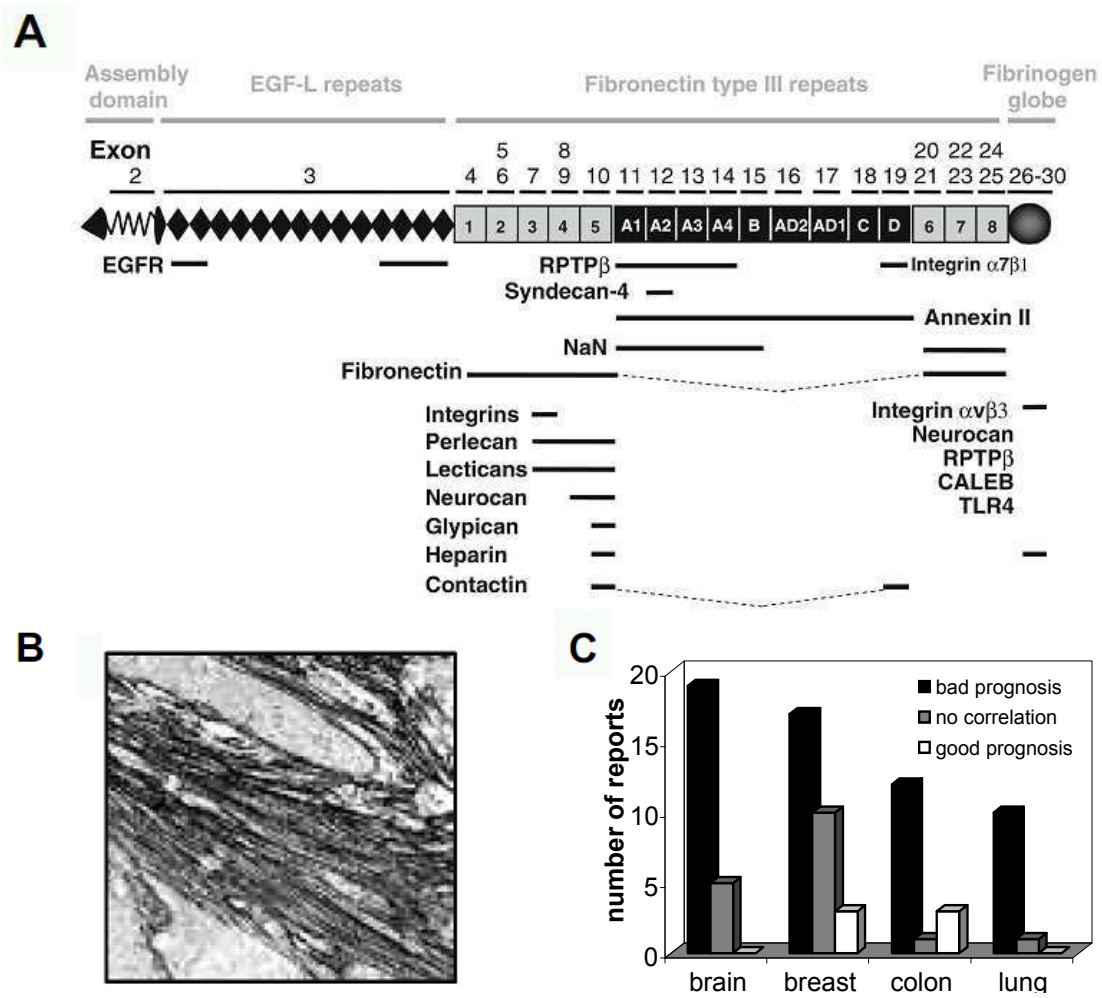

Figure 6: TNC characterization and expression. (A-B). Taken from Midwood and Orend, 2009**. (A)**. Organization of TNC into an assembly domain, EGF-L (epidermal growth factor-like), Fibronectin type III repeats (constant in grey and alternatively spliced in black) and the C-terminal fibrinogen globe domain. **(B)**. TNC presence in matrix conduit of paraffin preserved human colorectal carcinoma tissue, visualized by immunohistochemistry. **(C)**. Implication of TNC in cancer.

3. Mouse and human models to study the role of the tumor microenvironment in tumorigenesis

3.1 Murine Rip1Tag2 insulinoma model

Rip1Tag2 (RT2) is a well characterized multi-stage tumorigenesis mouse model (Figure 7). The SV40 large T-antigen (Tag) is expressed under the control of the rat insulin promoter (Rip). This model recapitulates all steps in tumor progression of neuroendocrine insulinoma (Hanahan, 1985). The logic in choosing the SV40 included the possibility to induce transformation of tumors in all cell types expressing SV40. The SV40Tag inhibits the p53

and pRb tumor suppressors, thus initiating transformation and hyperplasia which in turnS trigger angiogenesis and insulinoma formation in a reproducible and sequential manner. In addition, it allows to detect tumor cells by using T-antigen specific antibodies (Hanahan et al., 2007). In a C57Bl6 background RT2 mice barely develop visible macrometastasis which correlated with a lack of nuclear translocation of β-catenin (Herzig et al., 2007). Multi-step tumorigenesis in the RT2 transgenic mouse model consists in different stages. A normal islet also referred as islet of Langerhans (N) carries blood capillaries. By 5-7 weeks of age, almost all the islets become hyperplastic, but the number of vessels is not yet increased. At 7 to 12 weeks about 10% of the hyperplastic islets (H) become angiogenic (A) which results in a increased number of blood vessels. Finally, between 12 to 14 weeks of age, 2 to 4 % of primary hyperplastic islets become tumorigenic (T) and some invade the surrounding exocrine pancreas. The RT2 transgenic mouse model has been instrumental in visualizing the onset of tumor angiogenesis (Folkman et al., 1989; Bergers et al., 2000). The gain of survival signalling to overcome apoptosis during tumor development has been demonstrated by the upregulated expression of insulin-like growth factor II (IGF-II) during RT2 tumorigenesis (Christofori et al., 1994). In addition, RT2 mice have been instrumental to demonstrate the critical role of cell adhesion molecules, such as E-cadherin, during malignant tumor progression and metastasis (Perl et al., 1998).

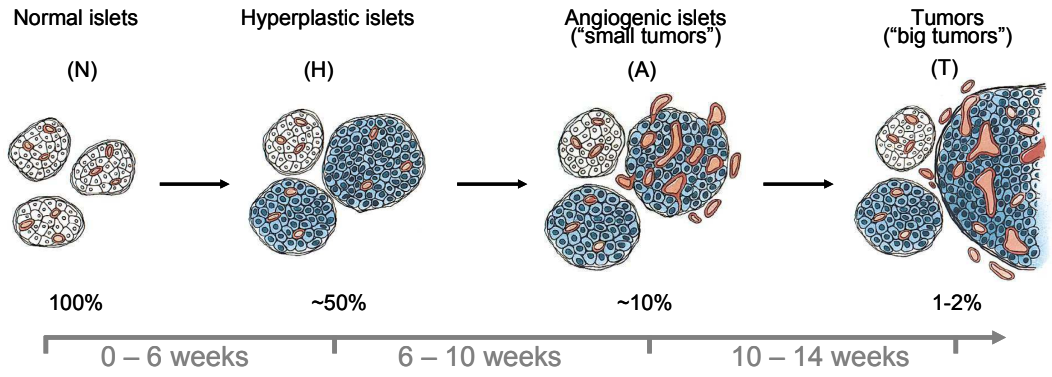

Figure 7: Multiple stages of tumorigenesis in the RT2 model system. Normal (N, <0.2 mm), hyperplastic (H, 0.2-0.5 mm), angiogenic (A, 0.5-1 mm) and tumorigenic (T, >1mm) islets were defined according to the size. Approximately 50% of the islets become hyperproliferative and develop into hyperplastic lesions. A subpopulation of these islets (~20%) becomes angiogenic and of these only a few progress into solid tumors. RT2 mice in the most commonly C57BL6 background do not exhibit formation of metastasis to other organs, because they die about 12 to 14 weeks of age due to hypoglycemia (Hanahan, 1985). **(Adapted from Hanahan and Folkman, 1996)**

3.2 Human colorectal cancer analysis

The intestine epithelial cells, which face the lumen of the gastrointestinal tract are organized as monolayer. The population of cells is very fluctuant, for example each minute, in the colon 20 to 50 million cells die and an equal number of newly minted cells replace them. Lining these epithelial cells, there is a basement membrane named basal lamina, to which cells are anchored. It is constituted of ECM proteins secreted by stromal and epithelial cells. The mesenchymal cells representing the stroma are essentially fibroblasts, endothelial cells and immune cells such as macrophages and mast cells. Lying underneath this layer of stromal cells is the intestinal wall that is a thick layer of smooth muscle responsible for the contraction of the intestinal tract.

CRC is known as bowel cancer, it takes place in the colon, rectum, or vermiform appendix. Under pathological conditions, the epithelial layer is the site of more changes, in particular in colon cancer. The notion of human tumor development as a multi-step process has been well documented for the epithelium of the intestine. Analysis of human cancers has revealed different tissue states. The TNM classification is used for classifying human CRC. Actually, T describes the size of the tumor and whether it has invaded the neighboring tissue, N describes regional lymph nodes that are involved, M describes distant metastasis TNM (Denoix, 1946). For example, invasive cancer that are localized within the intestinal wall (TNM stages I and II) might be cured by surgical resection. However, if it remained untreated, cancer cells can spread to local lymph nodes (and reach stage III). Finally, cancers that have disseminated (stage IV) are usually not curable.

CRC is one of the most common malignancies encountered in the western world and is the third most common cause of cancer related mortality (Kemp et al., 2004). Ferlay and collegues has estimated that approximately 9.7% of all newly diagnosed cancer are in the colon (Ferlay et al., 2007). The prognosis of patients with colon cancer is linked to the degree of penetration of the tumor through the intestine wall, the presence or absence of nodal involvement, and the presence or absence of distant metastases. Most colorectal carcinomas occur sporadically in the absence of well- defined familial syndromes. Like the

majority of cancers in other organs, there are conditions associated with the risk of tumor development. Epidemiologic of studies have shown that age is a large factor in the incidence of cancer. In the United States, the risk of dying from colon cancer is as much as 1000 times greater in a 70-year old man than in a 10-year-old boy. This suggests that this type of cancer requires years or even decades to develop (Harrison and Benzigen, 2011). A genetic pathway for this adenoma-carcinomas sequence has been proposed by Fearon and Vogelstein (Fearon and Vogelstein, 1990). But recent studies have characterized CRC as a very heterogenous disease, in fact four main molecular pathways have been identified resulting in malingnant transformation: Chromosomal Instability Pathway (CIN), CpG Island Methylator phenotype (CIMP), the microsatellite instability and serrated pathways (Worthley and Leggett, 2010)**.**

The CIN pathway is the most common genetic aberration which has been identified in 85% of all cases (Grady and Carethers, 2008), it is associated with a poorer prognosis and with mutation in the APC gene, which co-exist with deletion of the chromosome 5 (18q or 17q, (Pritchard and Grady, 2011). In addition, some other genes are involved in this pathway such as KRAS (Jiang et al., 2009). The CIMP pathway is characterized by epigenetic instability, consequence of silencing of tumor suppressor genes by hypermethlylation of the promoter (Kim et al., 2010). The microsatellite instability pathway involves mutations in the repeat sequences throughout the genome (Boland and Goel, 2010). To treat CRC surgery can be used to resect the tumor if it is localized. After surgery, chemotherapy is used. But in the last decade, targeted therapy to address the molecular abberations in a given cancer may improve cancer therapy.

4. Different targets on the road of cancer therapy: cancer cells, tumor vasculature and the tumor microenvironment

Nowadays, chemotherapy is frequently used in cancer therapy. This therapy is mostly used to target cancer cells, and it is used in combination with surgery and/or radiotherapy.

These drug families contain alkylating agents, anthracyclines, topoisomerase inhibitor and alkaloids (Takimoto and Calvo, 2008). All these drugs affect cell division and DNA synthesis. Unfortunately, they are not specific for cancer cells and lead to damage in normal proliferative cells. Therefore, targeting tumor angiogenesis appears to be a promising strategy, so that tumors will not get anymore blood support, as for example, anti-VEGF target therapy. The concept of targeted therapy had been described by Paul Ehrlich end of the nineteenth century, he proposed the "magic bullet" that would interact specifically with the micro-organisms. Later, this concept has been extended to cancer therapeutics (Imai and Takaoka, 2006). The American National Cancer Institute defined targeted cancer therapy as a major approach to block the growth and spread of cancer.

VEGF signalling appears to be preponderant in tumor angiogenesis, providing a rationale for targeting VEGF receptors (Bhargava and Robinson, 2011). There are five members of in VEGF family; VEGF-A, VEGF-B, VEGF-C, VEGF-D and a placental form named PLGF, they bind distinctly to their repceptors (VEGFR1, VEGFR2 and VEGFR3) and affect proliferation, migration, morphogenesis of endothelial cells to form new vessels (Rini et al., 2008; Zhang et al., 2009 and Jia et al., 2004). Some target molecules are designed to target tyrosine kinases, involved in VEGF signalling and thereby inhibit angiogenesis. As an example, Sorafenib (Nexavar®) is a small-molecule inhibitor of tyrosine kinases that is acting on the development of new blood vessels (Escudier et al., 2007). Sunitinib (Sutent®) is another small-molecule tyrosine kinases inhibitor (Motzer et al., 2007). It is also possible to target directly the ligand, actually it exists VEGF antibodies to prevent interactions with endothelial surface receptors, as an example Bevacizumab (Avastin®).

Rationale for an improved cancer therapy targeting cancer as an organ, in the last decade, it has been shown that the tumor microenvironment plays a crucial role in cancer progression (Bissell and Radisky, 2001), and it suggested that cancer should be targeted as an organ. It is important to not only target cancer and endothelial cells, but also other components of the tumor microenvironment such as immune cells since they have been

linked to tumor development and invasion. CAF are playing an important role in cancer, therefore they also should be targeted. The cell-surface serine protease known as fibroblast activation protein (FAP) has been suggested as target since it is not expressed by normal and activated fibroblasts (Rettig et al., 1993; Wang et al., 2005). Also emerging in cancer therapy is the targeting of TNC. It can be targeted by antibody-drug-conjugates (Niesner et al., 2002) and aptamers (Estevez et al., 2010). To summarize, it is possible that the next generation of therapeutic agents will not only kill tumor and tumor associated cells but will also destroy the tumor specific ECM thus potentialy causing a normalization of the tumor bed.

5. Limits of anti-angiogenic therapies: the case of Bevacizumab

5.1 A general introduction to Bevacizumab and resistance to anti-angiogenic drugs

Bevacizumab is a humanized monoclonal antibody directed against VEGF, which is currently extensively used in the clinics as anti-cancer drug. Bevacizumab traps VEGF and prevents the interaction with its receptor (VEGFR) and thereby blocks VEGF signalling that is crucial for survival, proliferation and migration of endothelial cells in tumor angiogenesis (Bergers and Hanahan, 2008).

But, like all anticancer therapies, agents that inhibit tumour angiogenesis are prone to resistance (Ellis and Reardon 2009). In both pre-clinical and clinical trials, the benefits of angiogenesis inhibitors are at the best transitory and are followed by a restoration of tumor growth and even foster tumor progression (Bergers and Hanahan, 2008)**.** Increasing evidence is demonstrating that progression and mortality are following a period of benefit, as for example in treated patients with late-stage colon cancers (Hurwitz et al., 2004). Indeed these therapies inhibiting VEGF, result in normalization of blood vessels, since pericytes which are unaffected by these treatments, improve endothelial cell coverage and by that improve blood vessel functionality (Stallcup and Huang, 2008; Mancuso et al., 2006; Bergers and Hanahan, 2008). Several mechanisms have been evoked to explain this

regrowth of the tumor vasculature including the survival of pericytes and the sleeves of extracellular matrix, endothelial basement membranes which can serve as guiding tracks for the regrowth of neo-vessels (Mancuso et al., 2006). In addition, anti-angiogenic treatment can result in hypoxia within the tumor (Figure 8), which can trigger the recruitment of bone marrow derived cells that have the capacity to form new vessels by differentiating into either endothelial cells which form the inner layer of blood vessels or into pericytes and thus initiate neo-vascularization (Bergers and Hanahan, 2008). Finally, a considerable number of patients treated with anti-angiogenic drugs failed to show even a transitory benefit which is not yet understood (Batchelor et al., 2007; Kindler et al., 2007).

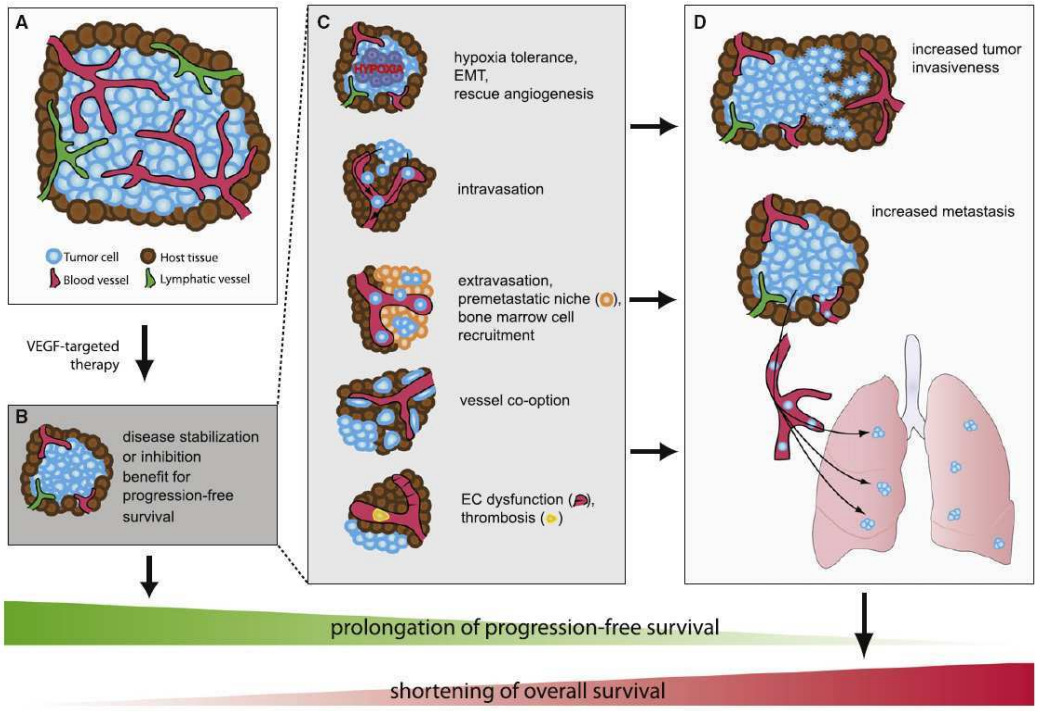

Figure 8: Resistance modes of anti-angiogenic therapies. (A). Tumors need blood (red) and lymphatic (green) vessels to grow. **(B-C)** VEGF-targeted therapies induce primary tumor shrinkage and inhibit tumor progression but can also initiate mechanisms that increase malignancy. **(D)** As result, anti-VEGF treatment can enhance tumor invasiveness and metastasis and reduce overall survival benefit. **(Taken from Loges et al., 2009)**

5.2 Human colorectal cancer and Bevacizumab treatment

Bevacizumab was approved by the FDA (Food and Drug Administration) in February 2004 to treat metastatic CRC (mCRC). It is now used as first line therapy with standard chemotherapy such as 5-Fluorouracil (5-FU) to treat patients with mCRC (Hurwitz et al., 2005). The EMEA (European Medicine Agency) approved the use of Bevacizumab in

association with oxaliplatin (which inhibits DNA synthesis in cancer cell) /5-FU/leucovorin (FOLFOX4) (Giantonio et al., 2007) based on the demonstration of a statistically significant improvement in overall survival of patients. Bevacizumab is administered intravenously at the dose of 5mg/kg once every 14 days until the tumor size increases.

Nevertheless, Bevacizumab treatment presents side effects and can induce gastrointestinal perforation, problems with surgery and wound healing and severe bleeding. Therefore, patients have to be selected for this kind of treatment. However, in the recent AVANT study (2011), Bevacizumab added to a standard adjuvant regimen for CRC failed to prevent relapses or improve overall survival. Furthermore, brief treatment of spontaneous and orthotopic tumor models with VEGF inhibitors caused a persistent switch to ''vasoinvasion'' of tumor cells, leading to increased metastasis. Increased metastasis had been demonstrated in an orthotopic xenograft mouse model treated with Bevacizumab. At first sight, these findings are inconsistent with previous observations that anti-VEGF reduces metastasis (Sini et al., 2008 and Verheul et al., 2007) and are difficult to assemble with the dogma that tumors, primary or metastatic ones, require blood supply for growth (discussed in Crawford and Ferrara, 2009). One possible explanation of anti-angiogenic treatment failure might rely on the active role of the microenvironment in tumor angiogenesis.

6. The role of the tumor microenvironment in tumor resistance and recurrence after anti-angiogenic therapies

It remains unclear how anti-angiogenic therapies affect the tumor microenvironment and in particular the "tumor bed". Studies with the anti-VEGF antibody DC101 in mice which was very potent in destroying the tumor and its vasculature, revealed that expression of TNC was unaffected by this treatment (Vosseler et al., 2005). These observations raise the possibility that TNC potentially is involved in the resurrection of the cancer upon removal of the anti-angiogenic drug. The possibility of an involment of tumor specific ECM is further supported by the observation that collagen IV-containing matrix sleeves persisted after an anti-angiogenic therapy and appeared to be instrumental in the regrowth of blood vessels

(Mancuso et al., 2006). It is possible that this matrix contains TNC. This process of tumor recurrence could be due to the up-regulation of alternative pro-angiogenic signals, protection of the tumor vasculature or by an improved vessel "normalization" through increased protective pericyte coverage, which altogether may participate to tumor recurrence and re-growth after anti-angiogenic therapy. In addition, it has been shown that TNC is promoting angiogenesis through different processes such as recruitment of endothelial cells progenitor or induction of endothelial cells proliferation and differentiation (reviewed by Midwood and Orend, 2009). These observations raise the possibility that TNC and other ECM components could support tumor re-vascularization upon removal of the anti-angiogenic drug.

Objectives

OBJECTIVES

Objective 1: Characterization of the extracellular matrix and cellular components of the tumor microenvironment in a murine tumor model and in human cancer tissue

In the insulinoma-prone SV40 Tag-expressing Rip1Tag2 (RT2) model that had been established in the laboratory to overexpress TNC, tumor angiogensis will be investigated in more detail by determining the presence of endothelial cells and carcinoma associated fibroblast (CAF) in dependence of TNC. Moreover expression and organization of TNC and other ECM molecules will be characterized. Cellular composition and ECM expression and organisation will also be determined in tissue from human colorectal carcinoma (CRC) and human insulinomas and will be compared to that in the RT2 model.

Objective 2: Development of a murine orthotopic xenograft model for investigating the role of tumor and host-derived TNC on tumor angiogenesis

To determine the role of host and tumor derived TNC on colorectal carcinoma angiogenesis an orthotopic immune-compromised Rag2KO model lacking B- and T- cells will be established that exhibits different TNC levels in the host and in the tumor cells. A particular attention will be paid to endothelial cells and CAF and the organization of ECM in dependence of TNC.

Objective 3: Preliminary results: development of a murine orthotopic xenograft model for investigating the impact of an anti-angiogenic therapy on the microenvironment

It is possible that the relative failure of anti-angiogenic therapies such as the ones using Bevacizumab could be due to an adaptive response involving the tumor microenvironment, and in particular TNC. The aim of this part was to establish an in-vivo model suitable to address the potential roles of TNC and of the tumor microenvironment on anti-angiogenic drug resistance and tumor recurrence.

Material and Methods

MATERIAL AND METHODS

1. In vitro experiments

1.1 Cell lines and culture conditions

SW480 human colon carcinoma cells, immortalized and tumorigenic human embryonic kidney HEK293 cells (Guan et al., 2001) and human osteosarcoma KRIB cells (Huang et al, 2001) were originally derived from ATCC. Cells were cultured in Dulbecco's Minimal Essential Medium (DMEM) containing 5% (v/v) fetal bovine serum (FBS), 100 U/ml penicillin and 100 µg/ml streptomycin. Cell cultures were maintained at 37°C and passaged at confluence.

1.2 Generation of cells for live imaging

An EcoRI site was added in the pCDNA-IFP1.4-IRES-cherry plasmid (kind gift from Dr R.Y. Tsien, La Jolla, USA) before the stop codon of the cherry cDNA using the GeneEditor™ *in vitro* Site-Directed Mutagenesis System according to the manufactory protocol (Promega,France), with primer 5'-P-TACAAGTAATCTAGAA TTCCCGTTTAAACCCGC-3'. After BamHI-EcoRI digestion, the cherry fragment was gel purified using the NucleoSpin® Extract II (Machery-Nagel, France) and cloned into the BamHI-EcoRI site of the pQCXIP retroviral vector (Clontech, Ozyme, France) generating the pQCXIP-cherry vector. Retroviral particles were produced with the pQCXIP-cherry (pQCXIP from Clonetech, construction generated by Dr. O. Lefebvre) and were then used to transduce cells according to standard protocols. Briefly, highly proliferative Bosc 23 cells (not described!) were plated at day 1. At day 2 Bosc 23 cells were transfected. The medium containing viral particles of the Bosc 23 cells were used to infect the cells of interest at day 4. Transduced cells were selected using puromycin (2.5µg/ml) at day 5.

1.3 Generation of cells with overexpression of DKK1

A BamHI and an EcoRI site were added in the the pCDNA 3.1 mDDK1 V5 His plasmid (constructed in the laboratory by Dr. O. Lefebvre), before the ATG or the stop codon of the mouse Dickkopf1 (mDKK1) cDNA respectively by using the GeneEditor™ *in vitro* Site-Directed Mutagenesis System and the following primers: 5'-P-GGT GGA ATT GCC CTT GGA TCC ACA TGA TGG TTG TGT-3' and 5'-P-ACC ATC ACC ATT GAG AAT TCA CCC GCT GAT CAG CC-3'. After BamHI-EcoRI digestion, the mDKK1 V5 His fragment was gel purified (NucleoSpin® Extract II) and cloned in the BamHI-EcoRI site of the pQCXIP retroviral vector (Clontech, Ozyme, France) generating the pQCXIP-mDKK1 V5 His vector. Retroviral particles were produced with the pQCXIP-mDKK1 V5 His vectors, that were then used to transduce cell according to standard protocols. Transduced cells were selected using puromycin (2.5µg/ml) (Table 1).

Table 1: Summary of engineered cell lines. Cells were engineered using either a retroviral or a lentiviral vector.

Cells engineered	VECTOR
SW480 shTNC 1	TCR2 lentiviral vector
SW480 shTNC 2	TCR2 lentiviral vector
SW480 shTNC 3	TCR2 lentiviral vector
SW480 TCR2 EV	TCR2 lentiviral vector
SW480 cherry	pQCXIP retroviral vector
HEK293 shTNC 1	TCR2 lentiviral vector
HEK293 TCR2 EV	TCR2 lentiviral vector
HEK293:DKK1	pQCXIP retroviral vector
HEK293 EV	pQCXIP retroviral vector
KRIB EV	pQCXIP retroviral vector
KRIB:DKK1	pQCXIP retroviral vector
T98G:DKK1	pQCXIP retroviral vector
T98G EV	pQCXIP retroviral vector

1.4 Generation of cells with knock down of TNC

At day 1, 6.5 X 10^5 cells were plated in a 6 well plate in complete medium. The second day polybrene at a final concentration of 8 µg/ml was added to each well. The appropriate amount of viral particles were added, according to a MOI (number of transducing lentiviral particles per well translate MOI!) and applying the following mathematical formula: (total number of cells per well) X (desired MOI) = total transducing units needed (TU) and (Total TU needed) / (TU/ML) = total of ml of lentiviral particles to add to each well, were used to found the proper amount of particles to add per well. Selection with puromycin (at a final concentration of 2.5 µg/ml) started at day 3 (Table 1).

1.5 Expression analysis by immunoblotting

Cultured HEK293WT and HEK293:TNC cells at 80% confluency in 6 well plate were washed with PBS, lysed in Laemmli buffer and the lysate was boiled at 95°C for 5 min. Protein lysates and purified TNC used as a loading control (100µg) were separated in a (6% sodium dodecylsulfate (SDS) gel (40% acrylamide/bis, 10% SDS, 1.5 M Tris-HCl [pH 8.8], N, N, N', N'-tetramethylethylenediamine (TEMED), 10% ammonium persulfate [APS] and distilled deionized water [ddH2O]) with a 4% stacking gel (40% acrylamide/bis, 10% SDS, 0,5 M Tris-HCl [pH 6.8], TEMED, 10% APS and ddH2O)) 6% PAGE SDS gel and transferred onto nitrocellulose membranes (Invitrogen© products, aisley PA4 9RF, UK). After blocking with 5% milk (Bio-rad) in PBS with 0.1% Tween 20 (PBS–T), the membrane was incubated with primary antibody against TNC (TNC1.2 Antibody in Table 2, dilution 1:1000, in PBS-T and 1:10 horse serum) overnight at 4°C, followed by 3 washes with PBS–T and incubation with an anti-rabbit IgG secondary antibody conjugated with horseradish peroxidase (polyclonal donkey, dilution 1:1000, Amersham GE Healthcare©) in PBS–T with 1.5% milk for 1 h at room temperature followed by 3 washes with PBS–T. Immunocomplexes were revealed with ECL Western blotting detection reagent on autoradiography film (Amersham GE Healthcare©). Prestained (Two Colors) Protein Ladder (10-170Kda) (Euromedex) was used.

2. Tumor material

2.1 Human colorectal carcinoma

The use of a human tissue collection was approved by the *CCPPRB d'Alsace N◦1 Strasbourg* ethics committee. Tissue from 10 human CRC and normal adjacent mucosa located more than 5 cm away were obtained from surgical specimens at the Department of Visceral Surgery (*Hôpitaux Universitaires de Strasbourg*), under the institutional review of the French ethics committee.

2.2 Human insulinoma

Seven human insulinomas and 2 samples from normal pancreas were obtained from the *Laboratoire de Biochimie et Biologie Moléculaire Plateforme Hospitalière de Génétique Moléculaire des Cancers CHU Strasbourg-Hautepierre*. Insulinomas are rare pancreatic neuroendocrine tumors and are the most common types of tumors arising from the islets of Langerhans cells. Estimates of malignancy (metastases) range from 5% to 30% (Metz et al., 2008). One of the obtained samples was malignant.

3. Animals

3.1 RT2 and RT2/TNC insulinoma mice

The well characterized Rip1Tag2 (RT2) transgenic tumor mouse model (Hanahan, 1985), was established by using the pancreas-specific rat insulin II promoter (Rip1) to induce the expression of the oncogenic Simian Virus-40 (SV40) large tumor antigen (Tag) in β-cells of the pancreatic islets. SV40Tag induces malignant transformation of β-cell with overt tumors over a period of 10-14 weeks. These mice reproducibly develop β-cell tumors in a multistage tumorigenic pathway involving islet hyperplasia, angiogenesis, adenoma and carcinoma formation.

Transgenic Rip1TNC mice, with ectopic expression of human TNC in the pancreatic β-cells under the control of the rat insulin promoter were generated in our team (Yundan Jia, PhD

thesis 2008). The human TNC cDNA sequence had been cloned into the Rip1 vector by using the intermediate pcDNA3.1/Hygro(-) vector. The 7.5 kbp sequence of human TNC (accession number X78565.1) harboring a polyadenylation signal was removed from the HxBL.pBS plasmid (Gherzi et al., 1995; Lange et al., 2007) by restriction enzyme cleavage with Not I and Kpn I and transferred into the intermediate pcDNA3.1/Hygro(-) vector (InVitrogen, Carlsbad, CA, USA). The resulting plasmid was cleaved with Xba I and Hind III before ligation downstream of the rat insulin II promoter into the corresponding cleavage sites of the 4.5 kb Rip1 vector containing an intron sequence (Hanahan, 1985). Successful cloning was confirmed by enzymatic restriction analysis and partial sequencing of 1000 base pairs around the start and the stop codon, respectively. Expression and secretion of the transgene product was determined 48h after transient transfection of the expression plasmid into the established RT2 β-tumor cell line bT2 by immunofluorescence for human TNC with the B28.13 antibody. The RipTNC expression vector was used for injection into the pronucleus of fertilized oocytes upon linearization with Sal I according to standard procedures (Labosky et al., 1994), giving rise to transgenic mice with stable transmission and expression of the transgene. Transgenic mice were genotyped by PCR with primers revP hTNC: 5`-GAA AGA CAC CTG CCA ACA GC-3` and RipES/VD: 5`-TAA TGG GAC AAA CAG CAA AG-3). For generation of double-transgenic RT2/TNC mice, single-transgenic RipTNC mice were crossed with RT2 mice (Hanahan, 1985). RT2/TNC and control mice were fed with 5% glucose starting at 10 weeks of age to prolong survival of hypogycemic tumor mice.

3.2 Ras and APC mice

The Apc^{1638N} mice express extremely low levels of C-terminal truncated Apc leading to the stochastic development of 5-6 tumors per mouse at an age of 10 month (Fodde, 1994). In pVillin-$Kras^{V12G}$ mice oncogenic Kras is expressed under the control of a 9 kb-regulatory region of the Villin gene. These mice develop 2-3 tumors after 20 months (Janssen, 2002). Tumor material was a kind gift of Dr. K.-P. Janssen.

3.3 Immunodeficient mice

3.3.1 Nude mice

Nude Nu/Nu Swiss mice were provided at the age of 8 weeks from Charles Rivers (France). These mice are hairless with an albino background. They are immunodeficient due to a defective development of the thymic epithelium. They lack T cells and present partial defects in B cell development. They have normal numbers of functional macrophages, natural killer cells, APC (antigen presenting cells) and normal complement activity.

3.3.2 Rag2KO and Rag2KO/TNCKO mice

Rag2KO mice are unable to produce B and T cells because of a knock out of the recombination activating gene Rag-2 which is necessary for VDJ joining (Chen et al., 1994). These mice are immuno-compromised and can therefore be used for tumor xenograft experiments (Greenberg et al., 2004). Rag2KO/TNCKO mice were generated by breeding of established transgenic TNCKO (Forsberg et al., 1996) and Rag2KO mice (Chen et al., 1994), respectively. Mice were genotyped by PCR with the following primers; TNCKO: TNCup 5`-CTG CCA GGC ATC TTT CTA GC-3`, TNCdown 5`- TTC TGC AGG TTG GAG GCA AC-3`, TNCNeoPA 5`-CTG CTC TTT ACT GAA GGC TC- 3`; Rag2KO: *Fw* (be homogenous with up and down) 5`- TTG GGA GGA CAC TCA CTT GCC AGT-3`, *Rv* 5`-GCA ACA TGT TAT CCA GTA GCC GGT-3`, KO 5`-GCT TCC TCT TGC AAA ACC ACA CTG-3`. Human colorectal carcinoma SW480 cells (ATCC)) were xenografted into the caecum (4 million cells in 100 µl, 2 injections) of 8 week-old Rag2KO/TNCKO mice. Tumors were dissected after 8 weeks and further analyzed as described.

4. Heterotopic and orthotopic xenograft models

4.1 Heterotopic xenograft model

4.1.1 Cell injection

Cells were trypsinised, counted and transferred into phosphate buffer saline (PBS). Four million cells were injected subcutaneously using an insulin syringe (BD Micro-Fine, 324893) on one side into the dorsum. The xenografts were resected approximately one month later.

4.1.2 Injection of human tumor material

Ten fresh human CRC tumors were obtained as described above and transferred into Dulbecco's modified Eagle's medium (DMEM) supplemented with 200 IU/ml penicillin, 200 µg/ml streptomycin and 5 µg/ml fungizone (Gibco, France). After removal of fibrotic and necrotic portions, the remaining cancerous tissue was minced with scissors and centrifuged for 10 min at 800 g. Mice were anaesthetized through isoflurane inhalation (Forane®; Abbott, France) and 0.4 ml of tumour tissue preparation was subcutaneously injected through a 18-gauge needle on both sides into the dorsum. The xenografts were resected when their volume reached approximately 1 cm^3. Grown tumors were resected and serially xenografted in nude mice up to passage 15. It was shown that the all over tumor morphology of the human CRC was recapitulated in the arising tumors derived from subcutaneous xenografts. Moreover, it was observed that the genetic alterations remained the same as in the original cancer (Guenot et al., 2006). Six xenografted human CRC tumors were analysed (collaboration D. Guenot, University of Strasbourg).

4.2 Orthotopic colon cancer xenograft model

After surgical access to the caecum, the organ was isolated with sterile gas and kept moist during the injection of tumor cells with sodium chloride (NaCl 0.9%). Four million cells (SW480) were injected into the caecum wall in 100 µl PBS with an insulin syringe. Between six and eight weeks later, the mice were sacrificed. The time frame is critical since mice can die from intestinal occlusion if the tumor becomes too big (Figure 9).

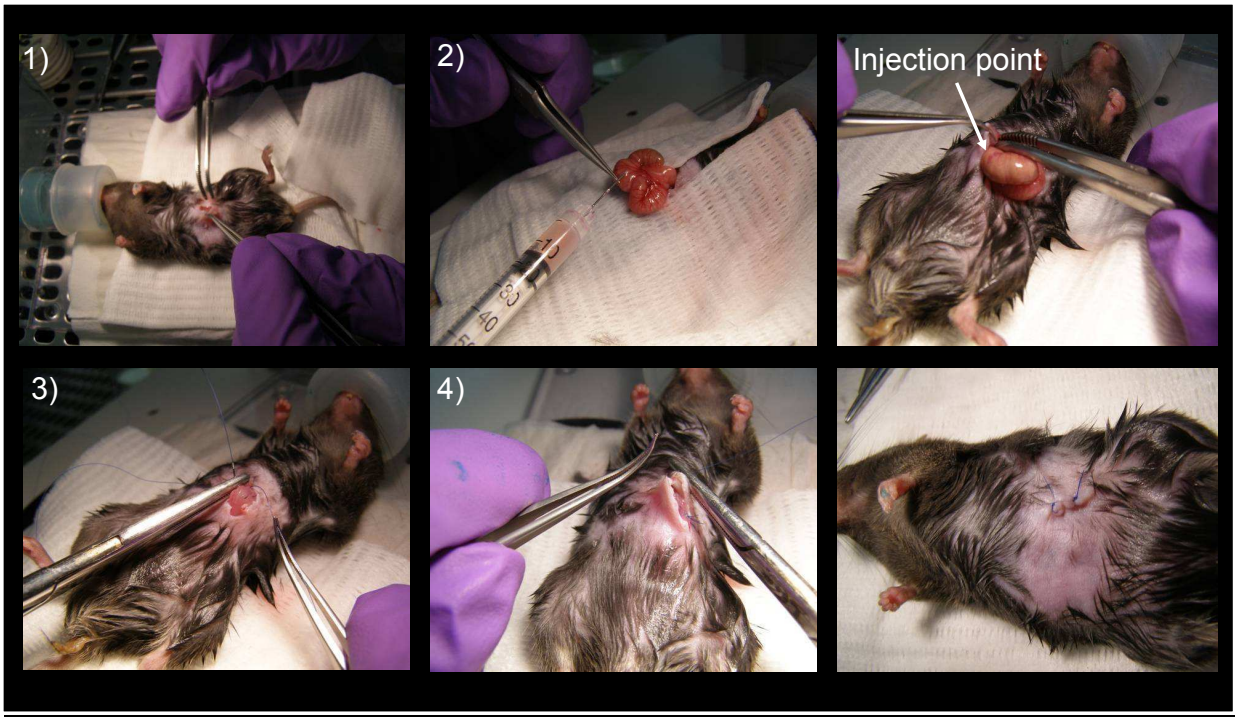

Figure 9: Surgical procedure for orthotopic injection into the caecum. 1 corresponds to the surgical access to the caecum, the second step 2 consists in isolation of the caecum that is kept moist during the experiment. Steps 3 and 4 represent the surgical closure.

5. Live imaging of tumorigenesis

In order to follow tumor growth of orthotopically grafted CRC cells in the living mouse, SW480 cells were labelled with the fluorescent protein "cherry" (pmCherry-N1 Vector) allowing live imaging by the NightOwl apparatus (Berthold Technologies, Germany) (Figure 10)**.**

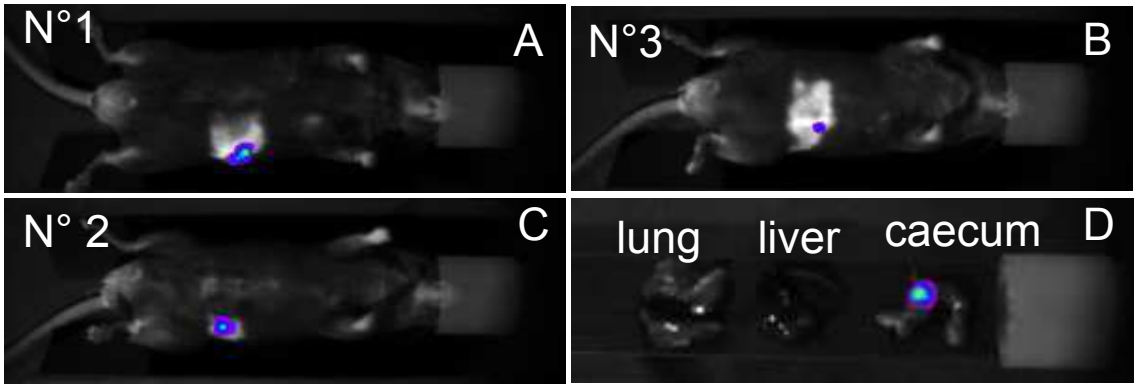

Figure 10 : NightOwl imaging of the caecum tumor from Rag2KO mice *in vivo* and *ex vivo*. (A-C). Correspond to three different mice that had been injected with SW480 cherry cells into the caecum wall three weeks before. **(D)**. Correspond to the different organs of the mice just after organ collection.

One limitation of this technique is that it was not possible to follow tumor growth, since the caecum moved inside the mouse during acquisition. If the caecum is just underneath the muscle layer it is possible to visualize the tumor. Nevertheless, it happens that from one day to the other the caecum is not at the same place and prevents fluorescence acquisition (Figure 11). Another point is that it is difficult to visualize tumors in mice with fur (like the Rag2KO). Therefore, mice need to be shaved before observation, which constitute a stressful procedure for the animals. Therefore live imaging was limited and spared for visualization of tumors before sacrifycing mice or before drug treatment.

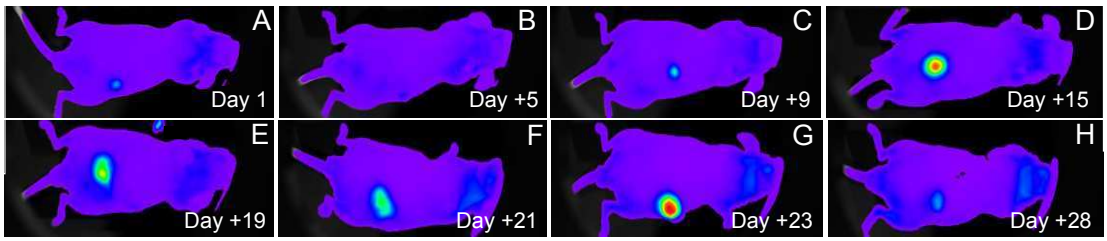

Figure 11 : In vivo fluorescence imaging: characterization of tumor growth in xenografted tumors in Rag2KO mice. (A-H). These images depict an example of *in vivo* imaging with the NightOwl apparatus, in a nude mice with a tumor in the caecum. The different pictures correspond to different days. Note that at day 28, there is less signal, potential due to the position of the caecum inside the abdominal cavity.

6. Experimental design of the anti-angiogenic treatment

Five weeks after orthotopic injection of SW480 tumor cells into the caecum wall, animals were divided into two groups. Animals from the control group received intra-peritoneal (IP) injection of NaCl, whereas animals from the treated group received Bevacizumab (5 mg/kg every 3 days), for a total of six injections. At the end of the treatment, animals were divided into two groups; one half was sacrificed just after the treatment and the rest one week after the end of the treatment.

7. Analysis of tumor volume and tissue preparation

7.1 Tumor volume

After sacrifice of RT2 mice, the tumors were isolated, kept in PBS and measured with a electronic calliper. The tumor diameter was measured and the volume was calculated

according to the mathematic formula: $V= (a^2*b)/2$ with a representing the small diameter and b the large diameter (Tomayko and Reynolds, 1989; Euhus et al., 1986).

7.2 Tissue preparation

7.2.1 Analysis of the vasculature (done by V. Djonov, Bern)

For preparation of vascular casts, the systemic vasculature was perfused with a freshly prepared Mercox solution (Vilene Company, Japan) containing 0.1 ml of accelerator per 5 ml of resin. One hour after perfusion, the pancreas was excised and tissue was removed in 7.5% potassium hydroxide for up to three weeks. After washing, the casts were dehydrated in ethanol and dried in a vacuum dessicator. The samples were then sputtered with gold to a thickness of 10 nm and examined by using a Philips XL-30 SFEG scanning electron microscope (SEM). For transmission electron microscopy (TEM) the samples were fixed in a 2% PFA/2.5% glutaraldehyde solution before further processing in a 1% OsO_4 solution, dehydrated in ethanol and embedded in epoxy resin. After staining with lead citrate and uranyl acetate, tissue sections were analyzed.

7.2.2 Tissue preparation

After mice sacrifice, organs were isolated and washed in 10X PBS, a piece of tumor tissue was cut and put directly into liquid nitrogen for later RNA analysis and stored at -80°C. The rest of the tumor was embedded in the Tissue-Tek® O.C.T. Compound (Sakura Finetek Europe B.V., Zoeterwoude, Netherlands) or was fixed in 4% paraformaldehyde (PFA) and then frozen in Tissue Tek® O.C.T. or embedded into paraffin. Some 4% PFA fixed samples were also placed overnight into sucrose to preserve certain structures and then was embedded into paraffin or Tissue Tek® O.C.T.

8. Analysis of protein expression by tissue staining

The tumor tissue architecture was characterized after staining with hematoxylin and eosin (H&E). Tissue sections were fixed in 4% PFA for 10 minutes, washed in H_2O for 5 min, then stained with Harris hematoxylin for 5 min and rinsed in water. Sections were then incubated in alcohol acid solution for 10 seconds, washed for 15 min, incubated in eosin

(Harris) for 15 seconds and washed again. The slides were mounted in non polymerizing aqueous medium (Swartz and Santi, 1996).

For immunochemical analyses, 7 µm sections were cut with a cryostat (at -20 °C) (LEICA CM3050S). Tissue was either fixed in PFA 4% for 10 minutes at room temperature or not fixed, depending on the antibody, washed 5 times for 5 minutes with PBS and incubated in a blocking solution containing 5% normal donkey serum for 1 hour at room temperature for blocking unspecific antibody binding. Tissue was incubated with the primary antibodies diluted in PBS, 5% normal donkey serum at 4°C overnight.

The following antibodies were used: rabbit against TNC; TNC1.2 (1:200, Lange et al., 2007), mouse antibodies B28.13 (1:50, Wagner et al., 2003), rat antibody against murine TNC (MTn12, 1:100, (Aufderheide and Ekblom, 1988), pan laminin-antibody recognizing all laminin isoforms, (1:2000, Simo et al., 1991), α smooth muscle actin αSMA) (1:400, Sigma), laminin α5 (1:400, Miner et al., 1997). For integrins, thrombospondin 1 (TSP1) and osteopontin (OPN) (details in Caroline Spenle, PhD thesis, 2010). For the antibody raised against TNC see Table 2. For fibronectin 2.2 (1:200, home made), EDA (recognizes the extra domain A from cellular fibronectin (c-fibronectin), gift from Ellen Van Obberghen-Schilling (ffrench-Constant and Hynes, 1989, Peters et al., 1996, White et al., 2008) vimentin (1:200, Santa Cruz Biotechnology), Mts1 (also called FSP1/ S100A4, 1:200 Ambartsumian et al., 1996) CD31 (1:50, BD Pharmingen, Newman, 1997), the guineapig antibody against insulin (1:200, DakoCytomation) and biotinylated rat anti-mouse TER119 (1:50, Caltag laboratories, Kina et al., 2000), rabbit anti-Lyve-1 (1/100, Reliatech, Carriera et al., 2003) rabbit anti-NG2 (1:200, Chemicon, Stallcup and Huang, 2008), rat against mouse F4/80 (1:50, AbD, Wohl et al., 2010), CD45 (1/20, BD pharmigen). Phospho-histone-3 (PH3) (1:200, Upstate). After incubation with the primary antibodies, sections were washed with PBS 5 times for 5 minutes, then incubated for 2 hours at room temperature with secondary antibodies produced in donkey, labelled with different fluorophores and specific to rabbit, rat and mouse immunoglobulins (Cy3 dilution 1:2000,

Dylight 488 dilution 1:1600, FITC 1:400, Cy5 dilution 1:1600, from Jackson ImmunoResearch Inc.©) and diluted in PBS containing 5% normal donkey serum. Sections were washed again with PBS 5 times for 5 minutes, then nuclei were stained with 4',6-diamidino-2-phenylindole (DAPI, 0.2 µg/ml) for 10 min at room temperature. Finally after 5 washes in 1X PBS, the slides were mounted with a polymerization medium (FluorSave™Reagent, CALBIOCHEM) under coverslips and stored at 4°C until analysis.

Table 2: Description of conditions for utilization of TNC antibodies.

	TNC1.2 (1:200)		TNC1.2 (1:400)		B28.13 (1:50)		MTn12 (1:10)	
	P	C	P	C	P	C	P	C
Human normal intestinal mucosa	+	+	+	+	+	+	-	-
Human colon cancer	+	+	+	+	+	+	-	-
Human colon cancer xenograft	+	+	+	+	+	+	+	+
Murine normal intestinal mucosa	Nd	+	Nd	-	Nd	Nd	Nd	+
RT2 insulinoma	Nd	+	Nd	+	Nd	Nd	Nd	+
RT2/TNC insulinoma	Nd	+	Nd	+	Nd	Nd	Nd	+
Pancreas TNCKO	Nd	-	Nd	-	Nd	-	-	-
Colon TNCKO	Nd	-	Nd	-	Nd	-	-	-

P, paraffin embedded tissue; C, cryopreserved tissue (without fixation), + means that the Ab is specifically recognizing TNC and – that it is not working, nd for not determined.

9. Tumor analysis: imaging and quantification

Tissue sections were examined with a Zeiss Apotome Imager Z2 fluorescence microscope equipped with fluorescence filters and a CCD camera. Staining was quantitatively evaluated by using the ImageJ v1.45e software (NIH). Briefly, images were converted to 8-bit pictures, and parameters such as brightness and contrast were adjusted. The same settings were used for all of the pictures by using the threshold function. The total areas of human TNC, mouse CD31, mouse NG2 and αSMA stainings were obtained by randomly choosing 3 to 5 fields for image acquisition on 1 to 3 sections per tumor. Signal intensity was calculated on a total of 15 pictures/tumor. The fraction of Ki67 positive cells amongst all cells was expressed in percentage of all nuclei stained by DAPI. Data were pooled for each tumor and are presented as mean +/- S.E.M.

10. Analysis of candidate gene expression by qRT-PCR

RNA isolation was performed on pieces of tumor tissue with the NucleoSpin® RNA II Purification Kit (Macherey-Nagel) according to the manufacturer's instructions. Specific primers for each gene were used. For normalization of gene expression mouse and human GAPDH and mouse porphobilinogen deaminase (PBDG) specific primers from Qiagen© were used (Gubin and Miller, 2001). For SYBR Green real-time RT-PCR, a total of 1 µg of RNA was reverse transcribed into cDNA by using the High capacity cDNA Reverse transcription kit (Applied Biosystem©) following the manufacturer's protocol. Samples were analyzed in 10 µl reactions using 2µl cDNA as template and using SYBR green (Applied Biosystems, Warrington, UK) or Taqman reaction mixtures (Applied Biosystems, Fostercity, CA, USA. Used primer sequences are listed in Table 3.

Table 3: Summary table of the different primers used for qPCR analysis

Gene	Forward primer	Reverse primer
CD31 human	ATTGCAGTGGTTATCATCGGAGTG	CTCGTTGTTGGAGTTCAGAAGTGG
CD31 mouse	GCTGGTGCTCTATGCAAGC	ATGGATGCTGTTGATGGTGA
DKK1 human	GACCATTGACAACTACCAGCCG	TACTCATCAGTGCCGCACTCCT
DKK1 mouse	CCGGGAACTACTGCAAAAAT	CCAAGGTTTTCAATGATGCTT
Sox4 human	CAGCAAGAGAAACTGTGTGTGA	AAGAGCGTGCAAGAACTAGAGA
Slug human	GAAAAGCACATTGCATCTTTTCT	TGTTCCTTTGGTTGAAATGGT
TNC human	CCTTGCTGTAGAGGTCGTCA	CCAACCTCAGACACGGCTA
TNC mouse	GCGCAGACACACACCCTAGC	TTTCCAGGTCGGGAAAAGCA
PBGD human	QT00014462 (Qiagen)	
PBGD mouse	QT00494130 (Qiagen)	
GAPDH human	ATCTTCTTTTGCGTCGCCAG	AATCCGTTGACTCCGACCTTC

11. Statistical analysis

Statistical analysis was done by using the GraphPad Prism program version 5.00. For significance of an association (contingency) Fisher's exact test or chi-square test were applied (tumor staging, gene expression). Statistical differences of events were analyzed by unpaired t-test (Gaussian distribution) or nonparametric Mann-Whitney test (no Gaussian distribution). Gaussian data sets with different variances were analyzed by unpaired t-test with Welch's correction. p-values < 0.05 were considered as statistically significant.

12. Analysis of liver metastasis

Livers of tumor bearing nude mice that had been treated with Bevacizumab or control solution were analysed with the NightOwl apparatus upon extraction of the organ. Since the cells are cherry positive, the NightOwl appartus detected a fluorescent signal.

Results

RESULTS

Paper contributions

Here, before starting to go further in the results that were obtained, I would like to precise my contribution to the manuscript entitled "In human and mice Tenascin-C matrix channel guide tumor angiogenesis and promote metastasis through activation of Wnt signalling". This paper was separated in two papers now, the first one is entitled "Tenascin-C promotes tumor angiogenesis and metastasis through repression of dickkopf-1" (Annex1) and where I am a co-first author and a second one concerning the conduits, where I am also a co-first-author (manuscript in draft stage).

I optimized the staining protocols for each Ab (more than 20) and in particular for three TNC Ab. Next, I characterized expression of several ECM molecules and the presence of tumor associated cells such CAF, endothelial cells and immune cells. I had analyzed ECM expression and organization and tumor associated cells in human insulinomas, CRC and corresponding heterotopic xenograft models. I had engineered cancer cells to ectopically express a fluorescent protein or DKK1 or a TNC knock down. I had established the orthotopic xenograft model in Rag2KO/TNCKO, Rag2KO and nude mice and had designed and performed the study with Bevacizumab treatment.

I also contributed to a review article entitled "Fibronectin and tenascin-C: accomplices in vascular morphogenesis during development and tumor growth" (Annex 2), by providing immunostaining results and ideas.

I also had contributed to a teaching program for high school students. This was a new operation to promote science in school. In this program I had designed PCR experiments and learned how to teach this information to the students. I got the chance to present this work and the concept, in a paper entitled ""'OpenLAB'': A 2-Hour PCR-Based Practical for High School Students" (Annex4), where I am a first co-author with 8 other authors.

PART A: CHARACTERIZATION OF THE EXTRACELLULAR MATRIX AND CELLULAR COMPONENTS OF THE TUMOR MICROENVIRONMENT IN A MURINE TUMOR MODEL AND IN HUMAN CANCER TISSUE

1. Description of the neuroendocrine Rip1Tag2 model with ectopic TNC expression

1.1 Tumor progression

Double transgenic mice with an ectopic expression of human TNC had been generated in the laboratory and were available for analysis (Y. Jia, PhD thesis 2008, Saupe, Gasser, Jia et al., in preparation, Annex1). First, in these mice a potential effect of TNC on tumor onset has been addressed. The diameter of Langerhans islet was measured at histological level as readout for the islet size, which correlates with the tumorigenic state (Hanahan, 1985). In 10 week old mice, this analysis revealed that the number of angiogenic and tumorigenic islets (> 0.5 mm) was significantly higher in RT2/TNC (45) compared to RT2 (28) mice (Figure 12A). At 12 weeks there was no difference in tumor number (Figure 12B) nor tumor volume (Figure 12C) detectable between genotypes at macroscopical level. Analysis of tumor progression had revealed an increase in carcinomas (more invasive) in RT2/TNC mice over that in RT2 controls (Saupe, Gasser, Jia et al., in preparation, Annex1).

RT2 mice usually did not exibit metastasis (Hanahan, 1985). Therefore, we determined potentially arising micrometastasis in various organs of 12 to 14 week old tumor bearing mice by IF staining for insulin. The presence of micrometastasis was visualized and quantified on section by H&E and insulin IF staining. This was possible since the SV40 T-antigen is expressed under the control of the rat insulin promoter (see Material and Methods). No differences in liver metastasis were noticed between genotypes, whereas micrometastasis in the lung were enhanced in double transgenic mice over control mice (Saupe, Gasser, Jia et al., in preparation, Annex1).

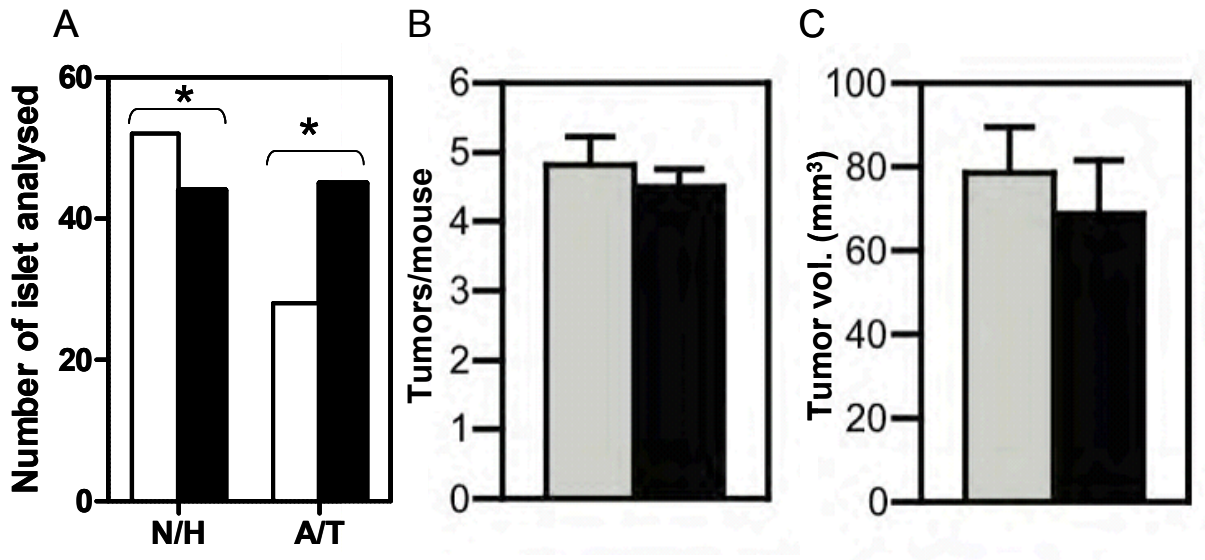

Figure 12: Tumor characterization in tumors from 10 and 12 week old RT2 and RT2/TNC mice. (A). Graph representing the number of analysed RT2 versus RT2/TNC islets in different classes; N/H and A/T. N, H, A and T mean normal, hyperplastic, angiogenic and tumorigenic islets. (p value=0.0449, Fisher test) (adapted from Y. Jia results). **(B-C)**. All macroscopical visible tumors from 12 week old mice were counted **(B)** and the tumor volume was determined **(C)** with the formula $V=4/3\pi(d/2)^3$, (d=diameter in mm). RT2 (N = 33 mice, n = 156 tumors), RT2/TNC (N = 26; n = 117), not significant.

1.2 Tumor growth

In RT2/TNC tumors it was observed that proliferation is enhanced (Saupe, Gasser, Jia et al., in preparation, Annex1). Moreover, glioblastoma cells cultivated on a TNC substratum enhanced proliferation (Huang et al., 2001). Therefore, it was determined whether TNC potentially triggers enhanced proliferation in RT2 tumors. Thus, tumor tissue from RT2 and RT2/TNC tumors was stained for TNC together with an antibody recognizing PH3 (Figure 13). It was observed that the cells with PH3 positive nuclei were adjacent or very close to the TNC signal. This observation supported the possibility that a contact with TNC had enhanced proliferation of tumor cells in this *in vivo* setting. Quantification of the PH3 signal revealed that proliferation is 1.7-fold higher in RT2/TNC tumors than in control RT2 tumors (Saupe, Gasser, Jia et al., in preparation, Annex1) suggesting that an increased contact with TNC in RT2/TNC tumor stroma had triggered tumor cell proliferation.

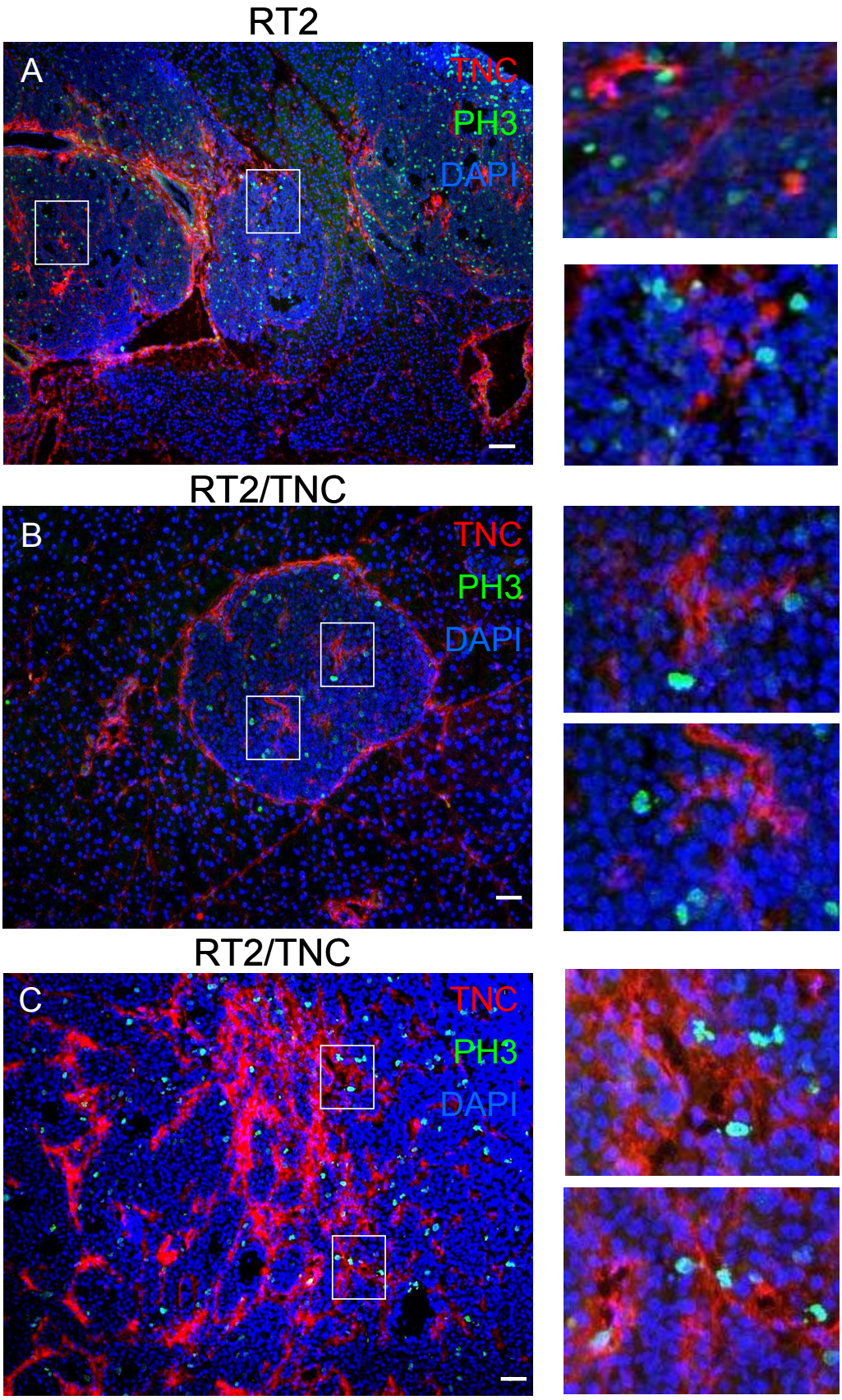

Figure 13: Proliferation in the RT2 tumors. (A-C). Immunostaing of proliferative cells (PH3) and total TNC (red) in RT2 **(A)** and in RT2/TNC **(B** and **C).** Enlargement of white box. Scale bars 50 µm.

1.3 Tumor angiogenesis

The role of TNC during tumor angiogenesis was analyzed by immunostaining (Figure 14A) specific for the endothelial cell marker CD31 followed by quantification of positive events by using the Image J software (Figure 14B). The CD31 counted events turned out to be significantly different in tumors of RT2/TNC mice than in tumors of RT2 control, 2.2-fold and 2.6-fold increased in RT2/TNC at 10 and 12 weeks respectively (Figure 14 B-C). These results suggested that ectopically expressed TNC promoted angiogenesis in these spontaneously arising tumors.

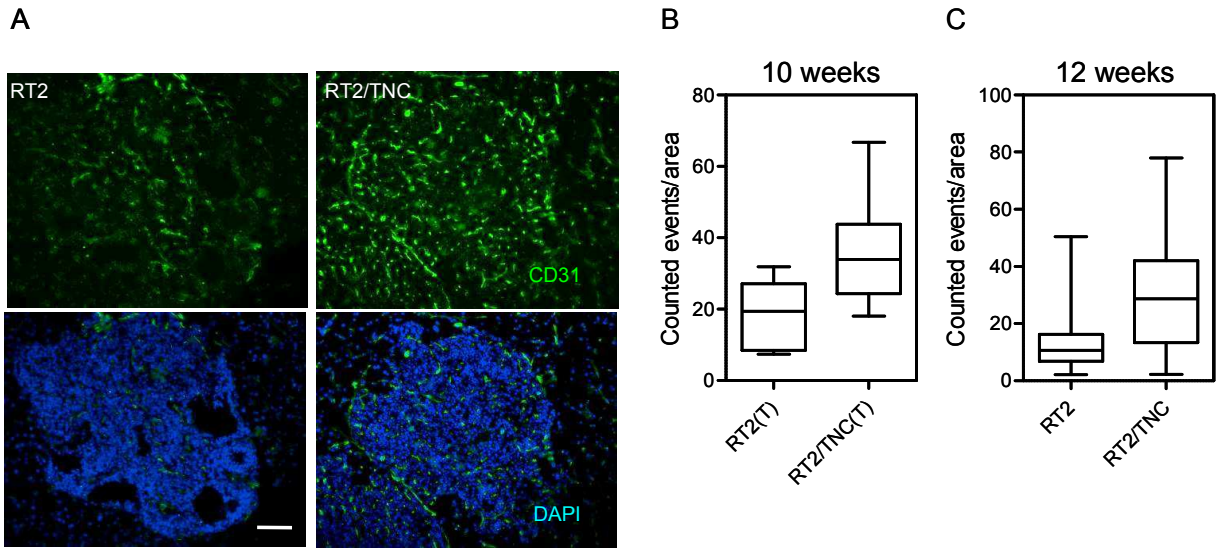

Figure 14: Overexpressed TNC promotes tumor angiogenesis in RT2 insulinoma. (A). Tissue staining of CD31 and quantification **(B-C)** of tumors from 10 **(B)** and 12 **(C)** week old RT2 and RT2/TNC mice. Relative expression was determined as event per mm^2. Number of samples; 10 weeks, RT2 (N = 5 mice, n = 13 tumors), RT2/TNC (N = 7, n = 19); 1.92-fold, S.E.M, p = 0.0006, unpaired t-test; 12 weeks, RT2 (N = 6, n = 34, 203 data points (fields)) and RT2/TNC (N = 4, n = 17, 106 data points (fields)), 2.27-fold, S.E.M., p < 0.0001, Mann Whitney test. Scale bar 100 µm.

By IF analysis of CD31 and TNC we observed that blood vessels were partially covered by TNC. It was also noticed that an aligned CD31 positive signal was interrupted and, an adjacent TNC signal appeared to provide a bridge between the two separated CD31 signals (Figure 15). This is reminiscent of endothelial tubulogenesis where TNC potentially served as scaffold. Moreover, it was also observed that all CD31 positive signal was adjacent to a TNC signal suggesting that TNC played an important role in angiogenesis. This should be further addressed in RT2 tumors lacking TNC to determine whether TNC is necessary in proper endothelial tubulogenesis.

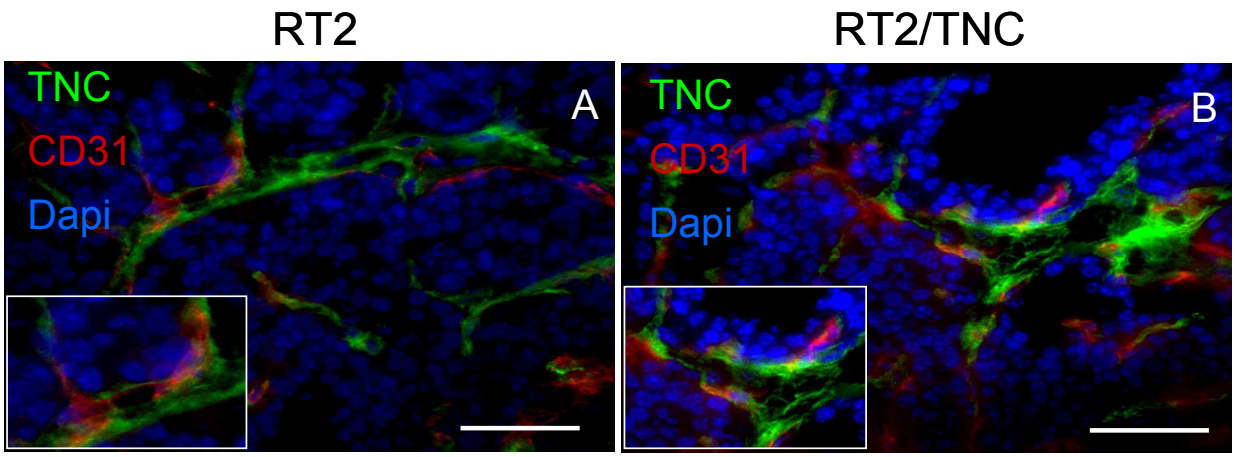

Figure 15: Blood vessel characterization in RT2 and RT2/TNC tumors. Representative pictures of endothelial cells stained with a specific antibody (CD31, in red) and TNC (in green) in RT2 **(A)** and in RT2/TNC **(B)**. Scale bars 20 µm**.**

1.4 Vessel anatomy

In collaboration with V. Djonov (University Bern, Switzerland) the vessel anatomy of RT2/TNC and control RT2 tumors was further analysed by SEM and TEM (see Material and Methods). The vasculature observed in RT2/TNC tumors was highly branched and leaky as indicated by Mercox escaping the vessels at multiple sites (Figure 16B) contrasting with the RT2 vasculature which did not exhibit these abnormalities (Figure 16A and C). Vessels seemed clearly aberrant and more disorganized in RT2/TNC and sometimes enlarged (Figure 16D-E). This raised the question whether vessel organization as e.g. lining by a basement membrane and coverage by pericytes was potentially different in RT2/TNC tumors. Therefore NG2 immunostaining was performed and revealed a strong staining of NG2 in RT2 tumors. Indeed pericytes were found all over the tumor in RT2 mice (Figure 17). A quantification of this result will be done in the future.

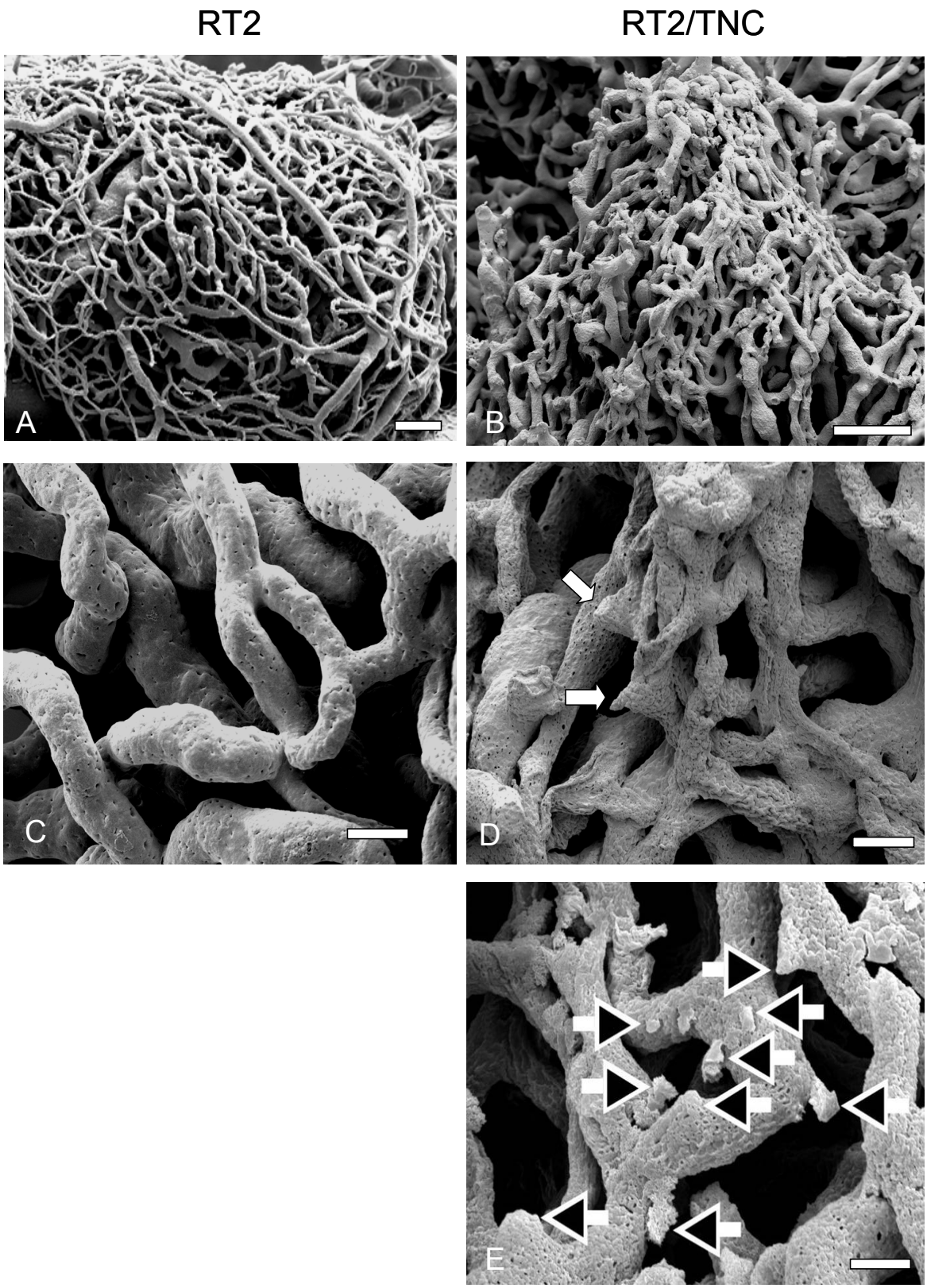

Figure 16: Anatomy of blood vessels in RT2 tumors. (A-E). Reproduction of the vasculature in tumors of 12 week old RT2 (**A** and **C**) and RT2/TNC (**B**, **D** and **E**) mice in corrosion casts upon Mercox perfusion. Arrows point at the leakage of vessels or branching points. Scale bars 50µm (**A** and **B**), 20 µm (**C**, **D** and **E**).

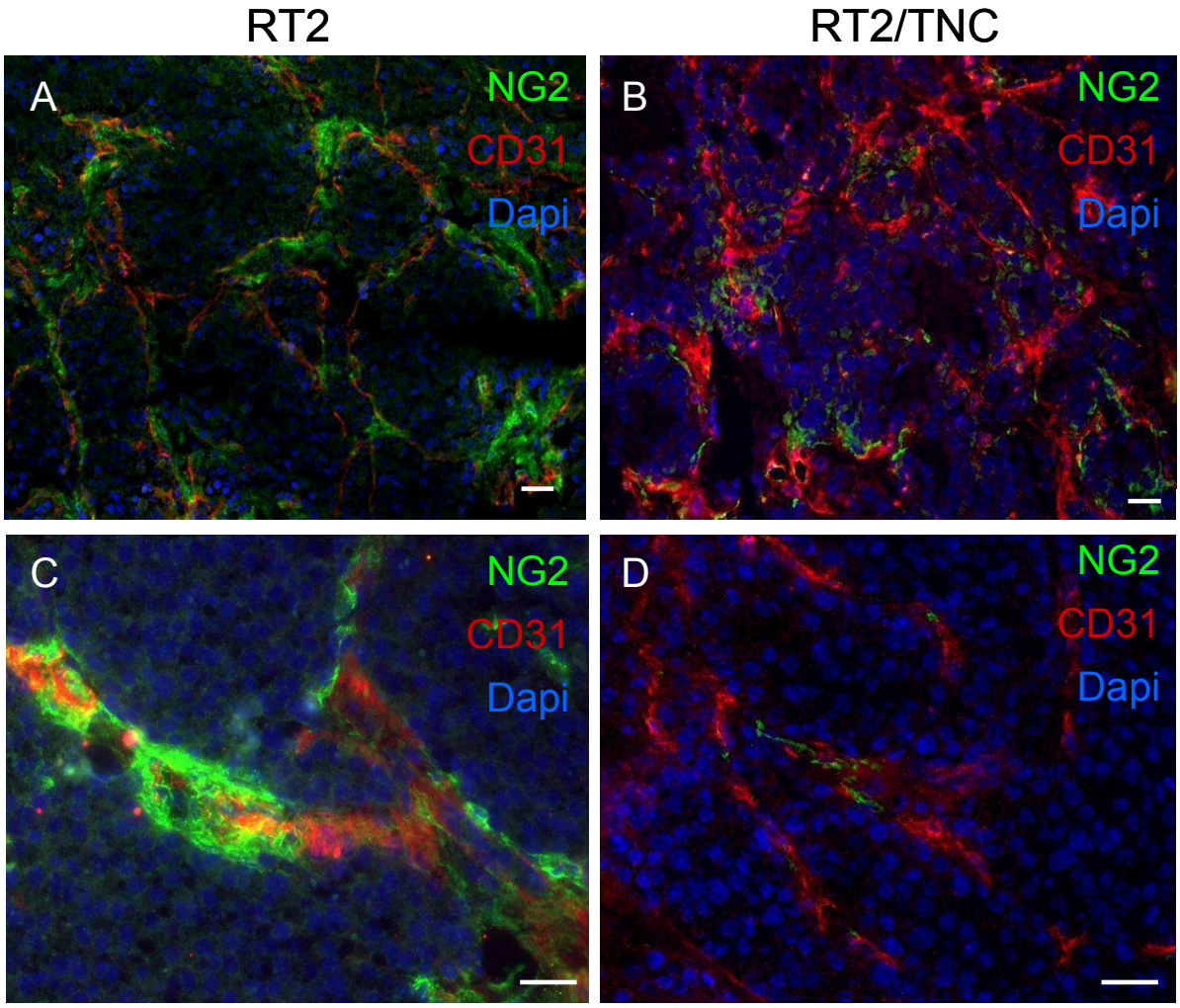

Figure 17: Tumor associated pericyte coverage of vessels in RT2 and RT2/TNC tumors. (A-D). Distribution of pericytes (NG2, green) and endothelia cells (CD31, red)) in tumors of 12 week old RT2 (**A** and **C**) and RT2/TNC (**B** and **D**) mice. Note that in RT2 vessels (**A-C)** the coverage by NG2 appears to be more extensive compared to that in RT2/TNC vessels (**B-D**). Scale bars 20 µm.

Subsequently a closer analysis of the vasculature was performed by V. Djonov on tumors from both genotypes by TEM (Figure 18). This analysis revealed that blood vessels in RT2 tumors exhibited a thin BM lining (Figure 18A). In contrast, some vessels in RT2/TNC tumors looked very different and exhibited a rough apical surface where matrix appeared to leak into the lumen (Figure 18 B-F). Moreover, atypical vessels were lined by a thick ECM layer and attached tumor cells (AtTu) that were characterized by few granular vesicles which is in contrast to most tumor cells that exhibited many of these vesicles. These atypical vessels will be coined here as conduits (see below) and were partially filled with non-fibrillar ECM material, fibroblasts (white asterisk), tumor cells (V. Djonov, personal

communication) and erythrocytes (Figure 18C and E). It was also observed that these conduits can be connected to regular blood vessels lined by BM and endothelial cells as shown in Figure 18D. Proof of erythrocytes inside TNC– rich vessels was provided by an adjacent TNC signal with that for the erythrocyte specific marker glycophorin (TER119) (Figure 19).

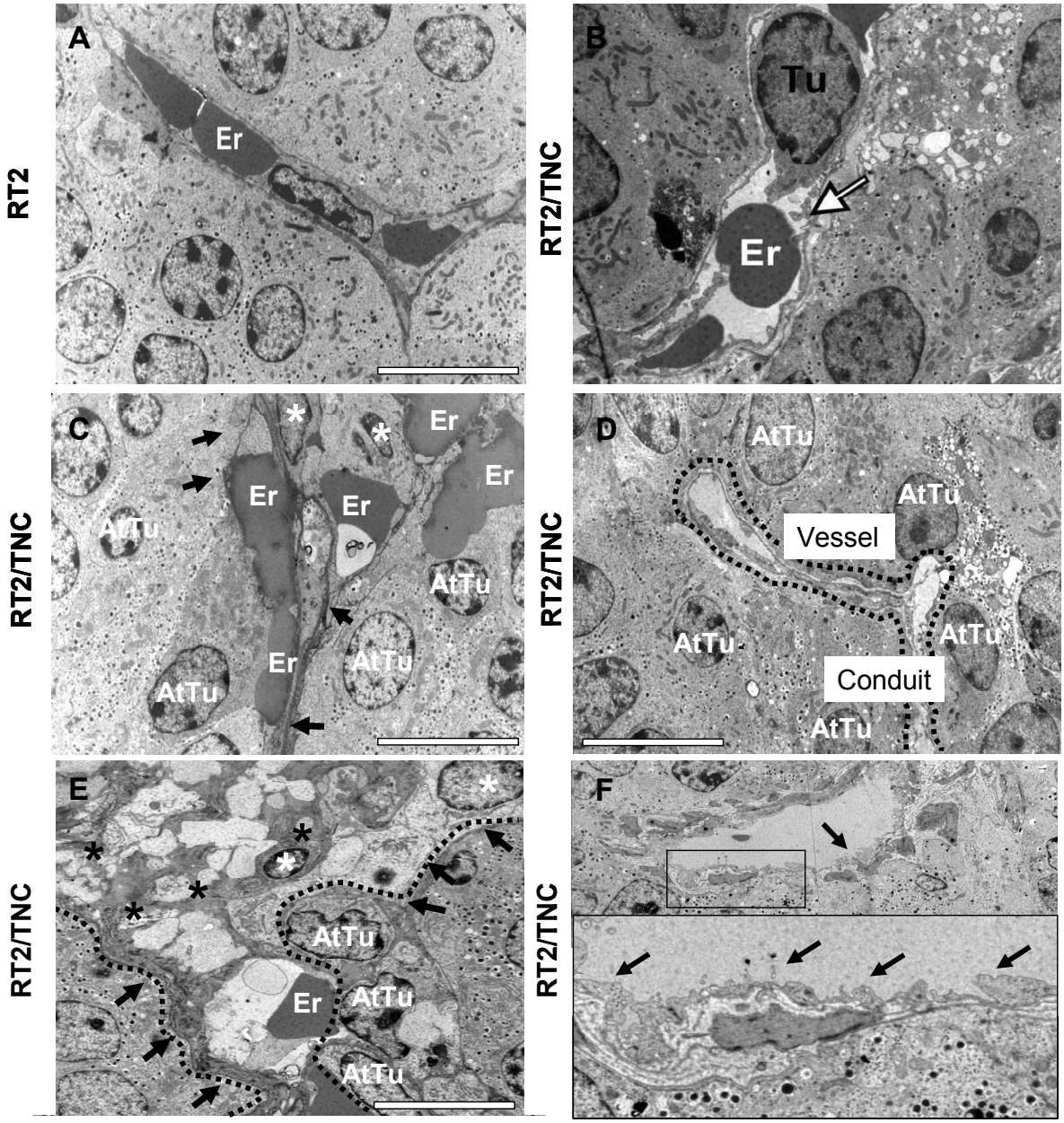

Figure 18: Vessel anatomy in RT2 and RT2/TNC tumors. (A-F). TEM pictures of vessels in RT2 **(A)** RT2/TNC tumor **(B-F)**. Tumor associated vessel containing erythrocytes (Er) in RT2 **(A)** and in RT2/TNC tumors (**B** and **C),** white and black arrows depict matrix deposition at the rim of the tumor. **(D)**. Continuum between a blood vessel characterized by a basement membrane, and a lumen within the conduit that exhibits lining by AtTu but not endothelial cell nor a BM. (**E-F)**. Black arrows, matrix deposits at the rim of the conduit that is lined by attached tumor cells (AtTu). Asterisks: nucleated cells within the tube. Note the presence of erythrocytes. Scale bars 10 µm **(A-F).**

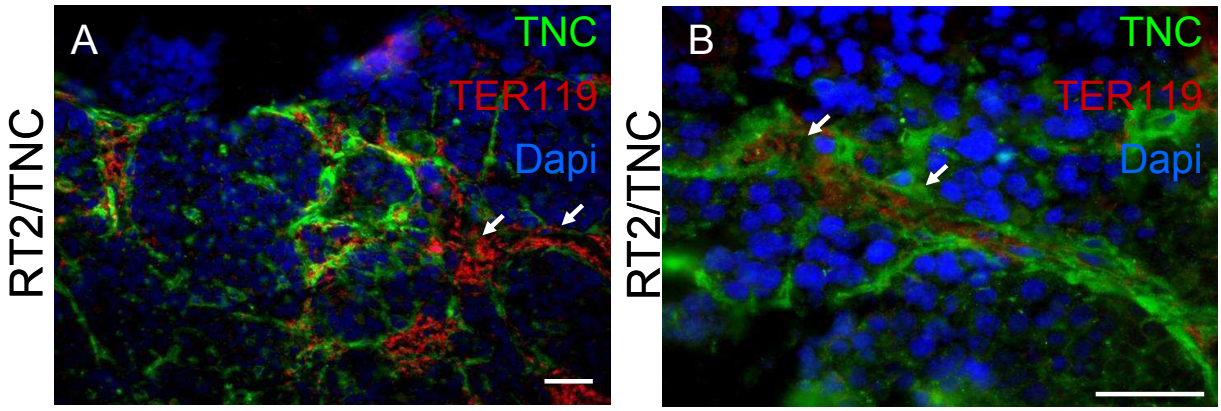

Figure 19: TNC expression in vessels of RT2/TNC tumors. **(A-B).** Immunostaining of vessel in a RT2/TNC tumor containing erythrocytes, pointed at by a white arrow. Scale bars 50 µm **(A),** 20 µm **(B)**

1.5 Expression and organization of TNC and other ECM molecules

The TNC1.2 antibody recognizes both human and mouse TNC, thus expression of total TNC was determined in RT2/TNC tumors by IF and was compared to that of endogenous TNC in RT2 tumors. Although in RT2/TNC tumors transgenic TNC should be expressed by all insulinoma cells this was not the case. In contrast to a homogenous TNC expression by all insulinoma cells, tumors of RT2/TNC mice displayed a similar expression pattern where TNC is present in conduits and other fibrillar structures ranging from 2.5 to 25 µm and more (Figure 20B, D and G).

TNC was surrounding blood vessels and, was also organized into CD31 negative tracks (Figure 15). By perfusion analysis and TEM we provided evidence that TNC tracks are connected to the circulation (Saupe, Gasser, Jia et al., in preparation). It was previously shown that endothelial cells (Zagzag et al., 1996) as well as endothelial precursor cells (Ballard et al., 2006) used the TNC matrix as guiding cue. In addition, tubular matrix channels composed of TNC, FN and procollagen (proColl), negative for CD31 and Lyve-1 (specific marker for lymphendothelial cells), were described earlier and their appearance was linked to metastasis in melanoma (Kaariainen et al., 2006). We decided to referTNC tracks that are not in association with CD31 as TNC conduits.

Since LM and TNC were expressed in melanoma channels (Kaariainen et al., 2006) and were highly expressed in the tumor specific conduits (De Arcangelis et al., 2001; Chiquet-Ehrismann and Chiquet, 2003), we asked the question whether LM was present in the TNC conduits of RT2 tumors. Therefore, tumor tissue of both genotypes was stained for TNC and LM. We found that both molecules formed conduits with discrete matrix layers that did not intermingle but were adjacent in tumors of both genotypes (Figure 20A and B). By confocal microscopy it was seen that these conduits formed hollow tubes about 13 to 15 µm in diameter (determined by confocal microscopy) that eventually contained nucleated cells (Figure 20E-G). It was noteworthy that TNC was mainly present in the core region of these conduits enwrapped by LM (Figure 20A).

TNC positive conduits were also positive for laminin γ2 and α5, two LM chains that previously had been seen to be expressed in melanoma conduits and in vasculogenic mimicry (Figure 20B-C). In some places TNC and laminins did not form discrete layers but an apparently unorganized matrix where both molecules were still in close vicinity to each other (Figure 20D). These observations suggest that both ECM molecules assemble into matrix conduits with an eventual lumen and cells inside.

In order to characterize the composition of the TNC rich conduits and to determine whether other ECM molecules are expressed and potentially form matrices together with TNC, tumor tissue was stained with specific antibodies for TNC together with those for collagen IV (Coll IV), collagen V (Coll V), FN, osteopontin (OPN) and thrombospondin-1 (TSP1). This analysis revealed that all analyzed ECM molecules were expressed in the tumor tissue, were partially coexpressed with TNC and accumulated into matrices that resembled the described TNC conduits and vessel like structures (Figure 21 and Figure 22). In the IF analysis on serial sections of the tumor tissue (Figure 21) it can be seen that the TNC matrix conduits contained FN, Coll IV and Coll V altogether, suggesting that these conduits exhibit a complex organization where several ECM molecules are present together with TNC.

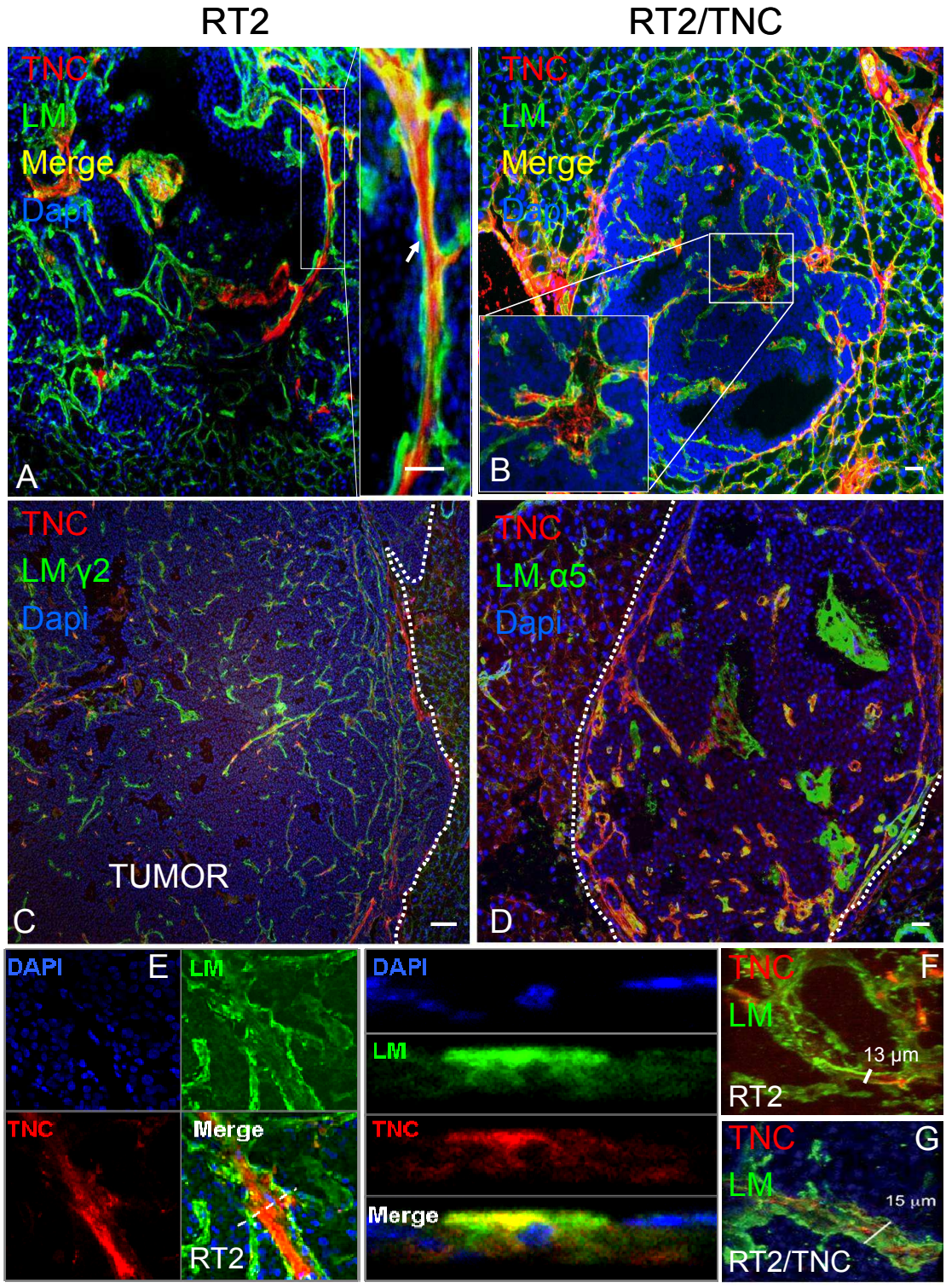

Figure 20: Organization of TNC matrix conduits in tumors of 12 week old RT2 and RT2/TNC mice. Immunostainings of tissue sections of RT2 **(A** and **C)** and RT2/TNC tumors **(B** and **D)** pancreas sections with the indicated antibodies. Arrows: nucleated cells, TNC and LM tubular **(A-B)**. White boxes, TNC-filled and LM-lined matrix track in the center of a tumor. **(C-D)**. γ2 (green, **C**) and α5 (green, **D**) LM composed conduit-like structures with TNC (red), which traversed the tumor. **(E-G).** Confocal pictures of ECM molecule-enriched conduits in RT2 **(E-F)** and RT2/TNC **(G)** tumors. **(E)**. Co-staining of LM (green) and TNC (red) observed by confocal microscopy (J. Mutterer, IBMP, Strasbourg). Z-stack was done through the conduit, where the white line was defined. Note the presence of a nucleated cell (blue) inside the conduit. **(F-G)**. 3D reconstruction of a conduit stained for LM (green) and TNC (red) in a RT2 **(F)** and RT2/TNC **(G)** tumor. Diameters of these conduits are 13 µm for RT2 and 15 µm for RT2/TNC tumors. Scale bars 50 µm **(C)**, 25 µm **(A)**, 20 µm **(B** and **D)** (Caroline Spenle, PhD Thesis, 2010).

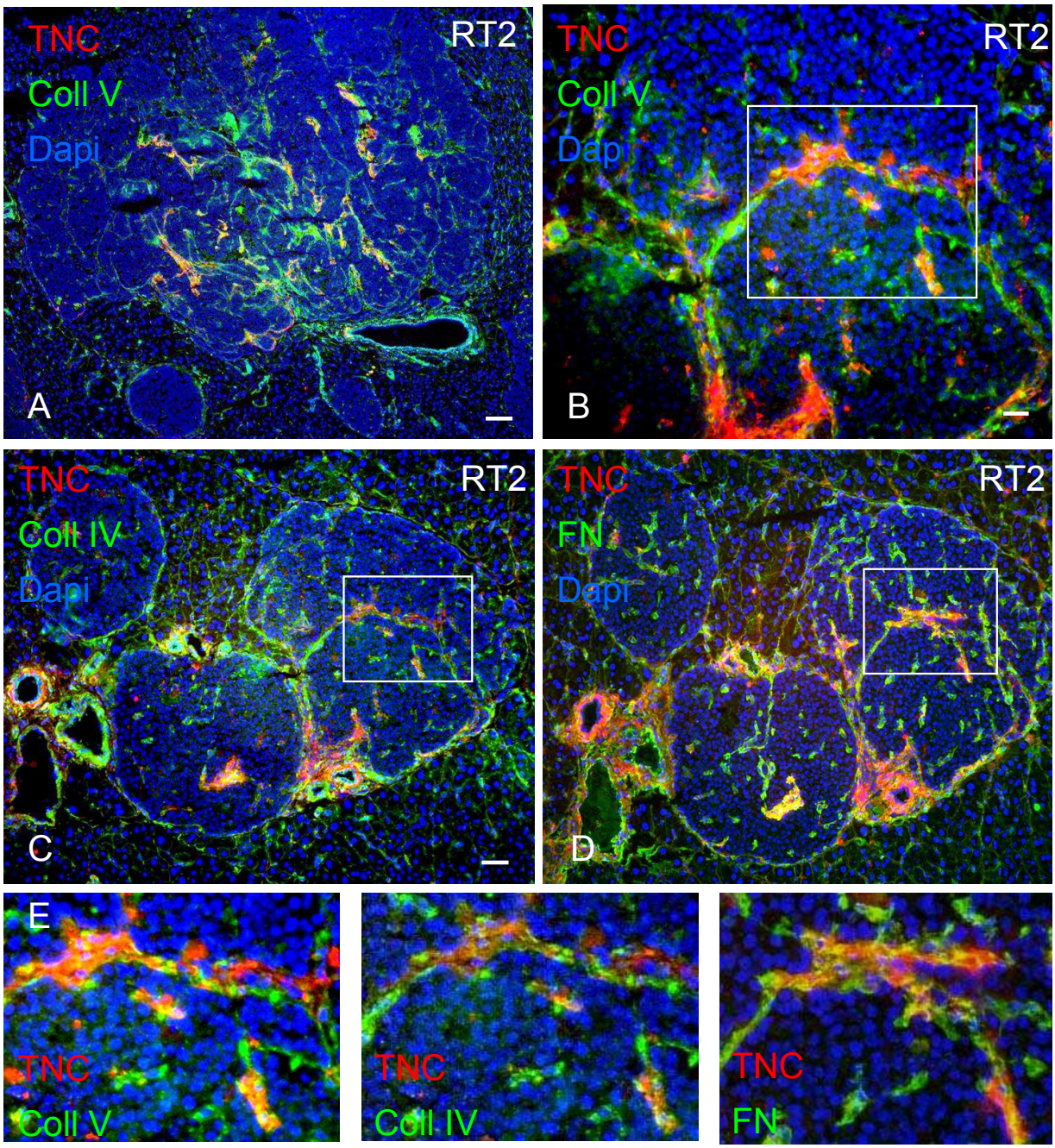

Figure 21: Co-alignment of TNC with other ECM molecules. Representative pictures of the indicated molecules in RT2 tumors on adjacent slides **(A-D),** enlargement of white box **(E).** TNC is organized into conduits together with FN **(D),** coll IV **(C)** and V **(A-B)** Scale bars 50 µm (**A**, **C** and **D**), 20 µm **(B)**.

OPN and TSP1 have been suggested to modulate the tumor phenotype by affecting cell migration, survival and angiogenesis (Liaw and Crawford 1999). Upon analysis of OPN and TSP1 expression by IF it was observed that both molecules were expressed in RT2 tumors in close vicinity to TNC (Figure 22 A-B). Moreover, they were both expressed in the capsule

that is surrounding the RT2 tumors. Whereas TNC and OPN expression were largely coexpressed (Figure 22B), TSP1 formed matrices that partially did not overlap with TNC matrices (Figure 22A). It was also noticed that the capsule extended into the tumor tissue by forming a tube-like structure. This histological observation could potentially be reminiscent of a mechanism by which the capsule may have served as a template for TNC tube formation within the tumor mass. This possibility needs to be addressed in the future.

Given that β1 integrins constitute receptors for ECM molecules found in the TNC matrix conduits, we asked whether cell contacts with the matrix tubes potentially could involve β1 integrins. Therefore, β1 integrin expression was analyzed and it was found that β1 integrin receptors are especially expressed in TNC-rich regions (Figure 22D). In particular, β1 integrins expressing cells were present inside the tumor capsule and adjacent to the TNC matrix. Next we analyzed the expression of the α6 chain since α6β1 is a laminin receptor and laminins were found in the TNC matrix tubes (Figure 20D). We observed a similar staining for α6 as for β1 integrin suggesting cells expressing this heterodimer are adjacent to the TNC matrix tubes. Thus cells expressive α6β1 might have been involved in the formation of these structures and potentially might interact with the matrix inside the conduits. Analysis on the expression of other integrins such as α9β1 (TNC receptor), α8β1 (TNC, OPN receptor) and α5β1 (FN receptor) amongst others remains to be done in the future.

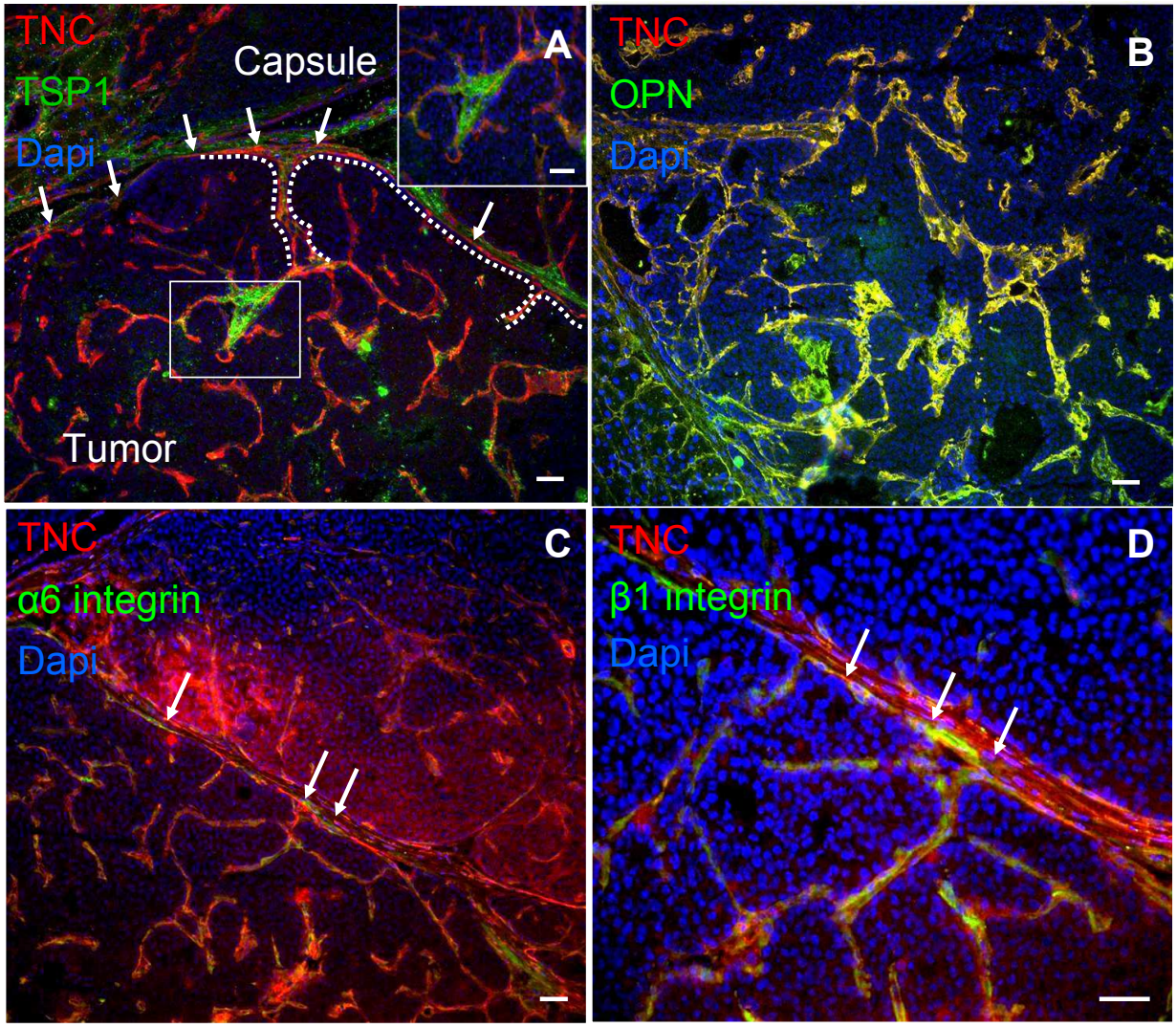

Figure 22: Characterization of TNC conduits in RT2 TNC tumors. (A-B) Immunostaining of other molecules for TSP1 **(A)**, OSP (green) **(B)**, α6 integrin (green) **(C)** and β1 integrin (green) **(D)**, which overlap with these conduits structures. Scale bars 20 µm. (Caroline Spenle PhD thesis, 2010).

Next we analyzed whether oncofetal FN potentially plays a role in RT2 angiogenesis as well as in TNC conduit formation. Indeed TNC and FN were expressed in matrix structures in adjacent layers (Figure 23). Stainings of RT2 insulinoma sections with an antibody directed against the extradomains of oncofetal FN (EDA and EDB) revealed that it was surrounding blood vessels but was also present in CD31 negative conduits (Figure 23 C-H). This suggested that oncofetal FN participates in angiogenesis and in TNC conduit formation.

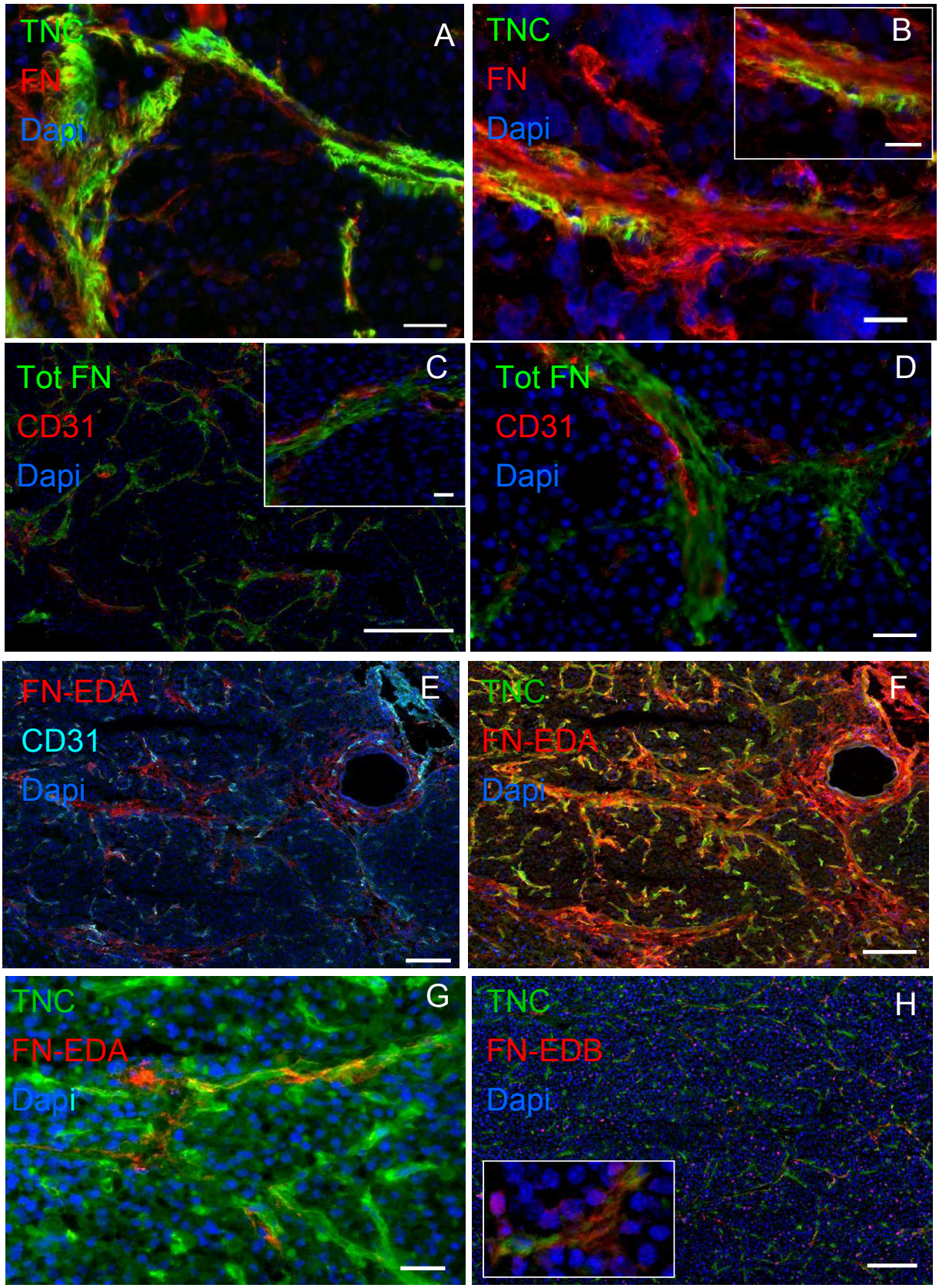

Figure 23: Representation of vessel like and conduit like structures in RT2 tumor. (A-B). Immunostainings showing TNC (green) and FN (red) organized as ECM rich conduits. **(C-D)**. Staining of FN (green) and CD31 (red). **(E-H)** Some of the oncofetal FN (FN-EDA and FN-EDB) was also surrounding blood vessels as well as CD31 negative conduits. Scale bars 100 and 20 µm (**C**), 50 µm **(E, F** and **H),** 20 µm **(A, B, D** and **G).**

In summary this study has shown that TNC was not ubiquitously expressed but organized into conduits together with other ECM molecules including collagens, laminins, FN, OPN and TSP1. Whether other ECM molecules such as periostin (reviewed by Ruan et al., 2009) were also present in these conduits remains to be determined. TNC was also closely lining oncofetal FN and seemed to serve as guiding cue for endothelial cells. Tumor cells expressing integrin α6β1 are lining the TNC matrix tubes and thus potentially played a role in the creation of these structures. Finally, the tumor capsule also seemed to play a role in the creation of the TNC matrix tubes as template.

1.6 TNC and tumor associated cells

1.6.1 Potential impact of TNC on fibroblasts

Given the importance of CAF in tumor angiogenesis (Kalluri and Zeisberg 2006), here it was investigated whether TNC had an impact on the occurrence and distribution of these cells. This was addressed by immunostaining for specific markers for CAF, in particular alpha smooth muscle actin (αSMA) (Kalluri and Zeisberg 2006), vimentin and S100A4/FSP1/Mts1 (Ambartsumian et al., 1996; Kalluri and Zeisberg 2006). First it was observed that cells expressing all three markers were present in RT2 and RT2/TNC tumors (Figure 24). By costaining with TNC it was noticed that CAF were adjacent to the TNC MATRIX. Vimentin, αSMA and Mts1 positive cells, reminiscent of CAF, were found surrounded by TNC potentially using the matrix conduits as guiding cue (Figure 24). At some places the Mts1 and TNC signal strongly overlapped, which may point towards these cells as source of TNC (Figure 24 G-H). This possibility needs to be further addressed by in situ hybridization.

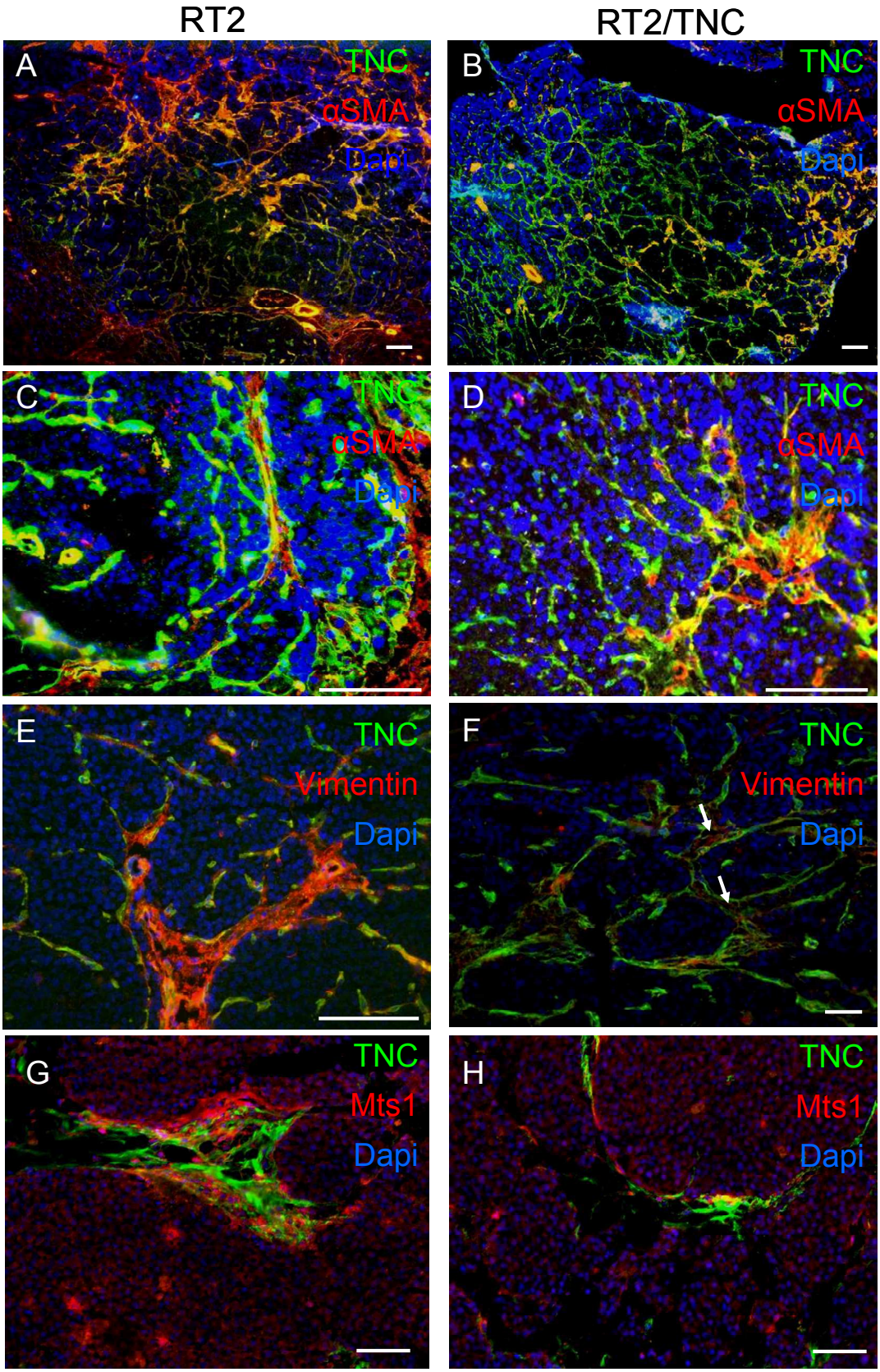

Figure 24: Characterization of different populations of fibrosblasts in murine and human tumors. Immunostaining of cryosections from tumors derived from 12 week old RT2 mice **(A, C, E** and **G**) and RT2/TNC mice **(B, D, F** and **H)**, for TNC in green and for fibroblasts (vimentin, α SMA and Mts1/ FSP1). Note that fibroblasts are in close vicinity to TNC. Scale bars 200 µm **(E),** 100 µm **(C-D),** 50 µm **(A, B, G and H)** and 20 µm **(F).**

Visual inspection of the stainings suggested that there were more CAF in RT2/TNC tumors. To address this possibility the αSMA signal was quantified with the Image J software. Quantification of the αSMA positive signal in tumors of both genotypes revealed that there were indeed about 4-times more CAF in RT2/TNC tumors than in RT2 control tumors (Figure 25). A separate analysis per transformation stage showed that the subgroup of normal/hyperplastic islets of RT2/TNC mice already had 4-times more CAF than the control tumors. Moreover, also in the angiogenic/tumorigenic subgroup the numbers of CAF were similarly increased in RT2/TNC tumors over that in RT2 controls by 4-times as was noticed for the first subgroup. This observation indicates that TNC stimulates the increase in CAF numbers in the tumor tissue. Moreover, this observation suggests that TNC has an impact on very early steps in tumorigenesis even before the angiogenic switch occurs. Whether this involves increased proliferation of CAF and/or enhanced recruitment of these cells by the TNC matrix needs to be further addressed.

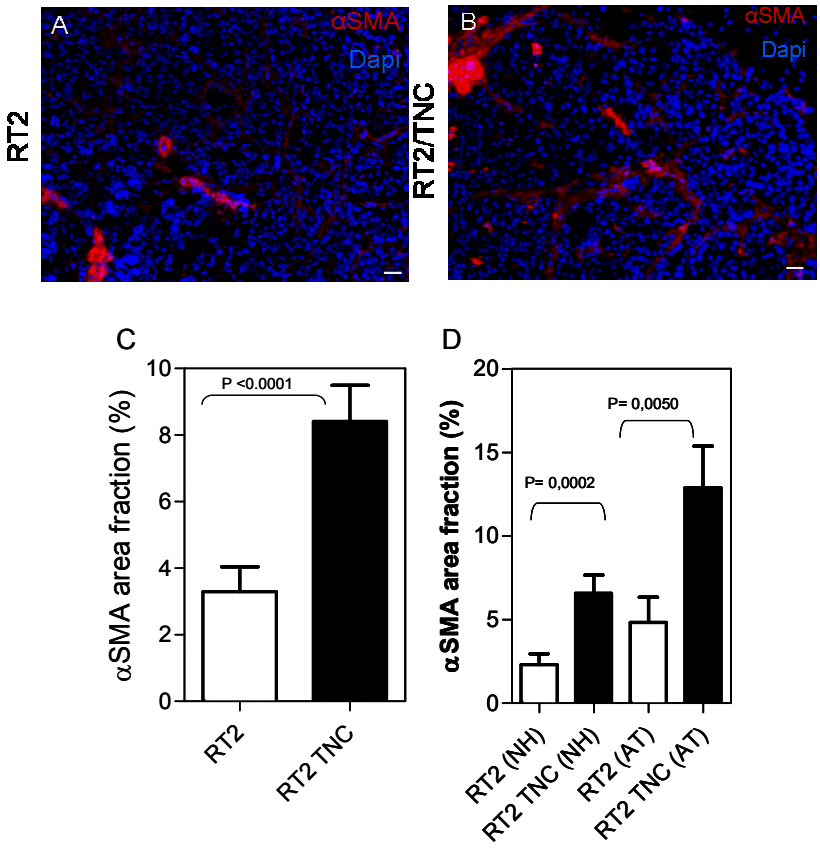

Figure 25: Quantification of CAF in RT2 and RT2/TNC tumors. (A- B). Representative pictures of tumors from 12 week old RT2 **(A)** AND RT2/TNC **(B)** mice. Scale bar 20µm. **(C).** Quantification of αSMA signal (area fraction: area in mm2 / tumor) in RT2 (N=3, n=45) compared to RT2/TNC (N=4, n=86), 2.54 fold, S.E.M., p<0.0001, Mann Whitney. **(D)**. Quantification of the αSMA signal (area in mm2 / tumor) in normal and hyperplastic (NH) islets in RT2 (N=3, n=27) and RT2/TNC (N=4, n=61)

mice, 3.9 – fold, S.E.M, p = 0.0001, Mann Whitney test and in antiogenic and tumorigenic islet (AT) in RT2 (n=18) and RT2/TNC (n=25) mice, 3.9 –fold, S.E.M., p= 0.0015, Mann Whitney test. N, number of mice and n, number of tumors.

1.6.2 Potential impact of TNC on macrophages

A potential impact of TNC on immune cells was addressed by immuostaining for CD45, a general immune cell marker. It was observed that the CD45 signal displayed a patchy pattern with a close association to the fibrillar TNC signal. This was confirmed by staining for macrophages with a F4/80 specific antibody which revealed again a close association with the TNC matrix. There appeared to be more macrophages in RT2/TNC (Figure 26B, D and F) tumor tissue than in RT2 (Figure 26A, C and E) control tumor tissue which needs to be confirmed by quantification.

1.6.3 No impact of TNC on lymph endothelial cells

Next, a potential impact of TNC on lymph endothelial cells was determined by immunostaining for Lyve-1. First, lymph node tissue from mouse pancreata was used for confirming antibody specificity, where the antibody indeed recognized lymphatic endothelial cells (Figure 27 A-B). Analysis of tumor tissue showed that the bulk of the tumor mass was negative but that the tumor rim exhibited lymphatic endothelial cells in RT2 tumors of both genotypes (Figure 27 C-F). No differences in genotypers were noticed.

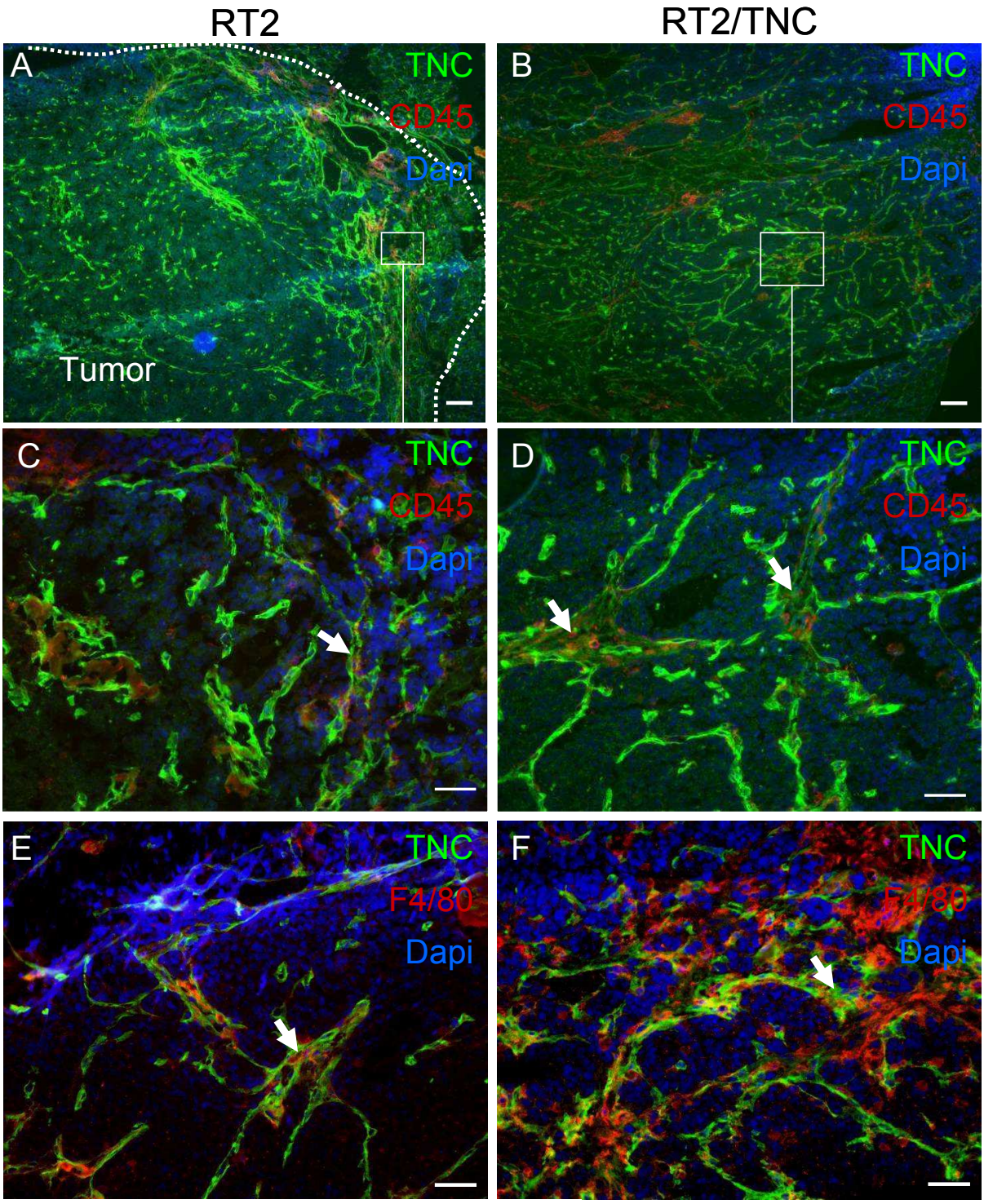

Figure 26: Characterization of immune cells in RT2 and RT2/TNC tumors. (**A-D**). Immune cells (red) and TNC (green) were stained in RT2 **(A and C)** and in RT2/TNC **(B and D)** tumors. CD45 positive cells were found in close vicinity to TNC conduits. **(E-F)**. Immunostaining of F4/80 positive cells in red in RT2 **(E)** and in RT2/TNC tumors (**F**). Scale bars 50 µm **(A-B)** and 20 µm **(C-F).**

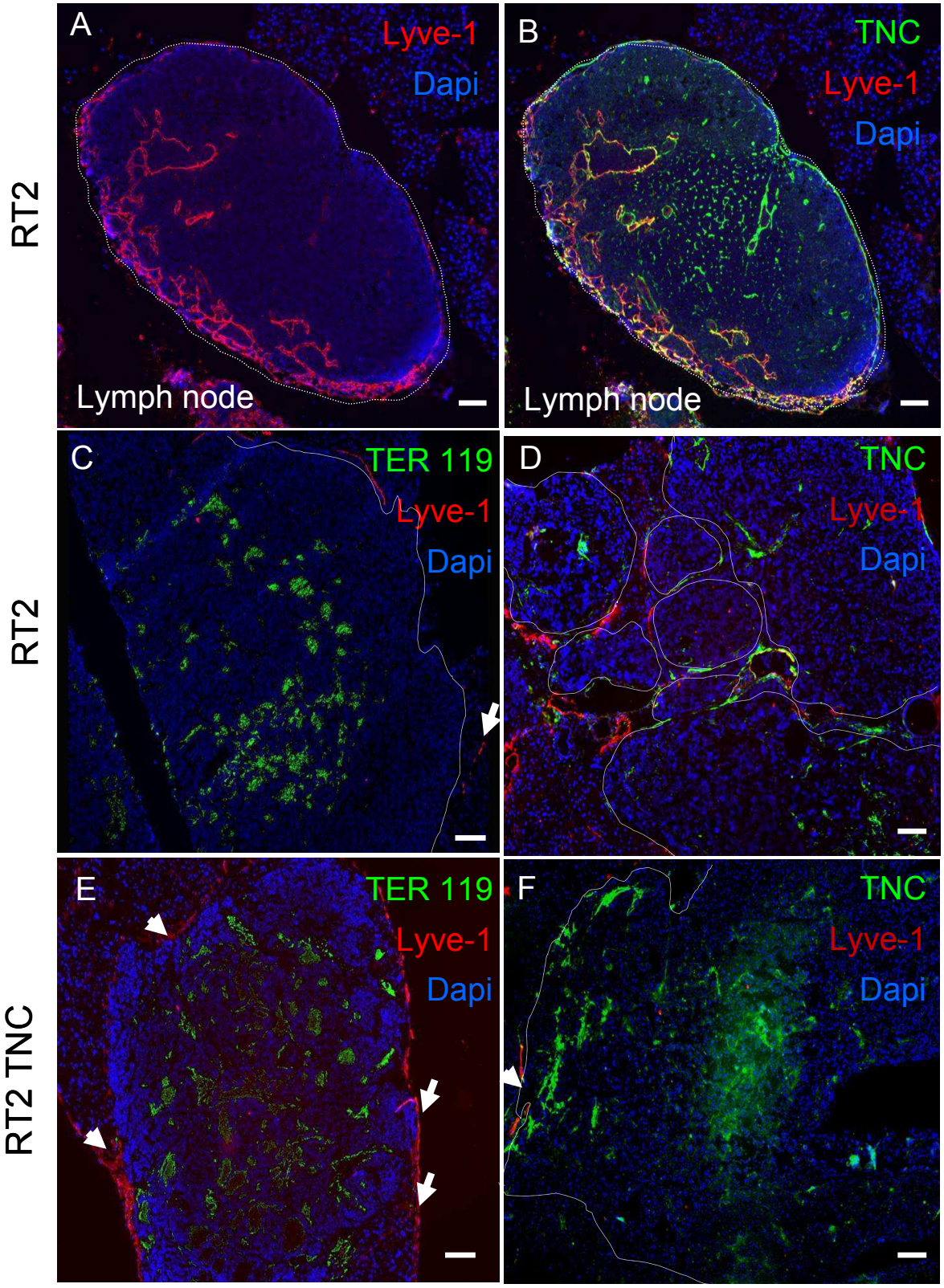

Figure 27: Representation of two conduit systems: lymphatic vessels and ECM tracks in tumors of 12 week old RT2 and RT2/TNC mice. (A-B). Representative pictures of a lymph node in a RT2 pancreas. The red signal corresponds to lymphatic endothelial cells (Lyve-1) and the green signal characterizes TNC expression. **(C** and **E).** Theses pictures represented lymph endothelial cells (red) pointed white arrows and erythrocytes (green) in RT2 **(C)** and RT2/TNC **(E**) tumors. Lymphatic vessels were localized at the rim of the tumor and were not connected to blood vessels**. (D** and **F).** Immunostaining of RT2 tumors **(D)** and RT2/TNC **(F)** tumors for TNC in green and Lyve-1 in red. Tumor circumference is marked by a white line. Scale bars 50 µm.

In summary this study had shown that TNC had an impact on CAF and macrophages but not on lymphatic endothelial cells. The close vicinity of CAF and macrophages with TNC suggested that these cells had interacted with TNC and might have promoted expansion of both cell types. It was also possible that CAF were involved in the formation of the TNC conduits and that a TNC matrix had served as guiding cue for CAF and macrophages. These possibilities need to be addressed by cell culture experiments in the future.

1.7 Potential link of TNC to DKK1 repression and tumor angiogenesis

Given that DKK1 was found to be repressed in cultured GBM cells on a TNC substratum (Ruiz et al., 2004), that DKK1 inhibited angiogenic Wnt signalling (Glinka et al., 1998) and negatively regulated angiogenesis (Min et al., 2011) here it was addressed whether DKK1 repression by TNC potentially played a role in enhanced angiogenesis by TNC. Therefore, DKK1 mRNA levels were determined by qRT-PCR in isolated RT2 and RT2/TNC tumors. It was observed that DKK1 levels in RT2/TNC tumors were significantly lower than in control tumors. In RT2/TNC tumors 7-times more tumors (50%) lacked DKK1 expression as compared to RT2 mice (7.1%) (Figure 28A). In tumors with detectable DKK1 expression, the levels were 3.2-fold reduced in RT2/TNC mice in comparison to RT2 controls (Figure 28B). To further address a potential inhibition of DKK1 expression by TNC in this model system, RT2 tumors that exhibited no TNC were analyzed in comparison to tumors with one TNC allele. Therefore TNCKO mice had been crossed with RT2 mice (Saupe, Gasser, Jia et al., in preparation). It was observed that in RT2 tumors with only one TNC allele, DKK1 levels were significantly lower (2-fold) than in RT2/TNC-/- tumors completely lacking TNC (Figure 28C) (Saupe, Gasser, Jia et al., in preparation, Annex1), which suggested that expression of TNC and DKK1 are inversely correlated.

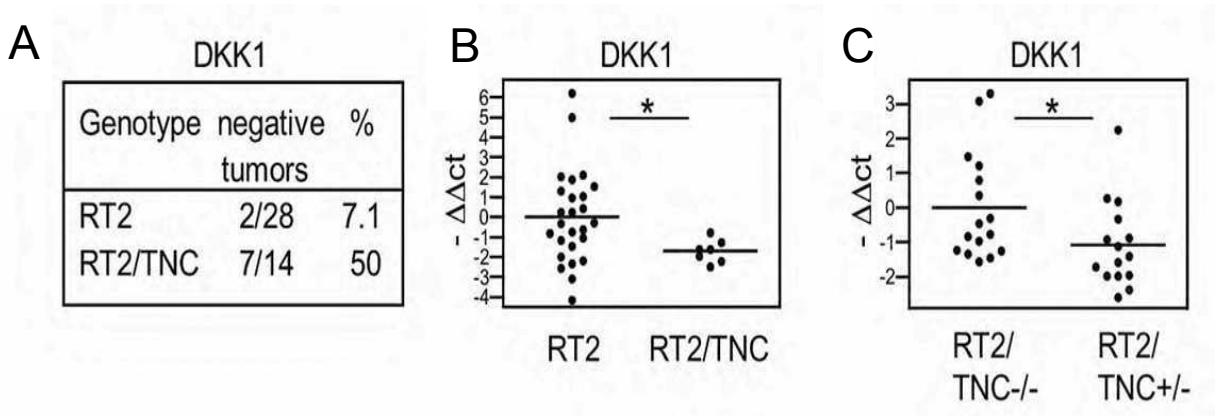

Figure 28: Impact of TNC on DKK1 expression in RT2 tumors. (**A-C).** DKK1 expression was determined by qRT-PCR on RNA from tumors of 14-17 week old mice. **(A).** The number of tumors per genotype that lacked any DKK1 RNA is expressed as % of all analysed tumors, p = 0.0031, Fisher`s exact test. **(B).** DKK1 levels in RT2/TNC and control tumors of 14 week old mice with detectable expression, p = 0.0021, unpaired t-test with Welsh`s correction. **(C).** DKK1 expression in RT2/TNC-/- and RT2/TNC+/- tumors. p = 0.0230, Mann-Whitney test. Number of samples, RT2 (N = 11 mice, n = 28 tumors) and RT2/TNC mice (N = 3, n =14). See details in Suppl. Table 3 in Saupe, Gasser, Jia et al,. manuscript in preparation, Annex1.

A potential functional link between TNC, DKK1 repression and tumorigenesis was further addressed in a xenograft model with tumor cells (T98G, KRIB) that were engineered to ectopically express murine DKK1 (Figure 29). Here the well characterized T98G GBM and the highly tumorigenic osteosarcoma cell line KRIB were chosen as model systems. Cells overexpressing DKK1 were obtained for both cell lines, whereas no cells could be generated with shRNA mediated DKK1 knockdown so far. First by qRTPCR (Figure 29A) and western blotting (Figure 29B) it was shown that engineered cells indeed expressed high levels of ectopically expressd murine DKK1. Similar results were observed in T98G cells (data not shown)

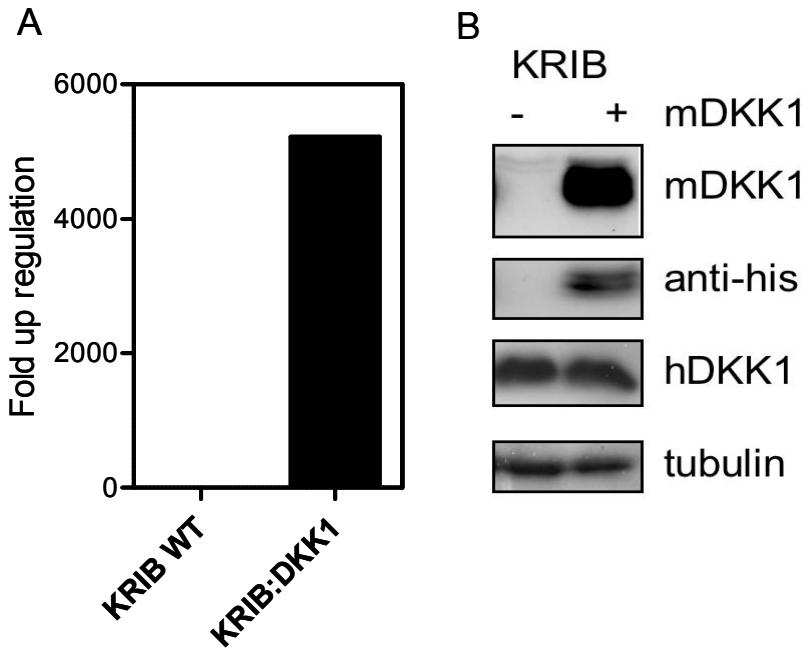

Figure 29: Engineering of KRIB cells to overexpress DKK1. (A). qPCR analysis on KRIB WT and KRIB:DKK1 cells to visualize DKK1 overexpression. **(B).** Western blot of KRIB cells (extracts) overexpressing DKK1.

Next, two sets of control cells had been used, KRIB parental cells (KRIB WT) and KRIB containing the empty vector (KRIB:EV) which were indistinguishable *in vitro* (see below) and thus were both used in the *in vivo* experiments. It was investigated whether high DKK1 levels had an impact on proliferation by determining cell numbers and, it was found that proliferation was indistinguishable between DKK1 overexpressing KRIB and T98G (not shown) and the corresponding parental cells (Figure 30A). In a wound closure migration assay it was investigated whether ectopically expressed DKK1 had an impact on cell migration. While KRIB control cells migrated to close the scratched area in 13h, KRIB:DKK1 cells were significantly retarded to do so (Figure 30B). T98G cells did not migrate under the chosen conditions (not shown).

To determine whether DKK1 had an impact on tumorigenesis and angiogenesis, DKK1 overexpressing (KRIB:DKK1), parental (KRIB WT) cells and cells containing the empty vector (KRIB:EV) were subcutaneously grafted into nude mice and tumors were sampled after 24 days. Upon measurement of tumor diameter the volume was calculated and it was observed that KRIB tumors overexpressing DKK1 remained significantly smaller (mean

value of 145 mm3) than tumors originating from parental KRIB cells (mean of 1028 mm3) and KRIB:EV cells (mean of 1345 mm3) (Figure 30C). Macroscopical inspection revealed that KRIB:DKK1 tumors were pale white which was in contrast to KRIB WT and KRIB:EV tumors that were reddish and exhibited multiple blood vessels on the tumor surface (Figure 30D). Neither wildtype nor DKK1 overexpressing T98G cells induced subcutaneous tumors (not shown).

To address the possibility that ectopically expressed DKK1 had an impact on endogenous DKK1 expression, expression of murine and human DKK1 was determined by qRT-PCR with species specific primers. It was observed that human DKK1 was reduced in KRIB:DKK1 tumors by 2.53-fold in comparison to the control tumors (Figure 30E).

By microscopical analysis of H&E stained tumor tissue it occurred that tumors derived from DKK1 overexpressing KRIB cells exhibited more necrotic areas than tumors from wildtype KRIB (Figure 31) and KIRB:EV control cells (data no shown). This needs to be quantified. Thus a high extent of necrosis potentially could have had an impact on proliferation. To address this possibility proliferation of the tumor cells was determined by staining for KI67. It was found that tumors from both cells had proliferative cells and that the reduced proliferation in KRIB:DKK1 tumors was not statistically significant (Figure 31 B-C).

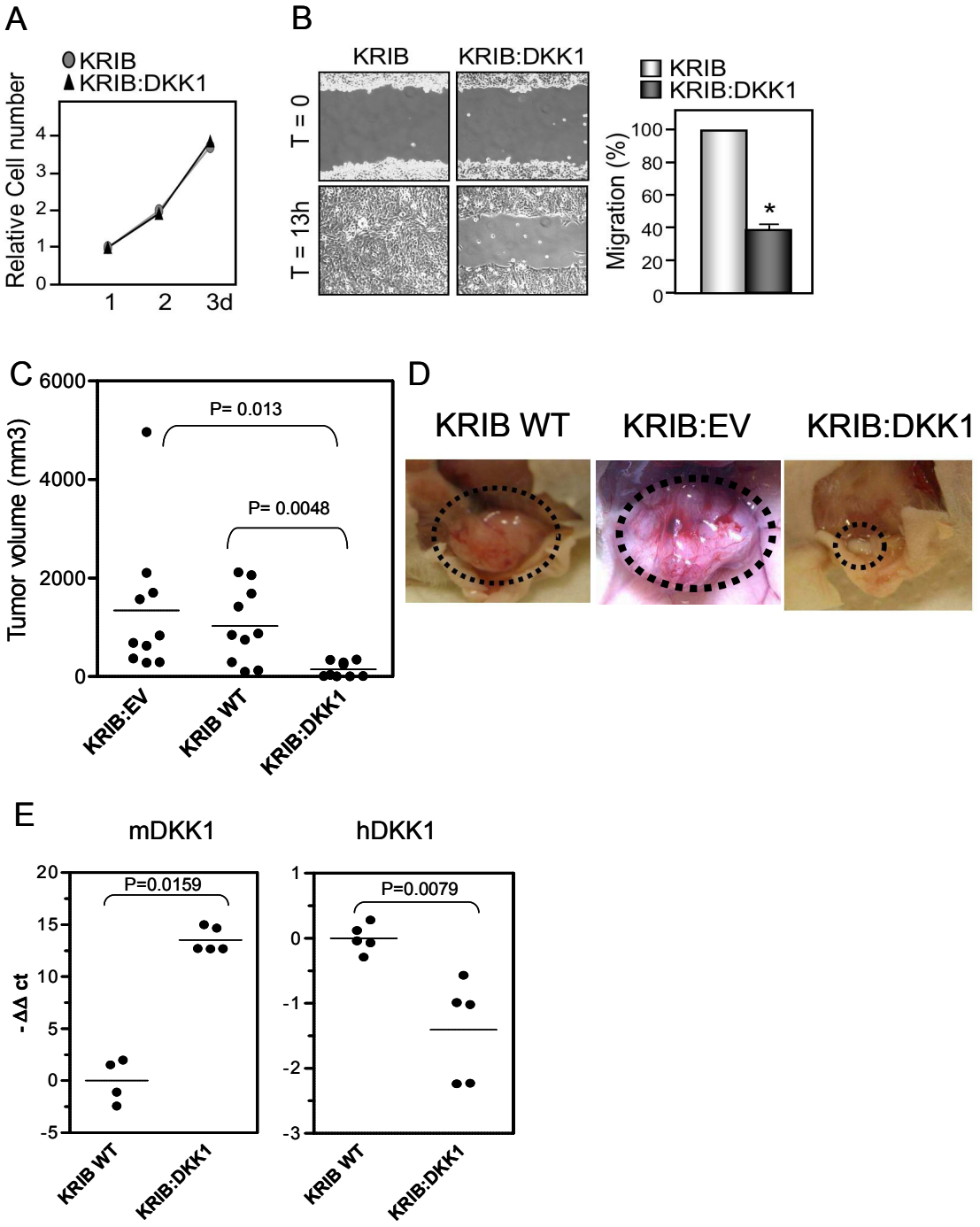

Figure 30: Consequences of DKK1 overexpression in KRIB cells *in vitro* and *in vivo*. (A). Proliferation of KRIB:DKK1 and parental cells was determined after the indicated time points by using the MTS assay. **(B).** Cell migration of KRIB:DKK1 and parental cells was determined as percentage of cell free area in a wound healing assay. The scratched area covered by cells at day 13 (t = 3) is represented in comparison to that at day 0 (t = 0) (%). Experiment was done in 3 independent repetitions, standard deviation, p<0.0001, Student`s t-test. **(C-D).** Consequences of DKK1 overexpression in KRIB cells upon xenografting in nude mice. **(C).** Determination of tumor volume, for KRIB:EV (N=10), 9.2 fold difference to KRIB:DKK1 (N=10), p value= 0.013, Mann Whitney test. For the KRIB WT (N=8), 7 fold difference to KRIB:DKK1 cells, p value= 0.0048, Mann Whitney test. There was no significant difference between KRIB WT and KRIB EV, unpaired t-test, p value= 0.5431. **(D).** Macroscopical appearance of tumors. **(E)**. Human and mouse DKK1 were analysed. Mouse DKK1 levels in KRIB:DKK1 and parental tumors with detectable expression, were determined by qRT-PCR on RNA from WT (N=4) and KRIB xenografted tumors (N=5). p = 0.0159, Mann-Whitney test. Human DKK1 levels in KRIB:DKK1 and parental tumors with detectable expression, p = 0.0079, Mann- Whitney test. N correspond to the number of mice used in the experiment.

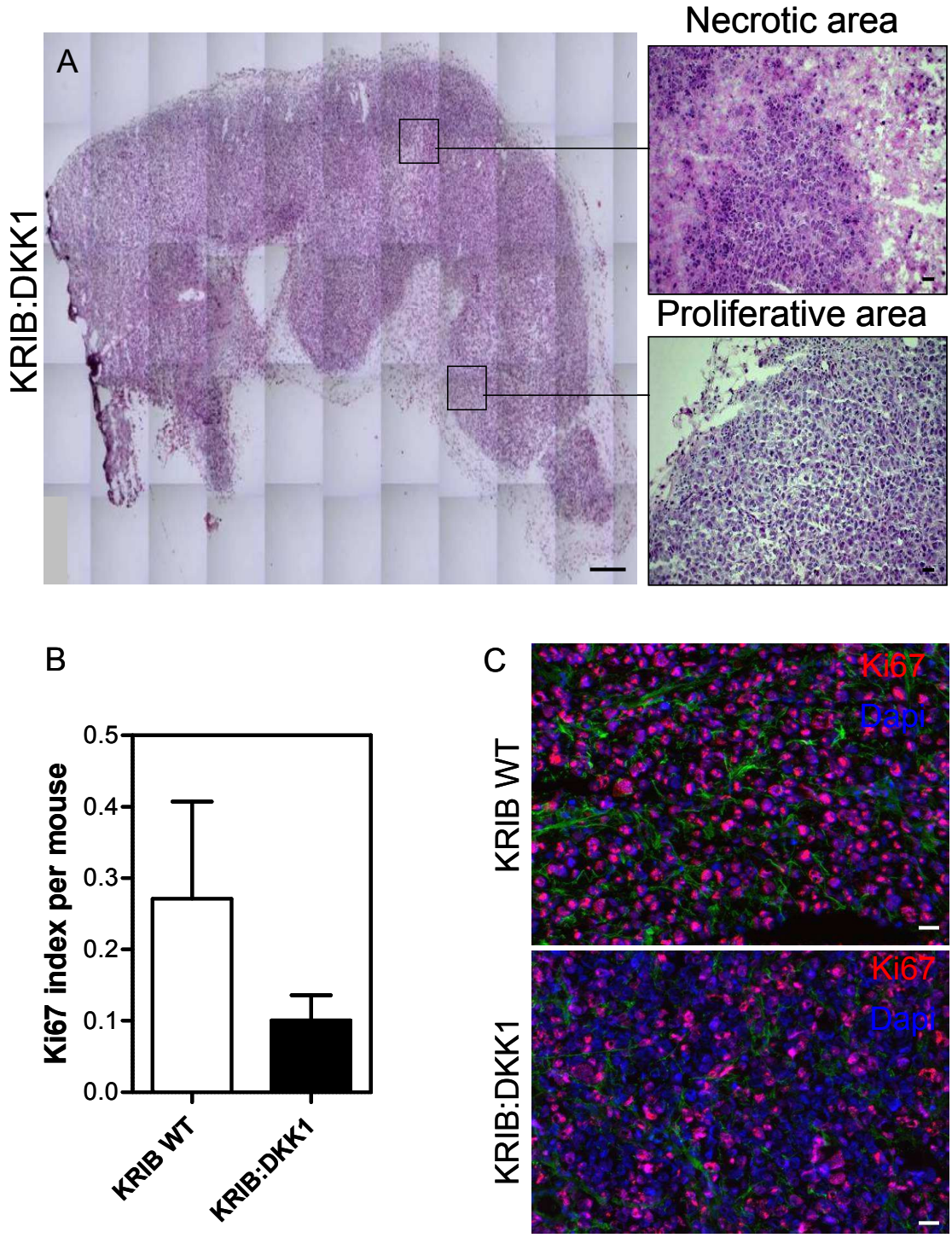

Figure 31: Characterization of KRIB:DKK1 and KRIB:WT tumor. (A). Overview of the whole KRIB:DKK1 xenografted tumor with in the two areas of higher magnification (black boxes). **(B-C)**. Proliferation rate in KRIB WT in comparison to KRIB:DKK1 tumors. Quantification of the KI67 signal with Image J software (KI67 INDEX= KI67 area fraction/ Dapi area fraction) in KRIB WT and KRIB:DKK1 tumors. KRIB WT (N=5) and KRIB:DKK1 (N=5) tumors, 2.69–fold, p=0.3095, Mann Whitney test. (**C**). Representative pictures of KRIB parental and overexpressing DKK1 tumors. Scale bar 200 and 20µm.

Since KRIB:DKK1 tumors were smaller and whiter than the control ones it was likely that high DKK1 had blocked angiogenesis in these tumors which may have caused the reduced

tumor size. To address this possibility, tumors were stained for CD31 (Figure 32 A-C). Subsequent quantification with the Image J program revealed a statistically significant reduction in CD31 in KRIB:DKK1 tumors compared to both control tumors (Figure 32 D-E). By IF analysis it was observed that TNC was expressed in all tumors. A quantification has not been done for all samples yet but analysis of 5 KRIB:DKK1 and 5 control tumors did not exhibit any differences in TNC expression levels (not shown), which suggested that high DKK1 levels did not have an impact on TNC expression. Altogether the data derived from the RT2 and the KRIB models suggest a link between repression of DKK1 and enhanced angiogenesis by TNC, namely that TNC presumably had promoted angiogenesis by repressing DKK1 (Saupe, Gasser, Jia et al., manuscript in preparation, Annex1).

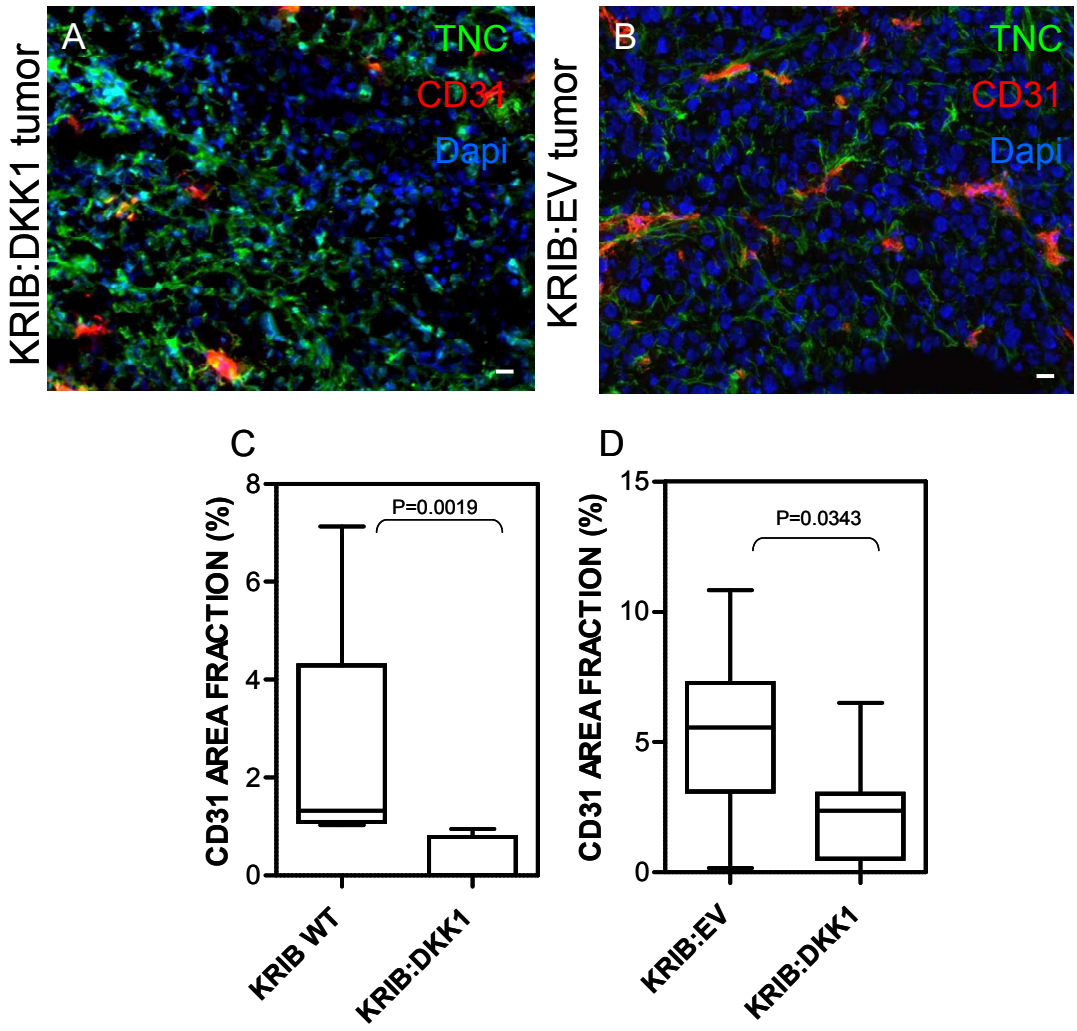

Figure 32: Angiogenesis in the KRIB parental and KRIB:DKK1 tumors. (A-B). Representative pictures for CD31 in red and TNC in green, the nuclei were represented in blue in KRIB:EV and KRIB:DKK1 xenografted tumors. Scale bar 20 µm. **(C).** Quantification of the CD31 signal (area in

mm2 / tumor) in KRIB parental (WT) (N= 5) and KRIB:DKK1 (N=5) tumors, 7.55 fold, p = 0.0119, Mann Whitney test. (**D).** Quantification of the CD31 signal (area in mm2 / tumor) in KRIB:EV (N= 10) and KRIB:DKK1 (N=8) tumors, 2.2 – fold, p = 0.0343, Mann-Whitney test.

2. Organization of TNC in the microenvironment of intestinal carcinomas

2.1 TNC expression and ECM organization

Tissue staining for TNC and CD31 showed the same tube-like organization as had been seen in RT2 tumors (Figure 33A-B). Moreover, these TNC tubes contained LM, Coll IV and FN which surrounded endothelial cells (Figure 33). The newly deposited TNC matrix also appeared to be used by endothelial cells as guiding cue as can be seen in Figure 33B where endothelial cells were directly following the nascent TNC matrix. TNC was also organized in conduits in human liver metastasis (originated from hCRC) where this matrix appeared to embed endothelial cells and pericytes thus potentially providing a favorable microenvironment for these cells (Figure 33 G-H).

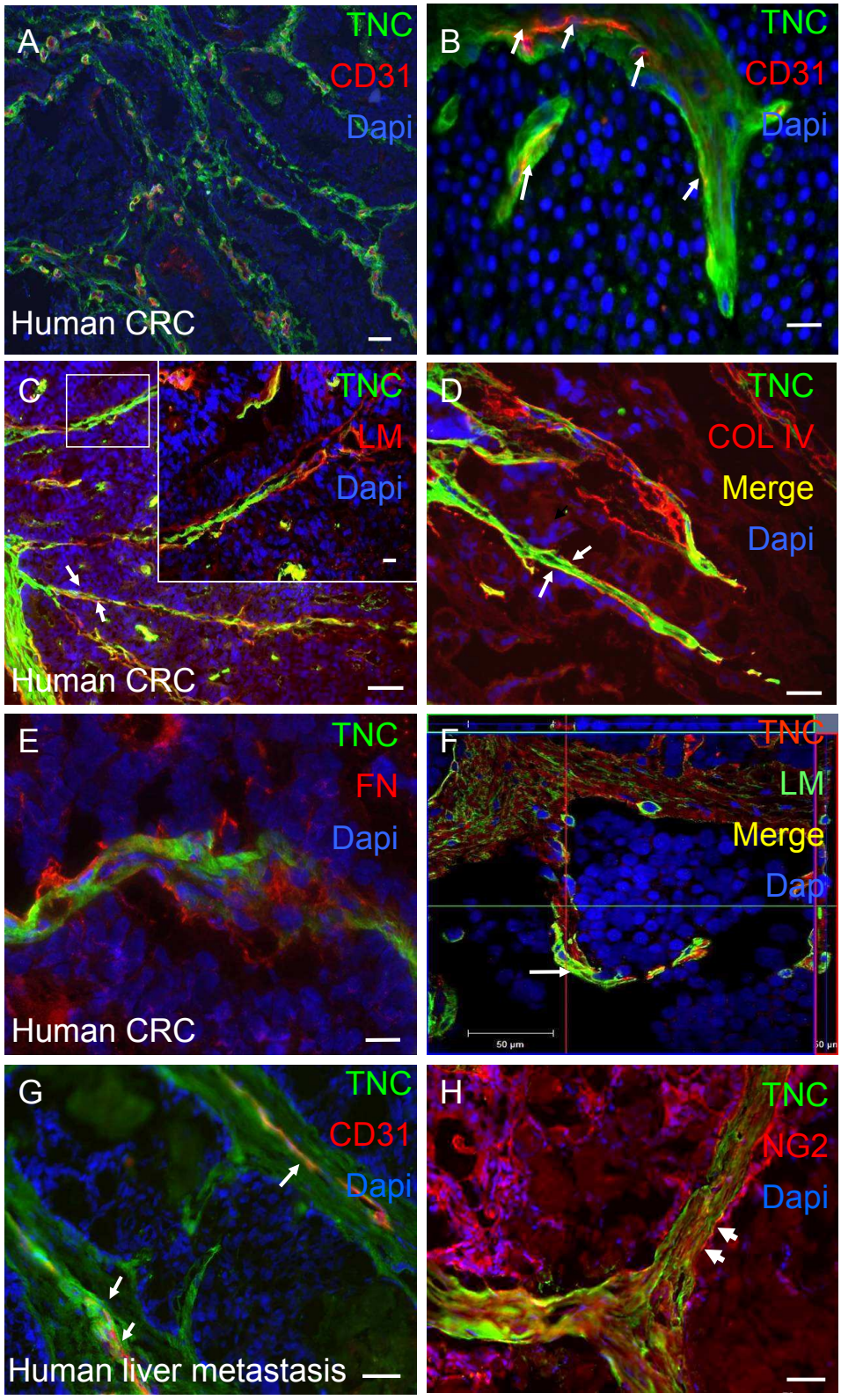

Figure 33: ECM organization in human CRC and corresponding liver metastasis. (A-H). Immunostaining of cryosections of human CRC with the indicated Ab, representing ECM matrix with TNC inside. Note that not all EC (CD31) were surrounded by TNC **(A-B)**. TNC is also forming conduits lined by LM **(C)** and by Coll IV **(D)**. In addition, TNC is also closely intermingled with FN **(E)**. **(F)** is a reconstruction picture of z-series acquired by confocal microscopy which was provided by K-P Janssen (TU Munich, Germany) showing a conduit enriched by TNC and LM. Arrows: cells inside matrix conduit. **(G-H)**. Corresponding human liver metastasis CD31 (red, **G**) and NG2 (red, **H**) positive cells are closely intermingled with TNC (green), arrows point at vessel-like structure or conduit. Scale bars 50 µm **(A, B, F, G** and **H)** and 20 µm **(C, D** and **E)**.

2.2 Establishment of an optimized staining protocol for tissue analysis

The establishment of an optimal protocol was necessary to be able to discriminate between human and murine TNC in xenografted human tumor cells into a murine host (see below). First the specificity of the available TNC antibodies for murine (Figure 34 A-B) and human (Figure 34 C-D) TNC was tested in fresh frozen tissue of normal human and murine normal intestinal tissue. The murine specific antibody MTn12 and the pan-TNC antibody TNC1.2 both recognized similar structures in the muscular layer and at the apical top of the intestinal glands. TNC1.2 recognized also other structures in the normal tissue in the lamina propria (Figure 34D). This could be due to different isoforms of TNC expressed at the different places that would be differentially recognized by the two antibodies. The rabbit polyclonal TNC1.2 antibody might recognize more isoforms of TNC than the rat monoclonal MTn12 antibody. It is also possible that the TNC1.2 antibody potentially recognizes something else that is not TNC specific although the major antigen was indeed TNC as determined by immunoblotting (not shown, Lange et al., 2008). Therefore it was important to see whether TNC1.2 would recognize a signal in intestinal tissue from a TNCKO mouse. It was observed that at the chosen dilution no signal was obtained with neither of the antibodies suggesting that the signal is TNC specific (Figure 34 A-C). Next it was addressed whether in paraffin embedded intestinal tissue TNC1.2 recognizes similar structures as in frozen tissue which turned out to be the case (Figure 34 G-H). The B28.13 antibody raised against human TNC was also tested and found to deliver a similar staining as obtained with the TNC1.2 antibody (Figure 34 E-F). Upon staining of intestinal tumor tissue of human (Figure 35 A-D) or murine origin Figure 35 E-F) it was observed that TNC was highly expressed and organized into tracks reminiscent of TNC matrix conduits. Application of the B28.13 delivered a strong staining whereas the TNC1.2 antibody showed a weaker signal. Therefore in the following analysis the TNC1.2 antibody was used for fresh frozen tissue analysis and the B28.13 for paraffin embedded tissue. A summary of optimized staining conditions is displayed in Table 2 (part Material and Methods).

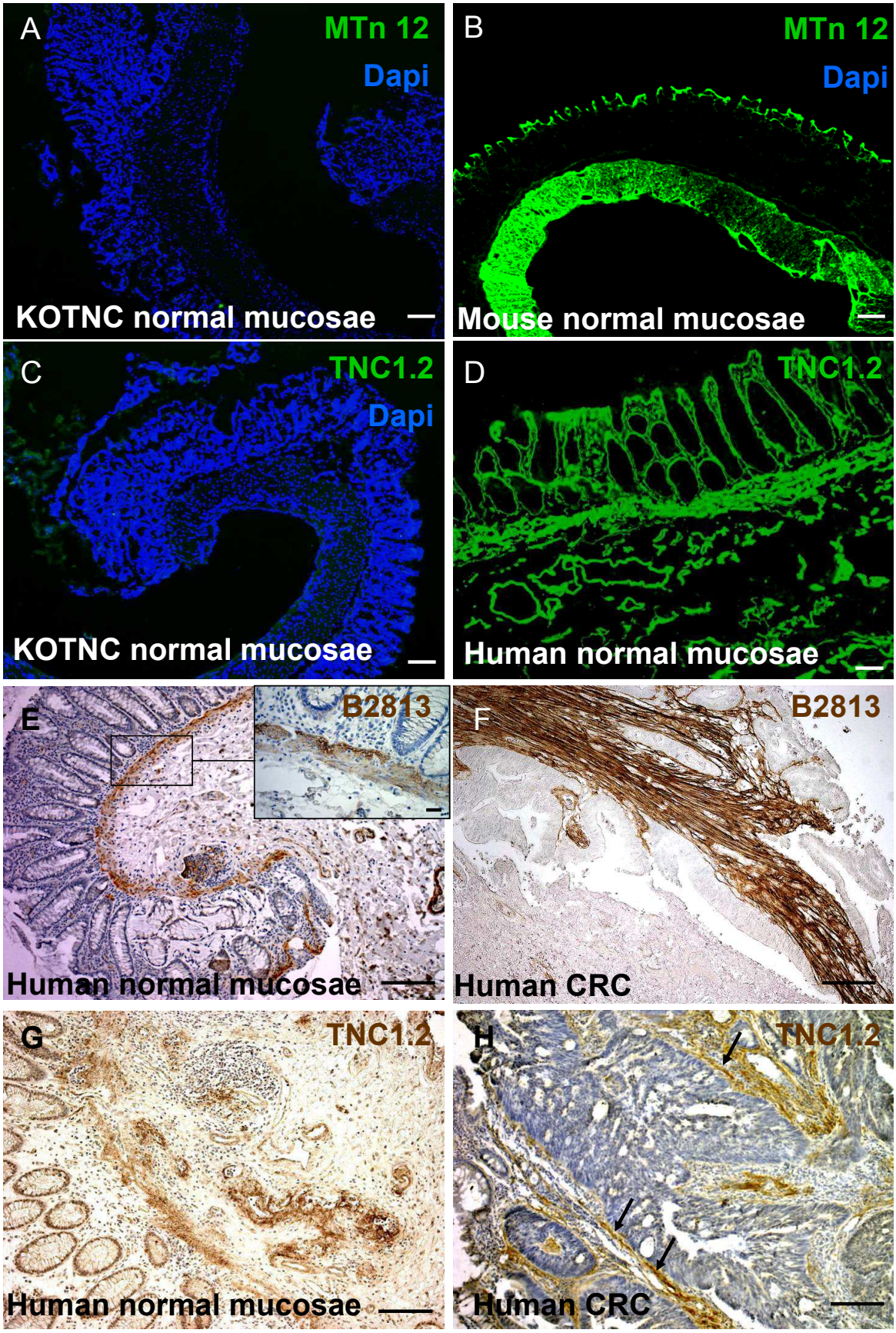

Figure 34: TNC antibody specificity. (A-D). Immunostaining on cryosections of normal human an murine mucosae and mucosae from KOTNC mice with MNT12 **(A-B)** and TNC1.2 **(C-D)** Representative pictures for TNC with B28.13 **(E-F)** and with TNC 1.2 **(G-H).** Scale bars 50 µm **(A, B, C, E, F, G** and **H)**, 20 µm **(D** and **E, enlargement)**.

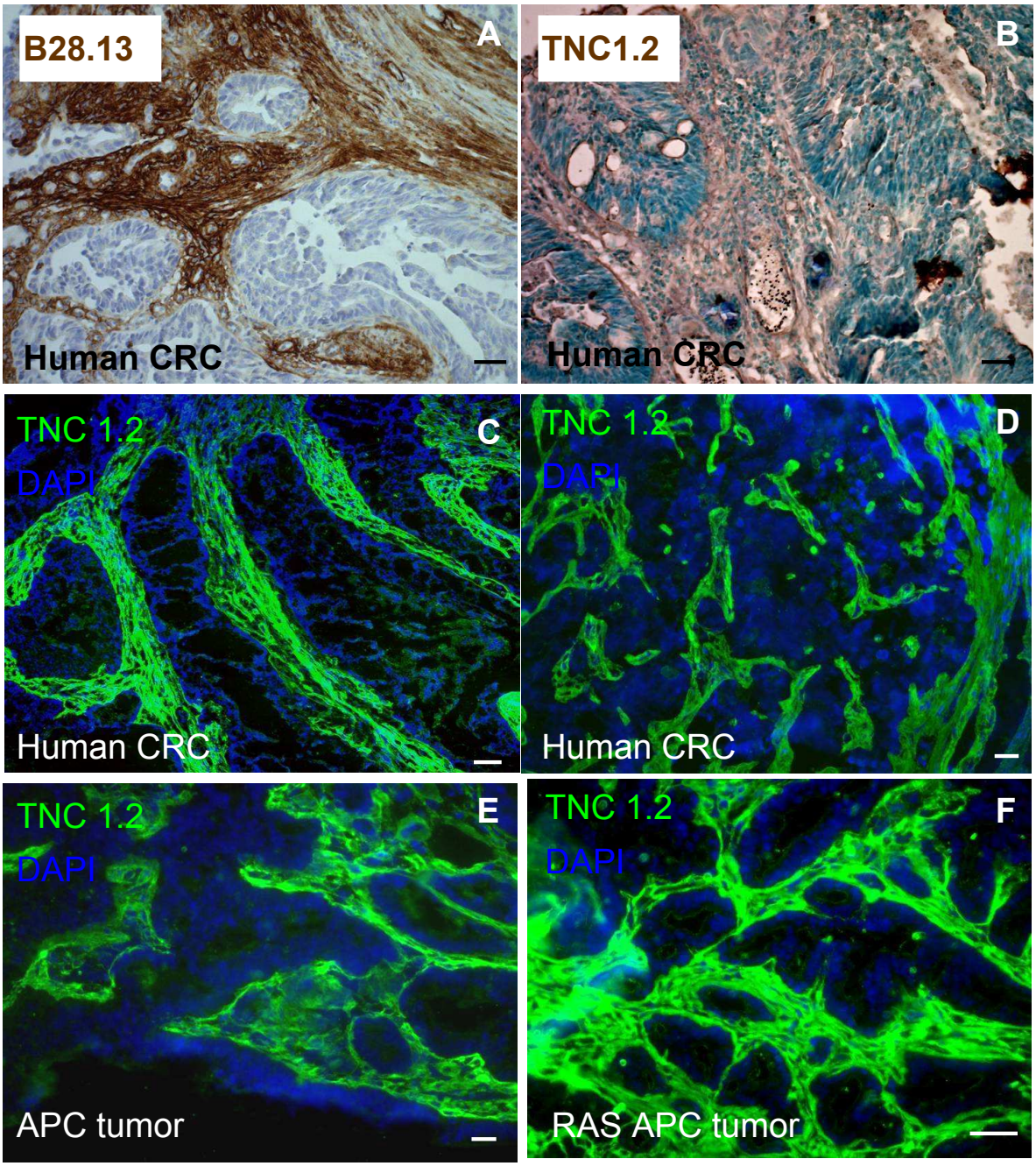

Figure 35: TNC expression in human and mouse tumors. (A-B). Representative pictures for TNC in human CRC using the B28.13 **(A)** and TNC1.2 **(B)** on paraffin sections. **(C-D).** Immunostainings for TNC in two different hCRC. Note that TNC is organized into matrix tracks. **(E-F)**. Immunostaining of mouse colorectal tumors. Scale bars 50 µm **(C)**, 20 µm **(A, B, D, E,** and **F)**.

2.3 TNC expression in human colon cancer xenografts

In order to develop and test patient tailored specific anti-cancer treatment a humanized murine cancer model is needed. Therefore human cancer material had been grafted into nude mice and the tissue organization and genetic alterations between the human cancer and the xenograft were investigated. It had been seen that the tissue organization found in

the primary human colorectal carcinoma is recapitulated upon grafting of minced and homogenized tumor tissue into nude mice. Moreover, the genetic alterations were also conserved (Guenot et al., 2006). These observations had suggested that the tissue organization is recapitulated to some extent within the murine host which raised the question how this applies to the microenvironment. To address this question human colorectal carcinoma specimen had been minced and homogenized prior to subcutaneous injection into nude mice (collaboration with D. Guenot). Tumors had been recovered after 2 weeks and tissue was analyzed by immunostaining. A comparison of total TNC expression between tumor xenograft (Figure 36 B-D) and primary cancer (Figure 36 A-C) was done by using the TNC1.2 Ab (Figure 23). It was observed that the patchy and conduit like expression found in the primary cancer was recapitulated in the xenograft with a similar pattern.

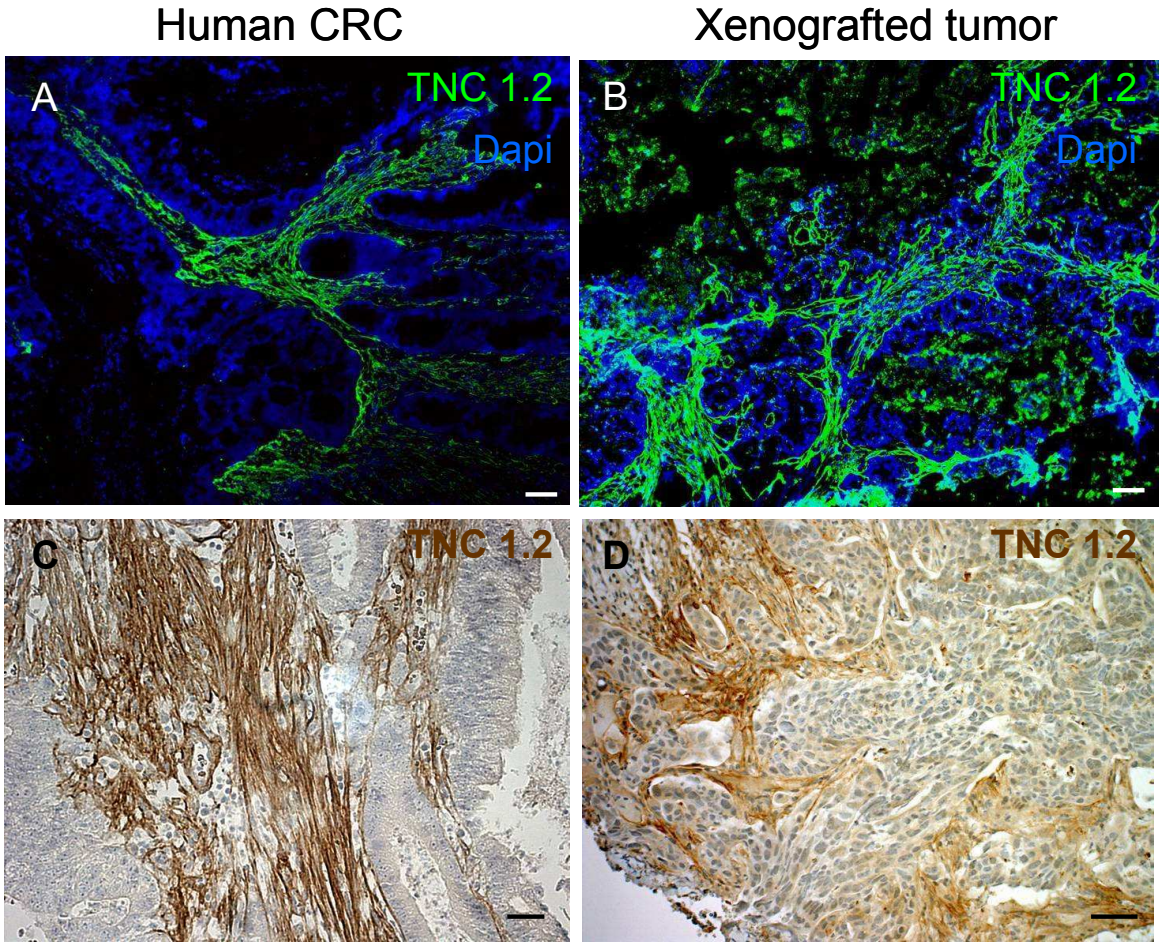

Figure 36: Comparison of TNC expression patterns in human CRC and corresponding human xenografted tumor. (A-B). Immunostainings with the TNC1.2 Ab showing a high TNC expression in the original tumor **(A)** and in the xenografted tumor **(B). (C-D).** Pictures of immunohistochemical staining representing TNC expression in human CRC **(C)** and corresponding xenografted tumors **(D)**. Scale bars 50 µm **(A, B** and **D)** and 20 µm **(C).**

By staining for murine TNC it was observed that there was little expression in the tumor xenograft which suggests that the grafted tumor had not significantly been infiltrated by murine cells that would express TNC (Figure 37). Upon continuous grafting of the first passage human xenograft, tumor tissue of the 5th passage was again analyzed for TNC expression. Now it was found that the human TNC was largely replaced by murine TNC which was again organized into TNC tracks reminiscent of the TNC matrix conduits. This observation questions the suitability of a tumor model where continuous xenografting of human tumor tissue in mice is used to phenocopy the properties of the original human cancer.

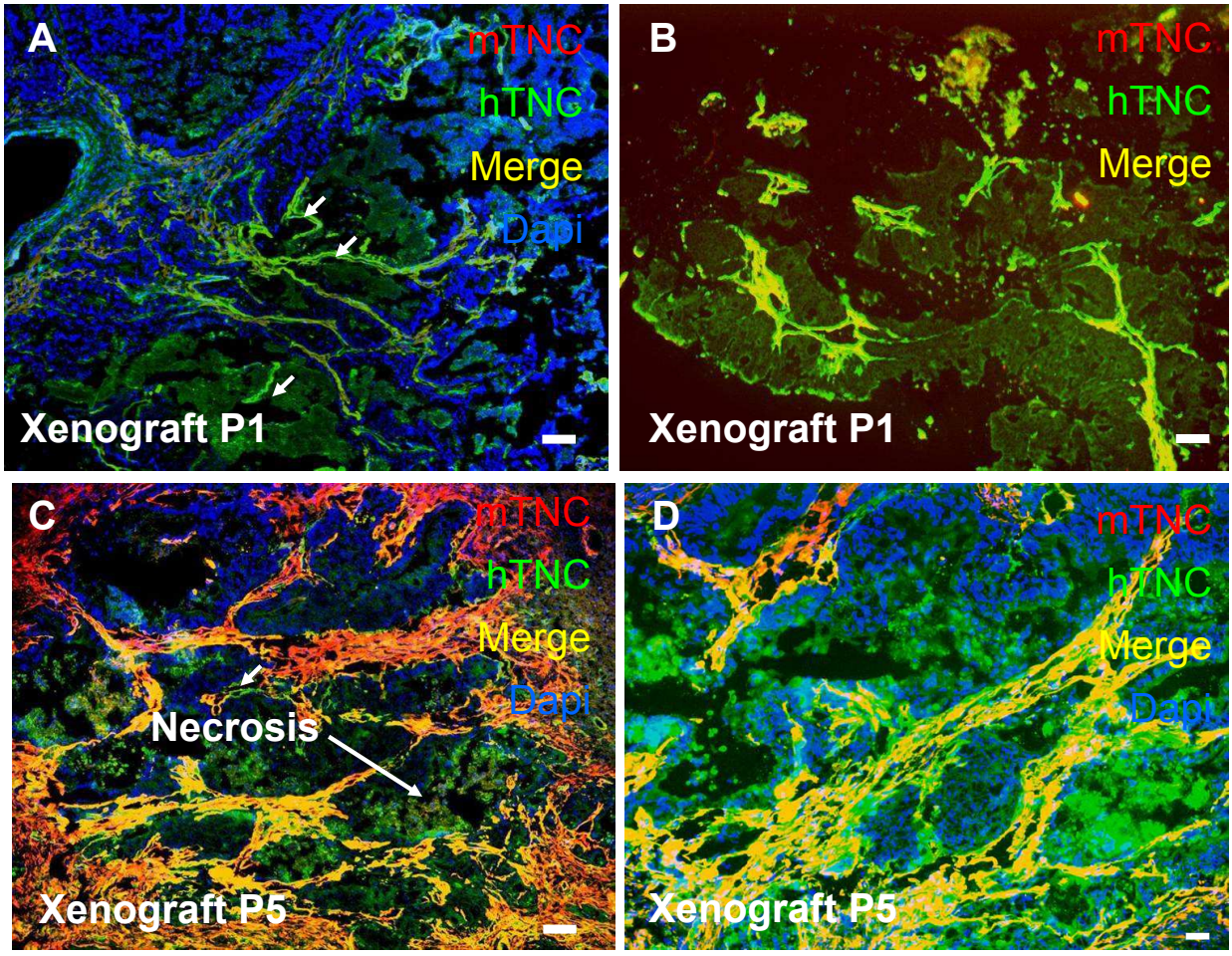

Figure 37: Presence of mouse and human TNC in different xenografted tumors. (A-D). Pictures represent tumor xenografts in the mouse. P1 represents the first tumor xenograft of homogenized human cancer material **(A and B)** whereas P5 represents the fifth continuous passage of the P1 tumor material in the nude mouse **(C and D)**. Note that after several passages human TNC (green) is replaced by murine TNC (red). Scale bars 50 µm **(A, B** and **C)** and 20 µm **(D).**

2.4 Association of CAF with TNC in human colorectal carcinoma and in the murine tumor xenografts

The question was addressed whether CAF are in vicinity to TNC by immunostaining of vimentin and αSMA. It was observed that indeed vimentin and αSMA positive CAF were embedded into a TNC-rich matrix and formed conduit structures similar to those observed in RT2 tumors (Figure 38).

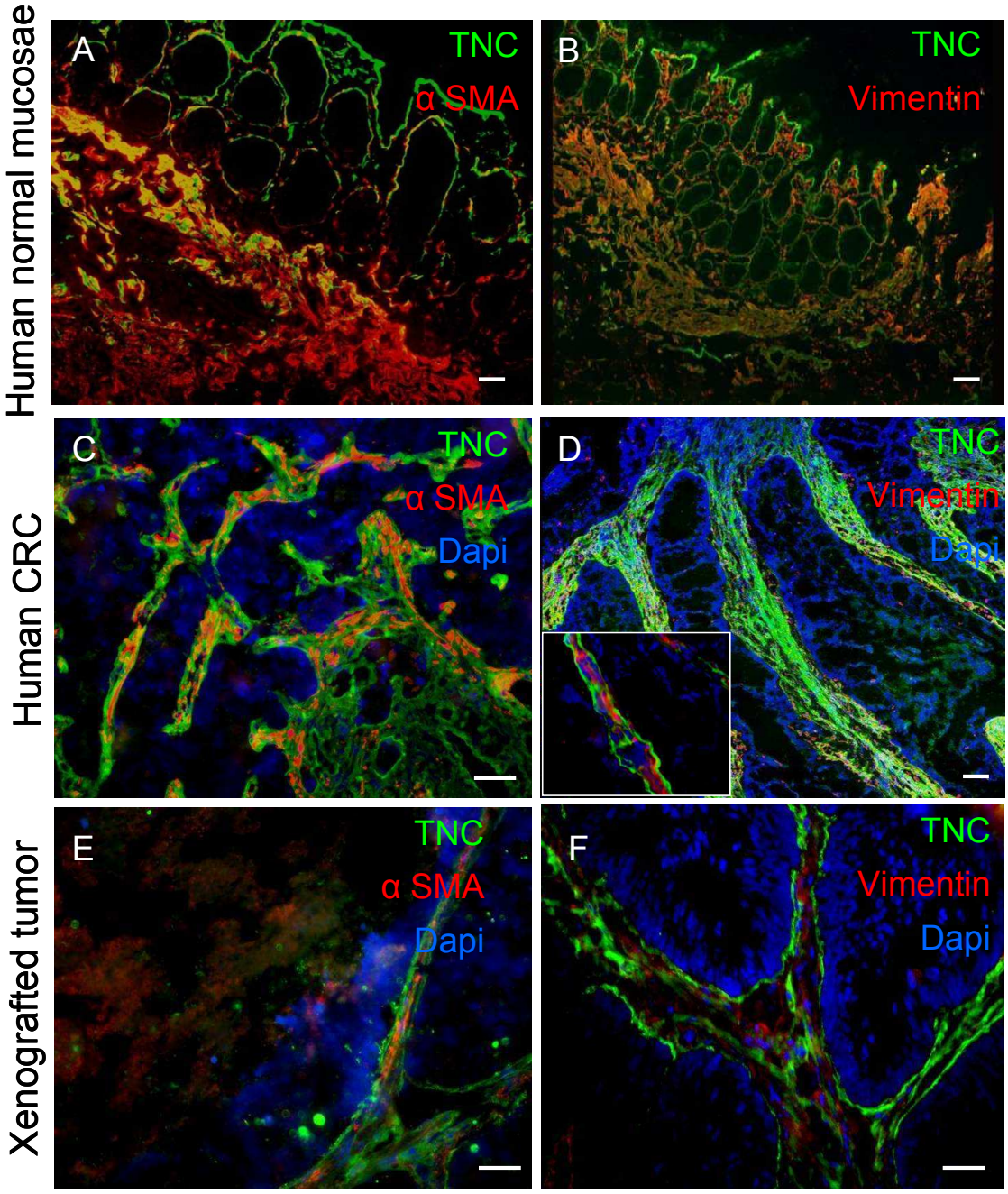

Figure 38: Cellular and fibrillar similarities of the tumor microenvironment in xenografted tumor in comparison to human tissues. **(A-B).** Immunostainings of cryosection of human normal mucosae, corresponding CRC **(C-D)** and xenografted tumor **(E-F)** for TNC, vimentin and αSMA. Scale bars 50 µm (**A, B, D** and **E**), 20 µm (**C** and **F**).

In summary, the all over morphology was recapitulated in the arising tumors that had derived from minced human hCRC tumor material upon xenografting into the murine host (nude mouse). Indeed, TNC was found organized into conduit like structures which are in close vicinity to CAF. Nevertheless, after several passaging in the murine host the human tumor microenvironment appeared to be replaced by the murine one.

3. Organization of TNC in the microenvironment of human insulinomas

Organization of tumor tissue derived from 7 human insulinomas and of adjacent normal pancreatic tissue was determined by H&E staining (Figure 39, Figure 40 and Gasser, Saupe, Jia et al., in preparation).

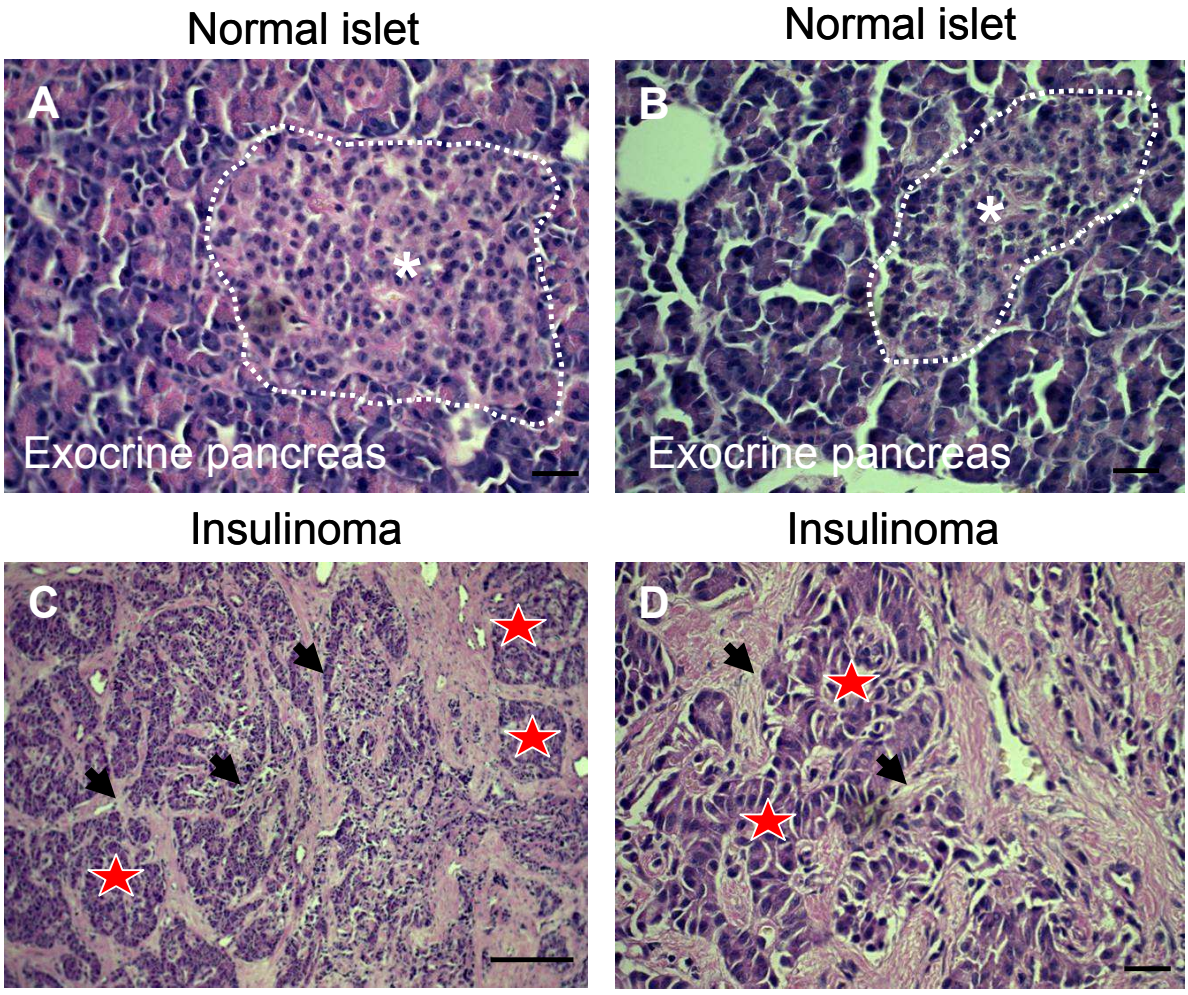

Figure 39: Histological characterization of normal and insulinoma tissue. (A-B). Representative pictures of H&E staining from human normal pancreatic islet surrounded by exocrine pancreas**. (C-D).** Representative pictures of one insulinoma **(D)** inset corresponds to a higher magnification of the insulinoma. Black arrows point at the stroma, asterisks at the normal tissue and red stars at tumorigenic tissue. Scale bars 100 µm **(C)** and 50 µm **(A, B** and **D.)**

Cell clusters with small nuclei were observed in the insulinomas that were partially infiltrated by stroma, which in some cases was very abundant (Figure 39 C-D, Figure 40B) and in others not (Figure 40D). In some specimen the insulinoma appeared to have invaded and some insulinoma seemed to be encapsulated; a feature that has also been seen in RT2 insulinomas (Figure 40 C-D). Expression of TNC was determined by immunostaining. Whereas in the normal tissue no TNC was detected (Figure 41A), TNC was found to be expressed in all analyzed insulinomas. Similar to the RT2 insulinoma tissue, TNC was not ubiquitously expressed but was specifically accumulated in TNC tracks ressembling the TNC matrix conduits observed in RT2 tumors. To address whether endothelial cells and CAF were also in close association with TNC as observed in the RT2 insulinomas, tissue was costained for TNC together with antibodies for CD31, vimentin (Figure 40). This analysis revealed that the tumor tissue was highly vascularised and that all CD31 signal was in close association with TNC suggesting that endothelial cells were embedded into a TNC rich matrix. This was especially prominent in Figure 40 (A, B and D). Vimentin staining revealed that all vimentin positive CAF were surrounded by TNC (Figure 40A-D).

By TNC staining of paraffin embedded human insulinoma tissue we observed that a TNC positive structure reminiscent of the described TNC matrix conduits was connected to a blood vessel with a typical BM and erythrocytes (Figure 41C). This observation suggested that the TNC matrix conduits also form a continuum with the vasculature in human insulinomas as was seen in RT2 insulinomas (Figure 41C).

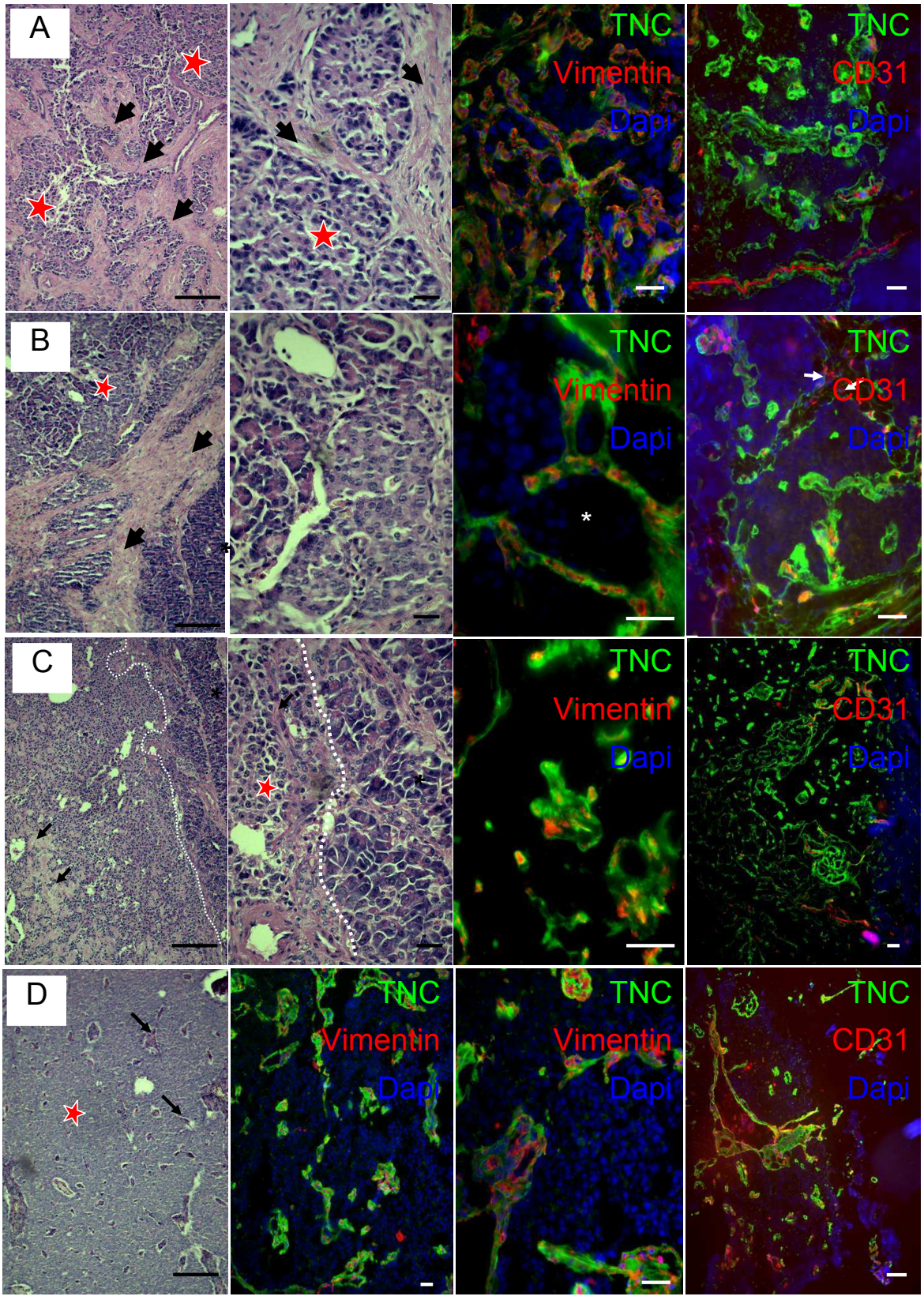

Figure 40: Organization of ECM in human insulinomas. (A-D). Immunostainings and H&E stainings of tissue sections corresponding to 4 different insulinomas with the indicated antibodies; black arrows at the stroma infiltration and red stars at the insulinoma. White arrows point at endothelial cells with a close alignment to TNC. Note that CAF and TNC are in close apposition forming tube-like structures. Scale bars 100 µm, 50 µm, 20 µm and 50 µm **(A)**, 100 µm, 50 µm, 20 µm and 20 µm **(B)**, 100 µm, 50 µm, 20 µm and 20 µm **(C)** and 100 µm, 20 µm, 20 µm and 50 µm **(D)**.

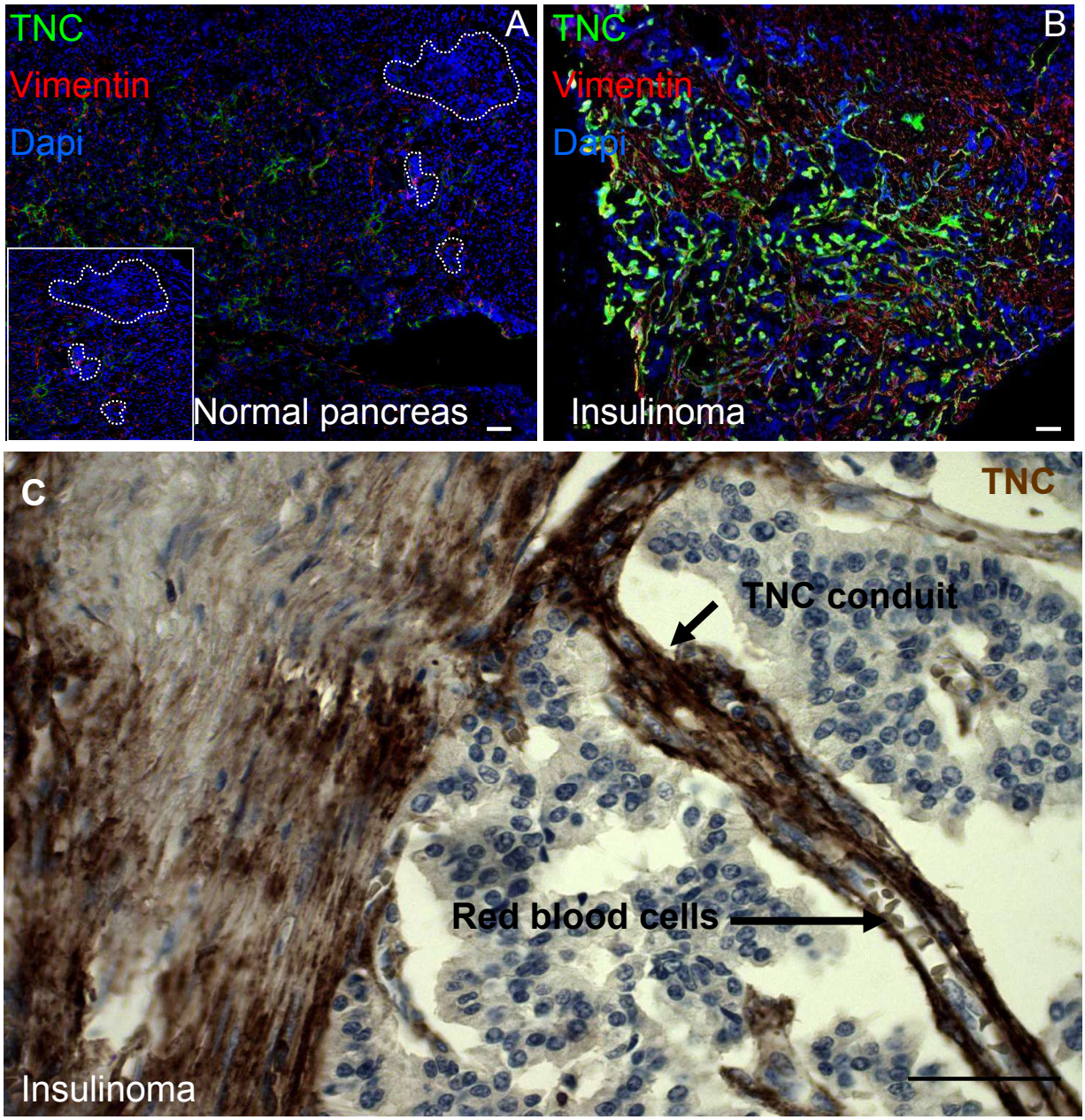

Figure 41: TNC expression in normal human pancreas and insulinoma. (A-B) Representative pictures of TNC (green) and vimentin (red) of normal human pancreas **(A)** and human insulinoma **(B)**. White doted line mark a normal pancreatic islet of Langerhans. **(C)** Representative picture of TNC expression (brown) in human insulinoma, blood vessel and TNC-enriched conduit are marked with an arrow. Scale bars 50 µm.

In summary this part of the study had shown that TNC is highly expressed in sporadic genetically modified murine intestinal tumors, and insulinomas and in colorectal carcinomas and their xenografts in mice. Moreover, TNC matrix assembly into conduits was described and revealed a complex organisation together with other ECM molecule. The conduits were seen to embed several tumor associated cells which is suggestive of a microenvironment that potentially promotes survival and expansion of these cells. A

mechanistic link of TNC to repression of DKK1 and enhanced tumor angiogenesis was shown. The presented results had also shown that RT2 tumors resemble human insulinomas in several aspects as in i) a high TNC expression, ii) organization of TNC into conduits and iii) TNC matrix surrounding endothelial cells and vimentin positive CAF. Thus the RT2 model is not only a valid model for studying spontaneously arising tumorigenesis and progression but may also be a proper model for studying human insulinomas which could improve our understanding about the origin of insulinomas and their eventual and rare progression into metastasizing carcinomas.

1. Use of immune-compromised Rag2KO mice for tumor engrafting

Next, it was addressed whether host-derived TNC would promote tumor angiogenesis. To address this question an immune compromised model was established that displayed defined TNC expression – wildtype (WT) or knockout. The immune compromised Rag2KO mouse was chosen, because it constitutes a relevant immune-compromised model for xenografting human tumor cells (Greenberg and Slayden 2004). First, it was determined whether grafting of HEK293 cells would induce tumors and indeed 2 weeks after engraftment under the skin tumors developed, mice were sacrificed 5 weeks after injection and tumor tissue was analyzed. Tumors appeared very whitish suggesting that they were not well vascularised (Figure 42D). Similarly, HEK293 cells overexpressing TNC (HEK293:TNC) (Figure 42 A-B) (Lange et al., 2008) were injected. Again tumors formed, but in contrast to HEK293 derived tumors they appeared highly vascularised in 2 of 3 mice as determined by macroscopical inspection. Upon TNC expression analysis in the tumor tissue it was observed that HEK293 cell-derived tumors expressed human TNC (as determined with the B28.13 antibody), which was in contrast to the cultured cells that lacked TNC expression in cell culture as determined by qRT-PCR and immunoblotting (Figure 42 A-B). This observation suggested that the tumor microenvironment may have triggered expression of TNC in the tumor cells. TNC was organized in conduits as already seen for several other tumors (see part A). Also in this model endothelial cells were in close association with TNC. In HEK293:TNC cell–derived tumors TNC was organized into thick tracks reminiscent of the TNC conduits described beforehand (see part A) (Figure 42C). CD31 staining revealed differences between the tumors. Whereas HEK293 cell-derived tumors exhibited few endothelial cells which could account for the whitish color, TNC overexpressing HEK293:TNC-derived tumors exhibited a strong CD31 signal which suggested the presence of multiple microvessels (Figure 42C). A potential promoting effect of TNC on angiogenesis in this model needs to be further substantiated by quantification of the CD31 signal in the future. Moreover, tumors should be analyzed to see whether TNC-induced angiogenesis had an impact on tumor growth in this model.

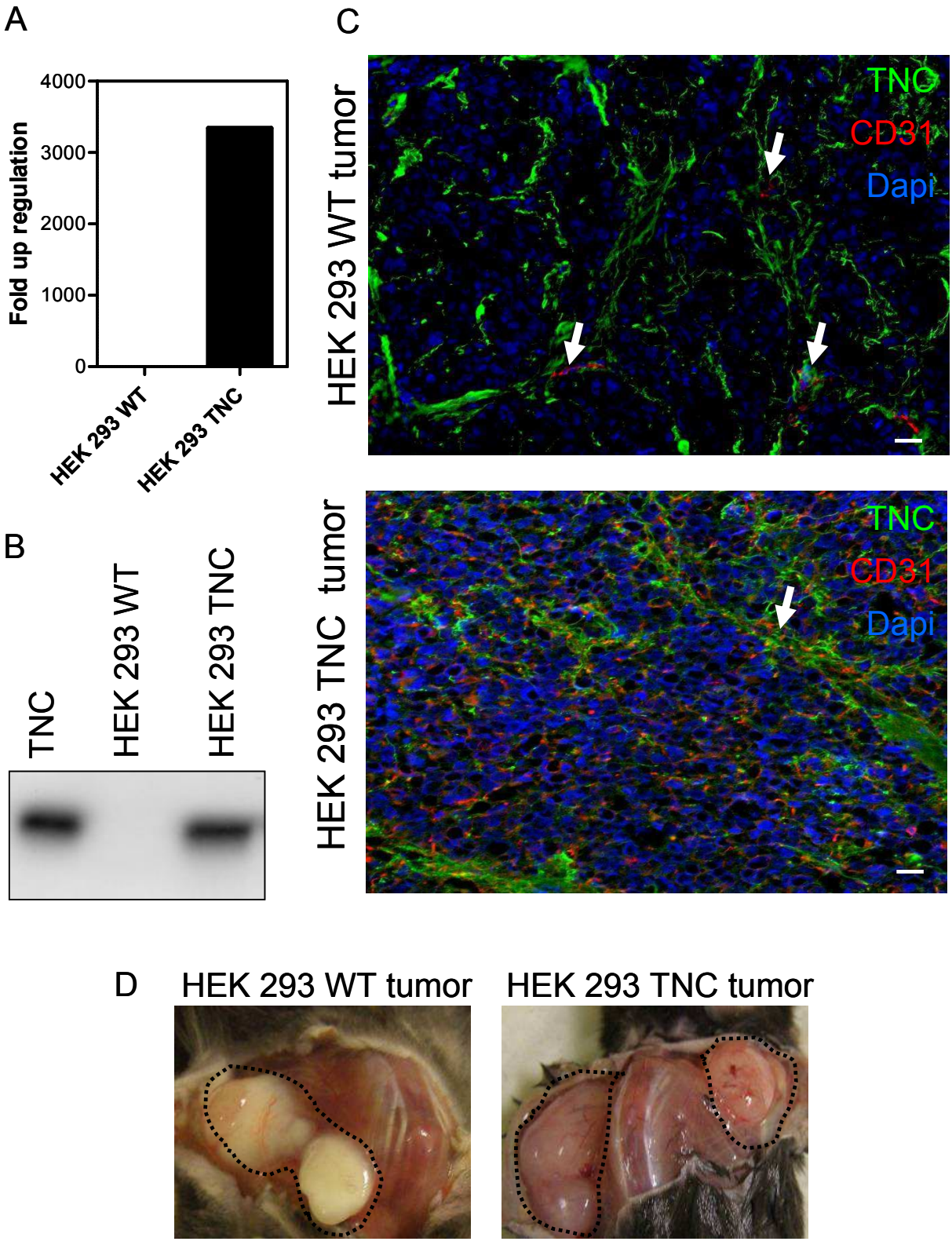

Figure 42: Consequences on tumor formation and ECM organization in a heterotopic grafting model with HEK293 cells overexpressing TNC. (A). qPCR analysis of cell extract of HEK293 WT and HEK293:TNC cells. **(B)**. WB analysis for TNC expression**. (C)**. Macroscopic pictures of tumors 5 weeks after injection of 2 million HEK293 and HEK293:TNC cells, respectively. Scale bars 20 µm. (**D)**. Representative pictures of HEK293 WT and HEK293:TNC tumors stained for CD31 in red and TNC in green. Arrow points at vessels in HEK293:TNC and in HEK WT tumors.

2. Establishment of immune-compromised Rag2KO mice lacking TNC expression for tumor cell grafting

TNC can be expressed by the tumor and the stromal cells of the host and it is not clear whether the cellular origin had an impact on the effects of TNC in tumorigenesis. Therefore, Rag2KO/TNCKO mice were generated by breeding. Moreover, to mimic the natural tumor microenvironment an orthotopic setting was chosen. Here, human SW480 colorectal carcinoma cells were injected into the caecum of Rag2KO wildtype or TNCKO mice. Mice were sacrificed after 6 to 8 weeks after grafting and exhibited tumors with high 71% (5/7) penetrance (Table 4).

Table 4: Summary of grafting experiment and treatment.

	Nude mouse		Rag2KO	Rag2KO/TNCKO
	orthotopic	subcutaneous	orthotopic	orthotopic
SW480shTNC	4/5	5/5	3/6	0/7
SW480wtTNC	22/28	5/5	5/7	6/8

SW480:shTNC were injected into 10 nude mice (5 orthotopic injections and 5 heterotopic sc. injections); control injections were done in 33 nude mice with SW480:cherry cells. 8 RagKO mice were injected with SW480shTNC and 7 with SW480 wtTNC cells.

Next, SW480 cells were orthotopically grafted into Rag2KO/TNCKO mice and also gave rise to tumors with a high penetrance of 75% (6/8) (Table 4). To address whether gross tumor morphology was different caecum tissue was stained by H&E. This analysis revealed that tumors had developed inside the muscular layer partially occluding the intestinal lumen (Figure 43). There were no apparent differences detectable between the different hosts. Upon immunostaining of tumor tissue from both hosts with a TNC antibody it was observed that TNC was highly expressed and had been organized into conduit like structures (Figure 43). In the Rag2KO/TNCKO host only unspecific background signal was obtained in the intestinal tissue (Figure 43B). This result suggests that tumor cell expressed TNC can be assembled into conduits.

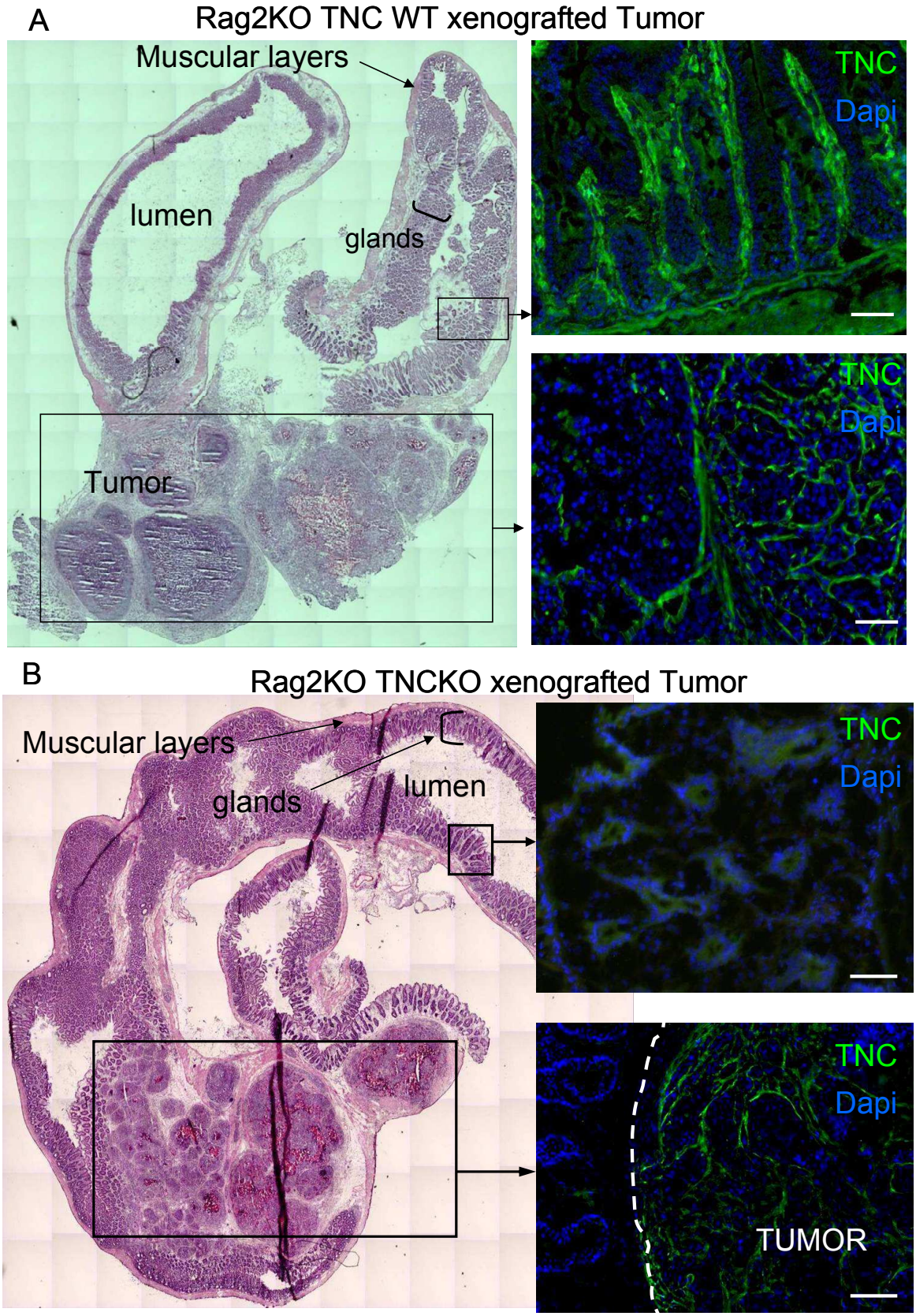

Figure 43: Histological and immunological characterization of the orthotopic xenografted SW480 tumors in the Rag2KO and Rag2KO/TNCKO mouse models. (A). General H&E overview (mosaic reconstruction picture) of orthotopic SW480 tumors in a Rag2KO/wtTNC mouse with higher magnification of the normal mucosa and tumor, corresponding to IF staining of TNC. Scale bar 50 µm. (**B**). General H&E overview (mosaic reconstruction picture) of an orthotopic SW480 tumor in a Rag2KO TNCKO mouse with higher magnification. Scale bars 50 and 100 µm.

A direct comparison of TNC expression levels between tumors of the two hosts showed that the TNC levels were several fold higher in a host that does express TNC in comparison to a host that lacks TNC (Figure 44). Although in a TNC-expressing host more TNC rich structures were observed, organization into conduits was detected in the TNCKO host. This observation suggests that both tumor and host cells contribute to the expression of TNC in tumor tissue and that organization into conduits does not depend on host-derived TNC. Alternatively the artificial absence of TNC in the stromal KO cells might induce tumor cell adaptation by upregulating TNC.

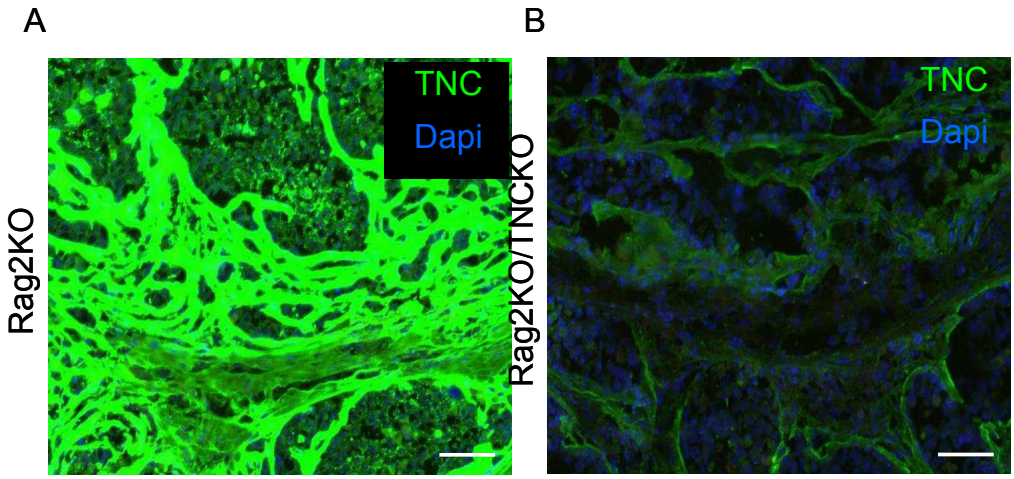

Figure 44: TNC expression in Rag2KO and Rag2KO/TNCKO SW480 orthotopic xenografted tumors. (A-B) were taken with the same exposure time to compare TNC level in Rag2KO and Rag2KO/TNCKO xenografted tumors. Scale bar 50 µm.

Next it was addressed whether tumor-derived TNC also had an impact on stromal cells such as endothelial cells and CAF as has been seen in other tumors (see part A). Therefore, tumor tissue of SW480 tumors grown in double KO mice (Rag2KO/TNCKO) were analyzed by immunostaining for CD31 and vimentin. It was observed that both cell types were surrounded by a TNC matrix in close apposition to it (Figure 45 A-B). By costaining for vimentin, and Mts1 (Figure 45 C-F), it turned out that the signals only partially overlapped which suggested that different types of activated fibroblasts are present in the tumor tissue (Kalluri and Zeisberg, 2006); CAF expressing vimentin and Mts1, and CAF that express only one of the markers.

Very few endothelial cells or CAF were found outside the TNC matrix which suggests that the TNC-rich microenvironment potentially provided a niche favouring survival and/or growth of these tumor associated cells. Finally, there were areas found with TNC conduits that did not exhibit endothelial cells (Figure 45 A-B). Nevertheless the tissue was not necrotic. This observation suggests that the TNC matrix might also play a role in diffusion of oxygen.

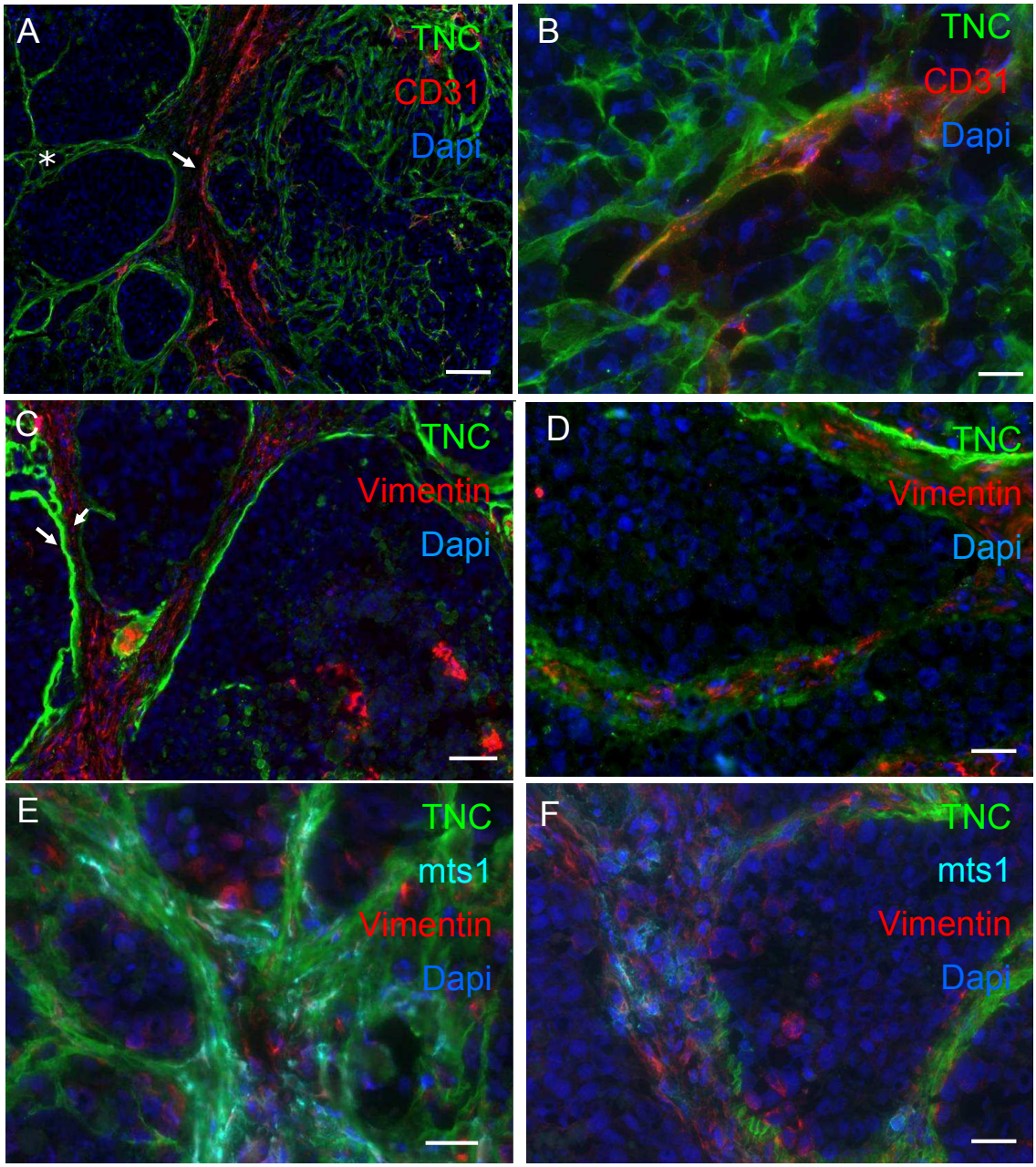

Figure 45: Characterization of the ECM and cellular tumor microenvironment in SW480 orthotopic xenografted tumors in a Rag2KO/TNCKO host. Representative pictures of TNC conduits **(A-B)**. Immunostainings of orthotopic xenografted tumor in Rag2KO/TNCKO host representing endothelial cells (red signal). Note that in some areas TNC covered blood vessels (arrow) and at some places TNC organized into conduits, which were not blood vessels (asterisks). **(C-D)**. Immunostainings presenting TNC organization (green) into conduits (white arrows) filled with

fibroblasts (red signal). **(E-F)**. Immunostainings of TNC, vimentin and Mts1 in orthotopic xenografted tumor demonstrating that Mts1 positive cells as well as vimentin positive cells could be found into TNC rich tubular structures. Scale bars 100 µm (**A)** and 50 µm **(C)**, 20 µm (**B, D, E** and **F**).

To address whether tumorigenesis is dependent on TNC, SW480 cells were engineered to down regulate TNC by shRNA technology using three differents shTNC lentiviruses (Figure Figure 46). As determined by qRT-PCR, knockdown cells did essentially not express TNC (Figure 46A). Orthotopic injection of SW480 shTNC cells into Rag2KO mice lacking TNC had been done and tumors could not be found in all seven injected Rag2KO/TNCKO mice which was done in three different experiments (Table 4). Microscopical inspection of the caecum did not reveal any abnormalities. A proper control experiment with engraftment of SW480 shTNC cells into Rag2KO mice has been done and 3 out of 6 mice develop tumors. This observation suggests that SW480 shTNC tumor cells did not engraft into a host that lacked TNC.

There are several possibilities to explain these results, first in SW480 cells a TNC knockdown may have consequences on proliferation. This was tested in cell culture. But proliferation in SW480 shTNC cells remained unchanged compared to the parental cells with wildtype TNC levels (Figure 46B). Another possibility is that SW480 shTNC cells are dependent on TNC and therefore cannot form tumors. To address this possibility SW480 shTNC cells were injected under the skin and into the caecum into nude mice exhibiting endogenous TNC. In both conditions engrafting and tumor formation occurred with a high penetrance of 100% (5/5) and 80% (4/5) upon subcutaneous and orthotopic grafting, respectively (Table 1). In conclusion, TNC appeared to be necessary for tumor initiation upon orthotopic implantation of SW480 cells in the caecum.

A

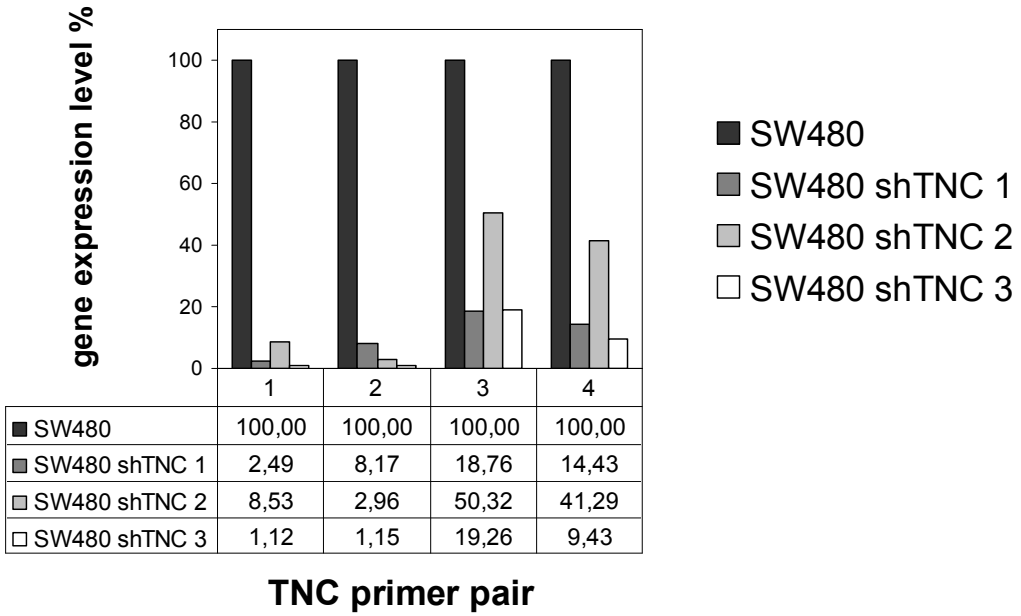

	1	2	3	4
SW480	100,00	100,00	100,00	100,00
SW480 shTNC 1	2,49	8,17	18,76	14,43
SW480 shTNC 2	8,53	2,96	50,32	41,29
SW480 shTNC 3	1,12	1,15	19,26	9,43

TNC primer pair

B

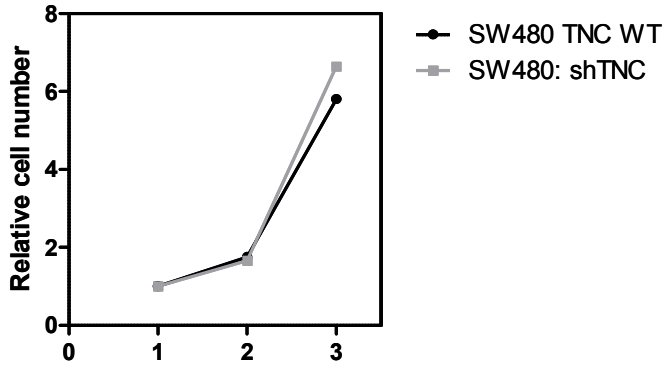

Figure 46: Characterization of SW480 shTNC cells. (A). qPCR analysis with different TNC primer pairs, showing downregulation of TNC expression in SW480 shTNC cells. ShTNC 1, 2 and 3 correspond to different cell lines that were derived upon transduction of three lentivirues expressing different shTNC sequences (see Material and Methods). Values are given in percentage**. (B).** Proliferation of SW480 and SW480 shTNC was determined after the indicated time points by using the MTS assay.

Together these experiments revealed that both tumor and stromal cells express TNC that was assembled into matrix-rich conduits. These TNC structures can already form if only tumor derived TNC is available. Moreover, whereas tumor-derived TNC tubes are less pronounced than structures formed by TNC of both cellular origin they appeared to have similar properties since they surrounded endothelial cells and CAF which is suggestive of the TNC matrix as providing a favourable niche that promoted survival and/or expansion of these cells.

It is possible that the relative failure of anti-angiogenic therapy such as the one using Bevacizumab (Bev) (Couzin-Frankel and Ogale, 2011) could be due to an adaptive response involving the tumor microenvironment, and in particular TNC. The aim of this part was to establish an in-vivo model suitable to address the potential roles of TNC and of the tumor microenvironment on anti-angiogenic drug resistance and tumor recurrence. Here the effect of Bev was determined on angiogenesis. Therefore, three consecutive experiments (named A (for Avastin) 1-3) were done with 9 (A1), 10 (A2) and 32 (A3) mice (Table 5). SW480:cherry cells were orthotopically grafted into the caecum of nude mice and, 5 weeks later mice were treated with Bevacizumab or NaCl (control) for another two weeks. Directly after the end of the treatment one group was sacrificed (T0), tumor tissue was prepared and analyzed. Another group was kept for another week (T1) to see whether removal of Bevacizumab had an impact on tumor angiogenesis.

Table 5: Summary of mice that survived the grafting experiment and treatment and that were used for analysis.

	All	C0	T0	C1	T1
A1	9	2	3	2	2
A2	10	1	4	1	4
A3	31	5	9	9	8
Total	50	8	16	12	14

Mice were classified into different groups, C0 and C1 corresponding to the control mice, that were sacrificed just after the end of the treatment (C0) and one week later (C1), respectively. T0 and T1 represent those mice that were Bevacizumab treated and sacrificed just after the treatment (T0) or one week later (T1).

1. Monitoring tumorigenesis by live imaging

SW480 cherry cells had been engineered to express the red fluorescent protein cherry which can be visualized by live imaging in the NightOwl bioluminometer. As can be seen in Figure 47 SW480:cherry derived caecum tumors can be imaged in the living mouse, before treating the mice, thus it was confirmed that mice had developed tumors before treatment was started.

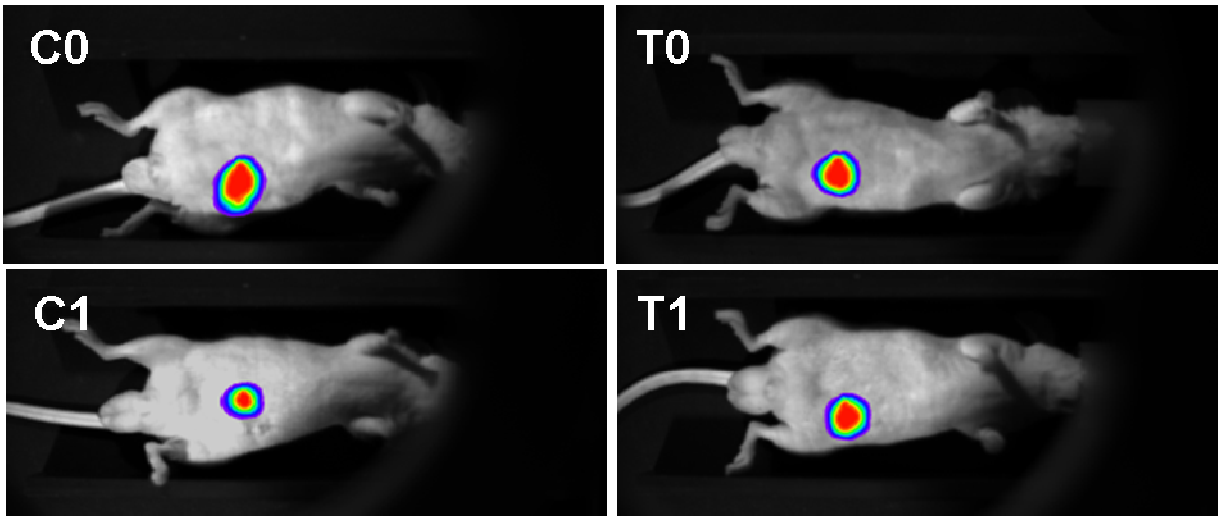

Figure 47: NightOwl pictures showing tumor growth in the xenografted nude mice. These pictures were taken 5 weeks after engraftment of SW480 cherry cells into the caecum wall. C0 and C1 correspond to control mice and T0 and T1 to the Bevacizumab treated mice, which were sacrificed just after the treatment (C0, T0) and one week after the end of the treatment (C1, T1). The red colour characterizes the strongest fluorescent signal, whereas the blue colour represents the weakest signal.

2. Histological characterization

To monitor a potential effect of Bevacizumab on tissue morphology, tumor sections were stained with H&E which revealed proliferative and necrotic areas in the tumor xenograft (Figure 48). There were no obvious differences noticed between Bevacizumab and control tumors but a detailed analysis should be performed to address a potential enhancing effect of Bevacizumab on necrosis. In the following experiment, only non-necrotic tissue was further analyzed to avoid unspecific trapping of the antybody.

First it was determined whether SW480-derived tumors would recapitulate important features of human CRC such as vascularization with pericyte coverage and expression of TNC. Indeed upon staining for CD31 and NG2 it was noted that xenografted tumors were vascularised with partial coverage by pericytes reminiscent of human CRC (Figure 49). In the tumor xenografts endothelial cells were also embedded into a TNC rich matrix similar to human CRC (Figure 50). Thus this model recapitulates features of human CRC and thus presents a suitable model to address the role of an anti-angiogenic treatment on tumorigenesis.

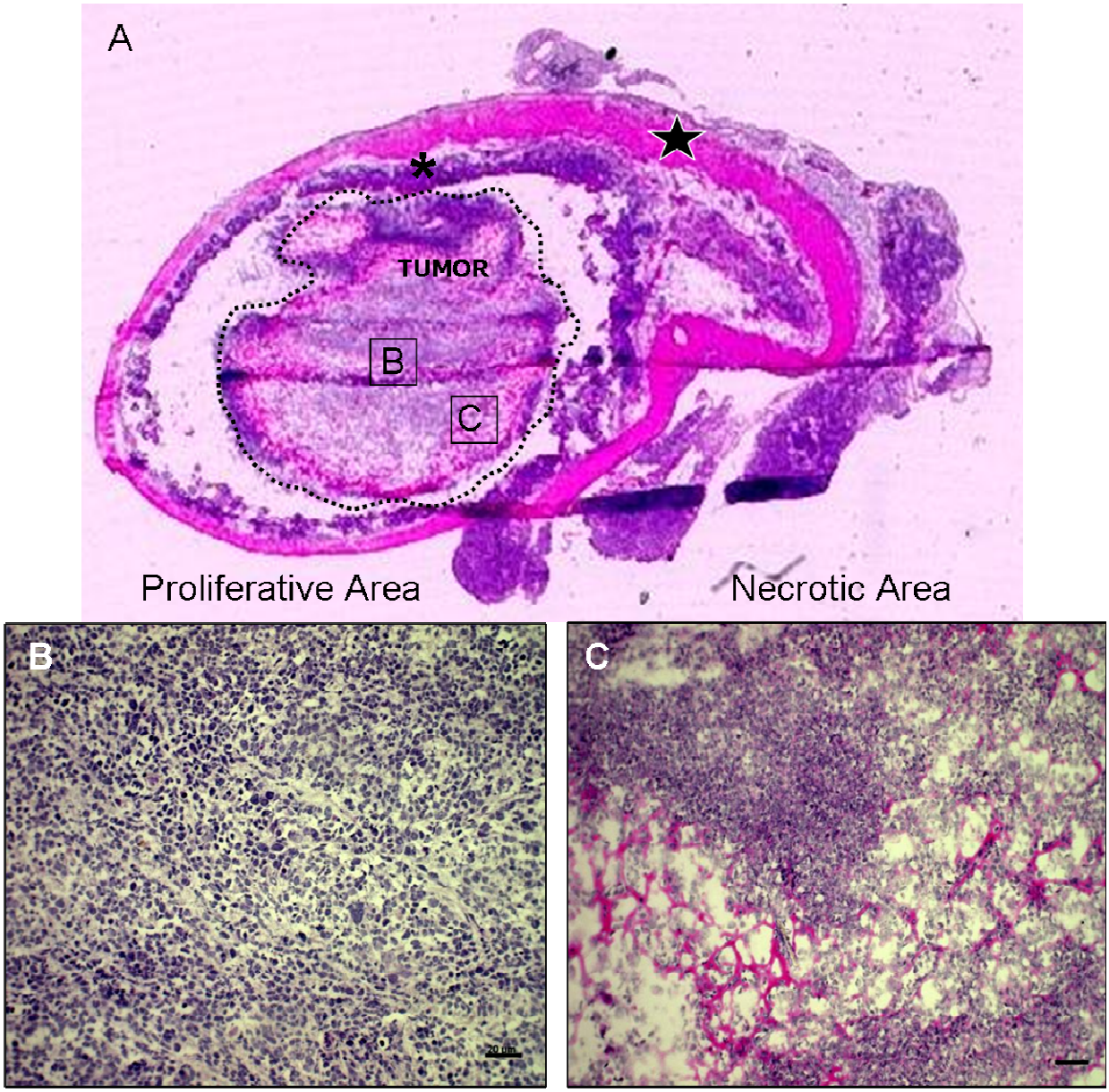

Figure 48 : Histology of caecum xenografted tumors. H&E staining of orthotopic tumor. **(A).** Global overview of the tumor upon grafting into the caecum. **(B).** H&E (Harris) staining corresponding to the tumor center**. (C).** H&E picture corresponding to a necrotic area**.** Black star: muscle layer and black asterisk: caecum wall. Scale bar 20µm.

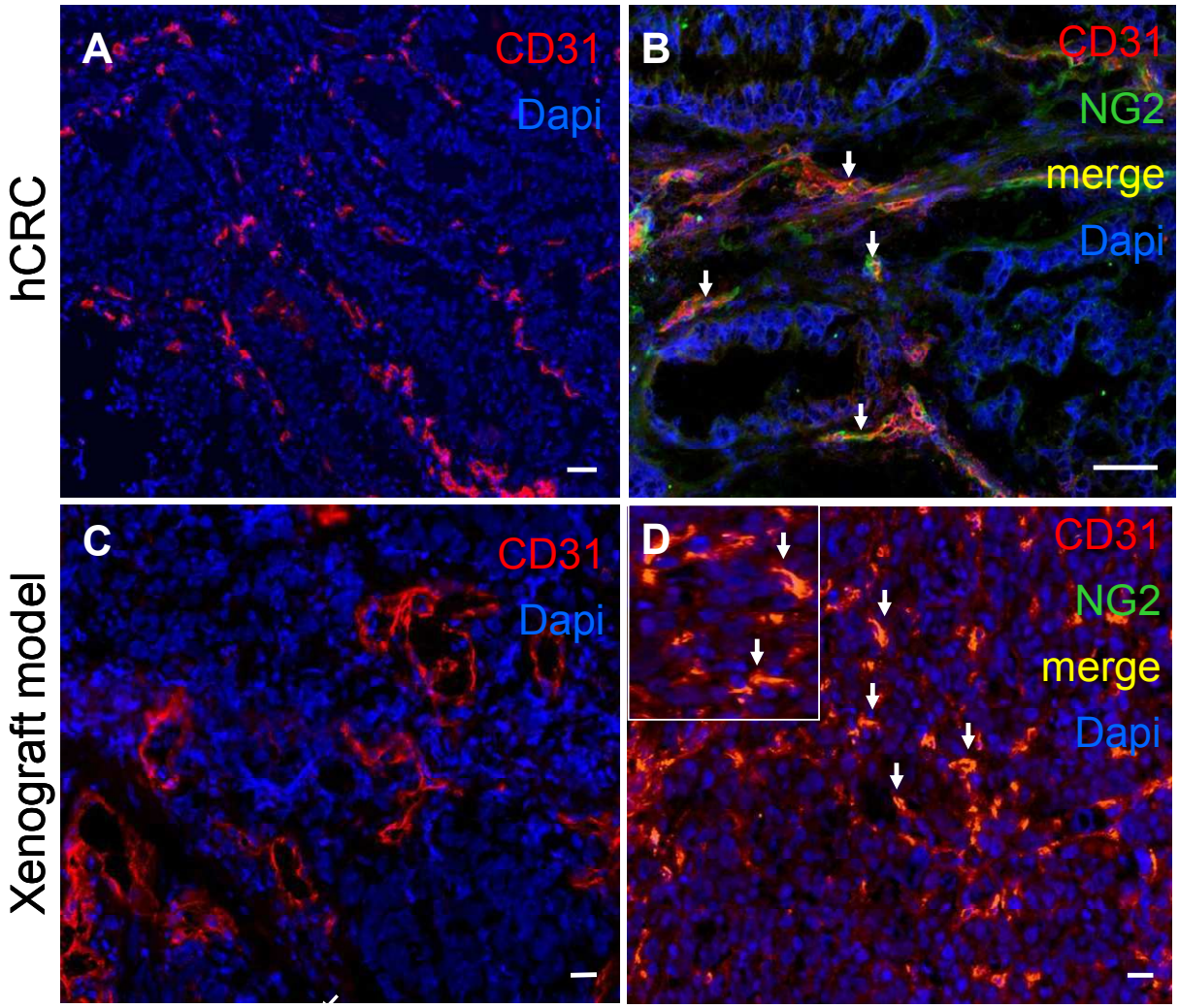

Figure 49 : Immunophenotypic characterization of stromal cells in human colorectal cancer cell line xenografts and human CRC. (A and C). Immunostainings of endothelial cells in human CRC **(A)** and in a orthotopic SW480 xenograft model **(C)**. Red signal corresponds to CD31. **(B and D).** Immunostainings of endothelial cells (red), of pericytes (green) and in human colorectal cancer (**B**) and orthotopic xenograft model **(D)**, merge between the red and green signal is represented in yellow and is pointed at with arrows. Scale bars 50µm (**A**, **B** and **D**), 20 µm **(C)**.

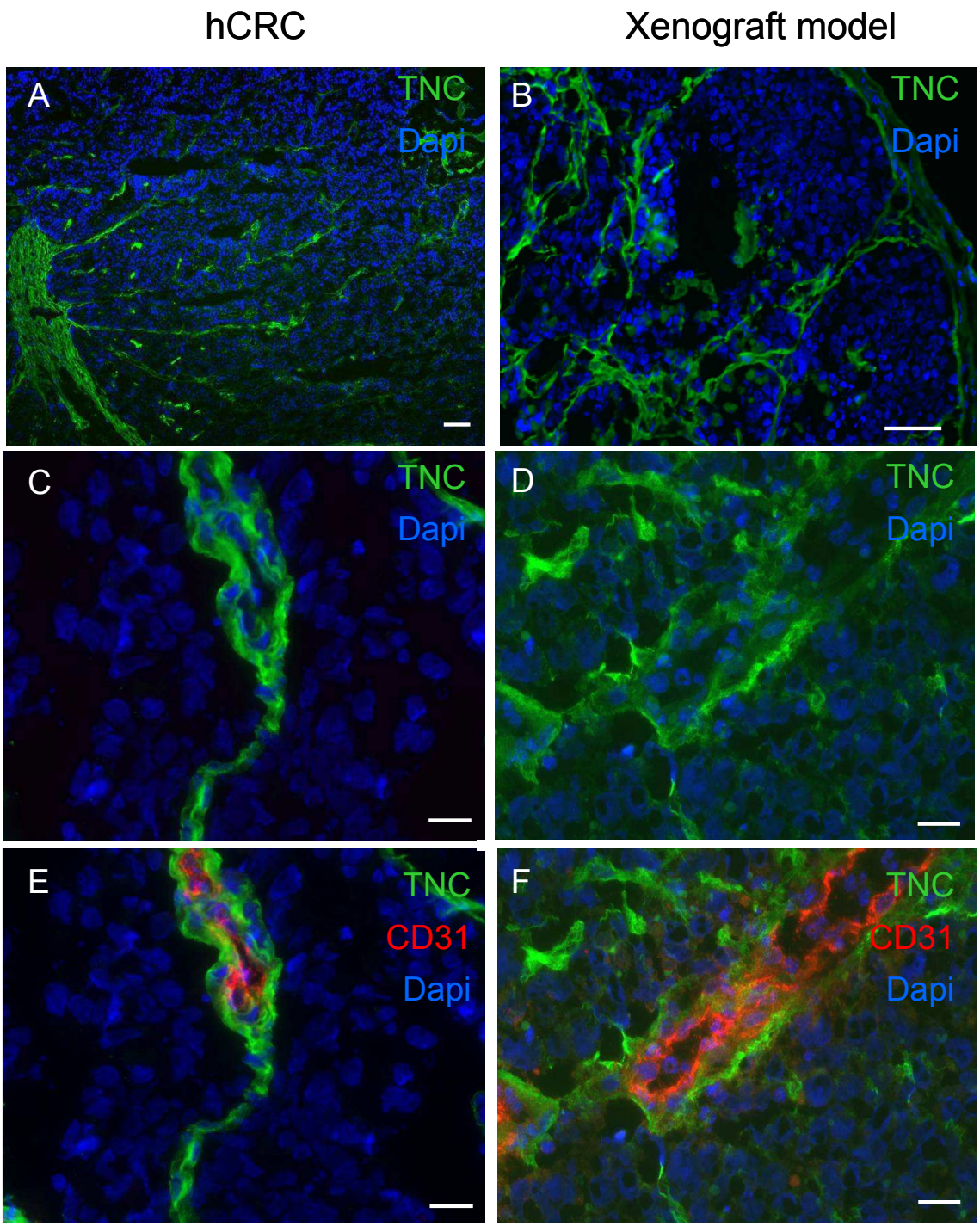

Figure 50: Immunostaning for the ECM molecule TNC in human CRC and in orthotopic xenografted tumors. (A-B) Immunostainings of hCRC **(A)** and of orthotopic tumor **(B**) representing TNC expression in green. **(C-F)** Pictures showing TNC expression in human tumor **(C)** together with endothelial cells **(E)** and in an orthotopic tumor in **(D)** and **(F).** Scale bars 50 µm **(A** and **B)**, 20µm **(C, D, E** and **F)**.

3. Effect of Bevacizumab on the tumor vasculature

A potential anti-angiogenic effect of Bevacizumab was determined by CD31 staining (Figure 51A) that was subsequently quantified with the Image J software (Figure 51C). It was seen that CD31 expression was very heterogenous in both the controls and the two treated groups. However, between the control group C0 and the treated group T0, a decrease of CD31 area fraction was observed, demonstrating that the treatment had triggered an anticipated anti-angiogenic response (Figure 51C). But after one week, the effect on CD31 was gone, since there was no difference between the control group C1 and the treated group T1 detectable anymore (Figure 51C).

TNC expression was addressed by immunostaining. It turned out that the expression was too heterogenous which was partially due to bad tissue and staining quality. Therefore the staining protocol needs to be optimized before quantification is possible.

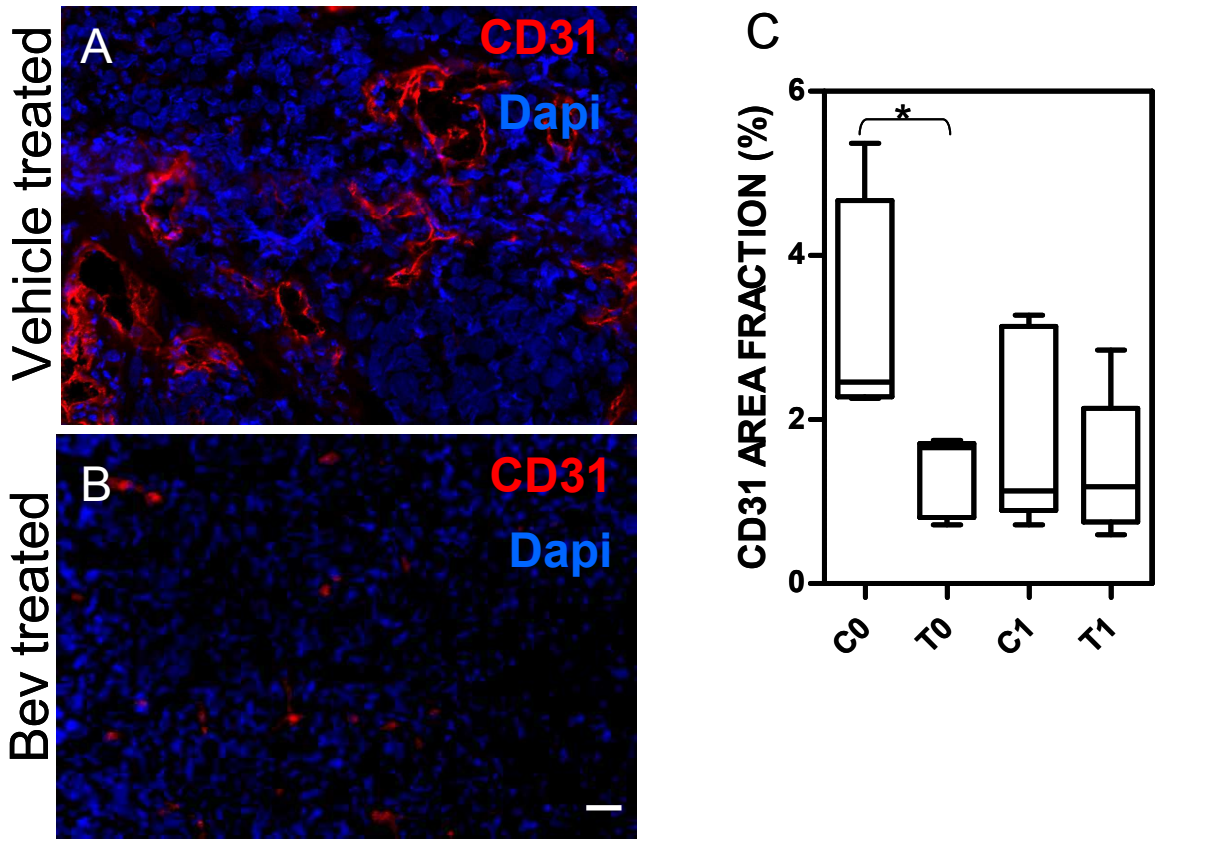

Figure 51: Quantification of CD31 in Bevacizumab and vehicle treated mice. (A-B). Representative pictures of endothelial cells in tumor of Bevacizumab **(B)** and in vehicle treated **(A)** mice**. (C).** Quantification of CD31 area fraction in percentage in the control and treated mice that were sacrificed after the end of the treatment (C0 and T0) and the mice that were sacrificed one week after the end of the treatment (C1 and T1). p value= 0.0159, Mann-Whitney test**.**

4. Effect of Bevacizumab on liver metastasis

To address whether Bevacizumab treatment potentially had an effect on metastasis was addressed by live imaging of disseminated cells at the end of the experiment (Figure 52). A fluorescent signal was observed in all experimental groups, indicating that the primary tumor cells had disseminated and had formed liver metastasis (Figure 52). Whereas both control groups exhibited a lower fraction of 33% and 20% of mice displaying fluorescence positive livers in the C0 and C1 groups, respectively, a high fraction of 67% and 75% of mice exhibited fluorescence positive livers in the T0 and T1 groups, respectively (Figure 52 and Table 6). This was in contrast to lung metastasis which was not observed. This results suggests that Bevacizumab treatment had increased liver metastasis substantially.

Table 6: Mice with liver metastasis in control mice and after Bevacizumab treatment

	C0	T0	C1	T1
Number	1/3	4/6	1/5	6/8
%	33	67	20	75

The number of mice exhibiting metastasis is compared to the total number of analyzed mice and presented in %.

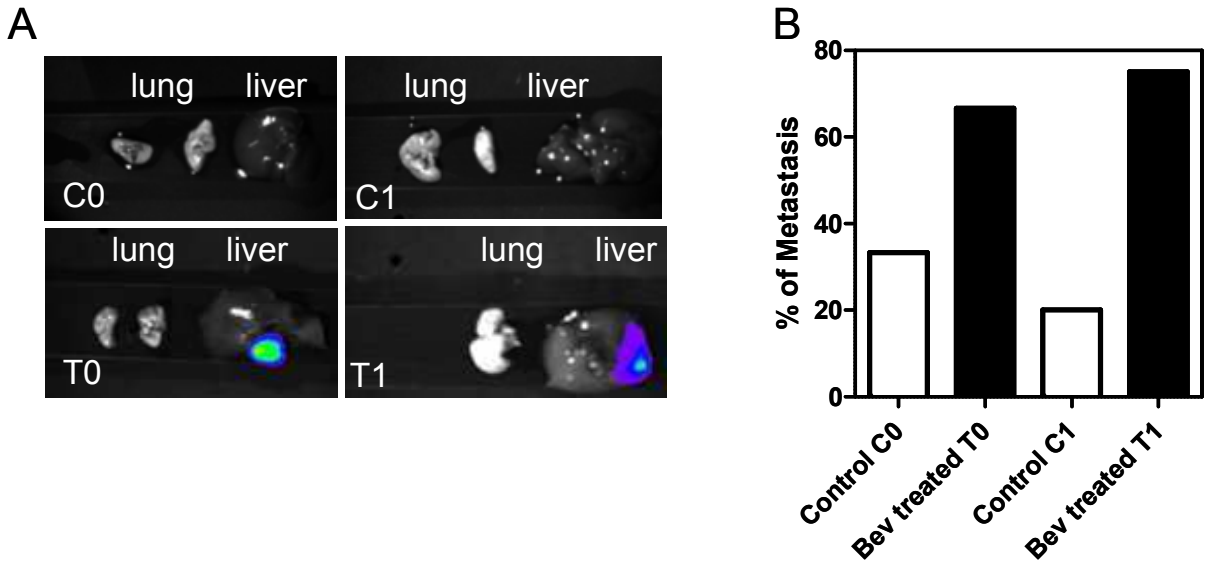

Figure 52 : Metastasis analysis in Bevacizumab treated mice. (A). NightOwl images corresponding to the different groups of Bevacizumab treated mice C0 and C1 for control and T0 and T1 for Bevacizumab treated mice. Organs had been prepared and were analyzed for signal emission. **(B).** Graphic representation of metastasis.

In summary, this experiment had shown that the xenograft model recapitulates important features of human CRC and that the treatment with anti-angiogenic Bevacizumab showed an effect in the majority of mice. In contrast to a decreased angiogenesis an enhanced liver metastasis was observed. It is possible that the fraction of necrotic tissue per tumor needs to be taken into account as readout for a response toward Bevacizumab. More experiments are needed to address these possibilities in detail. Importantly, despite a noticed anti-angiogenic effect Bevacizumab promoted liver metastasis. The underlying mechanisms and a potential involment of TNC need to be addressed in the future.

Discussion

DISCUSSION

The major interest of this study was the characterization of TNC expression in the tumor microenvironment of human cancers and murine cancer models. It further illustrates the crucial importance of TNC in tumor stroma that was described in previous studies correlating its high expression with bad prognosis in various tumor contexts (Midwood et al., 2011). In the present work we gathered new information concerning the specific distribution of TNC around tumor-associated vascular structures and established a link between its expression, tumor progression and angiogenesis in the Rip1Tag2 tumorigenesis mouse model. In addition we developed an orthotopic human colorectal cancer xenograft model in the mouse in order to evaluate anti-angiogenic therapy impacts on the tumor microenvironment. Given the differences of tissue organization and homeostasis between mouse and human, we first validated our cancer models by demonstrating that at least some characteristics of the human tumor microenvironment, such as TNC expression and distribution, were recapitulated in the murine tumors.

By analyzing tumor tissue of human insulinomas and human colorectal carcinomas we observed that TNC was organized into specific ECM "conduit-like" structures where endothelial cells and CAF were detectable. In the murine tumor models of spontaneous tumorigenesis, i. e. the Rip1Tag2, APC^{1638V} (Fodde et al., 1994) and $Kras^{V12G}$ (Janssen et al., 2002) mice, TNC was also expressed into these conduits. Further illustrating the relevance of this specific expression pattern, through heterotopic or orthotopic grafting of human tumor cells or human tumor material in immune compromised nude or Rag2KO mice, we also discovered TNC organization into tubular ECM fibers in close vicinity with endothelial cells and CAF. Altogether, this recurrent organization of TNC into matrix channels, observed in all analyzed tumors and tumor models, strongly suggests that these conduits might play a role in crucial steps of tumorigenesis. In the following section, this organization of TNC in the tumor microenvironment and potential implications on tumor angiogenesis and metastasis will be discussed.

1. TNC effects on tumor cells – impact on proliferation, migration, invasion and dissemination

In the RT2 model, TNC appeared to exhibit an early effect on tumorigenesis. We evidenced an increased proliferation of RT2/TNC islets as compared to RT2 controls suggesting that TNC may promote the progression of SV40Tag transformed cells into tumorigenic cells. Small tumors in 10 and 14 week old RT2/TNC mice seemed to be present in increased numbers than in RT2 counterparts. As fold change was close to statistical significance these preliminary observation would warrant further assessment on a larger set of mice (see Saupe, Gasser, Jia et al., manuscript in preparation, Annex1).

Contact of tumor cells with the TNC matrix may also promote their invasion. This assumption is supported by the observation that RT2/TNC mice exhibited more invasive carcinomas than RT2 littermates (Saupe, Gasser, Jia et al., manuscript in preparation, Annex1). Among these candidates, syndecan-4 is an ECM receptor which controls proliferation and migration of tumor cells (Huang et al., 2001). Interestingly, TNC was shown to inhibit syndecan-4 signalling in GBM cells and restoration of syndecan-4 activity reversed the TNC proliferation promoting effect in cultured GBM cells. In combination with pro-migratory factors such as LPA and PDGF it was seen that a TNC substratum could promote migration (Lange et al., 2008). Another study revealed that in a gain of function experiment activation of Wnt signalling increased the expression of Pdgfrα and β as well as proliferation of smooth muscle precursor cells (Cohen et al., 2009). They demonstrated that this effect was in part mediated by direct transcriptional regulation of TNC which was necessary and sufficient for Pdgfrα and β expression in lung explants. De Wever and collaborators (2004) demonstrated that myofibroblasts obtained by stimulation with transforming growth factor (TGF β) stimulated invasion of CRC into Coll I enriched matrigel. They identified two proinvasive agents secreted by myofibroblasts, scatter factor/ hepatocyte growth factor (SF/HGF) and TNC, each of them necessary but not sufficient.

2. TNC effects on tumor associated cells – role in angiogenesis

2.1 TNC effects on tumor associated cells

We had shown that the extent of angiogenesis correlated with the TNC copy number in transgenic RT2 mice. Indeed, an increased number of CD31 positive structures was detected in RT2/TNC than in RT2 tumors and angiogenesis was stimulated in RT2 as compared to RT2/TNCKO tumors (Saupe, Gasser, Jia et al., manuscript in preparation, Annex1). These observations suggest that TNC promotes angiogenesis in this stochastic tumor setting. Recently, Alves and collaborators (2011) had shown that a TNC-enriched matrix is implicated in the formation of defective tubular networks *in vitro*, which suggests that the presence of TNC in the tumor microenvironment may provide additional cues for endothelial branching morphogenesis.

TNC had previously been shown to act as a chemoattractant for endothelial cells and to promote transdifferentiation of neuroblastoma tumor cells into endothelial cells (Pezzolo *et al.*, 2011), to promote aggregation of endothelial cells which is reminiscent of early steps in tubulogenesis (Martina et al., 2010; Schenk et al., 1999) and to promote apoptosis with subsequent selection for highly proliferative endothelial cells (Alves et al., 2011). It was also shown that TNC promotes endothelial cell spreading and migration and vascularization of cardiac allografts since this was largely reduced in mice lacking TNC expression (Ballard *et al.*, 2006). We also had shown that TNC promoted sprouting angiogenesis in the CAM assay (Saupe, Gasser, Jia et al., manuscript in preparation, Annex1).

In RT2 tumors CAF and macrophages are found intermingled with TNC matrix. CAF are implicated in key steps of tumorigenesis; they play a role in cancer initiation (Olumi et al., 1999; Bhowmick et al., 2004), in cancer progression (Orimo et al., 2005) and in metastasis (Olaso et al., 1997). In addition, CAF exhibit pro-tumoral functions, such as promoting tumor cell survival, proliferation, and dissemination (Mantovan et al., 2002; Pollard 2004; Talmadge et al., 2007). CAF are considered as a major source of TNC (Degen et al., 2007) and also can be attracted by TNC (Gaggioli et al., 2007) suggesting a

close interdependence. Given that more CAF are found in RT2/TNC tumors it is possible that CAF contributed to enhanced angiogenesis.

In RT2 and RT2/TNC tumors immune cells were found in close contact with the TNC conduit. Indeed, inflammatory cells were shown to be an important actor in cancer (Coussens and Werb, 2002; de Visser et al., 2005). It is accepted that TAM show pro-tumoral functions, and can mediate tumor cell survival, proliferation, and dissemination (Mantovan et al., 2002; Pollard, 2004; Talmadge et al., 2007). In addition, high levels of TAM are often correlated with a bad prognosis. They secrete products such as reactive oxygens and proteinases (Gungor et al., 2009; Knaapen et al., 2006), which could promote proliferation, angiogenesis and metastasis (Huh et al., 2010). Therefore a quantification of TAM in tumors of both genotypes needs to be done in the future to address a potential angiogenesis promoting effect of these cells in RT2/TNC tumor angiogenesis.

Several bone marrow derived cells had been described to promote tumor angiogenesis upon recruitment into the tumor tissue (Grunewald et al., 2006; DePalma et al., 2005; Lyden et al., 2001) and it remains to be determined whether they play a role in TNC enhanced tumor angiogenesis which can be addressed in the RT2 model with different TNC expression. However the underlying molecular mechanisms involved in the TNC proangiogenic effect are yet poorly defined. Several candidate pathways notably a potential link of TNC to Wnt signaling and enhanced angiogenesis will be discussed.

2.2 Wnt/β-catenin pathway and angiogenesis

The Wnt/β-catenin pathway has been characterized as promoting vascular morphogenesis in the embryo and in organ-specific endothelial differentiation (reviewed by Dejana et al., 2010). In addition, cultured endothelial cells displayed activation of Wnt signalling and expressed multiple ligands, receptors and secreted modulators of Wnt signalling (Goodwin

et al., 2006). *In vivo* studies confirm that several Wnt ligands and Wnt inhibitors can regulate blood vessel formation (Wang et al., 2006).

In tumor cells cultured on a TNC substratum an increased expression of Wnt target genes such as fibronectin, Slug and Id2 was observed (Anja Heinke, personal communication). Moreover, in RT2/TNC tumors expression of some Wnt target genes such as cyclin D1, cyclin D2, CD44 and Slug was increased but it is not known in which cells this increased expression occurred. Nuclear β-catenin was eventually observed in RT2/TNC tumors but appeared to be a rare and local event (Saupe, Gasser, Jia et al., manuscript in preparation, Annex1).

2.3 DKK1 and angiogenesis

To address whether DKK1 levels had an impact on tumor angiogenesis, I had grafted osteosarcoma cells engineered to overexpress DKK1 under the skin of nude mice and had observed that these cells failed to induce vascularised tumors. Whereas proliferation of the DKK1 overexpressing cells was not diminished *in vitro* nor *in vivo*, tumors derived from DKK1 overexpressing tumor cells remained smaller which is presumably due to the reduced angiogenesis. Thus these observations suggest that DKK1 had a paracrine effect on tumor associated cells most likely on endothelial cells, CAF or other pro-angiogenic cells. The published role of DKK1 in tumor angiogenesis and progression is controversial. In colon cancer DKK1 is downregulated in comparison to the surrounding normal tissue (Gonzalez-Sancho et al., 2005). Whereas DKK1 is low in breast cancer cells with osteoblastic metastatic potential, DKK1 is highly expressed in breast cancer with an osteolytic metastasis potential and, DKK1 promoted osteolytic metastasis in myeloma (Pinzone et al., 2009). Finally, overexpression of DKK1 in canine Ace-1 prostate cancer cells promoted their metastatic potential upon intracardiac injection (Thudi et al., 2010).

2.4 Potential link between TNC and DKK1

Min and colleagues had demonstrated, that DKK1 and DKK2 are two regulators of Wnt signalling, with opposing functions in angiogenesis. They demonstrated that DKK2 stimulated filopodial dynamics and promoted endothelial cell proliferation/sprouting in an ischemia assay in mice. This activity was antagonized by DKK1 (Min et al., 2011). Preliminary results from the RT2 model do not support a potential role of DKK2 since there was no increased expression of DKK2 observed in RT2/TNC tumors (Falk Saupe, personal communication). Moreover, DKK2 was also not induced in several tumor cell lines on a TNC substratum while DKK1 was repressed under the same conditions (Anja Heinke, personal communication). Thus activation of Wnt signalling through repression of DKK1 by TNC may explain enhanced tumor angiogenesis by TNC in RT2 tumors.

We had shown an inverse correlation of the TNC copy number and DKK1 expression levels in RT2 tumors with knockout wildtype, and overexpression of TNC, which suggested a functional link of TNC to DKK1 repression, to Wnt signalling and enhanced angiogenesis.

3. Potential mechanism of TNC conduit formation and function

Previously it had been demonstrated that tumor vessels are tortuous, heterogenous and structurally abnormal (Jain et al., 2001, Mazzone et al., 2009, Nagy et al., 2010). Here, we demonstrated that tumors of RT2/TNC mice display an increased number of endothelial cells. But blood vessels appeared chaotic and were presumably less functional in blood supply which is supported by the observation that bigger tumors were less vascularized and less prominent in RT2/TNC mice (Falk Saupe, personal communication). We demonstrated the presence of atypical vessels by TEM and SEM in RT2/TNC tumors which were not seen in RT2 tumors suggesting a link to TNC expression levels. These atypical vessels exhibited a rough apical surface where matrix appeared to leak into the lumen. In addition, we also observed matrix rich conduits that lacked vessel features such as a basement membrane and lining endothelial cells. These conduits contained erythrocytes and presumably tumor cells which suggests a connection to the circulation. These conduits

did not appear to represent hemorraghies since signs of destroyed erythrocytes were missing.

These observations strongly suggest a functional link of TNC expression levels to tumor angiogenesis processes, in particular the distribution and specific deposition of TNC in subendothelial ECM may have a crucial impact on the establishment of an aberrant tumor-associated vessel network.

The conduits were lined by a thick ECM layer and atypical tumor cells. In 1999, Maniotis reported that blood vessels of highly aggressive uveal melanomas are formed by tumor cells and lacked endothelial cells. This novel concept in tumor vascularization was termed vasculogenic mimicry (Maniotis et al., 1999). This concept has gained credibility from recent evidence (Yao et al., 2011; Comito et al., 2011; Sun et al., 2011), but is still controversially discussed (McDonald and Foss, 2000). The presence of these networks is associated with bad prognosis. Electron microscopy has shown that during vasculogenic mimicry, channels are lined by a layer of ECM material and that a layer of tumour cells surrounded the ECM channels. Whether the TNC conduits represent vasculogenic mimicry needs to be addressed in 3D culture experiments in the future.

It is possible that TNC conduits represent the result of vessel pruning and may represent "mosaic vessels" which are characterized by endothelial cells that have lost their polarity and had died thus exposing tumor cells to the circulation with vessels that are highly leaky (Jain et al., 1988; Jain et al., 2005; Pettersson et al., 2000).

Our data showed that cells expressing β1 chain containing integrins are directly adjacent to the TNC conduits which raises the possibility that integrin mediated ECM interactions play a role in conduit formation. It needs to be addressed which β1 integrin heterodimers are expressed in these cells which may allow to deduce relevant cell – ECM interactions in conduit formation and maintenance. We had seen that cells expressing the α6β1 integrin

are adjacent to the conduits. This integrin was shown to be overexpressed in hepatocellular carcinoma (Le Bail et al., 1997; Carlioni et al., 1998) and its overexpression was associated with enhanced tumor growth. Integrins are major receptor for mechanotransduction (reviewed in Papachristou et al., 2009) and thus interactions of cells with the conduits through integrins could transduce a signal into the cells that potentially has an impact on their physiology. Indeed TEM analysis revealed that conduit lining tumor cells had a very different appearance as e.g. a reduced number of secretory vesicles. This raises the question whether these adjacent cells are involved in conduit formation and/or are transdifferentiating into other cells such as endothelial cells upon contact with the ECM in the conduits. Finally, integrin antagonists have been or are currently developed for anti-cancer intervention strategies. It will be interesting to see whether anti-β1 integrin targeting drugs potentially have an impact on the conduits.

Tumors including RT2 insulinomas were described to be surrounded by a capsule that is composed of ECM including OPN and TSP1 (Gulubova and Vlaykova, 2006). It was speculated that this capsule potentially protects the tumor from infiltrating immune cells. Moreover, OPN and TSP1 were shown to associate with LM which appears to modulate cell migration, survival and angiogenesis (Liaw and Crawford, 1999). Here we have shown that this capsule does express TNC in addition to OPN and TSP1. In RT2/TNC tumors more tumors exhibited a disrupted capsule thus displaying more carcinomas. Potentially this disruption of the capsule is linked to an increased number of infiltrating macrophages and fibroblasts as observed in RT2/TNC tumors. Our data also suggest that the capsule potentially serves as starting point for the formation of TNC containing ECM conduits.

Based on the observations presented in this study, we propose a working hypothesis in construction of TNC-driven ECM scaffolds that enable angiogenesis and metastasis (Figure 53). This possibility is supported by our observation that TNC is locally expressed at several sites which appear to grow in size and while increasing in size attracting endothelial cells and CAF and potentially other pro-angiogenic cells. This observation is not

in line with pruning as a potential mechanism of TNC conduit formation. In a tumor, several factors such as growth factors, cytokines and hypoxia as well as mechanical stress can trigger CAF, tumor cells and other cancer associated cells such as TAM, or other immune cells to secrete TNC (Orend & Chiquet-Ehrismann 2006, Midwood & Orend 2009). We observed in RT2 tumors a massive invasion of macrophages and CAF. Whether these cells express TNC needs to be addressed by in situ hybridization and/or FACS analysis. Tumor xenografting experiments into a TNC negative host showed that TNC assembles into conduits when expressed by the tumor cells. In addition in RT2/TNC tumors human TNC is expressed by the tumor cells and in both cases tumors expressed TNC assembled into conduits. Cancer associated cells are closely linked to TNC and some immunostaining results suggest that these cells might prepare space within the tissue, that is filled with matrix molecules such as LM, TNC, Coll IV, Coll V, Procoll III and FN. This hypothesis is supported by Gaggioli and colleagues who demonstrated that CAF prepare tracks into collagen enriched matrigel where they deposit TNC and FN (Gaggioli et al., 2007). Subsequently, these matrix channels were used by squamous carcinoma cells for invasion. Invasion of colorectal carcinoma cells into collagen gels was also guided by CAF, and this occurred in a TNC-dependent manner (De Wever et al., 2004).

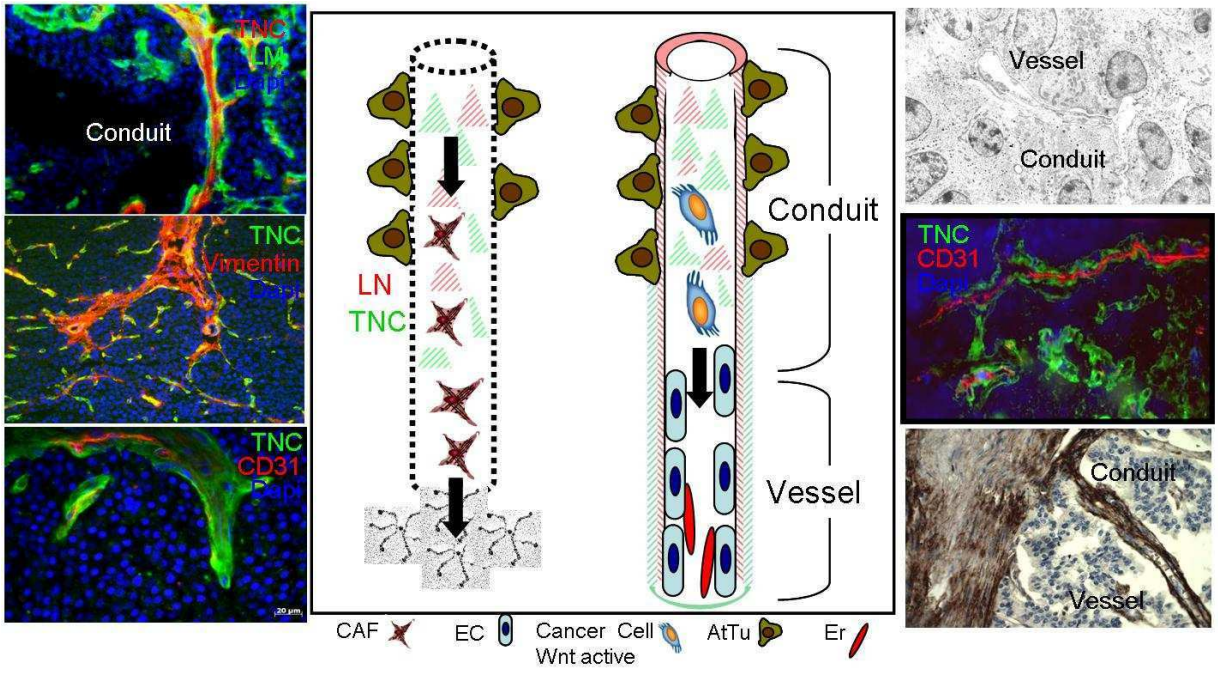

Figure 53: Summary of TNC conduit formation. TNC can be induced in tumor cells by various stimuli such as hypoxia, pro-inflammatory cytokines, TGFβ and mechanical stretch (Orend and Chiquet-Ehrismann, 2006). This occurs at multiple sites within a tumor thus generating a not

connected TNC network. Carcinoma associated fibroblasts migrate toward TNC, secrete metalloproteinase (MMPs) and create a lumen within the tissue that is filled with ECM molecules such as TNC and FN (Gaggioli et al., 2007). This structure may represent the origin of a matrix conduit. Tumor cells adjacent to this conduit may interact with the matrix through β1 integrins. This interaction presumably has an impact on the physiology causing tumor cells to differentiate into AtTu - attached tumor cells - that are characterized in the RT2/TNC model by less granular vesicles and potentially secrete other matrix molecules such as laminins, collagens, OPN, TSP1 and presumably more not yet identified matrix molecules. Adjacent tumor cells may also transdifferentiate into endothelial cells. Migratory CAF eventually will reach a blood vessel and thus produce a connection between a conduit and a blood vessel. Erythrocytes (Er) within the conduits do prove a connection between the conduit and the circulation. Endothelial cells or endothelial precursor cells may be attracted by TNC within the conduit (Zagzag et al., 1996) and potentially use the conduit as scaffold for angiogenesis (our observation). Motile tumor cells as e.g. colorectal carcinoma cells with an active Wnt signalling pathway may use the conduits for short distance trafficking (De Wever et al., 2004) which given the connection to the circulation may promote distant metastasis. The TNC conduits may resist an anti-angiogenic drug treatment (Vosseler et al., 2005) and could promote the reestablishment of the vasculature after destruction of endothelial cells and thus would represent a means of resistance against anti-angiogenic drugs.

Reticulars fibers in secondary lymphoid organs represent a TNC- containing tubular matrix system that exists under physiological conditions. The fibers in thymic conduits consist of a inner collagen core, a layer of LM and an outer lining by TNC and are about 2 µm in diameter (Drumea-Mirancea et al., 2005). In contrast, the matrix conduits that we characterized in murine and human tumors are several times bigger with up to 30 nm in diameter and more. Also the organization of TNC and LM is different in the tumor conduits with TNC frequently in the center and LM at the outer rim. Reticular fibers are believed to play a role in antigen maturation and as guiding cue for immune cells. Given the striking similarity in matrix composition and organization into conduits (Drumea-Mirancea et al., 2005), it is intriguing to speculate that a genetic program for TNC-containing reticular fibers is aberrantly activated in cancer and that these fibers serve a similar function as guiding cue in cancer. It will be interesting to see whether matrix conduits also form in RT2/TNCKO tumors which will provide information about the role of TNC in these conduits.

The TNC conduits might be responsible for enhanced metastasis in RT2/TNC tumors. In the RT2 model lung micrometastasis was higher in dependence on the TNC copy, lowest in RT2/TNCKO and highest in RT2/TNC mice. By TEM analysis tumor cells were seen inside the conduits. Given that the conduits are connected to the circulation it is possible that the conduits served as short distance guiding cue for tumor cells to reach the circulation and then the distant organ. A role of TNC in lung metastasis was indicated by different studies.

It was shown that TNC expression levels correlate with lung metastasis in breast cancer patients. TNC was found in the gene signature that predicts breast cancer lung metastasis (Minn et al., 2005). A knock down of TNC in xenografted breast cancer cells reduced metastasis in the lung (Calvo et al., 2008; Tavazoie et al., 2008). A mechanistic link of TNC to lung metastasis was demonstrated by Tavazoie and colleagues who showed that miR335 suppresses lung metastasis by down-regulating Sox4 and TNC (Tavazoie et al., 2008). Indeed TNC was recently found as a direct target of Sox4 (Scharer et al., 2009). Sox 4 had previously been uncovered as a TNC target gene in glioblastoma cells that had been grown on a TNC substratum (Ruiz et al., 2004) suggesting a positive interdependence. TNC appears to exhibit a pro-survival signal in metastasizing breast cancer cells and several candidate molecules and pathways had been identified. In particular Wnt signalling involving Lgr5 and Notch signalling involving Musashi-1 were shown to be relevant (Oskarsson et al., 2011). In the RT2/TNC model there is no indication that Lgr5 and Notch signalling play a role as deduced from gene expression analysis by qRT-PCR (Falk Saupe PhD thesis, 2011). Similarly, no induction of these genes was observed upon plating tumor cells on a TNC substratum (Anja Heinke, personal communication). In contrast, Wnt signalling potentially is linked to lung metastasis in the RT2 model since DKK1 expression was inversely linked to the TNC copy but this does not appear to include Lgr5. Thus it is possible that TNC promotes lung metastasis through different mechanisms in the different models. In the future it needs to be addressed whether an immune-compromised setting is suitable to address the role of TNC in lung metastasis (see below).

4. Murine model systems and their potential applications in addressing the role of TNC in cancer progression

4.1 Stochastic immune competent RT2 insulinoma model

The RT2 model has been extensively used in cancer research and provides the opportunity to address tumorigenesis upon sporadic induction in a setting that is relevant for human cancer. The SV40T-antigen interferes with the tumor suppressor genes p53 and RB which

are frequently inactivated in and associated with human cancer formation. Moreover, RT2 mice develop tumors in an immune competent setting which is important since the immune system plays a dual role in cancer (Coussens and Werb, 2002; Nathan, 2006) (see below). Here, it was shown that TNC is expressed in RT2 insulinomas in conduits and around newly formed blood vessels. Moreover, it was shown that CAF are in close association with the TNC matrix. In addition, we had shown that TNC levels correlate with lung micrometastasis suggesting that TNC promoted lung metastasis in this model. A similar organization of TNC into conduits and around blood vessels and a close association of the TNC matrix with CAF was also seen in human insulinomas. Thus, the RT2 model is not only a valid model for studying spontaneously arising tumorigenesis and tumor progression but also a proper model for human insulinoma which could improve our understanding about the origin of insulinomas and their eventual and rare progression into metastasis.

4.2 Tumor xenografting into immune-compromised mice lacking TNC

The Rag2KO mice are immune compromised since they lack the ability to make B and T cells and represent an established model for tumor xenografting experiments (Greenberg et al., 2004). Here these mice were used to address whether features of the tumor microenvironment such as TNC expression can be recapitulated in grafted tumors. We observed that upon grafting of human tumorigenic HEK293 (subcutaneous, heterotopic) and SW480 cells (caecum, orthotopic) tumors formed and exhibited an organisation of TNC into conduits where CAF and endothelial cells were embedded into the TNC rich matrix similar as in human colorectal carcinoma, human insulinomas and in RT2 tumors. Rag2KO/TNCKO mice were generated by breeding to address the role of host and tumor derived TNC in tumor cell engraftment, angiogenesis and conduit formation. It was seen that SW480 tumor cells with wildtype TNC formed tumors in a host lacking TNC. Arising tumors expressed TNC which was organized into conduits that embedded CAF and endothelial cells similar to human cancers. This experiment revealed that tumor cell derived TNC can assemble into conduits and with an apparently similar function as in a

TNC expressing host. Upon grafting of HEK293 cells with endogenous and ectopic TNC expression, respectively it turned out that more TNC conduits had formed when the tumor cells exhibited increased TNC levels. Together these studies revealed that tumor cells contributed to TNC conduit formation.

By engineering tumor cells to lack TNC expression we addressed whether TNC was necessary for tumor cell engraftment and growth. Upon injection into Rag2KO/TNCKO mice we could not detect any tumor formation and tissue analysis revealed that the tumor cells did not have engrafted. In contrast, in an immune-compromised nude mouse with wildtype TNC, a TNC knock down in SW480 tumor cells did not affect tumor formation. Moreover, SW480 cells with wildtype TNC had formed tumors in a TNC negative Rag2KO/TNCKO host. These results suggest that for tumor cell engraftment and tumor growth TNC appears to be necessary but that it is irrelevant whether the source is the host or the tumor cells. It is possible that TNC is required for survival and/or proliferation. Both survival and proliferation was shown to be stimulated by TNC (reviewed by Midwood and Orend, 2009). Thus the Rag2KO model with wildtype TNC and TNCKO together with cells that express or lack TNC offers the opportunity to address potential functions of TNC in very early steps of tumorigenesis.

The presented observations suggest the possibility that TNC is required for tumorigenesis. Thus it is expected that tumor prone mice with no TNC will not develop tumors. But this is not the case. It was shown that MMTV-Neu/TNCKO mice develop metastasizing mammary gland tumors with no difference in numbers and burden (Talts et al., 1999). Moreover, we had shown that RT2/TNCKO mice developed insulinomas that did not exhibit differences in numbers to that of RT2 mice with wildtype TNC (Saupe, Gasser, Jia et al., in preparation, Annex1). These results show that the absence of TNC does not interfere with tumorigenesis in stochastic tumor models with an intact immune system. The discrepancy between observations might be explained by a potential effect of TNC on the immune system. Indeed in the MMTV-Neu/TNCKO tumor tissue it was seen that the tumor

organization was different with more infiltration of macrophages. It was also shown that TNC modulates macrophage activities (Ruegg et al., 1989). Moreover, an RNA expression profiling derived from RipTNC islets revealed that ectopically expressed TNC had induced an immune signature (Falk Saupe, PhD thesis, 2011). Thus it is possible that TNC modulates the immune system which potentially has an impact on tumor onset and progression. Together these observations raise the question about the suitability of experiments in nude mice to address the role of TNC in lung metastasis (Oskarsson et al., 2011). Moreover, a potential link of TNC and inflammation in promoting human cancers such as in hepatitis virus associated hepatocellular carcinoma and inflammatory bowel diseases associated colon cancers should be revisited.

4.3 Orthotopic tumor xenografting mouse model for testing anti-angiogenic treatment

To recapitulate the features of human colorectal cancer a model in which tumors grow in a comparable tumor microenvironment is necessary. Therefore, the orthotopic grafting of SW480 cells was done into the caecum wall, which is part of the colon. This model recapitulates important features of human CRC such as high expression of TNC around blood vessels and organization of TNC into conduits that surround CAF.

This mouse model was used here with the aim to study the impact of an anti-angiogenic treatment on tumor progression and the tumor microenvironment. Here we used Bevacizumab alone, even if in the clinics, it is combined with cytotoxic agents such as 5-Fluorouracil (Hurwitz et al., 2004). A combination treatment in the mouse should be done in the future. Currently, patients with metastatic CRC receive Bevacizumab. In analogy, here we had used the human colorectal cancer cell line SW480 which was established from a primary adenocarcinoma of the colon that had metastasized to the liver (Leibovitz et al., 1976). These cells can form liver metastasis in the mouse. By using cherry labelled SW480 cells it was possible to decide when the Bevacizumab treatment should be started.

Nevertheless live imaging of labelled grafted tumor cells has some caveats which need to be taken into account, including masking of the signal that can occur during contractions of the intestine. Here, we observed that Bevacizumab treated mice had reduced angiogenesis since the CD31 quantification was significantly lowered when compared to controls. It was surprising however to observe that the frequency of metastasis to the liver was significantly increased in the Bevacizumab -treated group. A more detailed analysis is necessary to address the underlying mechanism and determine whether the tumor matrix and in particular TNC potentially concur to this increased propensity.

Preliminary results obtained from a heterotopic glioblastoma model showed that Bevacizumab treatment did not reduce either tumor size or angiogenesis. Interstingly, an increased TNC expression and organisation into tracks was specifically observed in tumors that did not respond to the Bevacizumab treatment (Tristan Rupp, Master thesis, 2011). These experiments suggested that Bevacizumab may have an impact on the tumor microenvironment and that TNC potentially plays a role in counteracting this anti-angiogenic treatment. This possibility is supported by experiments in xenografted squamous cell carcinomas where DC101 an anti-VEGFA antibody had caused destruction of blood vessels but did not affect the high TNC expression in the tumor bed (Vosseler et al., 2005).

A potential evasion mechanism involving the ECM was previously proposed. It was seen that matrix sleeves composed of laminins and coll IV which were interpreted as basement membranes had remained intact after an anti-angiogenic treatment and that these matrix structures were used for revascularization after the end of the anti-angiogenic treatment (McDonald and Foss, 2000). Currently it is not known whether these matrix sleeves contain TNC and potentially represent the described TNC conduits. Several evasion mechanisms are discussed that interfere with an anti-angiogenic cancer therapy which involve selection for other growth factors than VEGF (Berger and Hanahan, 2008). VEGF-targeted therapies can also initiate mechanisms that increase malignancy such as hypoxia

tolerance, intravasation and endothelial cell dysfunction. Anti-EGFR therapy represents another important approach in therapeutic treatment of metastatic CRC. However, a significant number of patients did not respond to this therapy (Loupakis et al., 2009; Viloria-Petit et al., 2004) presumably due to other evasion mechanisms. In the long run normalization of the tumor vasculature appears to be a more promising approach which would reduce hypoxia that is considered as a major pro-angiogenic condition. Moreover, a functional vasculature would also allow an improved delivery of cytotoxic or alternative drugs into the tumor tissue.

Given its prominent and exclusive expression in cancer tissue TNC appears as a prime candidate for targeting. Indeed several approaches have been developed such as in-situ imaging of TNC expression, delivery of cytokines or radionuclides using TNC specific Ab or aptamers (Reviewed in Midwood et al., 2011). Since tumor associated cells such as CAF express TNC it may also be necessary to destroy these cells to prevent expression of TNC and formation of a matrix bed that promotes tumorigenesis. For future targeting TNC it will be important to understand which cells in a tumor express TNC. It will also be necessary to determine whether host and tumor derived TNC is molecularly similar or different and exhibits potentially different functions. This can be addressed by in situ hybridization, FACS and in cell culture.

Altogether the presented murine tumor models offer several complementary opportunities to address the role of TNC in cancer progression which is summarized in Table 7.

Table 7: Summary of models

IS	Tissue / Cells	Mouse	Result	Conclusion
I	Human CRC	/	TNC conduits Embedding of EC, CAF	TNC conduits: scaffold angiogenesis
I	Human insulinoma	/	TNC conduits Connection to vasculature Embedding of EC, CAF	Similar features as in RT2 insulinomas
I		RT2 RT2/TNCKO RT2/TNC	Increased lung metastasis linked to TNC copy DKK1 inversely linked to TNC copy TNC around blood vessels TNC in conduits TNC: more CAF, EC, macrophages	TNC promotion of: tumor onset, angiogenesis, lung metastasis TNC conduits: alternative route for dissemination scaffold in angiogenesis result of pruning? TNC repression of DKK1 and activation of Wnt signaling
C	KRIB:DKK1	Nude sc	Smaller tumors Reduced angiogenesis	Inhibition of angiogenesis by DKK1
C	HEK293:TNC	Rag2KO sc	More TNC conduits	Contribution of tumor cell TNC to conduits
C	SW480	Rag2KO/TNCKO o	Tumor cell engraftment TNC conduits Embedding of EC, CAF	Conduit formation by tumor cell TNC with similar function
C	SW480shTNC	Rag2KO/TNCKO o	No tumors in absence of T and B cells	Importance of TNC for engraftment Pro-tumorigenic impact of TNC on immune cells
C	SW480shTNC	Nude sc / o	Tumor engraftment	Bypass of T and B cells by host TNC
C	Human CRC	Nude sc	TNC conduits Embedding of EC, CAF	Preservation of TNC organization and function in tumor microenvironment in murine host
C	SW480 Bevacizumab	Nude o	Reduced angiogenesis Enhanced liver metastasis	Adverse effect of Bevacizumab

The analyzed models are summarized according to tissue from human colorectal carcinoma (CRC), human insulinoma, murine RT2 and human tumor xenografts. Grafting experiments are sorted by immune competent (I) or immune compromised (C) immune system (IS), subcutaneous (sc) or orthotopic caecum (o) grafting. CAF, carcinoma associated fibroblast; EC, endothelial cells.

Conclusions and Perspectives

CONCLUSIONS AND PERSPECTIVES

In this thesis, the microenvironment, in particular TNC expression and organization, should be investigated in tumor tissue of human cancer and murine cancer models. Therefore, tumor tissue from human insulinomas and colorectal carcinomas as well as of 6 different tumor xenograft models had been analyzed by immunostaining (and subsequent quantification of some stainings) using a huge collection of antibodies (20). All staining protocols had been established. In addition several tumor cells had been engineered and partially characterized in cell culture before xenografting into immune compromised mice. Some of these mice such as the Rag2KO/TNCKO mouse had been generated by breeding and Live imaging using the NightOwl apparatus was established for this model. For orthotopic xenografting into the caecum wall a surgical protocol had been adjusted.

In addition, the well characterized sporadic RT2 insulinoma model was used here that had been engineered in the laboratory to express defined levels of TNC (wildtype, knock out and overexpression). Analysis of tumor tissue from these mice had shown that (i) TNC is highly expressd in the tumor tissue, ii) is organized into conduits that are composed of many ECM molecules , that iii) endothelial cells, CAF and macrophages are embedded into the TNC-rich matrix and that (iv) TNC had promoted angiogenesis and lung micrometastasis.

Upon analysis of human insulinoma tissue several parallels to the RT2 model were apparent which suggests that the RT2 model could be a valid model for studying insulinoma tumorigenesis and progression.

In the RT2 model DKK1 levels were found to be inversely linked to the TNC copy which suggested that repression of DKK1 by TNC is potentially linked to enhanced angiogenesis by TNC. This possibility was addressed in a xenograft model where high DKK1 turned out

to block angiogenesis. This result supports the possibility that TNC promotes tumor angiogenesis through repression of DKK1.

By comparing hCRC with heterotopic tumor xenografts, it was shown that the all over morphology was recapitulated including the organization of TNC into conduits as well as embedding of endothelial cells and CAF into the TNC rich matrix. It was further demonstrated that after several passages of the human tumor material in the mouse the human tumor microenvironment including TNC was replaced by murine matrix molecules raising the question about the usefulness of advanced passaging of human cancer tissue in the mouse as experimental model for human cancer.

By using a xenograft model with no TNC expression together with tumor cells that lack TNC it was observed that tumor engraftment was compromised which suggests that TNC has an impact on survival and/or tumor cell proliferation and that this involves an intact immune system (at least B and/or T-cells). Moreover, this observation raises the question about the suitability of immune compromised mouse models to study the role of TNC in tumorigenesis and metastasis.

Each of the murine cancer models was used to address a specific question. Together with information from the human cancer tissues here important information about the organization of TNC into conduits was obtained that allows to raise several hypotheses about the potential functions of the matrix conduits. It is possible that the TNC conduits are encoded by a program for reticular fibers in secondary lymphoid tissues and that they have a similar function in guiding cells in the tumor. TNC conduits potentially play an instrumental role in angiogenesis and metastasis. It is not clear what exact role the TNC conduits would play. It is possible that they arise as a result of vessel pruning. Our data suggest that it is more likely that the TNC conduits initiate a matrix network that serves as guiding cue for attracting pro-angiogenic cells such as endothelial cells, CAF and

macrophages. This would represent a different mechanism than sprouting angiogenesis and would give the ECM a central role in tumor angiogenesis. Finally it is possible that the TNC conduits represent physical niches that may counteract anti-angiogenic therapies by protecting cancer stem cells and endothelial cells from drugs. These hypotheses should be addressed in the future.

Pertinence and innovation

Targeting of TNC could present a strategy to improve destruction of cancer tissue. A custom made treatment for cancer patients is an important goal to improve cancer therapy in the future. *Ex vivo* treatment of human CRC upon xenografting into an immune compromised mouse seems to be a feasible strategy to improve the choice of treatment. Here, an immune compromised tumor model system that lacks endogenous TNC was established where TNC can be targeted in the xenografted human CRC tissue. Drugs targeting TNC had been established by us and other laboratories and may be available in the near future for cancer treatment. Our model system may deliver important informations about the role of TNC in CRC and will provide a basis for targeting TNC in combination with other drugs. The established model system may also allow to develop TNC-based strategies for a non-invasive live imaging of cancer progression in the future.

References

REFERENCES

Adams, M., Jones, J. L., Walker, R. A*., et al.* (2002). Changes in tenascin-C isoform expression in invasive and preinvasive breast disease. Cancer Res *62*, 3289-3297.

Adams, R. H., and Eichmann, A. (2010). Axon guidance molecules in vascular patterning. Cold Spring Harb Perspect Biol *2*, a001875.

Aguirre-Ghiso, J. A. (2007). Models, mechanisms and clinical evidence for cancer dormancy. Nat Rev Cancer *7*, 834-846.

Allegra, C. J., Yothers, G., O'Connell, M. J*., et al.* (2011). Phase III trial assessing bevacizumab in stages II and III carcinoma of the colon: results of NSABP protocol C-08. J Clin Oncol *29*, 11-16.

Alves, T. R., da Fonseca, A. C., Nunes, S. S*., et al.* (2011). Tenascin-C in the extracellular matrix promotes the selection of highly proliferative and tubulogenesis-defective endothelial cells. Exp Cell Res *317*, 2073-2085.

Ambartsumian, N. S., Grigorian, M. S., Larsen, I. F*., et al.* (1996). Metastasis of mammary carcinomas in GRS/A hybrid mice transgenic for the mts1 gene. Oncogene *13*, 1621-1630.

Astrof, S., and Hynes, R. O. (2009). Fibronectins in vascular morphogenesis. Angiogenesis *12*, 165-175.

Aufderheide, E., and Ekblom, P. (1988). Tenascin during gut development: appearance in the mesenchyme, shift in molecular forms, and dependence on epithelial-mesenchymal interactions. J Cell Biol *107*, 2341-2349.

Ballard, V. L., Sharma, A., Duignan, I*., et al.* (2006). Vascular tenascin-C regulates cardiac endothelial phenotype and neovascularization. Faseb J *20*, 717-719.

Baluk, P., Hashizume, H., and McDonald, D. M. (2005). Cellular abnormalities of blood vessels as targets in cancer. Curr Opin Genet Dev *15*, 102-111.

Baluk, P., Morikawa, S., Haskell, A*., et al.* (2003). Abnormalities of basement membrane on blood vessels and endothelial sprouts in tumors. Am J Pathol *163*, 1801-1815.

Barsky, S. H., Green, W. R., Grotendorst, G. R*., et al.* (1984). Desmoplastic breast carcinoma as a source of human myofibroblasts. Am J Pathol *115*, 329-333.

Benahmed, F., Gross, I., Guenot, D*., et al.* (2007). The microenvironment controls CDX2 homeobox gene expression in colorectal cancer cells. Am J Pathol *170*, 733-744.

Bergers, G., and Benjamin, L. E. (2003). Tumorigenesis and the angiogenic switch. Nat Rev Cancer *3*, 401-410.

Bergers, G., Brekken, R., McMahon, G*., et al.* (2000). Matrix metalloproteinase-9 triggers the angiogenic switch during carcinogenesis. Nat Cell Biol *2*, 737-744.

Bergers, G., and Hanahan, D. (2008). Modes of resistance to anti-angiogenic therapy. Nat Rev Cancer *8*, 592-603.

Betz, P., Nerlich, A., Tubel, J*., et al.* (1993). Localization of tenascin in human skin wounds--an immunohistochemical study. Int J Legal Med *105*, 325-328.

Bhowmick, N. A., Chytil, A., Plieth, D*., et al.* (2004). TGF-beta signaling in fibroblasts modulates the oncogenic potential of adjacent epithelia. Science *303*, 848-851.

Bissell, M. J., and Labarge, M. A. (2005). Context, tissue plasticity, and cancer: are tumor stem cells also regulated by the microenvironment? Cancer Cell *7*, 17-23.

Bissell, M. J., and Radisky, D. (2001). Putting tumours in context. Nat Rev Cancer *1*, 46-54.

Boland, C. R., and Goel, A. (2010). Microsatellite instability in colorectal cancer. Gastroenterology *138*, 2073-2087 e2073.

Burri, P. H., Hlushchuk, R., and Djonov, V. (2004). Intussusceptive angiogenesis: its emergence, its characteristics, and its significance. Dev Dyn *231*, 474-488.

Calvo, A., Catena, R., Noble, M. S*., et al.* (2008). Identification of VEGF-regulated genes associated with increased lung metastatic potential: functional involvement of tenascin-C in tumor growth and lung metastasis. Oncogene *27*, 5373-5384.

Carmeliet, P., and Jain, R. K. (2011). Principles and mechanisms of vessel normalization for cancer and other angiogenic diseases. Nat Rev Drug Discov *10*, 417-427.

Carnemolla, B., Castellani, P., Ponassi, M.*, et al.* (1999). Identification of a glioblastoma-associated tenascin-C isoform by a high affinity recombinant antibody. Am J Pathol *154*, 1345-1352.

Castellon, R., Caballero, S., Hamdi, H. K.*, et al.* (2002). Effects of tenascin-C on normal and diabetic retinal endothelial cells in culture. Invest Ophthalmol Vis Sci *43*, 2758-2766.

Chabas, D. (2005). [Osteopontin, a multi-faceted molecule]. Med Sci (Paris) *21*, 832-838.

Chang, H. Y., Chi, J. T., Dudoit, S.*, et al.* (2002). Diversity, topographic differentiation, and positional memory in human fibroblasts. Proc Natl Acad Sci U S A *99*, 12877-12882.

Chen, J., Chen, Z., Chen, M.*, et al.* (2009). Role of fibrillar Tenascin-C in metastatic pancreatic cancer. Int J Oncol *34*, 1029-1036.

Chen, J., Shinkai, Y., Young, F.*, et al.* (1994). Probing immune functions in RAG-deficient mice. Curr Opin Immunol *6*, 313-319.

Chiquet-Ehrismann, R., and Chiquet, M. (2003). Tenascins: regulation and putative functions during pathological stress. J Pathol *200*, 488-499.

Christofori, G., Naik, P., and Hanahan, D. (1994). A second signal supplied by insulin-like growth factor II in oncogene-induced tumorigenesis. Nature *369*, 414-418.

Cohen, E. D., Ihida-Stansbury, K., Lu, M. M.*, et al.* (2009). Wnt signaling regulates smooth muscle precursor development in the mouse lung via a tenascin C/PDGFR pathway. J Clin Invest *119*, 2538-2549.

Colognato, H., and Yurchenco, P. D. (2000). Form and function: the laminin family of heterotrimers. Dev Dyn *218*, 213-234.

Comito, G., Calvani, M., Giannoni, E.*, et al.* (2011). HIF-1alpha stabilization by mitochondrial ROS promotes Met-dependent invasive growth and vasculogenic mimicry in melanoma cells. Free Radic Biol Med *51*, 893-904.

Coussens, L. M., and Werb, Z. (2002). Inflammation and cancer. Nature *420*, 860-867.

Couzin-Frankel, J., and Ogale, Y. (2011). FDA. Once on 'fast track,' avastin now derailed. Science *333*, 143-144.

Crawford, Y., and Ferrara, N. (2009). Tumor and stromal pathways mediating refractoriness/resistance to anti-angiogenic therapies. Trends Pharmacol Sci *30*, 624-630.

De Arcangelis, A., Lefebvre, O., Mechine-Neuville, A.*, et al.* (2001). Overexpression of laminin alpha1 chain in colonic cancer cells induces an increase in tumor growth. Int J Cancer *94*, 44-53.

De Arcangelis, A., Neuville, P., Boukamel, R.*, et al.* (1996). Inhibition of laminin alpha 1-chain expression leads to alteration of basement membrane assembly and cell differentiation. J Cell Biol *133*, 417-430.

de Visser, K. E., Korets, L. V., and Coussens, L. M. (2005). De novo carcinogenesis promoted by chronic inflammation is B lymphocyte dependent. Cancer Cell *7*, 411-423.

De Wever, O., Nguyen, Q. D., Van Hoorde, L.*, et al.* (2004). Tenascin-C and SF/HGF produced by myofibroblasts *in vitro* provide convergent pro-invasive signals to human colon cancer cells through RhoA and Rac. Faseb J *18*, 1016-1018.

Degen, M., Brellier, F., Kain, R.*, et al.* (2007). Tenascin-W is a novel marker for activated tumor stroma in low-grade human breast cancer and influences cell behavior. Cancer Res *67*, 9169-9179.

Dejana, E. (2010). The role of wnt signaling in physiological and pathological angiogenesis. Circ Res *107*, 943-952.

Denoix, P. (1946). [Not available]. Bull Inst Natl Hyg *1*, 12-17.

Deryugina, E. I., Zijlstra, A., Partridge, J. J.*, et al.* (2005). Unexpected effect of matrix metalloproteinase down-regulation on vascular intravasation and metastasis of human fibrosarcoma cells selected in vivo for high rates of dissemination. Cancer Res *65*, 10959-10969.

Drumea-Mirancea, M., Wessels, J. T., Muller, C. A.*, et al.* (2006). Characterization of a conduit system containing laminin-5 in the human thymus: a potential transport system for small molecules. J Cell Sci *119*, 1396-1405.

Dvorak, H. F. (1986). Tumors: wounds that do not heal. Similarities between tumor stroma generation and wound healing. N Engl J Med *315*, 1650-1659.

Ebos, J. M., Lee, C. R., Cruz-Munoz, W.*, et al.* (2009). Accelerated metastasis after short-term treatment with a potent inhibitor of tumor angiogenesis. Cancer Cell *15*, 232-239.

Edwards, M. M., Mammadova-Bach, E., Alpy, F.*, et al.* (2010). Mutations in Lama1 disrupt retinal vascular development and inner limiting membrane formation. J Biol Chem *285*, 7697-7711.

Ellis, L. M., and Reardon, D. A. (2009). Cancer: The nuances of therapy. Nature *458*, 290-292.

Erickson, A. C., and Couchman, J. R. (2000). Still more complexity in mammalian basement membranes. J Histochem Cytochem *48*, 1291-1306.

Estevez, M. C., Huang, Y. F., Kang, H.*, et al.* (2010). Nanoparticle-aptamer conjugates for cancer cell targeting and detection. Methods Mol Biol *624*, 235-248.

Euhus, D. M., Hudd, C., LaRegina, M. C.*, et al.* (1986). Tumor measurement in the nude mouse. J Surg Oncol *31*, 229-234.

Farris, A. B., Misdraji, J., Srivastava, A.*, et al.* (2008). Sessile serrated adenoma: challenging discrimination from other serrated colonic polyps. Am J Surg Pathol *32*, 30-35.

Fearon, E. R., and Vogelstein, B. (1990). A genetic model for colorectal tumorigenesis. Cell *61*, 759-767.

Ferlay, J., Autier, P., Boniol, M.*, et al.* (2007). Estimates of the cancer incidence and mortality in Europe in 2006. Ann Oncol *18*, 581-592.

Ffrench-Constant, C., and Hynes, R. O. (1988). Patterns of fibronectin gene expression and splicing during cell migration in chicken embryos. Development *104*, 369-382.

Filsell, W., Rudman, S., Jenkins, G.*, et al.* (1999). Coordinate upregulation of tenascin C expression with degree of photodamage in human skin. Br J Dermatol *140*, 592-599.

Fodde, R., Edelmann, W., Yang, K.*, et al.* (1994). A targeted chain-termination mutation in the mouse Apc gene results in multiple intestinal tumors. Proc Natl Acad Sci U S A *91*, 8969-8973.

Folkman, J. (1971). Tumor angiogenesis: therapeutic implications. N Engl J Med *285*, 1182-1186.

Folkman, J. (1972). Anti-angiogenesis: new concept for therapy of solid tumors. Ann Surg *175*, 409-416.

Folkman, J., and Kalluri, R. (2004). Cancer without disease. Nature *427*, 787.

Folkman, J., Merler, E., Abernathy, C.*, et al.* (1971). Isolation of a tumor factor responsible for angiogenesis. J Exp Med *133*, 275-288.

Folkman, J., Watson, K., Ingber, D.*, et al.* (1989). Induction of angiogenesis during the transition from hyperplasia to neoplasia. Nature *339*, 58-61.

Forsberg, E., Hirsch, E., Frohlich, L.*, et al.* (1996). Skin wounds and severed nerves heal normally in mice lacking tenascin-C. Proc Natl Acad Sci U S A *93*, 6594-6599.

Gabbiani, G. (2003). The myofibroblast in wound healing and fibrocontractive diseases. J Pathol *200*, 500-503.

Gaggioli, C., Hooper, S., Hidalgo-Carcedo, C.*, et al.* (2007). Fibroblast-led collective invasion of carcinoma cells with differing roles for RhoGTPases in leading and following cells. Nat Cell Biol *9*, 1392-1400.

Gherzi, R., Carnemolla, B., Siri, A.*, et al.* (1995). Human tenascin gene. Structure of the 5'-region, identification, and characterization of the transcription regulatory sequences. J Biol Chem *270*, 3429-3434.

Glinka, A., Wu, W., Delius, H.*, et al.* (1998). Dickkopf-1 is a member of a new family of secreted proteins and functions in head induction. Nature *391*, 357-362.

Goerdt, S., and Orfanos, C. E. (1999). Other functions, other genes: alternative activation of antigen-presenting cells. Immunity *10*, 137-142.

Gonzalez-Sancho, J. M., Aguilera, O., Garcia, J. M.*, et al.* (2005). The Wnt antagonist DICKKOPF-1 gene is a downstream target of beta-catenin/TCF and is downregulated in human colon cancer. Oncogene *24*, 1098-1103.

Goodwin, A. M., Sullivan, K. M., and D'Amore, P. A. (2006). Cultured endothelial cells display endogenous activation of the canonical Wnt signaling pathway and express multiple ligands, receptors, and secreted modulators of Wnt signaling. Dev Dyn *235*, 3110-3120.

Gordon, S., and Taylor, P. R. (2005). Monocyte and macrophage heterogeneity. Nat Rev Immunol *5*, 953-964.

Grady, W. M., and Carethers, J. M. (2008). Genomic and epigenetic instability in colorectal cancer pathogenesis. Gastroenterology *135*, 1079-1099.

Greenberg, L. H., and Slayden, O. D. (2004). Human endometriotic xenografts in immunodeficient RAG-

2/gamma(c)KO mice. Am J Obstet Gynecol *190*, 1788-1795; discussion 1795-1786.

Grunewald, M., Avraham, I., Dor, Y.*, et al.* (2006). VEGF-induced adult neovascularization: recruitment, retention, and role of accessory cells. Cell *124*, 175-189.

Guan, L. S., Li, G. C., Chen, C. C.*, et al.* (2001). Rb-associated protein 46 (RbAp46) suppresses the tumorigenicity of adenovirus-transformed human embryonic kidney 293 cells. Int J Cancer *93*, 333-338.

Gubin, A. N., and Miller, J. L. (2001). Human erythroid porphobilinogen deaminase exists in 2 splice variants. Blood *97*, 815-817.

Guenot, D., Guerin, E., Aguillon-Romain, S.*, et al.* (2006). Primary tumour genetic alterations and intra-tumoral heterogeneity are maintained in xenografts of human colon cancers showing chromosome instability. J Pathol *208*, 643-652.

Guess, C. M., and Quaranta, V. (2009). Defining the role of laminin-332 in carcinoma. Matrix Biol *28*, 445-455.

Gulubova, M. V., and Vlaykova, T. I. (2006). Significance of tenascin-C, fibronectin, laminin, collagen IV, alpha5beta1 and alpha9beta1 integrins and fibrotic capsule formation around liver metastases originating from cancers of the digestive tract. Neoplasma *53*, 372-383.

Gungor, N., Knaapen, A. M., Munnia, A.*, et al.* (2010). Genotoxic effects of neutrophils and hypochlorous acid. Mutagenesis *25*, 149-154.

Hanahan, D. (1985). Heritable formation of pancreatic beta-cell tumours in transgenic mice expressing recombinant insulin/simian virus 40 oncogenes. Nature *315*, 115-122.

Hanahan, D., and Folkman, J. (1996). Patterns and emerging mechanisms of the angiogenic switch during tumorigenesis. Cell *86*, 353-364.

Hanahan, D., Wagner, E. F., and Palmiter, R. D. (2007). The origins of oncomice: a history of the first transgenic mice genetically engineered to develop cancer. Genes Dev *21*, 2258-2270.

Hanahan, D., and Weinberg, R. A. (2000). The hallmarks of cancer. Cell *100*, 57-70.

Hanahan, D., and Weinberg, R. A. (2011). Hallmarks of cancer: the next generation. In Cell, pp. 646-674.

Hancox, R. A., Allen, M. D., Holliday, D. L.*, et al.* (2009). Tumour-associated tenascin-C isoforms promote breast cancer cell invasion and growth by matrix metalloproteinase-dependent and independent mechanisms. Breast Cancer Res *11*, R24.

Harrison, S., and Benziger, H. (2011). The molecular biology of colorectal carcinoma and its implications: a review. Surgeon *9*, 200-210.

Hashizume, H., Baluk, P., Morikawa, S.*, et al.* (2000). Openings between defective endothelial cells explain tumor vessel leakiness. Am J Pathol *156*, 1363-1380.

Hellstrom, M., Gerhardt, H., Kalen, M.*, et al.* (2001). Lack of pericytes leads to endothelial hyperplasia and abnormal vascular morphogenesis. J Cell Biol *153*, 543-553.

Herlyn, M., Graeven, U., Speicher, D.*, et al.* (1991). Characterization of tenascin secreted by human melanoma cells. Cancer Res *51*, 4853-4858.

Herzig, M., Savarese, F., Novatchkova, M.*, et al.* (2007). Tumor progression induced by the loss of E-cadherin independent of beta-catenin/Tcf-mediated Wnt signaling. Oncogene *26*, 2290-2298.

Huang, W., Chiquet-Ehrismann, R., Moyano, J. V.*, et al.* (2001). Interference of tenascin-C with syndecan-4 binding to fibronectin blocks cell adhesion and stimulates tumor cell proliferation. Cancer Res *61*, 8586-8594.

Huh, S. J., Liang, S., Sharma, A.*, et al.* (2010). Transiently entrapped circulating tumor cells interact with neutrophils to facilitate lung metastasis development. Cancer Res *70*, 6071-6082.

Hurwitz, H., and Kabbinavar, F. (2005). Bevacizumab combined with standard fluoropyrimidine-based chemotherapy regimens to treat colorectal cancer. Oncology *69 Suppl 3*, 17-24.

Hurwitz, H. I., Fehrenbacher, L., Hainsworth, J. D.*, et al.* (2005). Bevacizumab in combination with fluorouracil and leucovorin: an active regimen for first-line metastatic colorectal cancer. J Clin Oncol *23*, 3502-3508.

Hynes, R. O. (2007). Cell-matrix adhesion in vascular development. J Thromb Haemost *5 Suppl 1*, 32-40.

Jain, R. K. (2001). Normalizing tumor vasculature with anti-angiogenic therapy: a new paradigm for combination therapy. Nat Med *7*, 987-989.

Jain, R. K. (2005). Normalization of tumor vasculature: an emerging concept in antiangiogenic therapy. Science *307*, 58-62.

Jain, R. K., and Baxter, L. T. (1988). Mechanisms of heterogeneous distribution of monoclonal antibodies and other macromolecules in tumors: significance of elevated interstitial pressure. Cancer Res *48*, 7022-7032.

Jallo, G. I., Friedlander, D. R., Kelly, P. J.*, et al.* (1997). Tenascin-C expression in the cyst wall and fluid of human brain tumors correlates with angiogenesis. Neurosurgery *41*, 1052-1059.

Janssen, K. P., el-Marjou, F., Pinto, D.*, et al.* (2002). Targeted expression of oncogenic K-ras in intestinal epithelium causes spontaneous tumorigenesis in mice. Gastroenterology *123*, 492-504.

Jiang, Y., Kimchi, E. T., Staveley-O'Carroll, K. F.*, et al.* (2009). Assessment of K-ras mutation: a step toward personalized medicine for patients with colorectal cancer. Cancer *115*, 3609-3617.

Jones, P. L., and Jones, F. S. (2000). Tenascin-C in development and disease: gene regulation and cell function. Matrix Biol *19*, 581-596.

Kaariainen, E., Nummela, P., Soikkeli, J.*, et al.* (2006). Switch to an invasive growth phase in melanoma is associated with tenascin-C, fibronectin, and procollagen-I forming specific channel structures for invasion. J Pathol *210*, 181-191.

Kalluri, R., and Zeisberg, M. (2006). Fibroblasts in cancer. Nat Rev Cancer *6*, 392-401.

Kaspar, M., Zardi, L., and Neri, D. (2006). Fibronectin as target for tumor therapy. Int J Cancer *118*, 1331-1339.

Katenkamp, K., Berndt, A., Hindermann, W.*, et al.* (2004). mRNA expression and protein distribution of the unspliced tenascin-C isoform in prostatic adenocarcinoma. J Pathol *203*, 771-779.

Kemp, Z., Thirlwell, C., Sieber, O.*, et al.* (2004). An update on the genetics of colorectal cancer. Hum Mol Genet *13 Spec No 2*, R177-185.

Kim, J. C., Choi, J. S., Roh, S. A.*, et al.* (2010). Promoter methylation of specific genes is associated with the phenotype and progression of colorectal adenocarcinomas. Ann Surg Oncol *17*, 1767-1776.

Kim, K. J., Li, B., Winer, J.*, et al.* (1993). Inhibition of vascular endothelial growth factor-induced angiogenesis suppresses tumour growth in vivo. Nature *362*, 841-844.

Kina, T., Ikuta, K., Takayama, E.*, et al.* (2000). The monoclonal antibody TER-119 recognizes a molecule associated with glycophorin A and specifically marks the late stages of murine erythroid lineage. Br J Haematol *109*, 280-287.

Knaapen, A. M., Gungor, N., Schins, R. P.*, et al.* (2006). Neutrophils and respiratory tract DNA damage and mutagenesis: a review. Mutagenesis *21*, 225-236.

Kurz, H., Burri, P. H., and Djonov, V. G. (2003). Angiogenesis and vascular remodeling by intussusception: from form to function. News Physiol Sci *18*, 65-70.

Labosky, P. A., Barlow, D. P., and Hogan, B. L. (1994). Embryonic germ cell lines and their derivation from mouse primordial germ cells. Ciba Found Symp *182*, 157-168; discussion 168-178.

Lange, K., Kammerer, M., Hegi, M. E.*, et al.* (2007). Endothelin receptor type B counteracts tenascin-C-induced endothelin receptor type A-dependent focal adhesion and actin stress fiber disorganization. Cancer Res *67*, 6163-6173.

Lange, K., Kammerer, M., Saupe, F.*, et al.* (2008). Combined lysophosphatidic acid/platelet-derived growth factor signaling triggers glioma cell migration in a tenascin-C microenvironment. Cancer Res *68*, 6942-6952.

Le Bail, B., Faouzi, S., Boussarie, L.*, et al.* (1997). Extracellular matrix composition and integrin expression in early hepatocarcinogenesis in human cirrhotic liver. J Pathol *181*, 330-337.

Leggett, B., and Whitehall, V. (2010). Role of the serrated pathway in colorectal cancer pathogenesis. Gastroenterology *138*, 2088-2100.

Leibovitz, A., Stinson, J. C., McCombs, W. B., 3rd*, et al.* (1976). Classification of human colorectal adenocarcinoma cell lines. Cancer Res *36*, 4562-4569.

Li, S., Edgar, D., Fassler, R.*, et al.* (2003). The role of laminin in embryonic cell polarization and tissue organization. Dev Cell *4*, 613-624.

Liaw, L., and Crawford, H. C. (1999). Functions of the extracellular matrix and matrix degrading proteases during tumor progression. Braz J Med Biol Res *32*, 805-812.

Liebner, S., Corada, M., Bangsow, T.*, et al.* (2008). Wnt/beta-catenin signaling controls development of the blood-brain barrier. J Cell Biol *183*, 409-417.

Loges, S., Mazzone, M., Hohensinner, P.*, et al.* (2009). Silencing or fueling metastasis with VEGF inhibitors: antiangiogenesis revisited. Cancer Cell *15*, 167-170.

Loupakis, F., Pollina, L., Stasi, I.*, et al.* (2009). PTEN expression and KRAS mutations on primary tumors and metastases in the prediction of benefit from cetuximab plus irinotecan for patients with metastatic colorectal cancer. J Clin Oncol *27*, 2622-2629.

Lyden, D., Hattori, K., Dias, S.*, et al.* (2001). Impaired recruitment of bone-marrow-derived endothelial and hematopoietic precursor cells blocks tumor angiogenesis and growth. Nat Med *7*, 1194-1201.

Malinda, K. M., and Kleinman, H. K. (1996). The laminins. Int J Biochem Cell Biol *28*, 957-959.

Mancuso, M. R., Davis, R., Norberg, S. M.*, et al.* (2006). Rapid vascular regrowth in tumors after reversal of VEGF inhibition. J Clin Invest *116*, 2610-2621.

Maniotis, A. J., Folberg, R., Hess, A.*, et al.* (1999). Vascular channel formation by human melanoma cells in vivo and in vitro: vasculogenic mimicry. Am J Pathol *155*, 739-752.

Mantovani, A., Sozzani, S., Locati, M.*, et al.* (2002). Macrophage polarization: tumor-associated macrophages as a paradigm for polarized M2 mononuclear phagocytes. Trends Immunol *23*, 549-555.

Martina, E., Degen, M., Ruegg, C.*, et al.* (2010). Tenascin-W is a specific marker of glioma-associated blood vessels and stimulates angiogenesis in vitro. Faseb J *24*, 778-787.

Mazzone, M., Dettori, D., Leite de Oliveira, R.*, et al.* (2009). Heterozygous deficiency of PHD2 restores tumor oxygenation and inhibits metastasis via endothelial normalization. Cell *136*, 839-851.

McDonald, D. M., and Foss, A. J. (2000). Endothelial cells of tumor vessels: abnormal but not absent. Cancer Metastasis Rev *19*, 109-120.

Metz, D. C., and Jensen, R. T. (2008). Gastrointestinal neuroendocrine tumors: pancreatic endocrine tumors. Gastroenterology *135*, 1469-1492.
Midgley, R., and Kerr, D. (2005). Bevacizumab--current status and future directions. Ann Oncol *16*, 999-1004.

Midwood, K. S., Hussenet, T., Langlois, B.*, et al.* (2011). Advances in tenascin-C biology. Cell Mol Life Sci *Published online August 2011*.

Midwood, K. S., and Orend, G. (2009). The role of tenascin-C in tissue injury and tumorigenesis. J Cell Commun Signal *3*, 287-310.

Min, J. K., Park, H., Choi, H. J.*, et al.* (2011). The WNT antagonist Dickkopf2 promotes angiogenesis in rodent and human endothelial cells. J Clin Invest *121*, 1882-1893.

Miner, J. H., Patton, B. L., Lentz, S. I.*, et al.* (1997). The laminin alpha chains: expression, developmental transitions, and chromosomal locations of alpha1-5, identification of heterotrimeric laminins 8-11, and cloning of a novel alpha3 isoform. J Cell Biol *137*, 685-701.

Minn, A. J., Kang, Y., Serganova, I.*, et al.* (2005). Distinct organ-specific metastatic potential of individual breast cancer cells and primary tumors. J Clin Invest *115*, 44-55.

Miyamoto, Y., Yoshimasa, T., Arai, H.*, et al.* (1996). Alternative RNA splicing of the human endothelin-A receptor generates multiple transcripts. Biochem J *313 (Pt 3)*, 795-801.

Mosher, D. F. (1980). Fibronectin. Prog Hemost Thromb *5*, 111-151.

Mueller, M. M., and Fusenig, N. E. (2004). Friends or foes - bipolar effects of the tumour stroma in cancer. Nat Rev Cancer *4*, 839-849.

Murata, H., Ratajczak, P., Meignin, V.*, et al.* (2008). Endothelial cell chimerism associated with graft rejection after human lung transplantation. Transplantation *85*, 150-154.

Nagy, J. A., Chang, S. H., Shih, S. C.*, et al.* (2010). Heterogeneity of the tumor vasculature. Semin Thromb Hemost *36*, 321-331.

Nakamura, T., Matsumoto, K., Mizuno, S.*, et al.* (2005). Hepatocyte growth factor prevents tissue fibrosis, remodeling, and dysfunction in cardiomyopathic hamster hearts. Am J Physiol Heart Circ Physiol *288*, H2131-2139.

Natali, P. G., Nicotra, M. R., Bartolazzi, A.*, et al.* (1990). Expression and production of tenascin in benign and malignant lesions of melanocyte lineage. Int J Cancer *46*, 586-590.

Nathan, C. (2006). Role of iNOS in human host defense. Science *312*, 1874-1875; author reply 1874-1875.

Newman, P. J. (1997). The biology of PECAM-1. J Clin Invest *99*, 3-8.

Niesner, U., Halin, C., Lozzi, L.*, et al.* (2002). Quantitation of the tumor-targeting properties of antibody fragments conjugated to cell-permeating HIV-1 TAT peptides. Bioconjug Chem *13*, 729-736.

Nikolova, G., Jabs, N., Konstantinova, I.*, et al.* (2006). The vascular basement membrane: a niche for insulin gene expression and Beta cell proliferation. Dev Cell *10*, 397-405.

Olaso, E., Santisteban, A., Bidaurrazaga, J.*, et al.* (1997). Tumor-dependent activation of rodent hepatic stellate cells during experimental melanoma metastasis. Hepatology *26*, 634-642.

Olumi, A. F., Grossfeld, G. D., Hayward, S. W.*, et al.* (1999). Carcinoma-associated fibroblasts direct tumor progression of initiated human prostatic epithelium. Cancer Res *59*, 5002-5011.

O'Reilly, M. S. (1997). Angiostatin: an endogenous inhibitor of angiogenesis and of tumor growth. Exs *79*, 273-294.

Orend, G., and Chiquet-Ehrismann, R. (2006). Tenascin-C induced signaling in cancer. Cancer Lett *244*, 143-163.

Orend, G., Huang, W., Olayioye, M. A.*, et al.* (2003). Tenascin-C blocks cell-cycle progression of anchorage-dependent fibroblasts on fibronectin through inhibition of syndecan-4. Oncogene *22*, 3917-3926.

Orimo, A., Gupta, P. B., Sgroi, D. C.*, et al.* (2005). Stromal fibroblasts present in invasive human breast carcinomas promote tumor growth and angiogenesis through elevated SDF-1/CXCL12 secretion. Cell *121*, 335-348.

Oskarsson, T., Acharyya, S., Zhang, X. H.*, et al.* (2011). Breast cancer cells produce tenascin C as a metastatic niche component to colonize the lungs. Nat Med *17*, 867-874.

Ozawa, M. G., Yao, V. J., Chanthery, Y. H.*, et al.* (2005). Angiogenesis with pericyte abnormalities in a transgenic model of prostate carcinoma. Cancer *104*, 2104-2115.

Paez-Ribes, M., Allen, E., Hudock, J.*, et al.* (2009). Antiangiogenic therapy elicits malignant progression of tumors to increased local invasion and distant metastasis. Cancer Cell *15*, 220-231.

Paik, D. C., Fu, C., Bhattacharya, J.*, et al.* (2004). Ongoing angiogenesis in blood vessels of the abdominal aortic aneurysm. Exp Mol Med *36*, 524-533.

Papachristou, D. J., Papachroni, K. K., Basdra, E. K.*, et al.* (2009). Signaling networks and transcription factors regulating mechanotransduction in bone. Bioessays *31*, 794-804.

Parsonage, G., Filer, A. D., Haworth, O.*, et al.* (2005). A stromal address code defined by fibroblasts. Trends Immunol *26*, 150-156.

Patarroyo, M., Tryggvason, K., and Virtanen, I. (2002). Laminin isoforms in tumor invasion, angiogenesis and metastasis. Semin Cancer Biol *12*, 197-207.

Penn, J. S., Madan, A., Caldwell, R. B.*, et al.* (2008). Vascular endothelial growth factor in eye disease. Prog Retin Eye Res *27*, 331-371.

Perl, A. K., Wilgenbus, P., Dahl, U.*, et al.* (1998). A causal role for E-cadherin in the transition from adenoma to carcinoma. Nature *392*, 190-193.

Peters, J. H., Chen, G. E., and Hynes, R. O. (1996). Fibronectin isoform distribution in the mouse. II. Differential distribution of the alternatively spliced EIIIB, EIIIA, and V segments in the adult mouse. Cell Adhes Commun *4*, 127-148.

Pettersson, A., Nagy, J. A., Brown, L. F.*, et al.* (2000). Heterogeneity of the angiogenic response induced in different normal adult tissues by vascular permeability factor/vascular endothelial growth factor. Lab Invest *80*, 99-115.

Pezzolo, A., Parodi, F., Marimpietri, D.*, et al.* (2011). Oct-4(+)/Tenascin C(+) neuroblastoma cells serve as progenitors of tumor-derived endothelial cells. Cell Res.

Pham, T., Landewe, R., van der Linden, S.*, et al.* (2006). An international study on starting tumour necrosis factor-blocking agents in ankylosing spondylitis. Ann Rheum Dis *65*, 1620-1625.

Pinzone, J. J., Hall, B. M., Thudi, N. K.*, et al.* (2009). The role of Dickkopf-1 in bone development, homeostasis, and disease. Blood *113*, 517-525.

Pollard, J. W. (2004). Tumour-educated macrophages promote tumour progression and metastasis. Nat Rev Cancer *4*, 71-78.

Pollard, J. W. (2008). Macrophages define the invasive microenvironment in breast cancer. J Leukoc Biol *84*, 623-630.

Pollard, J. W. (2009). Trophic macrophages in development and disease. Nat Rev Immunol *9*, 259-270.

Ponz-Sarvise, M., Rodriguez, J., Viudez, A.*, et al.* (2007). Epidermal growth factor receptor inhibitors in colorectal cancer treatment: what's new? World J Gastroenterol *13*, 5877-5887.

Pritchard, C. C., and Grady, W. M. (2011). Colorectal cancer molecular biology moves into clinical practice. Gut *60*, 116-129.

Raza, A., Franklin, M. J., and Dudek, A. Z. (2010). Pericytes and vessel maturation during tumor angiogenesis and metastasis. Am J Hematol *85*, 593-598.

Rettig, W. J., Garin-Chesa, P., Healey, J. H.*, et al.* (1993). Regulation and heteromeric structure of the fibroblast activation protein in normal and transformed cells of mesenchymal and neuroectodermal origin. Cancer Res *53*, 3327-3335.

Reynolds, A. R., Hart, I. R., Watson, A. R.*, et al.* (2009). Stimulation of tumor growth and angiogenesis by low concentrations of RGD-mimetic integrin inhibitors. Nat Med *15*, 392-400.

Rodemann, H. P., and Muller, G. A. (1991). Characterization of human renal fibroblasts in health and disease: II. In vitro growth, differentiation, and collagen synthesis of fibroblasts from kidneys with interstitial fibrosis. Am J Kidney Dis *17*, 684-686.

Ronnov-Jessen, L., Petersen, O. W., and Bissell, M. J. (1996). Cellular changes involved in conversion of normal to malignant breast: importance of the stromal reaction. Physiol Rev *76*, 69-125.

Ruan, K., Bao, S., and Ouyang, G. (2009). The multifaceted role of periostin in tumorigenesis. Cell Mol Life Sci *66*, 2219-2230.

Ruegg, C. R., Chiquet-Ehrismann, R., and Alkan, S. S. (1989). Tenascin, an extracellular matrix protein, exerts immunomodulatory activities. Proc Natl Acad Sci U S A *86*, 7437-7441.

Ruiz, C., Huang, W., Hegi, M. E.*, et al.* (2004). Growth promoting signaling by tenascin-C [corrected]. Cancer Res *64*, 7377-7385.

Ruoslahti, E. (2002). Specialization of tumour vasculature. Nat Rev Cancer *2*, 83-90.

Rybak, J. N., Roesli, C., Kaspar, M.*, et al.* (2007). The extra-domain A of fibronectin is a vascular marker of solid tumors and metastases. Cancer Res *67*, 10948-10957.

Said, N. A., and Williams, E. D. (2011). Growth factors in induction of epithelial-mesenchymal transition and metastasis. Cells Tissues Organs *193*, 85-97.

Saltz, L. B., Clarke, S., Diaz-Rubio, E.*, et al.* (2008). Bevacizumab in combination with oxaliplatin-based chemotherapy as first-line therapy in metastatic colorectal cancer: a randomized phase III study. J Clin Oncol *26*, 2013-2019.

Scharer, C. D., McCabe, C. D., Ali-Seyed, M.*, et al.* (2009). Genome-wide promoter analysis of the SOX4 transcriptional network in prostate cancer cells. Cancer Res *69*, 709-717.

Schenk, S., Chiquet-Ehrismann, R., and Battegay, E. J. (1999). The fibrinogen globe of tenascin-C promotes basic fibroblast growth factor-induced endothelial cell elongation. Mol Biol Cell *10*, 2933-2943.

Scholzen, T., and Gerdes, J. (2000). The Ki-67 protein: from the known and the unknown. J Cell Physiol *182*, 311-322.

Simo, P., Simon-Assmann, P., Bouziges, F.*, et al.* (1991). Changes in the expression of laminin during intestinal development. Development *112*, 477-487.

Simon-Assmann, P., and Kedinger, M. (2000). Tissue recombinants to study extracellular matrix targeting to basement membranes. Methods Mol Biol *139*, 311-319.

Sini, P., Samarzija, I., Baffert, F.*, et al.* (2008). Inhibition of multiple vascular endothelial growth factor receptors (VEGFR) blocks lymph node metastases but inhibition of VEGFR-2 is sufficient to sensitize tumor cells to platinum-based chemotherapeutics. Cancer Res *68*, 1581-1592.

Sporn, E., Davis, J. W., Thaler, K.*, et al.* (2008). Sentinel node mapping during laparoscopic distal gastrectomy for gastric cancer. Surg Endosc *22*, 2097.

Stallcup, W. B., and Huang, F. J. (2008). A role for the NG2 proteoglycan in glioma progression. Cell Adh Migr *2*, 192-201.

Steeg, P. S. (2006). Tumor metastasis: mechanistic insights and clinical challenges. Nat Med *12*, 895-904.

Subauste, M. C., Kupriyanova, T. A., Conn, E. M.*, et al.* (2009). Evaluation of metastatic and angiogenic potentials of human colon carcinoma cells in chick embryo model systems. Clin Exp Metastasis *26*, 1033-1047.

Sugimoto, H., Mundel, T. M., Kieran, M. W.*, et al.* (2006). Identification of fibroblast heterogeneity in the tumor microenvironment. Cancer Biol Ther *5*, 1640-1646.

Sun, T., Sun, B. C., Zhao, X. L.*, et al.* (2011). Promotion of tumor cell metastasis and vasculogenic mimicry by way of transcription coactivation by Bcl-2 and Twist1: A study of hepatocellular carcinoma. Hepatology.

Swartz, D. J., and Santi, P. A. (1996). Immunofluorescent artifacts due to the pH of antifading mounting media. Biotechniques *20*, 398-400.

Talmadge, J. E., Donkor, M., and Scholar, E. (2007). Inflammatory cell infiltration of tumors: Jekyll or Hyde. Cancer Metastasis Rev *26*, 373-400.

Talts, J. F., Wirl, G., Dictor, M.*, et al.* (1999). Tenascin-C modulates tumor stroma and monocyte/macrophage recruitment but not tumor growth or metastasis in a mouse strain with spontaneous mammary cancer. J Cell Sci *112*, 1855-1864.

Tan, K., and Lawler, J. (2009). The interaction of Thrombospondins with extracellular matrix proteins. J Cell Commun Signal *3*, 177-187.

Tanaka, K., Hiraiwa, N., Hashimoto, H.*, et al.* (2004). Tenascin-C regulates angiogenesis in tumor through the regulation of vascular endothelial growth factor expression. Int J Cancer *108*, 31-40.

Tavazoie, M., Van der Veken, L., Silva-Vargas, V.*, et al.* (2008). A specialized vascular niche for adult neural stem cells. Cell Stem Cell *3*, 279-288.

Thudi, N. K., Martin, C. K., Murahari, S.*, et al.* (2010). Dickkopf-1 (DKK-1) stimulated prostate cancer growth and metastasis and inhibited bone formation in osteoblastic bone metastases. Prostate *71*, 615-625.

Tomasek, J. J., Gabbiani, G., Hinz, B.*, et al.* (2002). Myofibroblasts and mechano-regulation of connective tissue remodelling. Nat Rev Mol Cell Biol *3*, 349-363.

Tomayko, M. M., and Reynolds, C. P. (1989). Determination of subcutaneous tumor size in athymic (nude) mice. Cancer Chemother Pharmacol *24*, 148-154.

Tsafrir, D., Tsafrir, I., Ein-Dor, L.*, et al.* (2005). Sorting points into neighborhoods (SPIN): data analysis and visualization by ordering distance matrices. Bioinformatics *21*, 2301-2308.

Tsukada, T., Tippens, D., Gordon, D.*, et al.* (1987). HHF35, a muscle-actin-specific monoclonal antibody. I. Immunocytochemical and biochemical characterization. Am J Pathol *126*, 51-60.

Tucker, R. P., and Chiquet-Ehrismann, R. (2009). The regulation of tenascin expression by tissue microenvironments. Biochim Biophys Acta *1793*, 888-892.

Van Obberghen-Schilling, E., Tucker, R. P., Saupe, F.*, et al.* (2011). Fibronectin and tenascin-C: accomplices in vascular morphogenesis during development and tumor growth. Int J Dev Biol.

Verheul, H. M., Hammers, H., van Erp, K.*, et al.* (2007). Vascular endothelial growth factor trap blocks tumor growth, metastasis formation, and vascular leakage in an orthotopic murine renal cell cancer model. Clin Cancer Res *13*, 4201-4208.

Villa, A., Trachsel, E., Kaspar, M.*, et al.* (2008). A high-affinity human monoclonal antibody specific to the alternatively spliced EDA domain of fibronectin efficiently targets tumor neo-vasculature in vivo. Int J Cancer *122*, 2405-2413.

Viloria-Petit, A. M., and Kerbel, R. S. (2004). Acquired resistance to EGFR inhibitors: mechanisms and prevention strategies. Int J Radiat Oncol Biol Phys *58*, 914-926.

Vosseler, S., Mirancea, N., Bohlen, P.*, et al.* (2005). Angiogenesis inhibition by vascular endothelial growth factor receptor-2 blockade reduces stromal matrix metalloproteinase expression, normalizes stromal tissue, and reverts epithelial tumor phenotype in surface heterotransplants. Cancer Res *65*, 1294-1305.

Wagner, S., Hofstetter, W., Chiquet, M.*, et al.* (2003). Early osteoarthritic changes of human femoral head cartilage subsequent to femoro-acetabular impingement. Osteoarthritis Cartilage *11*, 508-518.

Wang, H. Y., Liu, T., and Malbon, C. C. (2006). Structure-function analysis of Frizzleds. Cell Signal *18*, 934-941.

Wang, X. M., Yu, D. M., McCaughan, G. W*., et al.* (2005). Fibroblast activation protein increases apoptosis, cell adhesion, and migration by the LX-2 human stellate cell line. Hepatology *42*, 935-945.

White, E. S., Baralle, F. E., and Muro, A. F. (2008). New insights into form and function of fibronectin splice variants. J Pathol *216*, 1-14.

WHO (2008). World Cancer Report 2008. International Agency for Research on Cancer.

Widmaier, E., Raff, H., and Strang, K. T. (2007). Vander's Human Physiology. 11th edition: McGraw-Hill.

Wilson, K. E., Bartlett, J. M., Miller, E. P*., et al.* (1999). Regulation and function of the extracellular matrix protein tenascin-C in ovarian cancer cell lines. Br J Cancer *80*, 685-692.

Wohl, S. G., Schmeer, C. W., Witte, O. W*., et al.* (2010). Proliferative response of microglia and macrophages in the adult mouse eye after optic nerve lesion. Invest Ophthalmol Vis Sci *51*, 2686-2696.

Worthley, D. L., and Leggett, B. A. (2010). Colorectal cancer: molecular features and clinical opportunities. Clin Biochem Rev *31*, 31-38.

Yano, H., Hara, A., Takenaka, K*., et al.* (2000). Differential expression of beta-catenin in human glioblastoma multiforme and normal brain tissue. Neurol Res *22*, 650-656.

Yao, X. H., Ping, Y. F., and Bian, X. W. (2011). Contribution of cancer stem cells to tumor vasculogenic mimicry. Protein Cell *2*, 266-272.

Zagzag, D., Friedlander, D. R., Dosik, J*., et al.* (1996). Tenascin-C expression by angiogenic vessels in human astrocytomas and by human brain endothelial cells in vitro. Cancer Res *56*, 182-189.

Zeisberg, M., Bottiglio, C., Kumar, N*., et al.* (2003). Bone morphogenic protein-7 inhibits progression of chronic renal fibrosis associated with two genetic mouse models. Am J Physiol Renal Physiol *285*, F1060-1067.

Annex

ANNEX

ANNEX 1: Tenascin-C promotes tumor angiogenesis and metastasis through repression of dickkopf-1

ANNEX 2: Fibronectin and tenascin-C: accomplices in vascular morphogenesis during development and tumor growth

ANNEX 3: « OpenLAB »: A 2h PCR- based practical for high school students

Annex1:
Tenascin-C promotes tumor angiogenesis and metastasis through repression of dickkopf-1

Tenascin-C Promotes Tumor Angiogenesis and Metastasis through Repression of Dickkopf-1

Falk Saupe[1a], Isabelle Gasser[1a], Yundan Jia[1a,2], Anja Heinke[1b], Martial Kammerer[1b], Thomas Hussenet[1], Marija Marko[1], Olivier Lefebvre[1], Michael van der Heyden[1], Monika Hegi[3], Ruslan Hlushchuk[4], Jessica Kant[1], Wentao Huang[2], Anne-Catherine Feutz[2], Patricia Simon-Assmann[1], Michèle Kedinger[1], Valentin Djonov[4], Gerhard Christofori[5] and Gertraud Orend[1,2]*

a: equal contribution as first author

b: equal contribution as second author

* corresponding author, Phone: 33 (0)3 88 27 53 55, Fax:33 (0)3 88 26 35 38, E-mail: gertraud.orend@inserm.u-strasbg.fr

[1] Inserm, U682, Strasbourg, F-67200 France, University of Strasbourg, CHRU Strasbourg, Department of Molecular Biology, Strasbourg, 67200 France.

[2] Institute of Biochemistry and Genetics, Department of Biomedicine, University of Basel, Switzerland, team G. Orend

[3] Centre Hospitalier Universitaire Vaudois (CHUV), University Lausanne, Switzerland

[4] Department of Medicine, Gross Anatomy and Vascular Biology, University of Fribourg, Fribourg, Switzerland

[5] Institute of Biochemistry and Genetics, Department of Biomedicine, University of Basel, Switzerland, team G. Christofori

Characters (with spaces): 43`870

Abstract

The tumor microenvironment is instrumental in cancer progression. The extracellular matrix molecule tenascin-C (TNC) is a major component of the cancer specific matrix and high TNC expression is linked to bad prognosis in several cancers. To delineate TNC's functions in cancer, we established transgenic tumor mouse lines with varying levels of TNC expression and compared sporadic neuroendocrine tumor formation in abundance or absence of TNC. We show that TNC promotes tumor angiogenesis, carcinoma progression and lung micrometastasis formation. TNC represses the Dickkopf-1 (DKK1) promoter and induces Wnt target genes in TNC transgenic tumors and in cultured cells. While overexpression of DKK1 does not affect proliferation of tumor cells, it compromises the formation of vascularised tumors. Thus TNC-induced repression of DKK1 in tumor cells exerts a paracrine effect on the tumor microenvironment. Our results implicate canonical Wnt signalling as underlying mechanism for TNC-mediated promotion of tumor angiogenesis and subsequent metastasis. The transgenic cancer models will be useful to evaluate the efficacy of therapeutic approaches targeting TNC and downstream signalling pathways for repressing tumor angiogenesis and metastasis.

Key words: Angiogenesis, Dickkopf-1, metastasis, tenascin-C, Wnt signalling

Running title: Tumor progression by tenascin-C through DKK1 repression

Introduction

Manifestation of cancer requires many steps in which the microenvironment plays an essential role (Bissell and Labarge, 2005). Cells with oncogenic mutations do not readily cause cancer, a phenomenon known as tumor dormancy (Aguirre-Ghiso, 2007; Folkman and Kalluri, 2004). Angiogenesis presents an important step in awakening quiescent tumors and in promoting their development into malignant cancers (Almog 2010). Many factors are driving angiogenesis but the early events in tumor angiogenesis are poorly understood. Tumor cells secrete soluble factors that attract endothelial cells (EC) and EC progenitors. Blood and lymphatic EC invade the tumor tissue and establish a neovasculature within the tumor which provides the tumor with a connection to the blood circulation and the lymphatic vessel system. These routes may be used by disseminating cancer cells to seed metastasis in distant organs (Bergers and Benjamin, 2003; Kerbel, 2008). Thus in addition to the cancer cells other cell types and the extracellular matrix (ECM) constitute a major fraction of cancer tissue and contribute to tumor angiogenesis and metastasis.

An important component of the tumor specific ECM is tenascin-C (TNC). TNC is prominently expressed in the tumor microenvironment and plays a promoting role in malignant tumor progression (Midwood and Orend, 2009). TNC is causally linked to lung metastasis in experimental murine breast cancer (Calvo et al., 2008; Tavazoie et al., 2008) and melanoma (Fukunaga-Kalabis et al., 2010) models. Moreover, TNC is amongst a few genes with predictive value in glioma malignancy (Colman et al., 2010) and in human breast cancer metastasis to the lung (Minn et al., 2005). High levels of TNC are linked to tamoxifen resistance in breast cancer (Helleman et al., 2008). Although TNC is now well linked to cancer progression, and first mechanistic insights have been obtained (Midwood and Orend, 2009; Orend, 2005; Orend and Chiquet-Ehrismann, 2006; Tavazoie et al., 2008), it is still unknown how TNC promotes tumor angiogenesis and metastasis.

Since no *in vivo* model with TNC overexpression existed that would allow to address the role of TNC in tumor progression, here we generated mouse lines with different expression levels of TNC (overexpression, wildtype, knock out) in the neuroendocrine Rip1Tag2 (RT2) tumorigenesis model (Hanahan, 1985). In RT2 mice, oncogenic simian virus 40 T-antigen (SV40Tag) is expressed under the control of the rat insulin II promoter in the insulin-producing β-cells of the islets of Langerhans. SV40Tag sequesters and represses the function of the two tumor suppressor gene products p53 and pRb, thus initiating transformation and hyperplasia of β-cells, which in turn triggers angiogenesis and insulinoma formation in a reproducible and sequential manner (Hanahan, 1985). This model recapitulates multistage tumorigenesis as observed in a large fraction of human cancers (Nevins, 2001; Pipas and Levine, 2001).

Here, we demonstrate that TNC promotes tumor angiogenesis and tumor progression to metastasizing carcinoma. We provide a mechanistic basis for TNC's function by showing that TNC induces canonical Wnt signalling and the expression of specific Wnt target genes through repression of the soluble inhibitor Dickkopf-1 (DKK1). The described mechanism potentially applies to malignancy in human gliomas where high TNC expression correlates with low DKK1 and high Wnt target gene expression in a subset of glioblastoma (GBM) grade IV tumors. Thus, TNC and DKK1 could be attractive therapeutic targets for blocking tumor angiogenesis, tumor cell dissemination and metastasis.

Results

Tenascin-C promotes proliferation and carcinoma formation in a stochastic neuroendocrine tumor model

To determine the role of TNC in tumor onset and progression, we utilized the murine RT2 insulinoma model to generate double-transgenic mice with overexpression of human TNC. For the generation of RipTNC single-transgenic mice, the cDNA of human TNC was

cloned downstream of the rat insulin II promoter (**Suppl. Fig. 1**). Transgenic RipTNC mice ectopically expressed the human TNC protein in β-cells of the pancreas (**Fig. 1A**), were healthy and fertile and did not exhibit obvious alterations in tissue morphology. Pancreatic islets normally displayed glucagon-positive α-cells surrounding β-cells. RipTNC males also exhibited normal blood glucose levels after starvation (not shown). Thus, ectopic expression of TNC did not appear to interfere with the function of the endocrine pancreas in RipTNC mice.

RT2/TNC double-transgenic mice were generated by breeding. Tumors of double-transgenic mice expressed human TNC (**Fig. 1A**). To determine a potential effect of TNC on tumor onset, we analysed whether islet size, which correlates with the tumorigenic state (Hanahan, 1985), was different between RT2/TNC and RT2 mice. We measured islet diameter on tissue sections and observed that at 10 weeks the ratio of angiogenic and tumorigenic islets (> 0.5 mm) over that of normal and hyperplastic islets (< 0.5 mm) was higher in RT2/TNC (0.8) than in RT2 control mice (0.4) and was close to statistical significance ($p = 0.06$) (**Suppl. Table 1**). At 12 weeks there was no difference in tumor number (**Fig. 1B**) or tumor volume (**Fig. 1C**) detectable between genotypes.

Next, we addressed whether ectopically expressed TNC had an effect on apoptosis and proliferation. Staining for cleaved caspase-3, a marker of apoptotic cells, did not reveal differences between tumors from 12 week old RT2/TNC and RT2 mice (not shown). Upon immunofluorescent staining for the proliferation marker phospho-histone-H3 (P-H3) followed by quantification, we noticed that tumors of RT2/TNC mice exhibited about 1.7-fold more proliferating cells than those from RT2 mice (**Fig. 1D**).

To investigate whether TNC potentially influenced tumor invasion, we determined the percentage of carcinomas amongst tumors of RT2 and RT2/TNC mice using invasion of β-tumor cells into the exocrine pancreas, the lack of a continuous basement membrane and the presence of atypical nuclei as parameters for carcinomas. We observed that the

frequency of carcinomas and the ratio of carcinoma versus adenoma was higher in tumors of RT2/TNC mice (1.8) than in RT2 controls (0.8) (**Fig. 1E, Suppl. Table 2**).
In summary, in the spontaneous insulinoma model, ectopically expressed TNC promoted tumor cell proliferation and invasion.

Tenascin-C promotes tumor angiogenesis

We addressed the role of TNC during tumor angiogenesis by quantification of CD31-positive cells in tumor sections of both genotypes (**Fig. 2A**). The number of CD31-positive endothelial cells (EC) turned out to be 1.9-fold (10 weeks) and 2.2-fold (12 weeks) higher in tumors of RT2/TNC mice than in tumors of RT2 controls (**Fig. 2B, C**).

To determine a potential effect of TNC on vessel anatomy we investigated Mercox corrosion casts of the vasculature by scanning electron microscopy and observed that vessels of RT2/TNC tumors were very different to that of RT2 control tumors; vessels appeared larger, more dilated and disorganized (**Fig. 2D**).

A potential angiogenesis-promoting effect of TNC was addressed in the chick chorio-allantoic membrane (CAM) assay. Compared to control treatment purified TNC increased the number of vessels to a similar extent as PDGF-BB, a known angiogenic growth factor (**Fig. 2E**).
Together these data demonstrate that ectopically expressed TNC promoted angiogenesis in spontaneously arising tumors generating vessels with an abnormal morphology.

Tenascin-C increases lung micrometastasis

Since knock down of TNC reduced the ability of breast cancer cells (Calvo et al., 2008; Tavazoie et al., 2008) and melanoma cells (Fukunaga-Kalabis et al., 2010) to form lung metastasis in immune-compromised xenograft models we investigated whether expression levels of TNC had an effect on metastasis in RT2 tumor mice. In a C57Bl6 background, RT2 mice usually do not exhibit macrometastasis (Hanahan, 1985; our

result). Therefore, we determined potentially arising micrometastases in various organs (heart, liver, lung) of 12 to 14 week old tumor-bearing mice by qRT-PCR for insulin. In contrast to the background levels of insulin mRNA in lungs of control RipTNC and wildtype mice and in hearts of RT2/TNC mice (not shown), a strong insulin-specific signal was observed in livers and lungs of RT2 and RT2/TNC mice. Yet, while insulin expression of micrometastatic β-tumor cells was indistinguishable between liver tissues of RT2 and RT2/TNC mice (not shown), insulin levels in lungs of RT2/TNC double-transgenic mice were 6.5-fold higher in comparison to lungs of RT2 single-transgenic mice (**Fig. 3A**). This result suggests that ectopically expressed TNC enhanced lung but not liver metastasis.

In RT2/TNC-/- mice we investigated whether the absence of TNC had an impact on metastasis. Analysis of insulin expression by qRT-PCR revealed 10-fold lower insulin levels in the lungs of RT2/TNC-/- mice than in RT2 mice carrying one intact TNC allele (RT2/TNC+/-, **Fig. 3B**). Overall, insulin expression levels were lower (close to background) in lungs of tumor mice with no transgenic TNC expression. Moreover, less RT2/TNC-/- (4/13) mice exhibited significant insulin expression and thus less micrometastasis than RT2/TNC+/- littermates (8/13).

To determine whether the insulin-positive signals were indeed derived from tumor cells that had colonized the lung, we stained sections of lungs for insulin and could detect a considerable number of insulinoma cells in clusters of 50 and more cells within the lung parenchyma of RT2/TNC mice by immunofluorescence and histology (**Fig. 3C**).

Nuclear localization of β-catenin in RT2/TNC tumors

In search for a mechanism that could explain tumor progression by TNC, we investigated a potential link of TNC to Wnt signalling in RT2/TNC tumors, since Wnt signalling was activated by a TNC substratum in cultured GBM cells (Ruiz et al., 2004). Determining expression of β-catenin revealed a profound difference between tumors of the two

genotypes; in contrast to exclusively membraneous β-catenin in RT2 control tumors, in RT2/TNC tumors β-catenin was also found in the nucleus of cells inside the tumor and at the invading tumor front (**Fig. 4A, B**). In contrast, no nuclear β-catenin was found in RT2 tumors (**Fig. 4A**). Confocal microscopic analysis confirmed that the β-catenin signal was indeed nuclear (**Fig. 2C**, inlet). Together, these results demonstrate that in a tumor context with forced expression of TNC, β-catenin was stabilized and translocated into the nucleus.

Tenascin-C impact on Wnt signalling and DKK1 expression in RT2/TNC tumors

In RT2/TNC tumors we determined expression of Wnt target genes by qRT-PCR on RNA extracted from isolated tumors. We observed that expression of cyclin D1 (2.5-fold), cyclin D2 (1.6-fold), CD44 (1.8-fold) and Slug (1.8-fold) was significantly increased in small still mostly differentiated tumors of RT2/TNC mice over that in RT2 controls (**Fig. 5A, Suppl. Table 3**). This was in contrast to other Wnt target genes (c-myc, Id2 and Lgr5) which were not elevated (not shown). These results suggest induction of a subset of Wnt target genes in a TNC-dependent manner in nascent carcinomas potentially driving progression of adenomas into carcinomas.

To elucidate whether TNC potentially activated Wnt signalling through DKK1 repression in RT2/TNC tumors*,* as had been demonstrated in cultured GBM cells (Ruiz et al., 2004), we determined DKK1 levels in RT2 tumors by qRT-PCR. In RT2/TNC mice, 7-times more tumors (50%) lacked DKK1 expression as compared to RT2 mice (7.1%) (**Fig. 5B**). In tumors with detectable DKK1 expression, the levels were 3.2-fold reduced in RT2/TNC mice in comparison to RT2 controls (**Fig. 5C, Suppl. Table 3**). Moreover, in RT2 tumors with only one TNC allele DKK1 levels were significantly lower (2-fold) than in RT2/TNC-/- tumors completely lacking TNC (**Fig. 5D**), which suggests that expression of TNC and DKK1 are inversely linked.

Impact of tenascin-C on DKK1 expression and Wnt signalling in cultured tumor cells

We investigated DKK1 mRNA levels in various cultured cancer cells that were grown on fibronectin (FN) and on FN/TNC, a valid condition to investigate TNC functions as previously described (Chiquet-Ehrismann, 1990; Huang et al., 2001). We observed that in T98G cells, DKK1 levels exhibited 20-fold repression after 5h and 24h of culture in the presence of TNC. DKK1 levels remained more than 5-times lower over a period of 12 days representing 80 - 95% repression (**Fig. 6A**). Although DKK1 protein levels still remained high after 5h, they were reduced after 1, 2 and 6 days on the TNC containing substratum (**Fig. 6B**).

We determined whether DKK1 repression is a general response of tumor cells on a TNC substratum. Therefore we compared expression of DKK1 in T98G cells with that in KRIB osteosarcoma, MCF7 and MDA-MB435 breast carcinoma and Caco-2 colon cancer cells. We observed that in all tested tumor cells DKK1 expression was lowered ranging from 23.2 - fold (KRIB) to 2.8 - fold (MCF7) 24h after plating on FN/TNC (**Fig. 6C**).

To address whether a TNC substratum had an effect on DKK1 promoter activity we determined DKK1 promoter-driven luciferase expression. Therefore we cloned a 3.0 kbp DKK1 promoter sequence upstream of the transcriptional start site in front of the luciferase gene. This reporter construct was used to measure luciferase activity upon transfection into T98G cells in the presence or absence of TNC. On a FN substratum luciferase expression was high which was in contrast to growth on FN/TNC where luciferase expression driven by the DKK1 promoter was significantly and more than 2.5-fold reduced in comparison to FN (**Fig. 6E**). This suggests that cell adhesion to TNC blocked transcription of DKK1.

We investigated expression of Wnt target genes on a TNC substratum by qRT-PCR. Whereas expression of some Wnt target genes (c-myc, cyclin D1, cyclin D2, CD44, Lgr5)

was not elevated (not shown), Id2 and FN levels were increased on the TNC substratum in T98G cells up to 3.4- and 2.6-fold at 7 and 12 days of culture, respectively (**Fig. 6D**). Slug was also induced in the presence of TNC in a delayed response up to 2.1-fold and 2.4-fold after 7 and 12 days, respectively. To investigate induction of Wnt signalling by TNC in more detail we determined expression of Wnt target genes in other cell lines. Whereas in MDA-MB435 cells no induction by TNC was noted, in KRIB cells on a TNC substratum an increased expression of the Wnt target genes Sox4 (van der Flier et al., 2007) (2.1-fold) at 24h and of Slug (2.4-fold) and FN (2.2-fold) at 6 days was observed (**Suppl. Table 4**). This was in contrast to CD44, Id2, c-myc, Lgr5 and cyclin D1 that were not elevated in KRIB cells (not shown).

To address whether low DKK1 levels were responsible for derepression and activation of Wnt signalling by TNC we engineered T98G cells stably overexpressing DKK1 (**Fig. 6F**). Upon plating of T98G:DKK1 cells on FN/TNC for 24h we determined Wnt target gene expression and observed that Id2 dropped to levels as on FN (**Fig. 6G**) which was in contrast to parental cells with an elevated expression of Id2 on FN/TNC. This result suggests that expression of Id2 is regulated by a TNC substratum through DKK1.

Together our data had revealed that in RT2 tumors TNC and DKK1 are inversely expressed and that in cultured tumor cells a TNC substratum represses DKK1 transcription through promoter inhibition in an early and sustained manner which results in the induction of Wnt target genes.

Role of DKK1 in proliferation, migration, angiogenesis and tumorigenesis

A potential functional link between TNC, DKK1 repression and tumorigenesis was further addressed in a xenograft model with DKK1 overexpressing tumor cells (T98G, KRIB) that we had generated (**Fig. 6F, 7A**). First we determined whether high DKK1 expression had an impact on proliferation and noticed that proliferation was indistinguishable between parental and DKK1 overexpressing KRIB (**Fig. 7B**) and T98G cells (data not shown). In a wound closure migration assay we investigated whether ectopically expressed DKK1 had

an impact on cell migration. KRIB cells migrated to close the scratched area in 13h, while KRIB:DKK1 cells were significantly retarded to do so (**Fig. 7C**).

Parental and DKK1 overexpressing cells were subcutaneously grafted into nude mice. Whereas T98G cells failed to induce tumors, KRIB cells induced tumors with 100% penetrance independent of the DKK1 expression levels. But KRIB tumors overexpressing DKK1 were highly necrotic (not shown) and remained significantly smaller (15.1 mm^3) than tumors originating from parental KRIB cells (591.3 mm^3) (**Fig. 7D**). By staining for KI67 we noticed that DKK1 overexpressing tumor cells were nevertheless proliferative (not shown). Macroscopical inspection revealed that KRIB:DKK1 tumors were pale white which was in contrast to KRIB tumors that were reddish and exhibited multiple blood vessels at the tumor surface (**Fig. 7E**). This almost complete absence of vessels in the DKK1 overexpressing tumors was confirmed by largely reduced CD31 staining (**Fig 7F, G**).

Correlated expression of TNC, DKK1 and Wnt target genes in a subgroup of GBM tumors

Finally, we investigated DKK1 expression in human primary GBM with documented high expression of TNC and Id2 (Ruiz et al., 2004). Protein expression levels were determined by immunohistochemistry in human GBM (WHO IV) on a tissue microarray (Murat et al., 2008, visualized in **Fig. 8**). We observed that in 70% (28/40) of GBM with no or low DKK1 immuno-positivity a robust expression of TNC coincided with elevated levels of Id2 and/or cyclin D1 in the majority of cases (**Fig. 8**). Unlike with other Wnt-pathway antagonists (Lambiv et al. *in press*) the DKK1 promoter is not methylated in primary GBM (Gotze et al., 2010). Hence, repression of DKK1 and induction of Wnt signalling by TNC might be specifically relevant in the subset of GBM that exhibit high expression of TNC, Id2 and cyclin D1 and low DKK1 expression. We also correlated the expression of DKK1 mRNA to survival of patients with GBM IV that had been treated with combined chemoradiotherapy comprising temozolomide (Murat et al., 2008; Stupp et al., 2009). Interestingly, increased expression of DKK1 mRNA was associated with better outcome

as indicated by a Hazard ratio below 1.0 (0.73, with 95% confidence interval 0.548-0.981, n = 42; p = 0.037; Cox model corrected for MGMT methylation and age).

Discussion

TNC plays an instrumental role in events causing cancer progression and metastasis (Midwood and Orend, 2009; Orend and Chiquet-Ehrismann, 2006) but the underlying mechanisms are poorly understood. Here, we have phenocopied TNC actions in human cancer by ectopically expressing TNC in insulinoma-prone RT2 mice and observed that increased TNC expression promotes carcinoma progression by promoting proliferation, invasion, angiogenesis and lung micrometastasis formation. Our results prove for the first time in an immune-competent stochastic tumor model that TNC drives tumorigenesis resulting in enhanced lung metastasis.

Our data suggest that enhanced tumor progression by TNC occurs through the repression of DKK1, a soluble inhibitor of canonical Wnt signalling (Glinka et al., 1998), and subsequent activation of Wnt signalling. The Wnt/β-catenin signalling pathway has been documented to promote tumor angiogenesis (Dejana 2010), cancer progression (Giles et al., 2003) and metastasis (Nguyen et al., 2009). By using RT2 mice with different TNC expression levels (wildtype, knock out, overexpression) we showed that DKK1 expression inversely correlates with the TNC copy number suggesting that TNC has an impact on DKK1 expression in spontaneously arising tumors. We had previously shown that a TNC substratum repressed DKK1 in GBM cells, stabilized β-catenin and induced Wnt target genes (Ruiz et al., 2004). Now we extended this observation by showing that DKK1 was robustly and consistently repressed by TNC in several tumor cell lines derived from breast, brain, colon and bone cancer tissue. Repression of DKK1 by TNC was already detectable after 4h and DKK1 remained repressed until the last time point of analysis (12 days) which correlated with low DKK1 protein levels. Signalling pathways involving p53 (Wang et al., 2000), c-jun (Grotewold and Ruther, 2002), vitamin D3 (Pendas-Franco et al., 2008) and NANOG (Zhu et al., 2009) have been

shown to induce DKK1 gene transcription. Conversely, promoter methylation (Aguilera et al., 2006), histone acetylation, polycomb family members (Hussain et al., 2009), and endothelin-1 signalling (Clines et al., 2007) downregulate DKK1 expression. Here, we have shown that cell adhesion to TNC represses DKK1 transcription. It is intriguing to speculate that endothelin signalling could be involved in TNC-induced DKK1 repression since TNC induced the endothelin receptor type A (Lange et al., 2007).

In agreement with an effect of DKK1 on Wnt signalling, we observed activation of Wnt signalling in small yet mostly differentiated tumors of RT2/TNC mice as evidenced by nuclear localization of β-catenin and increased expression of the Wnt target genes cyclin D1, cyclin D2, CD44 and Slug. Elevated expression of these genes in still differentiated tumors could have been instrumental in driving their evolution into carcinomas which is supported by an enhanced carcinoma formation seen in RT2/TNC mice.

In tumor cells cultured on a TNC substratum we also observed induction of Wnt targets, Id2 (T98G) and Sox4 (KRIB) and, FN and Slug in both cell lines. We conclude that tumor cells repress DKK1 and induce autocrine Wnt signalling resulting in cell type-specific transcriptional responses that are presumably affected by the Wnt ligand/receptor status and intrinsic signalling components. Functionally, we showed that DKK1 overexpression diminished tumor cell migration *in vitro*. Our results are consistent with a model where DKK1 repression in tumor cells could result in an autocrine activation of Wnt signalling thus promoting tumor cell migration and carcinoma formation. Nevertheless, in tumors reduced levels of secreted DKK1 may also lead to activation of Wnt signalling in stromal cells in a paracrine fashion and thus promote tumor angiogenesis and metastasis (**Fig. 9**).

Angiogenesis represents an important step on the road to metastasis. Here, we have demonstrated that tumors of RT2/TNC mice display an increased number of EC which is a hallmark of enhanced angiogenesis. In RT2/TNC tumors, blood vessels appeared

chaotic and were presumably not functional in supplying blood but may still have contributed to metastasis as was documented for non functional blood vessels in another study (Rolny et al., 2011). TNC has been shown to act as chemoattractant for EC, to play a role in the generation of tumor derived endothelial cells (Pezzolo et al., 2011), and to promote EC tube formation *in vitro* (Martina et al., 2010; Orend and Chiquet-Ehrismann, 2006). Now, using the CAM assay, we showed that TNC also induced EC sprouting. Despite a documented role of VEGFA-associated signalling in TNC-stimulated tumor angiogenesis (Tanaka et al., 2004) and induction of several pro-angiogenic factors (Ruiz et al., 2004), by qRT-PCR we have not found evidence for an increased expression of any of these molecules and pathways in RT2/TNC tumors (data not shown). In contrast, our results suggest an important role of DKK1 and Wnt signalling in TNC-driven angiogenesis. To address whether DKK1 levels had an impact on tumorigenesis/angiogenesis *in vivo*, we had utilized KRIB osteosarcoma cells overexpressing DKK1 and indeed observed that these cells failed to induce vascularised tumors.

The role of DKK1 in tumor progression has remained controversial with apparently contradictory observations published. In colon cancer (Gonzalez-Sancho et al., 2005), melanoma (Kuphal et al., 2006) and advanced prostate cancer (Hall et al., 2006), DKK1 is downregulated in comparison to the corresponding healthy tissues. Whereas DKK1 is low in breast cancer cells with an osteoblastic metastasis potential, it is highly expressed in breast cancer cells with an osteolytic metastasis potential and, DKK1 promotes osteolytic metastasis in myeloma (Pinzone et al., 2009). Finally, overexpression of DKK1 in canine Ace-1 prostate cancer cells promoted their metastatic potential upon intracardiac injection (Thudi et al., 2010). The role of DKK1 in tumor angiogenesis is also not clear. Whereas DKK1 appears to mobilize EC progenitor cells (Aicher et al., 2008; Smadja et al. 2011) and slightly enhanced tumor angiogenesis of already established xenografted human HBCx-12 breast cancer cells upon peri-tumoral injection of recombinant DKK1 (Smadja et al. 2011) here we observed that DKK1 overexpressed by

osteosarcoma cells blocked tumor growth, presumably by inhibiting tumor angiogenesis. Possible explanations for the different effects of DKK1 may be found in the different experimental systems and settings used and the influence of non-canonical Wnt signalling pathways involving JNK (Thudi et al., 2010).

In summary, for the first time we had demonstrated that the TNC levels determine the extent of angiogenesis and metastasis in an immune competent sporadic tumorigenesis model. These results provide formal proof of a decisive role of TNC in cancer progression. We also provide a mechanistic basis for the described TNC actions by showing that TNC induces canonical Wnt signalling through transcriptional repression of DKK1 thus triggering expression of selective Wnt targets. The described mechanism may also apply to malignancy in human gliomas and could be relevant for therapy since a high expression of DKK1 was linked to a better chemo- and radiotherapy response rate in GBM patients. Based on these observations, TNC presents an attractive target for blocking tumor angiogenesis and tumor cell dissemination. Drugs targeting TNC in cancer are already in clinical trials (Brack et al., 2006; Pedretti et al., 2009; Reardon et al., 2008). Our tumor mice with transgenic human TNC in a TNC negative background could serve as an excellent preclinical model for evaluating the efficacy of drugs targeting human TNC.

Experimental Procedures *(additional information in Suppl. information)*

Generation of transgenic RipTNC mice

The human TNC cDNA sequence (accession number X78656.1, (Aukhil et al., 1993) was cloned into the Rip1 vector by using the intermediate pcDNA3.1/Hygro(-) vector (**Suppl. Fig. 1**). The construct was partially sequenced and transferred into fertilized oocytes. Three transgenic mouse lines with stable expression and transmission of the transgene in a C57Bl6 background were established. Transgenic mice were identified by PCR. All experimental procedures involving mice were done according to the guidelines of the Swiss Federal Veterinary Office and of Inserm.

Generation of tumor mice with different TNC expression levels

RT2/TNC and RT2/TNC-/- mice were generated by breeding RT2 transgenic mice (Hanahan, 1985) with RipTNC (this study) and TNC-/- mice (Forsberg et al., 1996), respectively. RT2/TNC and control mice were fed with 5% glucose starting at 10 weeks of age. Tumors in RT2/TNC-/- and RT2/TNC+/- mice were investigated in a mixed C57Bl6/129/Sv background at 15-17 weeks of age.

Generation of rabbit anti-TNC antibodies and tissue analysis

Rabbit antisera recognizing human and murine TNC were derived upon injection of recombinant human TNC protein (Lange et al., 2007). Pancreata were dissected and tumors were collected. Tumor diameter was measured with a caliper and used to determine the tumor volume with the formula $V = 4/3\ \pi\ (d/2)^3$. Pancreata or xenograft tumors were embedded in the Tissue Tek O.C.T. compound or were fixed in 4% paraformaldehyde (PFA) followed by freezing in Tissue Tek O.C.T. or embedding into paraffin. Tissue sections were stained with primary and Cy3-, Cy5-, FITC- or Dylight 488-labeled secondary antibodies. CD31-or PH3-positive signals were quantified per constant field by using the Image J software. Tumor material from patients had been acquired upon written consent according to conventional ethics standards, was frozen or

embedded into paraffin before tissue analysis. Relative expression of the indicated gene products was determined in 68 GBM (WHO IV) on a tissue micro array (Murat et al., 2008) using immunohistochemistry. The immunostainings were scored semi-quantitatively (score 0–3) and categorized as described previously (Sivasankaran et al., 2009). Briefly, tumors were ordered by similarity of protein expression profiles using the SPIN software (data are centered, divided by the mean) (Tsafrir et al., 2005).

DKK1 promoter luciferase assay

A 3kb human DKK1 promoter sequence was cloned into the multiple cloning site of pGL3-basic Luciferase reporter vector (Promega). T98G cells were transiently transfected with TK-Renilla and pGL3-DKK1 Promoter construct or empty pGL3-basic vector. Transfections were performed with JetPEI^{TM} (Polyplus transfection). Cells were cultured in 1% DMEM and transfected with the reporter gene constructs 40 hours before using the Dual-Luciferase Reporter Assay System (Promega). Transfection with the renilla luciferase vector was used for normalization. Luciferase activity is presented as the ratio of pGL3-DKK1/pGL3-basic.

Cell culture

The indicated cell lines (ATCC) were plated onto FN or FN/TNC coated dishes for up to 12 days in DMEM supplemented with 10% FCS (MCF7 and MDA MB435) or 1% FCS (T98G, KRIB, Caco2 and HT29; see details in Huang et al. (2001)). RNA was isolated with the NucleoSpin RNA extraction kit (Macherey-Nagel, France) according to the manufacturer's instructions. Expression of candidate genes was determined by qRT-PCR using expression of ß2-microglobulin for normalization. Primer sequences are available in **Supplemental Table 6**. Cells were lysed in Laemmli buffer and immunoblotting was performed with antibodies recognizing Anti-DKK1 (Sigma-Aldrich, AV48015), 1:400, Anti-DKK1, N-terminal (Sigma-Aldrich, D3195), 1:1500, Anti-6xHis tag (Abcam, ab18184), 1:5000, Anti-α-tubulin (CP06, Oncogene, Boston, MA, USA).

Generation of DKK1 overexpressing cells

A BamHI and an EcoRI site were added in the pCDNA 3.1 mDDK1 V5 His plasmid before the ATG or the stop codon of the mouse Dickkopf cDNA respectively, using the GeneEditor™ *in vitro* Site-Directed Mutagenesis System, with the primers 5'-P-GGTGGAATTGCCCTTGGATCCACATGATGGTTGTGT-3' and 5'-P-ACCATCACCATTGAGAA TTCACCCGCTGATCAGCC-3'. After BamHI-EcoRI digestion, the mDKK1 V5 His fragment was gel purified (NucleoSpin® Extract II, Machery-Nagel, France) and cloned in the BamHI-EcoRI site of the pQCXIP retroviral vector (Clontech, Ozyme, France) generating the pQCXIP-mDKK1 V5 His vector. Retroviral particles were produced with the pQCXIP-cherry and pQCXIP-mDKK1 V5 His vectors, that were then used to transduce the cell lines according to standard protocols. Transduced cells were selected using Puromycin.

Tumor xenograft experiment

KRIB osteosarcoma cells (ATCC) with parental and ectopic DKK1 expression (4 million cells/100μl) were injected in the left upper back of nude mice (Charles River, 5 mice per condition). Mice were sacrificed after 3.5 weeks before measurement of the tumor size with a caliper. Tumor tissue was embedded in OCT, frozen on dry ice, and conserved at -80° C.

Expression analysis of candidate genes in the RT2 tumor model

Tissue from 12 – 17 week old mice was isolated, immediately snap frozen and RNA was extracted using the RNA kit according to the manufacturer's protocol (NucleoSpin Extract II, Machery-Nagel, France). RNA was reverse transcribed and qRT-PCR was performed using SYBR green or Taqman reaction mixtures. Primer sequences are available (see **Suppl. Table 5**). Data were normalized to the average of three reference genes RPL9, TBP and GAPDH. Relative expression between RT2 and RT2/TNC samples was calculated based on the mean ΔΔCt-values.

Analysis of the vessel morphology

For preparation of vascular casts, a Mercox solution containing accelerator was perfused before the pancreas was excised and further processed. Tissue samples were sputtered with gold and examined in a scanning electron microscope. For TEM the samples were fixed in a 2% PFA/2.5% glutaraldehyde solution before further processing in a 1% OsO_4 solution, dehydration in ethanol and embedding in epoxy resin. Upon staining with lead citrate and uranyl acetate, tissue sections were analysed.

CAM assay

Egg white (5 ml) was removed from chicken eggs at day 3 after fertilization before incubation at 37°C in a humidified chamber. At day 8 Whatman paper (0.5 cm in diameter, Whatman) soaked with 20 µl PDGF-BB (200 ng/ml, Sigma), purified human TNC (2 µg/ml) in PBS/0.01% Tween-20 and PBST control was placed onto the CAM in a region devoid of blood vessels. At day 11 the CAMs were removed from the embryo and analysed for blood vessel density by light microscopy. The number of vessels in 20 squares of 1 mm x 1 mm were used to quantify vessel density around and on top (not shown) of each sample. Results derived from 3 independent experiments.

Statistical analysis

Statistical analysis was done on original data using GraphPad Prism version 5.00. For significance of an association (contingency) Fisher's exact test or chi-square test was applied (tumor staging, gene expression, metastasis incidence, GBM analysis). Statistical differences of events were analysed by unpaired t-test (Gaussian distribution) or nonparametric Mann-Whitney test (no Gaussian distribution). Gaussian data sets with different variances were analysed by unpaired t-test with Welch's correction. p-values < 0.05 were considered as statistically significant.

Acknowledgement

We thank A. Klein, C. Arnold, C. Alcon, K. Strittmatter, H. Antoniadis, P. Lorentz, M.-F. Hamou and S. Kraemer for excellent technical assistance, J. Mutterer for capturing the confocal pictures, B. Scolari and R. Buergy for preparation of tissue samples for electron microscopy and E. Domany for the SPIN software. We are grateful to R. Chiquet-Ehrismann and the transgene facility of the Friedrich Miescher Institute for Biomedical Research for assistance with the generation of the transgenic mice. We also like to thank R. Fässler for providing the TNC knock out mice. I.G. was supported by a grant from Inserm/Region Alsace. O.L. and P.S.A. were supported by Ligue contre le Cancer. G.O. was supported by Krebsliga Beider Basel, Association for International Cancer Research, Swiss National Science Foundation, Oncosuisse, Novartis Foundation for Biological and Medical Sciences, the Hospital Hautepierre, Association pour la Recherche contre le Cancer and a grant from the Institut National du Cancer.

Author contribution

F.S., I.G., Y.J., A.H., M.K., T.H., M.M., O.L., M.H., R.H. J.K., W.H. and A.C.F. had performed experiments and contributed results. G.O., V.J. and G.C. supervised experiments. G.O., F.S., I.G. and Y.J. designed the study and G.O. wrote the manuscript with support from G.C., T.H.,M.K., F.S. and P.S.A.

Conflict of interest

The authors declare no conflict of interests.

References

Aguilera, O., Fraga, M.F., Ballestar, E., Paz, M.F., Herranz, M., Espada, J., Garcia, J.M., Munoz, A., Esteller, M. and Gonzalez-Sancho, J.M. (2006) Epigenetic inactivation of the Wnt antagonist DICKKOPF-1 (DKK-1) gene in human colorectal cancer. *Oncogene*, **25**, 4116-4121.

Aguirre-Ghiso, J.A. (2007) Models, mechanisms and clinical evidence for cancer dormancy. *Nat Rev Cancer*, **7**, 834-846.

Aicher, A., Kollet, O., Heeschen, C., Liebner, S., Urbich, C., Ihling, C., Orlandi, A., Lapidot, T., Zeiher, A.M. and Dimmeler, S. (2008) The Wnt antagonist Dickkopf-1 mobilizes vasculogenic progenitor cells via activation of the bone marrow endosteal stem cell niche. *Circ Res*, **103**, 796-803.

Almog, N. (2010) Molecular mechanisms underlying tumor dormancy. *Cancer Lett*, **294**, 139-146.

Aukhil, I., Joshi, P., Yan, Y. and Erickson, H.P. (1993) Cell- and heparin-binding domains of the hexabrachion arm identified by tenascin expression proteins. *J Biol Chem*, **268**, 2542-2553.

Bergers, G. and Benjamin, L.E. (2003) Tumorigenesis and the angiogenic switch. *Nat Rev Cancer*, **3**, 401-410.

Bissell, M.J. and Labarge, M.A. (2005) Context, tissue plasticity, and cancer: are tumor stem cells also regulated by the microenvironment? *Cancer Cell*, **7**, 17-23.

Brack, S.S., Silacci, M., Birchler, M. and Neri, D. (2006) Tumor-targeting properties of novel antibodies specific to the large isoform of tenascin-C. *Clin Cancer Res*, **12**, 3200-3208.

Calvo, A., Catena, R., Noble, M.S., Carbott, D., Gil-Bazo, I., Gonzalez-Moreno, O., Huh, J.I., Sharp, R., Qiu, T.H., Anver, M.R., Merlino, G., Dickson, R.B., Johnson, M.D. and Green, J.E. (2008) Identification of VEGF-regulated genes associated with increased lung metastatic potential: functional involvement of tenascin-C in tumor growth and lung metastasis. *Oncogene*.

Chiquet-Ehrismann, R. (1990) What distinguishes tenascin from fibronectin? *Faseb J*, **4**, 2598-2604.

Clines, G.A., Mohammad, K.S., Bao, Y., Stephens, O.W., Suva, L.J., Shaughnessy, J.D., Jr., Fox, J.W., Chirgwin, J.M. and Guise, T.A. (2007) Dickkopf homolog 1 mediates endothelin-1-stimulated new bone formation. *Mol Endocrinol*, **21**, 486-498.

Colman, H., Zhang, L., Sulman, E.P., McDonald, J.M., Shooshtari, N.L., Rivera, A., Popoff, S., Nutt, C.L., Louis, D.N., Cairncross, J.G., Gilbert, M.R., Phillips, H.S., Mehta, M.P., Chakravarti, A., Pelloski, C.E., Bhat, K., Feuerstein, B.G., Jenkins, R.B. and Aldape, K. A multigene predictor of outcome in glioblastoma. (2010) *Neuro Oncol*, **12**, 49-57.

Dejana, E. (2010) The role of wnt signaling in physiological and pathological angiogenesis. *Circ Res*, **107**, 943-952.

Folkman, J. and Kalluri, R. (2004) Cancer without disease. *Nature*, **427**, 787.

Forsberg, E., Hirsch, E., Frohlich, L., Meyer, M., Ekblom, P., Aszodi, A., Werner, S. and Fassler, R. (1996) Skin wounds and severed nerves heal normally in mice lacking tenascin-C. *Proc Natl Acad Sci U S A*, **93**, 6594-6599.

Fukunaga-Kalabis, M., Martinez, G., Nguyen, T.K., Kim, D., Santiago-Walker, A., Roesch, A. and Herlyn, M. Tenascin-C promotes melanoma progression by maintaining the ABCB5-positive side population. (2010) *Oncogene*, **29**, 6115-6124.

Giles, R.H., van Es, J.H. and Clevers, H. (2003) Caught up in a Wnt storm: Wnt signaling in cancer. *Biochim Biophys Acta*, **1653**, 1-24.

Glinka, A., Wu, W., Delius, H., Monaghan, A.P., Blumenstock, C. and Niehrs, C. (1998) Dickkopf-1 is a member of a new family of secreted proteins and functions in head induction. *Nature*, **391**, 357-362.

Gonzalez-Sancho, J.M., Aguilera, O., Garcia, J.M., Pendas-Franco, N., Pena, C., Cal, S., Garcia de Herreros, A., Bonilla, F. and Munoz, A. (2005) The Wnt antagonist DICKKOPF-1 gene is a downstream target of beta-catenin/TCF and is downregulated in human colon cancer. *Oncogene*, **24**, 1098-1103.

Gotze, S., Wolter, M., Reifenberger, G., Muller, O. and Sievers, S. (2010) Frequent promoter hypermethylation of Wnt pathway inhibitor genes in malignant astrocytic gliomas. *Int J Cancer*, **126**, 2584-2593.

Grotewold, L. and Ruther, U. (2002) The Wnt antagonist Dickkopf-1 is regulated by Bmp signaling and c-Jun and modulates programmed cell death. *Embo J*, **21**, 966-975.

Hall, C.L., Kang, S., MacDougald, O.A. and Keller, E.T. (2006) Role of Wnts in prostate cancer bone metastases. *J Cell Biochem*, **97**, 661-672.

Hanahan, D. (1985) Heritable formation of pancreatic beta-cell tumours in transgenic mice expressing recombinant insulin/simian virus 40 oncogenes. *Nature*, **315**, 115-122.

Helleman, J., Jansen, M.P., Ruigrok-Ritstier, K., van Staveren, I.L., Look, M.P., Meijer-van Gelder, M.E., Sieuwerts, A.M., Klijn, J.G., Sleijfer, S., Foekens, J.A. and Berns, E.M. (2008) Association of an extracellular matrix gene cluster with breast cancer prognosis and endocrine therapy response. *Clin Cancer Res*, **14**, 5555-5564.

Huang, W., Chiquet-Ehrismann, R., Moyano, J.V., Garcia-Pardo, A. and Orend, G. (2001) Interference of tenascin-C with syndecan-4 binding to fibronectin blocks cell adhesion and stimulates tumor cell proliferation. *Cancer Res*, **61**, 8586-8594.

Hussain, M., Rao, M., Humphries, A.E., Hong, J.A., Liu, F., Yang, M., Caragacianu, D. and Schrump, D.S. (2009) Tobacco smoke induces polycomb-mediated repression of Dickkopf-1 in lung cancer cells. *Cancer Res*, **69**, 3570-3578.

Kerbel, R.S. (2008) Tumor angiogenesis. *N Engl J Med*, **358**, 2039-2049.

Kuphal, S., Lodermeyer, S., Bataille, F., Schuierer, M., Hoang, B.H. and Bosserhoff, A.K. (2006) Expression of Dickkopf genes is strongly reduced in malignant melanoma. *Oncogene*, **25**, 5027-5036.

Lambiv, W.L., Vassallo, I., Delorenzi, M., Shay, T., Diserens, A-C., Misra, A., Feuerstein, B.G., Murat, A., Migliavacca, E., Hamou, M-F., Sciuscio, D., Burger, R., Domany, E., Stupp, R., Hegi, M.E. The Wnt inhibitory factor 1 (WIF-1) is targeted in

glioblastoma and has tumor suppressing function potentially mediated by induction of senescence. Neuro Oncol. *in press.*

Lange, K., Kammerer, M., Hegi, M.E., Grotegut, S., Dittmann, A., Huang, W., Fluri, E., Yip, G.W., Gotte, M., Ruiz, C. and Orend, G. (2007) Endothelin receptor type B counteracts tenascin-C-induced endothelin receptor type A-dependent focal adhesion and actin stress fiber disorganization. *Cancer Res*, **67**, 6163-6173.

Martina, E., Degen, M., Ruegg, C., Merlo, A., Lino, M.M., Chiquet-Ehrismann, R. and Brellier, F. (2010) Tenascin-W is a specific marker of glioma-associated blood vessels and stimulates angiogenesis in vitro. *Faseb J*, **24**, 778-787.

Midwood, K.S. and Orend, G. (2009) The role of tenascin-C in tissue injury and tumorigenesis. *J Cell Commun Signal*. 3, 287 - 310.

Minn, A.J., Gupta, G.P., Siegel, P.M., Bos, P.D., Shu, W., Giri, D.D., Viale, A., Olshen, A.B., Gerald, W.L. and Massague, J. (2005) Genes that mediate breast cancer metastasis to lung. *Nature*, **436**, 518-524.

Murat, A., Migliavacca, E., Gorlia, T., Lambiv, W.L., Shay, T., Hamou, M.F., de Tribolet, N., Regli, L., Wick, W., Kouwenhoven, M.C., Hainfellner, J.A., Heppner, F.L., Dietrich, P.Y., Zimmer, Y., Cairncross, J.G., Janzer, R.C., Domany, E., Delorenzi, M., Stupp, R. and Hegi, M.E. (2008) Stem cell-related "self-renewal" signature and high epidermal growth factor receptor expression associated with resistance to concomitant chemoradiotherapy in glioblastoma. *J Clin Oncol*, **26**, 3015-3024.

Nevins, J.R. (2001) The Rb/E2F pathway and cancer. *Hum Mol Genet*, **10**, 699-703.

Nguyen, D.X., Chiang, A.C., Zhang, X.H., Kim, J.Y., Kris, M.G., Ladanyi, M., Gerald, W.L. and Massague, J. (2009) WNT/TCF signaling through LEF1 and HOXB9 mediates lung adenocarcinoma metastasis. *Cell*, **138**, 51-62.

Orend, G. (2005) Potential oncogenic action of tenascin-C in tumorigenesis. *Int J Biochem Cell Biol*, **37**, 1066-1083.

Orend, G. and Chiquet-Ehrismann, R. (2006) Tenascin-C induced signaling in cancer. *Cancer Lett*, **244**, 143-163.

Pedretti, M., Soltermann, A., Arni, S., Weder, W., Neri, D. and Hillinger, S. (2009) Comparative immunohistochemistry of L19 and F16 in non-small cell lung cancer and mesothelioma: two human antibodies investigated in clinical trials in patients with cancer. *Lung Cancer*, **64**, 28-33.

Pendas-Franco, N., Aguilera, O., Pereira, F., Gonzalez-Sancho, J.M. and Munoz, A. (2008) Vitamin D and Wnt/beta-catenin pathway in colon cancer: role and regulation of DICKKOPF genes. *Anticancer Res*, **28**, 2613-2623.

Pezzolo, A., Parodi, F., Marimpietri, D., Raffaghello, L., Cocco, C., Pistorio, A., Mosconi, M., Gambini, C., Cilli, M., Deaglio, S., Malavasi, F. and Pistoia, V. (2011) Oct-4(+)/Tenascin C(+) neuroblastoma cells serve as progenitors of tumor-derived endothelial cells. *Cell Res*. Mar 15, Epub ahead of print.

Pinzone, J.J., Hall, B.M., Thudi, N.K., Vonau, M., Qiang, Y.W., Rosol, T.J. and Shaughnessy, J.D., Jr. (2009) The role of Dickkopf-1 in bone development, homeostasis, and disease. *Blood*, **113**, 517-525.

Pipas, J.M. and Levine, A.J. (2001) Role of T antigen interactions with p53 in tumorigenesis. *Semin Cancer Biol*, **11**, 23-30.

Reardon, D.A., Zalutsky, M.R., Akabani, G., Coleman, R.E., Friedman, A.H., Herndon, J.E., 2nd, McLendon, R.E., Pegram, C.N., Quinn, J.A., Rich, J.N., Vredenburgh, J.J., Desjardins, A., Guruangan, S., Boulton, S., Raynor, R.H., Dowell, J.M., Wong, T.Z., Zhao, X.G., Friedman, H.S. and Bigner, D.D. (2008) A pilot study: 131I-antitenascin monoclonal antibody 81c6 to deliver a 44-Gy resection cavity boost. *Neuro Oncol*, **10**, 182-189.

Rolny, C., Mazzone, M., Tugues, S., Laoui, D., Johansson, I., Coulon, C., Squadrito, M.L., Segura, I., Li, X., Knevels, E., Costa, S., Vinckier, S., Dresselaer, T., Akerud, P., De Mol, M., Salomaki, H., Phillipson, M., Wyns, S., Larsson, E., Buysschaert, I., Botling, J., Himmelreich, U., Van Ginderachter, J.A., De Palma, M., Dewerchin, M., Claesson-Welsh, L. and Carmeliet, P. (2011) HRG inhibits tumor growth and metastasis by inducing macrophage polarization and vessel normalization through downregulation of PlGF. *Cancer Cell*, **19**, 31-44.

Ruiz, C., Huang, W., Hegi, M.E., Lange, K., Hamou, M.F., Fluri, E., Oakeley, E.J., Chiquet-Ehrismann, R. and Orend, G. (2004) Growth promoting signaling by tenascin-C [corrected]. *Cancer Res*, **64**, 7377-7385.

Sivasankaran, B., Degen, M., Ghaffari, A., Hegi, M.E., Hamou, M.F., Ionescu, M.C., Zweifel, C., Tolnay, M., Wasner, M., Mergenthaler, S., Miserez, A.R., Kiss, R., Lino, M.M., Merlo, A., Chiquet-Ehrismann, R. and Boulay, J.L. (2009) Tenascin-C is a novel RBPJkappa-induced target gene for Notch signaling in gliomas. *Cancer Res*, **69**, 458-465.

Smadja, D.M., d'Audigier, C., Weiswald, L.B., Badoual, C., Dangles-Marie, V., Mauge, L., Evrard, S., Laurendeau, I., Lallemand, F., Germain, S., Grelac, F., Dizier, B., Vidaud, M., Bieche, I. and Gaussem, P. (2011) The Wnt antagonist Dickkopf-1 increases endothelial progenitor cell angiogenic potential. *Arterioscler Thromb Vasc Biol*, **30**, 2544-2552.

Stupp, R., Hegi, M.E., Mason, W.P., van den Bent, M.J., Taphoorn, M.J., Janzer, R.C., Ludwin, S.K., Allgeier, A., Fisher, B., Belanger, K., Hau, P., Brandes, A.A., Gijtenbeek, J., Marosi, C., Vecht, C.J., Mokhtari, K., Wesseling, P., Villa, S., Eisenhauer, E., Gorlia, T., Weller, M., Lacombe, D., Cairncross, J.G. and Mirimanoff, R.O. (2009) Effects of radiotherapy with concomitant and adjuvant temozolomide versus radiotherapy alone on survival in glioblastoma in a randomised phase III study: 5-year analysis of the EORTC-NCIC trial. *Lancet Oncol*, **10**, 459-466.

Tanaka, K., Hiraiwa, N., Hashimoto, H., Yamazaki, Y. and Kusakabe, M. (2004) Tenascin-C regulates angiogenesis in tumor through the regulation of vascular endothelial growth factor expression. *Int J Cancer*, **108**, 31-40.

Tavazoie, S.F., Alarcon, C., Oskarsson, T., Padua, D., Wang, Q., Bos, P.D., Gerald, W.L. and Massague, J. (2008) Endogenous human microRNAs that suppress breast cancer metastasis. *Nature*, **451**, 147-152.

Thudi, N.K., Martin, C.K., Murahari, S., Shu, S.T., Lanigan, L.G., Werbeck, J.L., Keller, E.T., McCauley, L.K., Pinzone, J.J. and Rosol, T.J. (2010) Dickkopf-1 (DKK-1)

stimulated prostate cancer growth and metastasis and inhibited bone formation in osteoblastic bone metastases. *Prostate*, **71**, 615-625.

Tsafriri, D, Tsafrir, I., Ein-Dor, L., Zuk, O., Notterman, D.A. and Domany, E. (2005) Sorting points into neighborhoods (SPIN): data analysis and visualization by ordering distance matrices. *Bioinformatics*, **21**, 2301-2308.

Van der Flier, L.G., Sabates-Bellver, J., Oving, I., Haegebarth, A., De Palo, M., Anti, M., Van Gijn, M.E., Suijkerbuijk, S., Van de Wetering, M., Marra, G. and Clevers, H. (2007) The Intestinal Wnt/TCF Signature. *Gastroenterology*, **132**, 628-632.

Wang, J., Shou, J. and Chen, X. (2000) Dickkopf-1, an inhibitor of the Wnt signaling pathway, is induced by p53. *Oncogene*, **19**, 1843-1848.

Zhu, Y., Sun, Z., Han, Q., Liao, L., Wang, J., Bian, C., Li, J., Yan, X., Liu, Y., Shao, C. and Zhao, R.C. (2009) Human mesenchymal stem cells inhibit cancer cell proliferation by secreting DKK-1. *Leukemia*, **23**, 925-933.

Figure legends

Fig. 1 TNC promotes tumor proliferation and invasion

Expression of transgenic TNC in pancreatic islets (encircled) of a RipTNC pancreas and in RT2/TNC tumors (**A**) was determined by immunohistological staining of tissue sections with a human TNC specific antibody. (**B, C**) All macroscopical visible tumors from 12 week old mice and the tumor volume was determined with the formula $V=4/3\ \pi\ (d/2)^3$, (d=diameter in mm). RT2 (N = 33 mice, n = 156 tumors), RT2/TNC (N = 26; n = 117), not significant. (**D**) Proliferating cells in islets of 12 week old RT2 and RT2/TNC mice were identified with a phospho histone H3 (P-H3) specific antibody and quantified as event per mm^2 using the Image J program. RT2 (N = 13, n = 199 sections), RT2/TNC (N = 13, n = 176). $p < 0.0001$, Mann Whitney test. (**E**) The number of adenomas (Ad) and carcinomas (Ca) per mouse was determined in microscopic tumor sections of RT2 and RT2/TNC mice. RT2 (N = 22, n = 120 tumors), RT2/TNC (N = 24, n = 157). SEM, $p = 0.001$, unpaired t-test. Scale bar, 100 μm (upper panels), 500 μm (lower panels).

Fig. 2 Overexpressed TNC promotes tumor angiogenesis

(**A**) Staining and quantification of CD31 in tumors of 10 (**B**) and 12 (**C**) week old RT2 and RT2/TNC mice. Relative expression was determined as event per mm^2. Number of samples; (**B**) 10 weeks, RT2 (N = 5 mice, n = 13 tumors), RT2/TNC (N = 7, n = 19); 1.92-fold, SEM, $p = 0.0006$, unpaired t-test; (**C**) 12 weeks, RT2 (N = 6, n = 34, 203 data points) and RT2/TNC (N = 4, n = 17, 106 data points), 2.27-fold, SEM, $p < 0.0001$, Mann Whitney test. Scale bar 100 μm. (**D**) Reproduction of the vasculature in tumors of 12 week old RT2 and RT2/TNC mice in corrosion casts upon Mercox perfusion. (**E**) Blood vessel quantification in the CAM assay. Number of samples, PBS-Tween (PBST) = 12, PDGF = 10 and TNC = 9, 1.85 – fold (TNC over PBST), SD, $p = 0.001$, unpaired t-test.

Fig. 3 TNC enhances lung micrometastasis

(**A, B**) Relative expression of insulin in lung tissue of RT2, RT2/TNC, RT2/TNC-/- and RT2/TNC+/- tumor mice was determined by qRT-PCR. (**C**) Immunofluorescent anti-

insulin and H & E staining of lung tissue from a RT2/TNC mouse. Number of samples; (**A**) 14 weeks, RT2 (N = 26), RT2/TNC (N = 24), 6.5 – fold, p = 0.0229, unpaired t-test, (**B**) 16 – 17 weeks, RT2/TNC-/- (N = 13), RT2/TNC+/- (N = 13), 10.2 –fold, p = 0.0283 Mann Whitney test. Scale bar 50 μm.

Fig. 4 Nuclear localization of β-catenin in RT2/TNC tumors

Expression analysis of β-catenin was done by immunohistochemistry and immunofluorescence in tumors of 14 week old RT2 (N = 5) and RT2/TNC (N = 8) mice. Pictures display tumor cells with nuclear β-catenin inside the tumor (**A**), at the invading front (**B**) and at the tumor rim (**C,** inlet: confocal picture). White asterisks (**B, C**), cells with nuclear β-catenin. Scale bars, 100 μm (**B** inlet), 200 μm (**B – C**), 10 μm (**C**, inlet). Boxes represent areas of higher magnification.

Fig. 5 TNC impact on Wnt signalling and DKK1 expression in RT2 tumors

(**A**) Wnt target gene and (**B-D**) DKK1 expression was determined by qRT-PCR on RNA from tumors of 14-17 week old mice. (**B**) The number of tumors per genotype that lacked any DKK1 RNA is displayed as % of all analysed tumors, p = 0.0031, Fisher`s exact test. (**C**) DKK1 levels in RT2/TNC and control tumors of 14 week old mice with detectable expression, p = 0.0021, unpaired t-test with Welsh`s correction. (**D**) DKK1 expression in RT2/TNC-/- and RT2/TNC+/- tumors. p = 0.0230, Mann-Whitney test. Number of samples, RT2 (N = 11 mice, n = 28 tumors) and RT2/TNC mice (N = 3, n = 14). See details in **Suppl. Table 3**.

Fig. 6 Impact of TNC on DKK1 expression and Wnt signalling in cultured tumor cells

Different tumor cells were plated on a FN or FN/TNC substratum for the indicated time points, before extraction of RNA and subsequent qRT-PCR (**A**, **C**, **D**), or protein lysis and immunoblotting for DKK1 (T98G cells) (**B, F**). Gene expression levels in the presence of TNC are displayed in comparison to the absence of TNC (T98G). Note that a TNC

substratum strongly reduced DKK1 expression in multiple tumor cell lines after 24 hours (KRIB, MDA-MB435 (MDA), MCF7, Caco2 and T98G) (**C**) and over a period of 5 hours up to 12 days (T98G) (**A**). This correlated with induction of Wnt target genes in T98G (**D**) and KRIB cells (**Suppl. Table 4**). Unpaired t-test $*$ $p < 0.05$, $**$ $p < 0.01$, $***$ $p < 0.001$. (**E**) DKK1 promoter inhibition by TNC. T98G cells were transfected with a DKK1-promoter/luciferase (or empty pGL3 control) plasmid together with TK-Renilla before plating on FN or FN/TNC (triplicates) and subsequent determination of luciferase activity which is presented upon normalization to Renilla. $p < 0.01$. Paired t-test. (**F**) Ectopically expressed murine DKK1 is detected by immunoblotting for murine DKK1 and the His-tag. In contrast to indistinguishable levels of endogenous DKK1 a high expression of ectopic murine DKK1 is noted in T98G:DKK1 cells. (**G**) Id2 expression in parental and T98G:DKK1 cells on FN and FN/TNC was determined by qRT-PCR. SD, $p< 0.05$, unpaired t-test.

Fig. 7 Consequences of DKK1 overexpression in KRIB cells in vitro and in vivo

(**A – C**), Consequences of DKK1 overexpression in cultured KRIB cells. (**A**) Western blot of KRIB cells overexpressing DKK1. (**B**) Proliferation of KRIB:DKK1 and parental cells was determined after the indicated time points by using the MTS assay. (**C**) Cell migration of KRIB:DKK1 and parental cells was determined in a wound healing assay. The scratched area covered by cells at day 13 (t = 3) is represented in comparison to that at day 0 (t = 0) (%). Experiment was done in triplicates, SD, $p< 0.0001$, student`s t-test. (**D – G**) Consequences of DKK1 overexpression in KRIB cells upon xenografting in nude mice. (**D**) Determination of tumor volume, 39 – fold, $p = 0.0079$, Mann Whitney test. (**E**) Macroscopical appearance of tumors. (**F**) Quantification of the CD31 signal (area in mm^2 / tumor) in parental and KRIB:DKK1 tumors. 7.5 – fold, SEM, $p = 0.0079$, Mann Whitney test. (**G**) Immunostaining of representative slides from KRIB:DKK1 and parental KRIB derived tumors for the indicated molecules. d, days. Scale bar represents 100 μm.

Fig. 8 Correlated expression of TNC, DKK1 and Wnt target genes in a subgroup of GBM tumors

Relative expression of the indicated gene products was determined in 68 GBM (WHO IV) on a tissue microarray (Murat et al., 2008) using immunohistochemistry. Low DKK1 expression was significantly correlated with high cyclin D1 expression (Fisher`s exact test $p < 0.05$).

Fig. 9 Proposed model of TNC effect on Wnt signalling and subsequent tumor invasion, tumor angiogenesis and metastasis formation

(**A**) Adhesion of tumor cells to a TNC substratum blocks expression of the soluble Wnt inhibitor DKK1 by promoter inhibition which subsequently leads to stabilization and nuclear translocation of β-catenin and induction of Wnt target genes with an appropriate Wnt receptor/ligand setting. (**B**) Repression of DKK1 by TNC in tumor cells does not only have an autocrine effect on tumor cells such as promoting their invasion, but also may de-repress and promote Wnt signalling in stromal cells in a paracrine manner thus promoting tumor angiogenesis. This possibility is supported by DKK1 overexpressing tumor cells forming poorly vascularised tumors.

Fig. 1

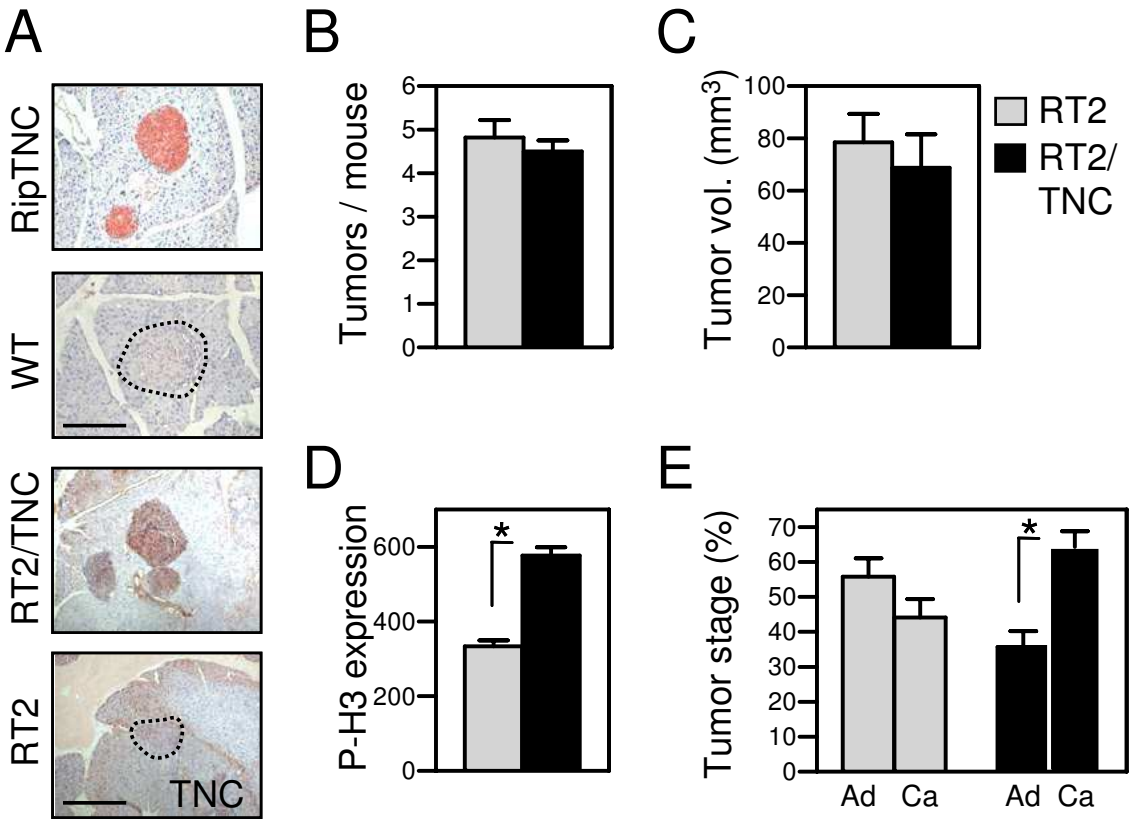
A
RipTNC
WT
RT2/TNC
RT2
TNC
B
Tumors / mouse
0
1
2
3
4
5
6
C
Tumor vol. (mm3)
0
20
40
60
80
100
RT2
RT2/
TNC
D
P-H3 expression
0
200
400
600
*
E
Tumor stage (%)
0
10
20
30
40
50
60
70
*
Ad
Ca
Ad
Ca

Fig. 2

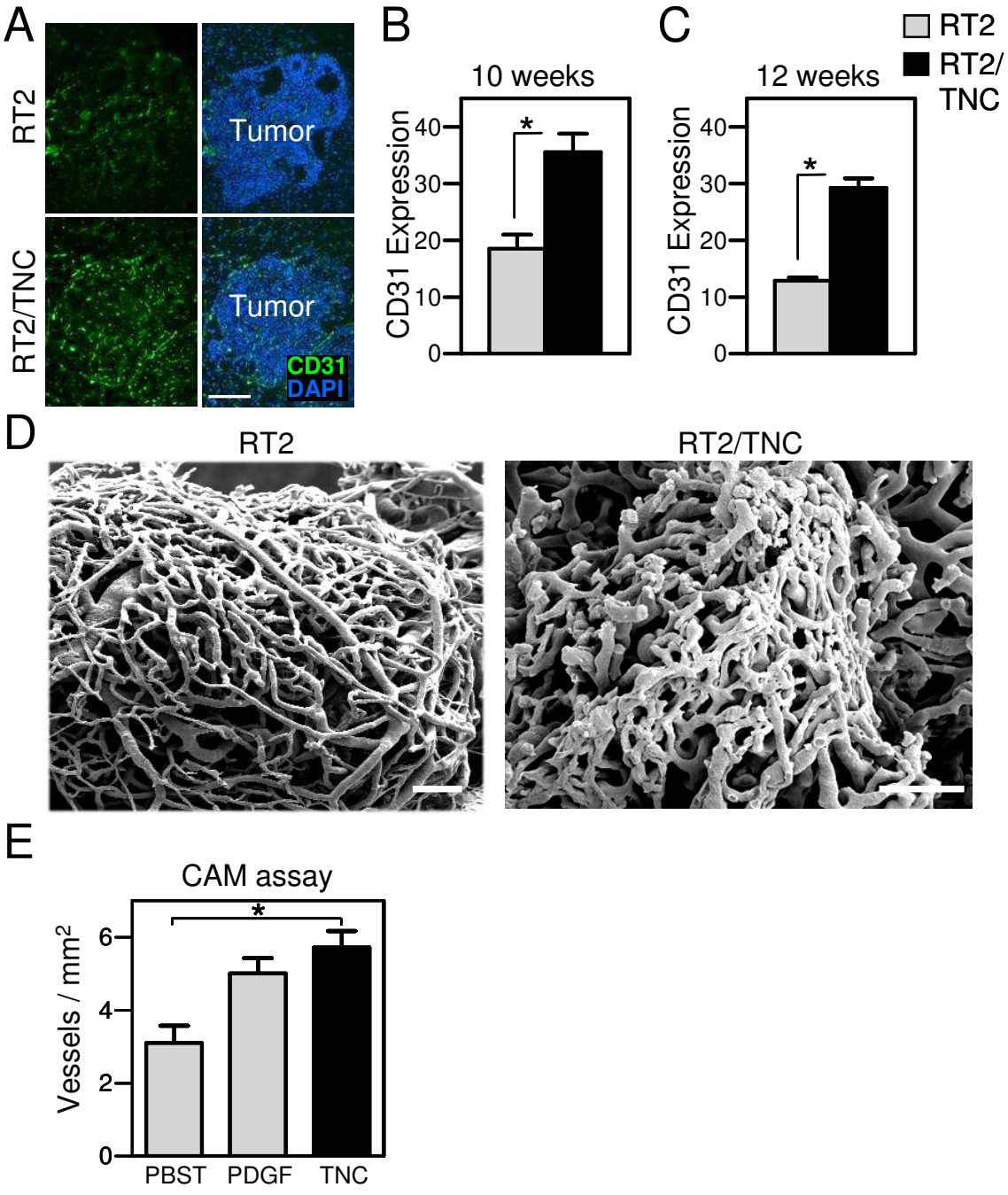
A
RT2
RT2/TNC
Tumor
Tumor
CD31
DAPI
B
10 weeks
CD31 Expression
40
30
20
10
0
*
C
12 weeks
RT2
RT2/
TNC
D
RT2
RT2/TNC
E
CAM assay
Vessels / mm2
6
4
2
0
*
PBST
PDGF
TNC

Fig. 3

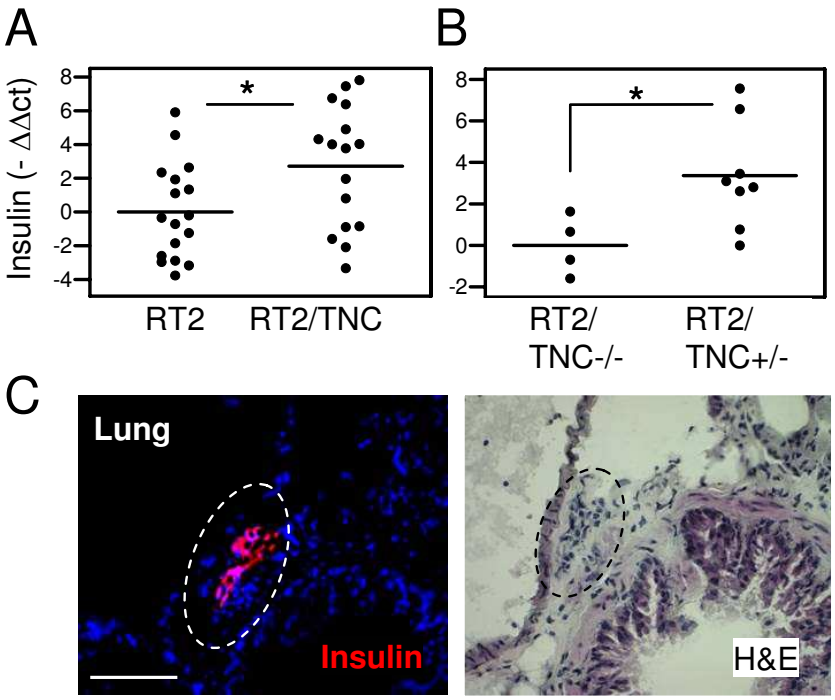
A
B
C
Insulin (- ΔΔct)
8
6
4
2
0
-2
-4
*
RT2
RT2/TNC
RT2/
TNC-/-
RT2/
TNC+/-
Lung
Insulin
H&E

Fig. 4

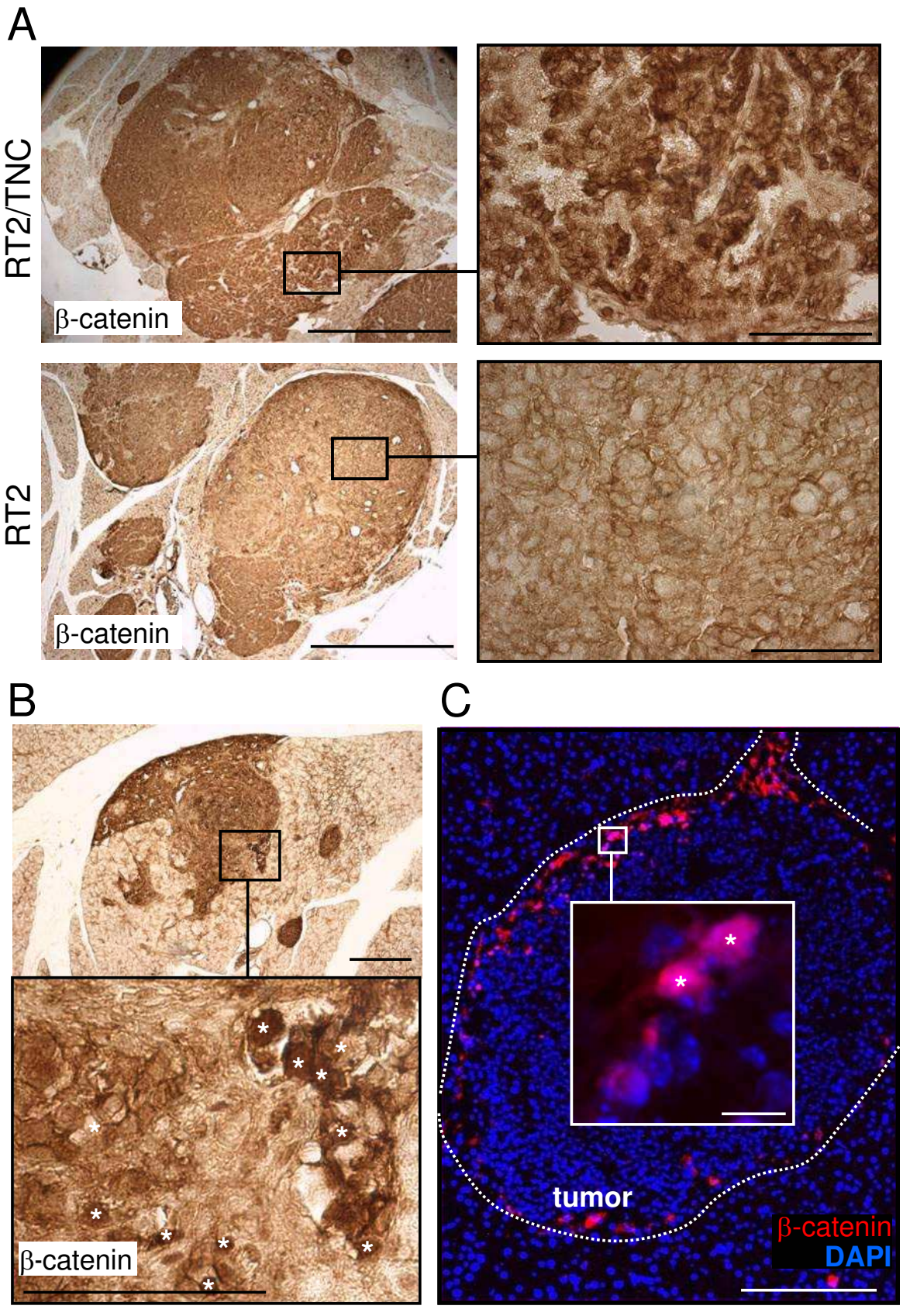
A
RT2/TNC
β-catenin
RT2
β-catenin
B
β-catenin
C
tumor
β-catenin
DAPI

Fig. 5

A

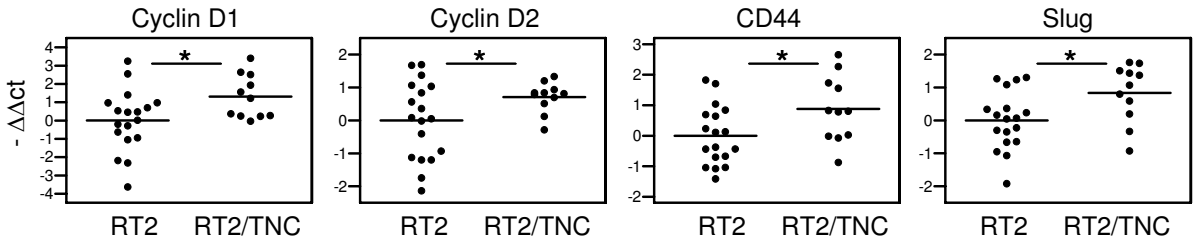

B

DKK1

Genotype	negative tumors	%
RT2	2/28	7.1
RT2/TNC	7/14	50

C

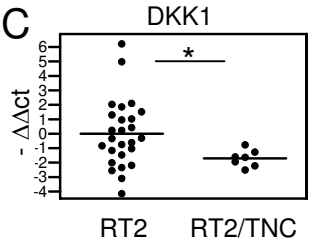

D

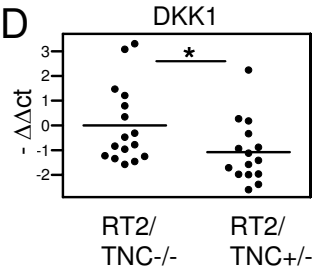

Fig. 6

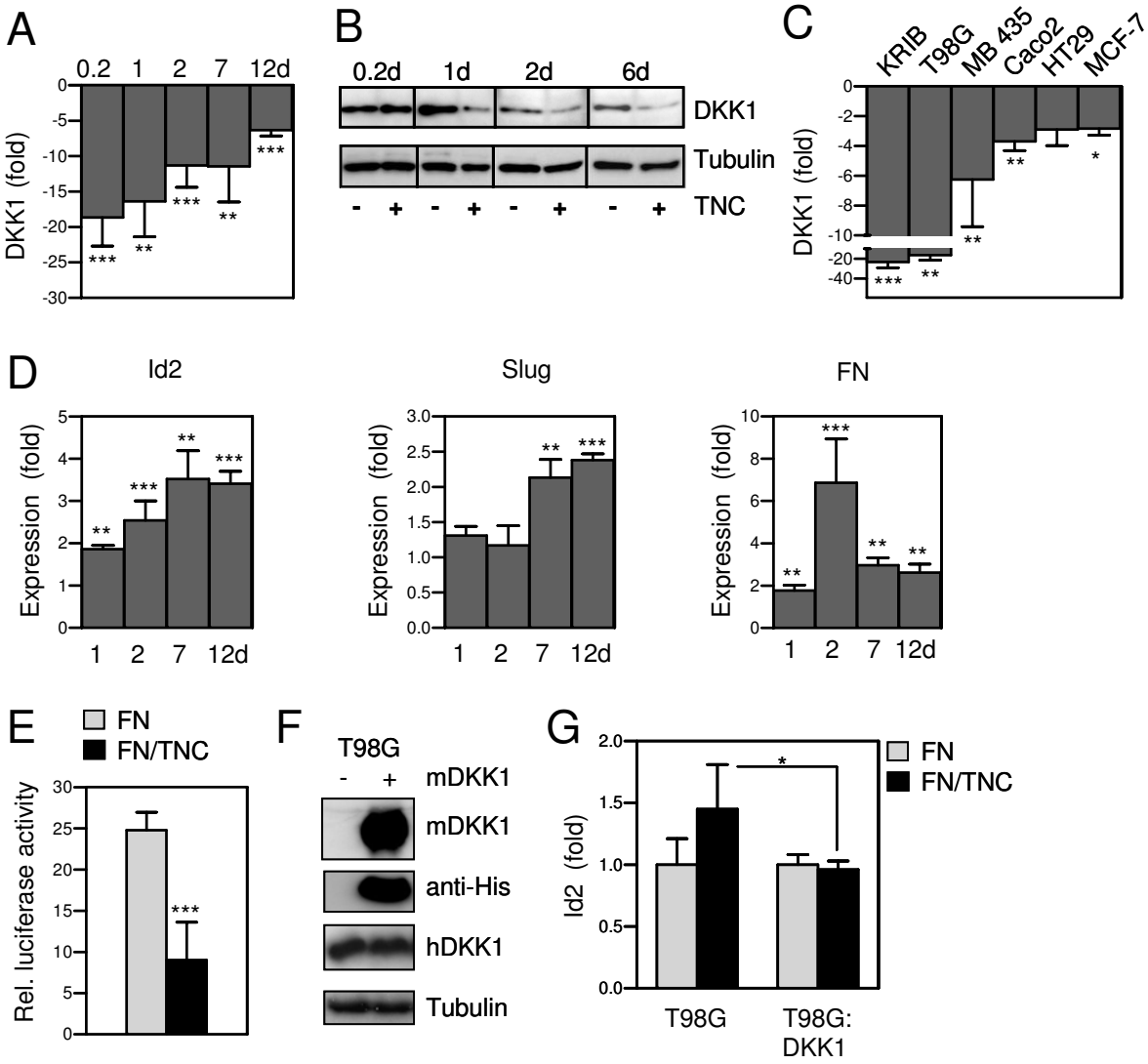
A
0.2 1 2 7 12d
DKK1 (fold)
B
0.2d 1d 2d 6d
DKK1
Tubulin
- + - + - + - +
TNC
C
KRIB T98G MB 435 Caco2 HT29 MCF-7
DKK1 (fold)
D
Id2
Slug
FN
Expression (fold)
1 2 7 12d
E
FN
FN/TNC
Rel. luciferase activity
F
T98G
- + mDKK1
mDKK1
anti-His
hDKK1
Tubulin
G
FN
FN/TNC
Id2 (fold)
T98G
T98G: DKK1

Fig. 7

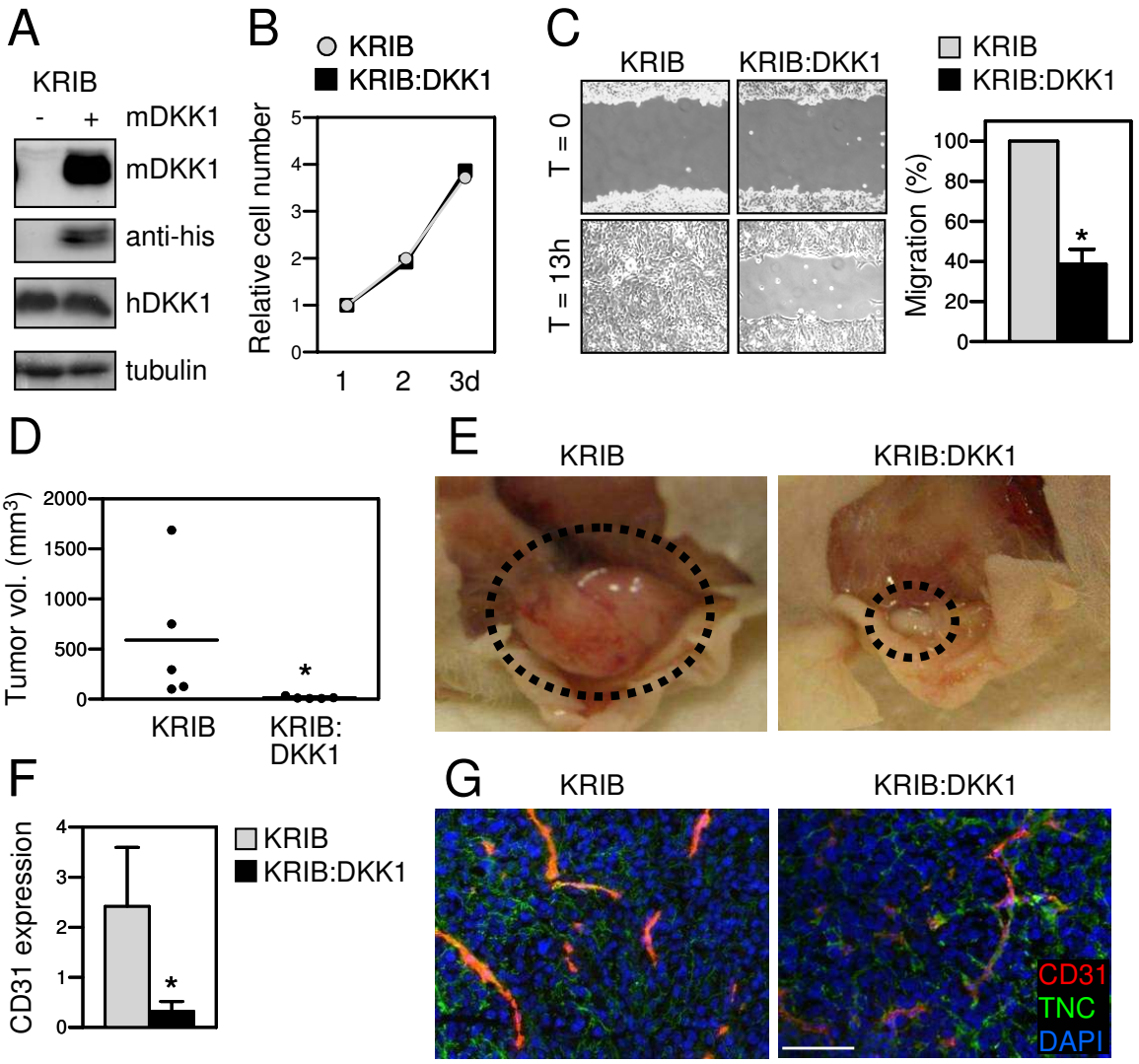
A
KRIB
- + mDKK1
mDKK1
anti-his
hDKK1
tubulin
B
KRIB
KRIB:DKK1
Relative cell number
0 1 2 3 4 5
1 2 3d
C
KRIB
KRIB:DKK1
T = 0
T = 13h
KRIB
KRIB:DKK1
Migration (%)
0 20 40 60 80 100
*
D
Tumor vol. (mm3)
0 500 1000 1500 2000
*
KRIB
KRIB: DKK1
E
KRIB
KRIB:DKK1
F
CD31 expression
0 1 2 3 4
*
KRIB
KRIB:DKK1
G
KRIB
KRIB:DKK1
CD31
TNC
DAPI

Fig. 8

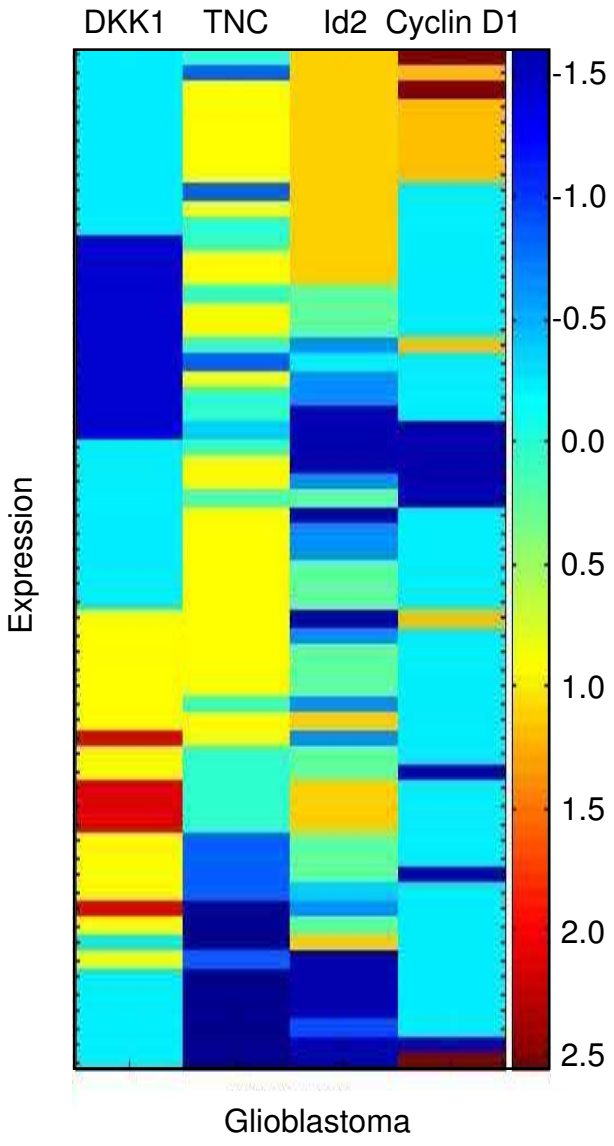
DKK1
TNC
Id2
Cyclin D1
Expression
Glioblastoma
-1.5
-1.0
-0.5
0.0
0.5
1.0
1.5
2.0
2.5

Fig. 9

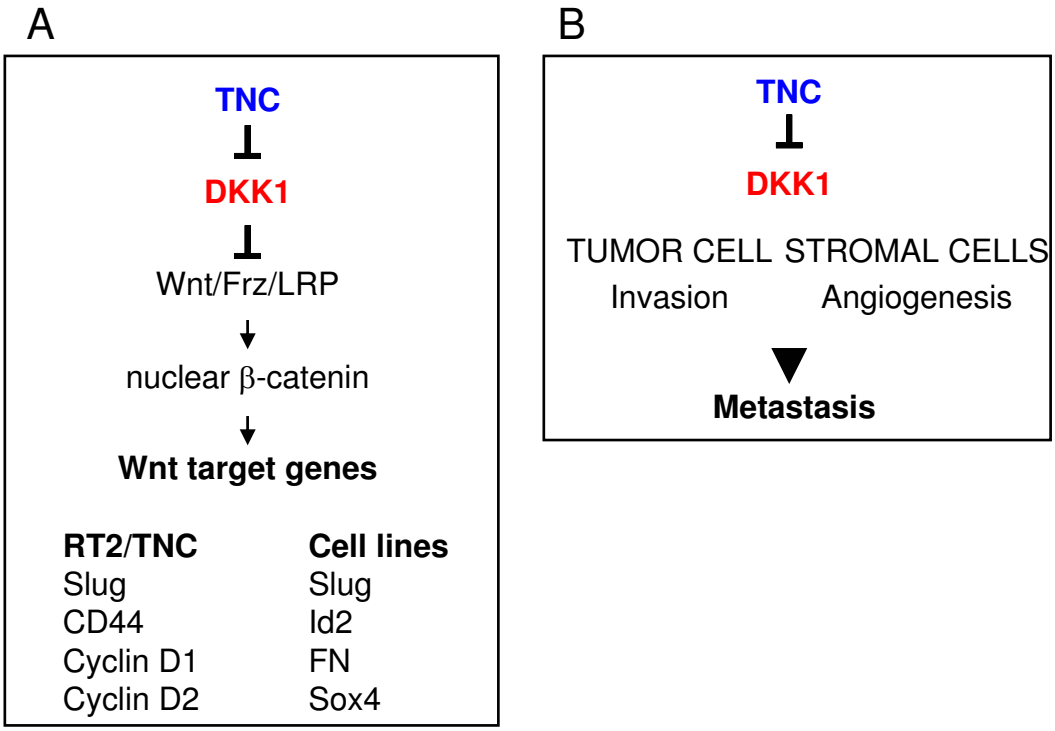
A
TNC
DKK1
Wnt/Frz/LRP
nuclear β-catenin
Wnt target genes
RT2/TNC
Slug
CD44
Cyclin D1
Cyclin D2
Cell lines
Slug
Id2
FN
Sox4
B
TNC
DKK1
TUMOR CELL
Invasion
STROMAL CELLS
Angiogenesis
Metastasis

Supplemental Fig. 1

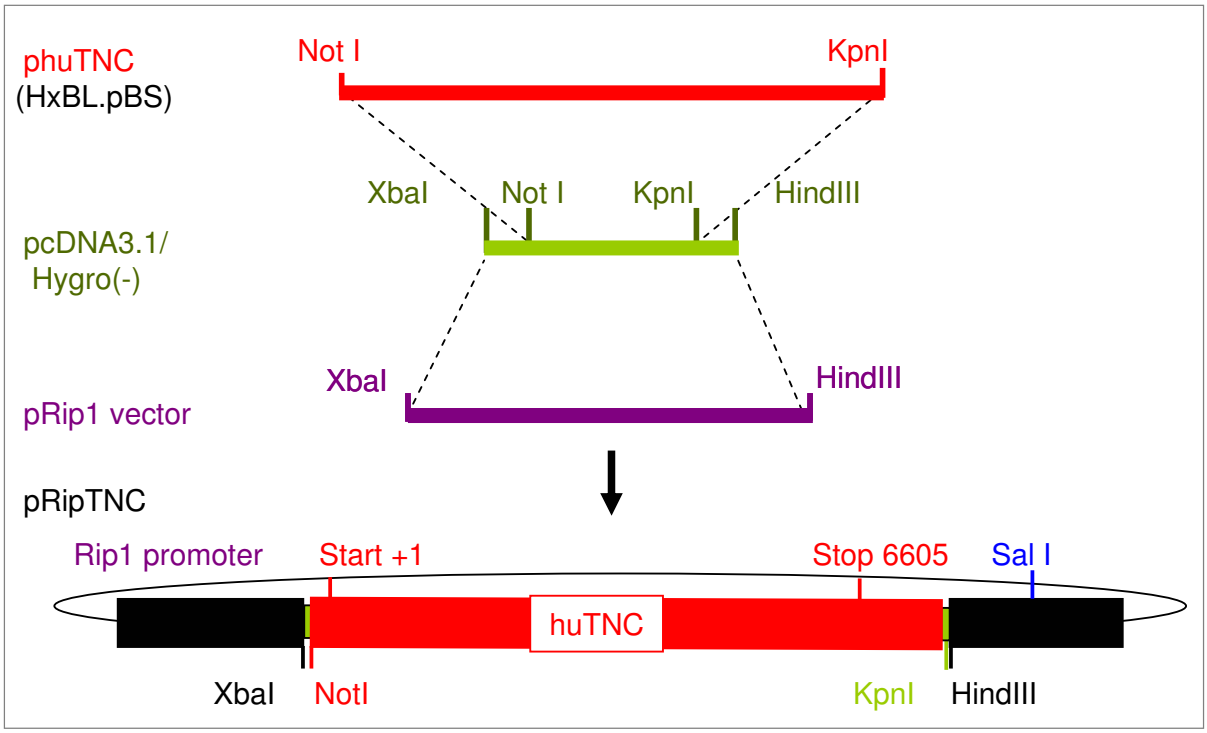

Supplemental Material and Methods

Construction of the TNC expression plasmid, generation of transgenic RipTNC mice and genotyping

The 7.5 kbp sequence of human TNC (accession number X78565.1) harboring a polyadenylation signal was removed from the HxBL.pBS plasmid (Aukhil et al., 1993; Gherzi et al., 1995) by restriction enzyme cleavage with NotI and KpnI and transferred into the intermediate pcDNA3.1/Hygro(-) vector (InVitrogen, Carlsbad, CA, USA). The resulting plasmid was cleaved with XbaI and HindIII before ligation behind the rat insulin II promoter into the corresponding cleavage sites of the 4.5 kb Rip1 vector containing an intron sequence (Hanahan, 1985). Successful cloning was confirmed by restriction enzyme cleavage and, by partial sequencing of 1000 bp around the start and the stop codon, respectively. Expression and secretion of the transgene product was determined upon 48h transient transfection of the expression plasmid into the established RT2 β-tumor cell line βT2 by immunofluorescence for human TNC with the B28.13 antibody (Wagner et al., 2003) in the absence of detergent for detection of secreted TNC. Secretion of human TNC was also determined by sandwich ELISA on conditioned medium from βT2 cells 48h after transfection using the B28.13 antibody for capturing and the TNC1.2. antibody (see below) for detection of bound human TNC (not shown). The RipTNC expression vector was used for injection into the pronucleus of fertilized oocytes upon linearization with SalI according to standard procedures (Labosky et al., 1994), giving rise to transgenic mice with stable transmission and expression of the transgene. Transgenic mice were identified by PCR with primers revP1 hTNC: 5`-GAA AGA CAC CTG CCA ACA GC-3` and RipES/VD: 5`-TAA TGG GAC AAA CAG CAA AG-3). For generation of double-transgenic RT2/TNC mice, single-transgenic RipTNC mice were crossed with RT2 mice (Hanahan, 1985).

Generation of RT2/TNCKO tumor model

RT2/TNCKO mice were generated by breeding of established transgenic Rip1Tag2 (Hanahan, 1985), TNCKO (Forsberg et al., 1996), respectively that had been crossed

into a C57Bl6 background. The respective genotype was determined by PCR with the following primers; RT2: Tag1 5`-GGACAAACCACAACTAGAATGCAG-3`, Tag2 5`-CAGAGCAGAATTGTGGAGTGG-3`; TNCKO: TNCup 5`-CTGCCAGGCATCTTTCTAGC-3`, TNCdown 5`-TTCTGCAGGTTGGAGGCAAC-3`, TNCNeoPA 5`-CTGCTCTTTACTGAAGGCTC-3`. Tumors in RT2/TNCKO and RT2/TNC+/- mice were investigated in a mixed C57Bl6 background containing 50-75% of 129/Sv. In this background tumorigenesis was delayed and mice were sacrificed at 15-17 weeks of age.

Generation of rabbit anti-TNC antibodies

Recombinantly expressed his-tagged human TNC was purified as described (Lange et al., 2007) and was used for injection into 2 rabbits, which gave rise to antisera TNC1.2 and TNC2.2 recognizing human and murine TNC by western blotting, IF and IHC.

Histological analysis and confocal microscopy

Pancreata from transgenic and control mice were isolated and fixed in 4% paraformaldehyde (PFA) overnight, fixed for 2h in 4% PFA and 20% sucrose overnight, and embedded in paraffin or Tissue Tek O.C.T. (Sakura Finetek Europe B.V., Zoeterwoude, Netherlands). Freshly isolated tissue was embedded in Tissue Tek O.C.T., frozen on dry ice or was snap frozen in liquid nitrogen. Histological analysis was done on H&E-stained paraffin sections. Immunostaining was done on paraffin sections (5 µm) or on cryosections (7 and 30 µm) as described (Compagni et al., 2000). The following antibodies were used: rabbit against TNC (TNC1.2, 1:200), phospho-histone-H3 (1:200, Upstate), cleaved caspase 3 (Cell Signalling), β-catenin (1:200, BD Transduction Laboratories), E-cadherin (1:200, BD Transduction Laboratories), KI67 (1:200, Thermo Scientific (RM-9106)), rat antibodies against murine TNC (MTn12, 1:100, (Aufderheide and Ekblom, 1988), CD31 (1:50, BD Pharmingen), the guineapig antibody against insulin (1:200, DakoCytomation) and mouse antibody B28.13 (1:50, Wagner et al., 2003). Nuclei were stained with 4`,6-diamino-2-phenylindole (DAPI).

The tumor diameter in 10 and 12 week old mice was measured on pictures of DAPI-stained tissue. Intra-tumoral microvessel density was analysed by quantifying CD31-positive signals per constant field using the Image J software (National Institute of Mental Health, Bethesda, MD). Students t-test was performed by using the Graph Pad Prism 4 Demo software. Histologic staging and grading of tumors was done on H&E sections. All sections were analysed with either an Axioskop2 plus light microscope using Axiovision 3.1 Software (Zeiss) or a Nikon Diaphot 300 immunofluorescence microscope (Nikon) using the Openlab 3.1.7. software (Improvision). Pancreatic islets were classified according to their size in diameter: normal islets (less than 0.2 mm), hyperplastic/dysplastic islets (0.2 – 0.5 mm), angiogenic islets (more than 0.5 up to 1.0 mm) and tumorigenic islets (more than 1.0 mm). Pancreatic islets were categorized according to size and morphology as normal/hyperplastic, including normal as well as enlarged islets; as angiogenic/tumorigenic (more than 0.5 mm), as adenoma (more than 1 mm), with well differentiated tumor cells, encapsulation, no invasive tumor edges; carcinoma grade 1, well differentiated and homogenous appearance of tumor cells, tumor capsule partially absent, one invasive tumor edge; carcinoma grade 2, partially dedifferentiated and heterogenous appearance of tumor cells, tumor capsule largely absent, more than one invasive tumor edge, carcinoma grade 3 or anaplastic tumor, complete loss of tumor cell differentiation, very heterogenous tumor appearance. For proliferation analysis tissue sections were stained with DAPI, insulin, and anti-PH3 antibody. Phospho-histone-H3 positive nuclei were counted in defined fields upon costaining with DAPI and insulin.

Immunohistochemical investigations of a panel of primary GBM was performed on a tissue micro array (Murat et al., 2008) according to standard procedures for paraffin sections using a heat induced epitope retrieval technique in citrate buffer (pH 6.0; pressure cooker, 3–5 min) and overnight incubation with the primary antibody. The following antibodies were used, anti-TNC (monoclonal, B28.13; dilution 1:2500; anti-DKK1 (IMGENEX ;1:500), Cyclin D1 (NeoMarker 1:500), and Id2 (Santa-Cruz; 1:10’000). The immunostainings were scored semiquantitatively. The tumors were

ordered by similarity of the expression profiles (scores 0–3) using the SPIN software (Tsafrir et al., 2005).

Expression analysis of candidate genes by qRT-PCR

Tissue from tumors, liver and lung of 12 – 17 week old mice was isolated and immediately snap frozen in liquid nitrogen. Total RNA was extracted using NucleoSpin RNA II kit (Macherey-Nagel, Düren, Germany) according to the manufacturer's protocol. Tissue from liver (1 µg), tumor or lung (2 µg) was treated with DNase I (Invitrogen) and reverse transcribed using MultiScribe reverse transcriptase (Applied Biosystems, Fostercity, CA, USA). cDNA was diluted with water to 100 µl (liver, lung) or 200 µl (tumors). QRT-PCR was performed on a 7500 Real Time PCR System (Applied Biosystems) using SYBR green (Applied Biosystems, Warrington, UK) or Taqman reaction mixtures (Applied Biosystems, Fostercity, CA, USA). Primers were found in the database (http://medgen.ugent.be/rtprimerdb/), designed using appropriate tools (Primer3 or Roche software, Roche) or Applied Biosystems (Taqman assay) and are listed in **Suppl. Tables 5** and **6**. Samples were analysed in 10 µl using 1 –5 µl (tumors) or 2.5 µl (liver, lung) cDNA. Data were normalized to a reference (sum of RPL9, TBP and GAPDH (tumors), TBP (liver, lung) and β2MG (cells). Relative expression between RT2 and RT2/TNC and, FN and FN/TNC samples was calculated based on the mean ΔΔct-value.

Scanning electron microscopy and transmission electron microscopy

For preparation of vascular casts, the systemic vasculature was perfused with a freshly prepared Mercox solution (Vilene Company, Japan) containing 0.1 ml of accelerator per 5 ml of resin. One hour after perfusion, the pancreas was excised and tissue was removed in 7.5% potassium hydroxide for up to 3 weeks. After washing, the casts were dehydrated in ethanol and dried in a vacuum desiccator. The samples were then sputtered with gold to a thickness of 10 nm and examined in a Philips XL-30 SFEG scanning electron microscope (SEM). Sections (80 - 90 nm) were prepared and mounted

on copper grids coated with Formvar (polyvinyl formal; Fluka, Buchs, Switzerland). They were stained with lead citrate and uranyl acetate prior to viewing in a Philips EM-400 electron microscope.

References to Supplemental Material

Aufderheide, E. and Ekblom, P. (1988) Tenascin during gut development: appearance in the mesenchyme, shift in molecular forms, and dependence on epithelial-mesenchymal interactions. *J Cell Biol*, **107**, 2341-2349.

Aukhil, I., Joshi, P., Yan, Y. and Erickson, H.P. (1993) Cell- and heparin-binding domains of the hexabrachion arm identified by tenascin expression proteins. *J Biol Chem*, **268**, 2542-2553.

Compagni, A., Wilgenbus, P., Impagnatiello, M.A., Cotten, M. and Christofori, G. (2000) Fibroblast growth factors are required for efficient tumor angiogenesis. *Cancer Res*, **60**, 7163-7169.

Forsberg, E., Hirsch, E., Frohlich, L., Meyer, M., Ekblom, P., Aszodi, A., Werner, S. and Fassler, R. (1996) Skin wounds and severed nerves heal normally in mice lacking tenascin-C. *Proc Natl Acad Sci U S A*, **93**, 6594-6599.

Gherzi, R., Carnemolla, B., Siri, A., Ponassi, M., Balza, E. and Zardi, L. (1995) Human tenascin gene. Structure of the 5'-region, identification, and characterization of the transcription regulatory sequences. *J Biol Chem*, **270**, 3429-3434.

Hanahan, D. (1985) Heritable formation of pancreatic beta-cell tumours in transgenic mice expressing recombinant insulin/simian virus 40 oncogenes. *Nature*, **315**, 115-122.

Labosky, P.A., Barlow, D.P. and Hogan, B.L. (1994) Embryonic germ cell lines and their derivation from mouse primordial germ cells. *Ciba Found Symp*, **182**, 157-168; discussion 168-178.

Murat, A., Migliavacca, E., Gorlia, T., Lambiv, W.L., Shay, T., Hamou, M.F., de Tribolet, N., Regli, L., Wick, W., Kouwenhoven, M.C., Hainfellner, J.A., Heppner, F.L., Dietrich, P.Y., Zimmer, Y., Cairncross, J.G., Janzer, R.C., Domany, E., Delorenzi, M., Stupp, R. and Hegi, M.E. (2008) Stem cell-related "self-renewal" signature and high epidermal growth factor receptor expression associated with resistance to concomitant chemoradiotherapy in glioblastoma. *J Clin Oncol*, **26**, 3015-3024.

Tsafrir, D., Tsafrir, I., Ein-Dor, L., Zuk, O., Notterman, D.A. and Domany, E. (2005) Sorting points into neighborhoods (SPIN): data analysis and visualization by ordering distance matrices. *Bioinformatics*, **21**, 2301-2308.

Wagner, S., Hofstetter, W., Chiquet, M., Mainil-Varlet, P., Stauffer, E., Ganz, R. and Siebenrock, K.A. (2003) Early osteoarthritic changes of human femoral head cartilage subsequent to femoro-acetabular impingement. *Osteoarthritis Cartilage*, **11**, 508-518.

Supplemental Figures

Suppl. Fig. 1 TNC expression vector

Cloning of the sequence encoding human TNC harboring a polyadenylation signal was removed from the HxBL.pBS plasmid by restriction enzyme cleavage with NotI and KpnI and was transferred into the Rip1 vector by using the indicated restriction enzymes and the pcDNA3.1 vector as intermediate. The inserted human cDNA sequence comprises 45 nucleotides upstream of the start site and 639 nucleotides downstream of the stop signal.

Suppl. Table 1 TNC-dependent pancreatic islet size in RT2 tumors

Genotype	N (%)	H (%)	A (%)	T (%)	N, H (%)	A,T (%)	AT/NH
RT2	12.3	58.9	24.7	4.1	71.2	28.8	0.4
RT2/TNC	15.2	40.5	35.4	8.9	55.7	44.3	0.8

Analysis of pancreatic islets of RT2 (n = 5) and RT2/TNC (n = 7) mice at 10 weeks of age. Islet diameter on tissue sections (average 12 tumors per mouse, total 73 RT2 and 79 RT2/TNC) was used for classification. Normal (N) (< 0.2 mm), hyperplastic (H) (0.2 - 0.5 mm), angiogenic (A) (> 0.5 - 1 mm) and tumorigenic (T) (> 1.0 mm). AT/NH, $p = 0.06$, Fisher`s exact test.

Suppl. Table 2 Carcinoma progression by TNC

Genotype	Adenoma (%)	Carcinoma (%) Grade 1	Grade 2	Grade 3	Grade 1 - 3	Ca/Ad
RT2	55.8	32.7	10.5	0.9	44.2	0.8
RT2/TNC	35.7	39.9	21.3	3.2	64.3	1.8

Analysis of numbers of adenomas and carcinomas grade 1 – 3 in 12 week old mice. The distribution of adenomas and compiled carcinomas grade 1 – 3 between genotypes was significantly different, $p < 0.05$, Fisher`s exact test.

Suppl. Table 3 Analysis of Candidate Gene expression in RT2 Tumors

Candidate gene	Tumor	ΔΔCt RT2/TNC versus RT2	p value	Relative expression
CD44	All	-0.46	0.22	1.38
	Small	-0.54	0.19	1.45
	Small + Diff	**-0.88**	**0.03**	**1.84**
	Big	0.71	0.11	-1.64
	Big + Diff	0.71	0.11	-1.64
	Diff	-0.54	0.15	1.46
Cyclin D1	All	-0.77	0.13	1.70
	Small	-1.02	0.11	2.02
	Small + Diff	**-1.30**	**0.03**	**2.46**
	Big	0.13	0.86	-1.10
	Big + Diff	0.51	0.50	-1.43
	Diff	-0.91	0.07	1.88
Cyclin D2	All	-0.38	0.29	1.30
	Small	-0.50	0.14	1.42
	Small + Diff	**-0.71**	**0.03**	**1.64**
	Big	0.43	0.37	-1.35
	Big + Diff	0.67	0.21	-1.59
	Diff	-0.41	0.21	1.33
DKK1	All	**1.71**	**<0.01**	**-3.23**
	Small	**1.61**	**0.02**	**-3.03**
	Small Diff	**1.36**	**0.02**	**-2.56**
	Big	1.88	n.a.	-3.70
	Big Diff	0.74	n.a.	-1.67
	Diff Only	**1.22**	**0.01**	**-2.33**
	Diff	n.a.	n.a.	n.a.
Slug	All	-0.25	0.43	1.19
	Small	**-0.72**	**0.04**	**1.64**
	Small + Diff	**-0.84**	**0.02**	**1.79**
	Big	1.29	0.05	-2.44
	Big + Diff	1.00	0.19	-2.00
	Diff	-0.44	0.18	1.36

Relative gene expression of candidate genes (alphabetical order) in RT2/TNC tumors versus RT2 tumors is based on ΔΔCt values that were determined by SYBR Green qRT-PCR on RNA isolated from 14 week old RT2 (N = 11 mice, n = 28 tumors) and RT2/TNC mice (N = 3, n = 14). Gene expression was normalized to the median value of three genes, TBP, GAPDH and RPL-9 and was used to determine ΔΔCt. Data are presented for all tumors (All), small tumors (Small, 1 – 3 mm in diameter, RT2 (n = 20), RT2/TNC (n = 11), big tumors (Big > 3 mm, RT2 (n = 8), RT2/TNC (n = 3), differentiated tumors (Diff., high expression of insulin and E-cadherin), RT2 (n = 23), RT2/TNC (n = 14), small and differentiated tumors (Small diff.), RT2 (n = 18), RT2/TNC (n = 11) and big and

differentiated tumors (Big diff.), RT2 (n = 5), RT2/TNC (n = 3). Statistical differences were calculated for the ΔΔCt values using adequate Student's t-test. Bold numbers represent statistically significant data: p values, cyclin D1 (p = 0.0336, t-test), cyclin D2 (p = 0.0321, t-test with Welsh correction), CD44 (p = 0.031, t-test), Slug (p .0195, t-test). n.a., not applicable due to too small sample number with detectable expression. DKK1, Dickkopf 1, Id2, inhibitor of differentiation 2.

Suppl. Table 4 TNC-dependent Gene Expression of Wnt Target Genes in Cultured Tumor Cells

Cell line	Time (days)	Id2	Slug	FN	Sox4
T98G	1	**1.9**	1.3	**1.8**	1.5
	2	**2.5**	1.2	**6.9**	0.9
	7	**3.5**	**2.1**	**3.0**	**2.0**
KRIB	1	0.9	0.8	1.0	**2.1**
	6	0.9	**2.4**	**2.2**	1.1
MDA MB435	1	0.6	0.7	0.3	1.0
	6	0.6	0.7	0.4	1.3

Gene expression was determined by qRT-PCR on RNA isolated from the indicated cell lines upon plating on FN or FN/TNC and is expressed as ratio FN/TNC versus FN (fold). Experiments were done in triplicates per time point. Bold, p value < 0.05.

Suppl. Table 5 Primer List for qRT-PCR on tumor and lung tissue

Gene	Forward primer	Reverse primer
CD44	GTCTGCATCGCGGTCAATAG	GGTCTCTGATGGTTCCTTGTTC
CyclinD1	CGCACTTTCTTTCCAGAGTCA	AAGGGCTTCAATCTGTTCCTG
CyclinD2	CACCGACAACTCTGTGAAGC	TCCACTTCAGCTTACCCAACA
DKK1	Taqman mDKK1 Mm00438422_m1	
DKK1	CCGGGAACTACTGCAAAAAT	CCAAGGTTTTCAATGATGCTT
E-Cadherin	CAGCCTTCTTTTCGGAAGACT	GGTAGACAGCTCCCTATGACTG
Insulin	TGGCTTCTTCTACACACCCAAG	ACAATGCCACGCTTCTGCC
Insulin	Taqman mIns1 Mm01259683_g1	
Slug	GAAAAGCACATTGCATCTTTTCT	TGTTCCTTTGGTTGAAATGGT
TNC mouse	GCGCAGACACACACCCTAGC	TTTCCAGGTCGGGAAAAGCA
TNC human	CCTTGCTGTAGAGGTCGTCA	CCAACCTCAGACACGGCTA
RPL9	ACCCTGGCCCGACGG	TACCCTTCCTCTTCCCTATGCC
TBP	CCCCACAACTCTTCCATTCT	GCAGGAGTGATAGGGGTCAT
GAPDH	Taqman Mm99999915_g1	

Suppl. Table 6 Primer List for qRT-PCR on cultured cells

Gene	Forward primer	Reverse primer
DKK-1	GACCATTGACAACTACCAGCCG	TACTCATCAGTGCCGCACTCCT
Id2	TCAGCCTGCATCACCAGAGA	CTGCAAGGACAGGATGCTGATA
Slug	ATGAGGAATCTGGCTGCTGT	CAGGAGAAAATGCCTTTGGA
Fibronectin	CCCATCAGCAGGAACACCTT	GGCTCACTGCAAAGACTTTGA A
Sox4	CAGCAAGAGAAACTGTGTGTGA	AAGAGCGTGCAAGAACTAGAGA
β2-Microglobulin	GTGGGATCGAGACATGTAAGCA	AATGCGGCATCTTCAAACCT

Annex2:
Fibronectin and tenascin-C: accomplices in vascular morphogenesis during development and tumor growth

Int. J. Dev. Biol. 55: 511-525
doi: 10.1387/ijdb.103243eo

THE INTERNATIONAL JOURNAL OF DEVELOPMENTAL BIOLOGY
www.intjdevbiol.com

Fibronectin and tenascin-C: accomplices in vascular morphogenesis during development and tumor growth

ELLEN VAN OBBERGHEN-SCHILLING*[,1,2], RICHARD P. TUCKER[3], FALK SAUPE[4], ISABELLE GASSER[4], BOTOND CSEH[1,2], GERTRAUD OREND*[,4,5,6]

[1]CNRS UMR6543, IBDC, Nice, France, [2]University of Nice-Sophia Antipolis, Nice, France, [3]Cell Biology and Human Anatomy, University of California at Davis, USA, [4]Inserm U682, Strasbourg, France, [5]University of Strasbourg, UMR-S682, Strasbourg, France and [6]Department of Molecular Biology, CHRU Strasbourg, Strasbourg, France

ABSTRACT In addition to soluble factors, the extracellular matrix (ECM) also plays a vital role in normal vasculogenesis and in the pathological angiogenesis of many disease states. Here we will review what is known about the role of the ECM molecules fibronectin and tenascin-C in the vasculature and highlight a potential collaborative interplay between these molecules in developmental and tumorigenic angiogenesis. We will address the evolution of these modular proteins, their cellular interactions and how they become assembled into an insoluble matrix that impacts the assembly of other ECM proteins and the bioavailability of pro-angiogenic factors. The role of fibronectin and tenascin-C networks in tumor angiogenesis and metastasis will be described. We will elaborate on lessons learned about their role in vessel function from the functional ablation or the ectopic expression of both molecules. We will also elaborate on potential mechanisms of how fibronectin and tenascin-C affect cell adhesion and signaling that are relevant to angiogenesis.

KEY WORDS: tumor angiogenesis, matrix assembly, fibronectin, tenascin-C

Introduction

Cells and extracellular matrix (ECM) form tissues, and collections of tissues form organs. In the organism different organs act together through blood and lymphatic vessels. Solid tumors resemble organs that are structurally and functionally abnormal. They contain multiple cell types and ECM components and develop through complex interactions between these different components using processes that often resemble those used by developing organs (reviewed in Egeblad *et al.*, 2010). It is long known that tumors need to turn on angiogenesis in order to grow more than a few millimeters in diameter. Tumors have developed several strategies to trigger the so called "angiogenic switch" in order to develop a connection to the hemapoietic and lymphatic vasculature which is believed to be essential for nourishment and oxygenation. Connections to the vasculature also present pathways for motile cancer cells to travel to distant organs to seed metastasis.

In the initial concept of sprouting angiogenesis, largely supported by angiogenesis observed in tumor xenograft experiments, tumors secrete factors that stimulate the process of the outgrowth of new blood vessels from preexisting vessels (Risau, 1997). The development of new vasculature by angiogenesis occurs in two stages. First, a dense, immature, evenly spaced network of new vessels develops by recursive sprouting and fusion of sprouts. Second, the network is remodeled into a hierarchically spaced network by adaptive pruning events and blood flow. How vessel branching is regulated at the molecular level is a matter of debate. Whether the tip cell represents the default state or is actively induced is not clear. At least it is known that VEGFR2, Wnt and notch signaling

Abbreviations used in this paper: αTM, alpha tropomyosin; DKK, dickkopf; E, embryonic day; ECM, extracellular matrix; EDA, extra domain A; EDB, extra domain B; EDNRA (B), endothelin receptor type A (B); ET1, endothelin 1; FAK, focal adhesion kinase; FGF, fibroblast growth factor; Id2, inhibitor of differentiation 2; ILK, integrin-linked kinase; JNK, c-Jun N-terminal kinase; LPA, lysophosphatidic acid; MEK, mitogen-activated protein kinase kinase; MMP, matrix metalloproteinase; MMTV, mouse mammary tumor virus; PDGFR, platelet-derived growth factor receptor; PI3K, phosphoinositide 3-kinase; PLCγ, phospholipase C gamma; RT2, Rip1Tag2, SV40 T antigen induced insulinoma; TFGβ1, transforming growth factor beta 1; VEGF, vascular endothelial growth factor; VM, vasculogenic mimicry.

***Address correspondence to:** Ellen Van Obberghen-Schilling. CNRS UMR6543, Centre A. Lacassagne, 33 Ave de Valombrose, 06189 Nice, France. Fax: +33 (0)492.03.1235. e-mail: vanobber@unice.fr - web: http://www.unice.fr/ibdc/
Gertraud Orend. INSERM UMR-S682, 3 Avenue Molière, 67200 Strasbourg, France. Fax: 33 (0)388.26.3538. e-mail: gertraud.orend@inserm.u-strasbg.fr - web: http://u682-inserm.u-strasbg.fr

Final, author-corrected PDF published online: 12 July 2011.

ISSN: Online 1696-3547, Print 0214-6282

are involved in tip cell organization (Bentley *et al.*, 2008). Apart from sprouting angiogenesis, there are several other mechanisms of tumor vascularization, including intussusceptive angiogenesis, vessel co-option, and recruitment of endothelial progenitor cells. In addition, lymphangiogenesis and vasculogenic mimicry are involved in the formation of the tumor microcirculation (Dome *et al.*, 2007; Hillen and Griffioen, 2007; Kucera *et al.*, 2009).

Much emphasis has been placed on the role of angiogenic cytokines such as vascular endothelial growth factor (VEGF) in endothelial cell biology. However, considerable evidence indicates that the matrix is equally important in vessel homeostasis and remodeling. Its role at the molecular level is still poorly understood. ECM proteins provide instructive signals to cells during development, homeostasis and in disease states. The ECM can regulate cell and tissue behavior by serving as a structural network as well as initiating biochemical signaling cascades in cells through interactions with a number of specialized transmembrane ECM receptors such as integrins (reviewed in Erler and Weaver, 2009). Emerging evidence indicates that distinct ECM molecules act in concert to elicit their biological effects. Thus, deciphering the coordinated action of ECM proteins is key to understanding how the ECM network can support normal vascular function and influence the tumor microenvironment to promote angiogenesis.

Fibronectin is a large multi-domain ECM glycoprotein with a fundamental role in blood vessel morphogenesis during embryonic development and pathological angiogenesis. Since the first investigation of fibronectin distribution by Linder and collaborators in chick embryos (Linder *et al.*, 1975), countless studies have documented its elevated expression at sites of tissue remodeling, organogenesis and in numerous disease states. Whereas fibronectin is strongly expressed around developing blood vessels during embryogenesis (Peters and Hynes, 1996), its expression is barely detectable in the normal adult vasculature (ffrench-Constant and Hynes, 1989; Peters *et al.*, 1996). Re-expression of fibronectin occurs during pathological angiogenesis in various diseases such as cancer, late stage artherosclerosis and in blinding ocular conditions (Astrof and Hynes, 2009; Neri and Bicknell, 2005; Pedretti *et al.*, 2009, 2010; Roy *et al.*, 1996, and references therein).

Fibronectin is commonly classified into two forms, plasma fibronectin (p-fibronectin), a soluble form produced by hepatocytes that circulates in blood at high concentrations, and cellular fibronectin (c-fibronectin) produced in tissues where it is incorporated in a fibilllar matrix. c-Fibronectin differs from p-fibronectin by the presence of additional domains, including the highly conserved fibronectin type III "extra" domains B (EDB) and/or A (EDA), that arise from alternative splicing of the pre-mRNA. (Fig. 1, ffrench-Constant and Hynes, 1989; Peters *et al.*, 1996; White *et al.*, 2008,

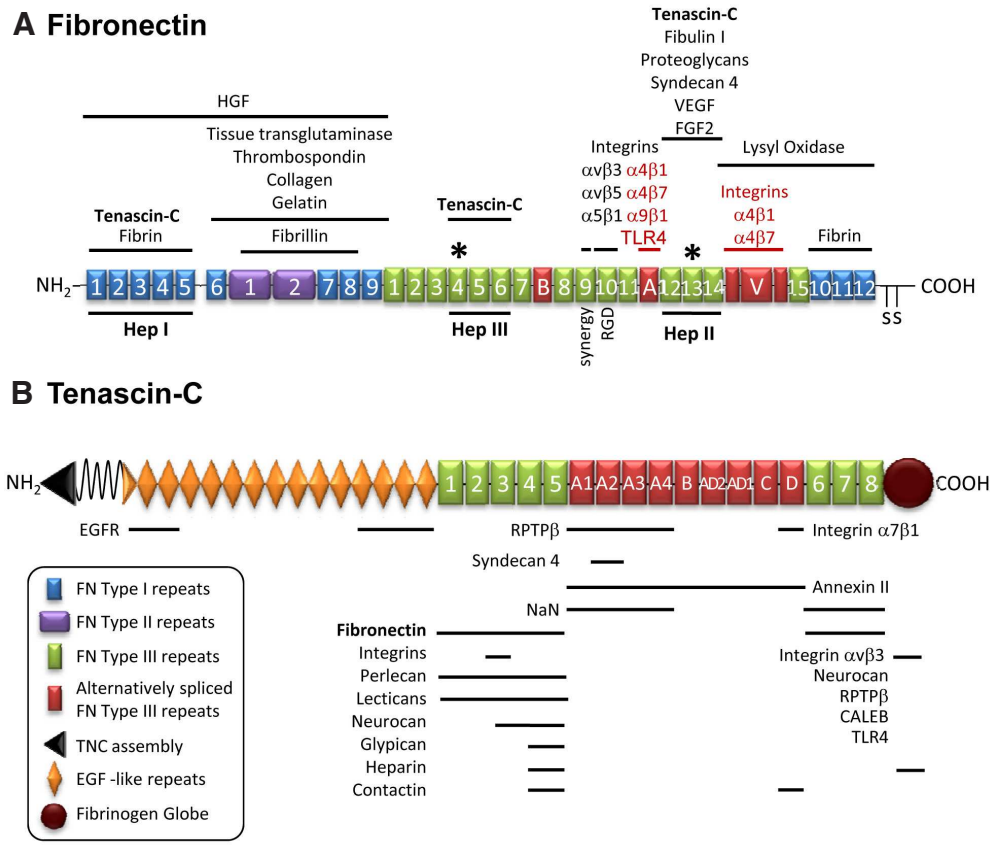

Fig. 1. Domain structure of fibronectin and tenascin-C and potential binding partners. (A) *Fibronectin is a dimeric protein of 240-270KDa, composed of 2 similar or identical monomers joined by a pair of disulfide bonds near the C terminus. Each monomer is organized into type I, type II and type III repeats (FN I-III). Extra Domains B (B) and A (A) correspond to type III repeats. Alternate splicing at a third site (V) gives rise to inserts of variable length (up to 5 in humans) that are nearly always included in c-fibronectin. Heparin-binding domains (Hep) I-III and binding domains for cellular receptors, ECM components, enzymes and growth factors are indicated. Multiple cellular binding sites for fibronectin contribute to angiogenesis (reviewed in Avraamides et al., 2008; Hynes, 2007). Most notably, the tri-peptide motif Arg-Gly-Asp (RGD) located in the 10th FN type III repeat (FN III-10) is the site of binding to α5β1 integrin, as well as αv-based integrins (Leiss et al., 2008; Pankov and Yamada, 2002) including αvβ3 and αvβ5, which are all currently targeted in anti-angiogenic strategies (Desgrosellier and Cheresh, 2010). The asterisks correspond to sites of mutations FN1 identified in patients with glomerulopathy and fibronectin deposits (GFND) (Castelletti et al., 2008). Integrin α5β1 binding to the RGD motif in FN III-10 requires the synergy region in the 9th FN type III repeat (Danen et al., 1995).* **(B)** *Tenascin-C is a modular molecule composed of an oligomerization domain, EGF-L and FN type III (constant and alternate) repeats, and a fibrinogen like domain (see Orend and Chiquet-Ehrismann, 2006). Binding sites for interacting molecules are indicated. CALEB, chicken acidic leucine-rich EGF like domain containing brain protein, EGFR, epidermal growth factor receptor, NaN, sodium channel subunit β 2, RPTPβ, protein tyrosine phosphatase β, TLR4, toll like receptor 4.*

and references therein). Importantly for clinical applications, fibronectin splice variants containing the EDB and EDA domains, often referred to as oncofetal variants, are amongst the most specific markers of angiogenic blood vessels to date (Kaspar *et al.*, 2006). In addition to promoting adhesion and signaling through cell surface receptors, the fibronectin matrix functions as a fibrillar scaffold for the assembly of other matrix proteins. Itprovides a platform for angiogenic signaling by increasing the bioavailability of soluble angiogenic factors, and cooperating with their transmembrane receptors (Hynes, 2007; Hynes, 2009; Miyamoto *et al.*, 1996; Mosher *et al.*, 1980).

Tenascin-C is another large modular ECM protein that exhibits a restricted and low expression in normal tissue. It is the founding member of the tenascin familiy with four members, tenascin-C, -R, -W and tenascin-X (reviewed in Chiquet-Ehrismann and Chiquet, 2003). All tenascins harbor several homologous domains that have been extensively described elsewhere (reviewed in Chiquet-Ehrismann and Chiquet, 2003; Orend, 2005; Orend and Chiquet-Ehrismann, 2006, Fig. 1). Tenascin-C can assemble into hexamers, it can be processed into monomers and it interacts with several cell surface receptors and other matrix molecules (reviewed in Midwood and Orend, 2009, Fig. 1). Its expression is elevated in embryonic tissues and in tissue of several cancers, and high tenascin-C expression has been found to correlate with lymph node metastasis and poor prognosis (reviewed in Midwood and Orend, 2009). Tenascin-C is one of the few genes within the signature of predictive value for lung metastatis in breast cancer patients (Minn *et al.*, 2005). Moreover, a robust expression of tenascin-C is associated with resistance to tamoxifen therapy in patients with estrogen receptor positive breast cancer (Helleman *et al.*, 2008). Tenascin-C plays a yet poorly defined role in enhancing tumor cell proliferation, promoting angiogenesis, invasion and metastasis (Orend and Chiquet-Ehrismann, 2006). Tenascin-C interacts with several ECM molecules and cell surface receptors, thus affecting tissue architecture, tissue resilience and cellular responses relevant in angiogenesis, metastasis and the stem cell niche (reviewed in Midwood and Orend, 2009).

At present, little is known about the interdependence of tenascin-C and fibronectin, yet a functional complicity of these two ECM molecules is strongly supported by their overlapping expression, physical interaction and modulatory role in cell adhesion-dependent processes (reviewed in Midwood and Orend, 2009). Here, we will address when both matrix molecules have evolved and how this may further our knowledge about their potential role in the vasculature of vertebrates in normal tissue homeostasis and in cancer. We will describe how the ablation of fibronectin and tenascin-C affects developmental and pathological angiogenesis. Finally, we will summarize and discuss what is known about fibronectin and tenascin-C in angiogenesis, in pathologies including cancer.

Evolutionary aspects of fibronectin and tenascin-C in the vasculature

The vasculature of vertebrates has a number of anatomical features that sets it apart from the vasculature of other members of the phylum Chordata. Notably, it is composed of a closed system of tubes lined by endothelial cells that are in turn invested by a basement membrane (Fig. 2). The urochordates (also known as tunicates or sea squirts), which are generally believed to be the closest relatives to the vertebrates (e.g., Putnam *et al.*, 2008)), have what appear to be inside-out vessels, at least from a vertebrate's point of view: the lumen of the tunicate heart and major vessels is lined by the basement membrane of myoepithelial cells and not by an endothelium (Davidson, 2007). Cells are occasionally encountered lining the lumen of urochordate vasculature, and though these may represent endothelial-like cells, recent evidence suggests that in at least some colonial tunicates they are Piwi-positive stem cells (Rinkevich *et al.*, 2010). In contrast to the closed system of vertebrates, the circulatory system of the tunicates is open, with the vessels leading from the heart emptying into lacunae where the hemolymph can bathe the organs. The cephalochordates (also known as lancelets or amphioxus), which are most likely a more distantly related invertebrate chordate, also have an open vascular system lined by ECM, but it lacks the epithelial lining of tunicate vessels (Fig. 2). For example, the aorta of amphioxus forms from the basement membranes of the gut endoderm and the ECM of the surrounding mesenchyme (Kucera *et al.*, 2009). This primitive acellular matrix-tube vasculature is widely found in other invertebrates as well (Rupert

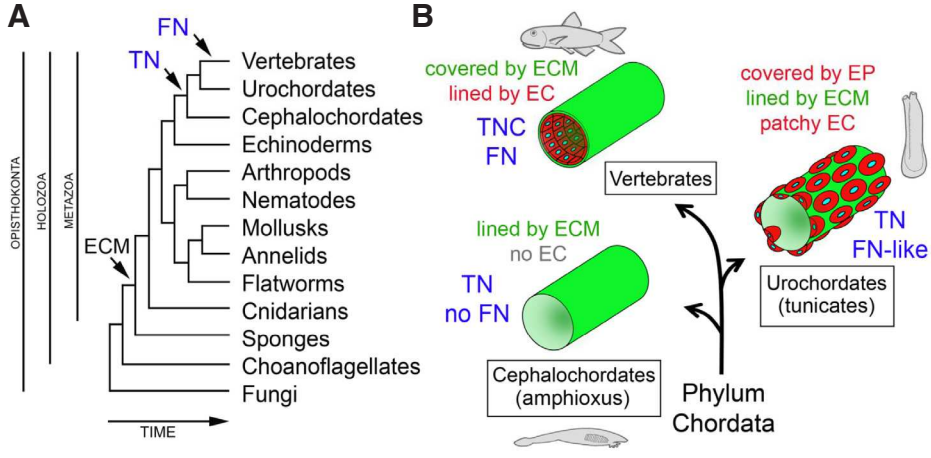

Fig. 2. Evolution of fibronectin and tenascin-C. (A) *Integrins are found in single-celled holozoans and fungi, but extracellular matrix (ECM) first appeared in early metazoans. Tenascins (TN) and fibronectin (FN) evolved much later in basal chordates.* **(B)** *The evolution of blood vessels in the Phylum Chordata. In cephalochordates (also known as lancelets or amphioxus) the circulatory system is open, and blood vessels are matrix tubes without endothelial cells (EC) or surrounding epithelial cells (EP). Cephalochordates have a tenascin gene, but not a fibronectin gene. In urochordates (also known as tunicates or sea squirts) the circulatory system is also open. Blood vessels are lined by extracellular matrix and surrounded by epithelial cells. Occasionally cells are encountered lining the lumen of the vessels, but it is not known if these are endothelial cells. The urochordate Ciona has a tenascin gene and a fibronectin-like gene that lacks key features of vertebrate fibronectin. In vertebrates the circulatory system is closed and lined by endothelial cells; all vertebrates examined have multiple tenascin genes and a highly conserved fibronectin gene.*

and Carle, 1983; reviewed by Kucera and Lammert, 2009), even though invertebrates are perfectly capable of making tubular organs lined with epithelia like the trachea or salivary glands (e.g., see Castillejo-Lopez *et al.*, 2004). Other anatomical features that are unique to the vertebrates include a lymphatic system and thymus (Bajoghli *et al.*, 2009): no comparable systems are found in tunicates or amphioxus.

On the cellular, physiological and molecular levels the vertebrate circulatory system also has a number of unique features. For example, an adaptive immune system appears to have evolved with jawed fish (e.g., see Bajoghli *et al.*, 2009), and amphioxus and tunicates lack the complex coagulation systems of vertebrates (Doolittle, 2009). Amphioxus and tunicates have many blood cells that appear to share roles with leukocytes, but they do not have erythrocytes (Cima *et al.*, 2001; Huang *et al.*, 2007). The tunicate *Ciona* has both globin and hemocyanin-related genes, but it is unknown if one or both play roles in respiration (Ebner *et al.*, 2003).

Many ECM genes have origins that coincide with the appearance of basal metazoa, including collagens (Exposito *et al.*, 2008), thrombospondins (Bentley and Adams, 2010) and syndecans (Chakravarti and Adams, 2006). Wnt and key players that make up the Wnt signaling pathways are present in sponges but not choanoflagellates, suggesting that they also evolved with the first metazoans (Richards and Degnan, 2009). Even more ancient are the integrins and molecules involved in integrin signaling like paxilin, talin and Integrin-linked Kinase (ILK) (Sebe-Pedros *et al.*, 2010), some of which are in single-celled holozoans as well as fungi. In contrast, tenascins and fibronectin are encoded by relatively new genes, having evolved early in the chordate lineage. Of the two, tenascins appear to have evolved first, as the amphioxus *Branchiostoma* has a gene that encodes a tenascin that closely resembles vertebrate tenascins, but it lacks a fibronectin gene (Tucker and Chiquet-Ehrismann, 2009). Nothing is known about the expression of the amphioxus tenascin, but it is remarkable for having multiple (at least 7) copies of RGD motifs predicted to be exposed to integrin binding. It is interesting to speculate that at least some of the functions of fibronectin in vertebrates may be carried out in amphioxus by this RGD-rich form of tenascin. In contrast, the tunicate *Ciona* has a tenascin gene and a fibronectin-like gene, but the predicted protein encoded by the latter has distinctive features (e.g., it lacks an RGD motif and domains that correspond to EDA and EDB domains) that leads one to suggest that it may play different roles than its highly conserved vertebrate counterpart (Tucker and Chiquet-Ehrismann, 2009). Interestingly, the *Ciona* tenascin gene is expressed in the notochord and muscle cells, and is not associated with the developing heart (Kawashima *et al.*, 2009; Tucker *et al.*, 2006).

What can we learn from the evolution of ECM about the origins of the distinctive anatomical and molecular features of the circulatory system in vertebrates? Only in vertebrates do we see a closed circulatory system with proper endothelial cells, and during vertebrate development cells lining blood vessels, which are likely to be endothelial cells, express both tenascin (Tucker, 1993) and fibronectin (Astrof and Hynes, 2009; ffrench-Constant and Hynes, 1989). As we will see below, both tenascin-C and fibronectin are critical for normal vascularization, so the appearance of these interrelated matrix molecules may have played a role in the evolution of this distinctive feature of vertebrates.

Fibronectin and tenascin-C in loss of function models

Effect of a loss of fibronectin and its receptors on the vasculature

Genetic evidence points to a major role for fibronectin and its receptors in vascular development. Ablation of the fibronectin gene leads to embryonic lethality at embryonic day 9.5 (E9.5) with severe cardiovascular defects and aberrant somitogenesis (George *et al.*, 1993). Interestingly, the severity of the defects was found to vary as a function of the genetic background of the fibronectin-null mice (George *et al.*, 1997). A search for gene modifiers of the heart defects led to the identification of potential candidates on chromosome 4, proposed to affect a migratory process involved in coalescence of the two heart primordia into a single heart tube (Astrof *et al.*, 2007b). The gene encoding tenascin-C is also located on chromosome 4, at a distinct locus. It is intriguing to speculate that tenascin-C could participate in genetic interactions that determine the severity of the phenotype. Integrin α5-null mice lacking the main fibronectin receptor, $\alpha5\beta1$, die at E10.5 with a phenotype similar to fibronectin-null mice (Francis *et al.*, 2002; Yang *et al.*, 1993). A comparable phenotype was observed in mice with an inactivating mutation of the $\alpha5\beta1$-binding motif of fibronectin (RGD to RGE) (Takahashi *et al.*, 2007), attesting to the functional importance of this ligand-receptor pair for vascular morphogenesis. Concerning the role of other fibronectin-binding integrins in vascular development and angiogenesis (reviewed in Hynes, 2007)), $\alpha v\beta3$ and $\alpha v\beta5$ integrins that bind to the RGD sequence in the cell-binding domain of fibronectin have received the most attention. Studies of integrin antagonists indicate that αv integrins promote angiogenesis, while genetic deletion studies indicate that αv integrins are not required for angiogenesis. Although their exact function in angiogenesis has been subject to much debate (see (Astrof and Hynes, 2009; Desgrosellier and Cheresh, 2010; Hodivala-Dilke, 2008), αv-targeting agents are currently being developed or used in the clinic for cancer therapeutics.

Genetic ablation of the fibronectin gene deletes all fibronectin variants (up to 20 in humans). What about the role of the alternately spliced isoforms, and their cellular receptors? Selective ablation of EDB and EDA domains suggests that these domains confer essential functions to fibronectin, as evidenced by the early embryonic death of mice lacking both exons (Astrof *et al.*, 2007a). However, the precise roles of these domains and the molecular events involved have yet to be fully understood, as compensatory mechanisms can rescue mice with single knock outs of either the EDB or EDA variant (recently reviewed in Astrof and Hynes, 2009; White *et al.*, 2008). The EDB domain has been proposed to generate a conformational modification of fibronectin and improve the access to nearby integrin binding domains (see Balza *et al.*, 2009; Bencharit *et al.*, 2007; Carnemolla *et al.*, 1992; Hashimoto-Uoshima *et al.*, 1997; Ventura *et al.*, 2010). This function is consistent with results from isoform-selective knockdown studies in endothelial cells (Cseh *et al.*, 2010).

Whereas no EDB-specific cellular receptor has been identified to date, inclusion of the EDA repeat in c-fibronectin creates new binding sites for $\alpha4\beta1$, $\alpha4\beta7$ and $\alpha9\beta1$ integrins (Kohan *et al.*, 2010; Liao *et al.*, 2002) (Fig. 1). $\alpha4\beta1$ and $\alpha9\beta1$ are structurally similar integrins that can bind to several ECM proteins; in the case of $\alpha9\beta1$ this includes tenascin-C (Humphries *et al.*, 2006; Yokosaki *et al.*, 1998). Genetic and pharmacological studies in mice reveal a

role for these integrins in the lymphatic vasculature. Hence, $\alpha 9\beta 1$ null mice die between 8-12 days after birth from major defects in development of the lymphatic system (Huang *et al.*, 2000). More recently, it was shown that the interaction between integrin $\alpha 9$ and fibronectin containing the EDA domain is required for fibronectin matrix assembly during lymphatic valve morphogenesis (Bazigou *et al.*, 2009). Integrin $\alpha 4$ knock out mice die at E11.5 with cardiac malformations and placental defects. Interestingly, targeted deletion of $\alpha 4$ in lymphatic vessels or pharmacological inhibition of $\alpha 4\beta 1$ was found to suppress growth factor- and tumor-induced lymphangiogenesis and prevent metastatic spread *in vivo*. In this same study, $\alpha 4\beta 1$ and c-fibronectin were identified as markers of proliferative lymphatic endothelium in invasive tumors (Garmy-Susini *et al.*, 2010). In addition to the EDA domain, sequences in the variable (V) region (Fig. 1) can also bind to $\alpha 4\beta 1$ integrin and thus contribute to the observed effects. Collectively, these findings shed light on the role of c-fibronectin variants as fundamental regulators of both blood and lymphatic vessels.

In humans, mutations in the fibronectin gene were identified in patients with glomerulopathy with fibronectin deposits (GFND), an autosomal dominant disease characterized by proteinuria, microscopic hematuria, hypertension, and massive glomerular deposits of non-fibrillar fibronectin in the mesangium and subendothelial space that lead to end-stage renal failure (Castelletti *et al.*, 2008). These mutations affect the heparin binding domains Hep-II and Hep-III. Functional studies showed that mutant recombinant Hep-II fragments display lower binding to endothelial cells and podocytes, compared to wild-type Hep-II, and an impaired ability to induce endothelial cell spreading and cytoskeletal reorganization. Hep-II and -III domains participate in fibronectin assembly in ECM, through complex fibronectin-fibronectin and fibronectin-cell surface proteoglycan interactions (Singh *et al.*, 2010). Interestingly, heparin-binding domains of fibronectin are sites of tenascin-C binding and have been shown to mediate functional interactions between fibronectin and tenascin-C that involve cell surface proteoglycans of the syndecan family, as discussed below.

Effect of tenascin-C knock out on the vasculature

Tenascin-C knock out mouse was generated in two different laboratories (Forsberg *et al.*, 1996; Saga *et al.*, 1992). In both studies the signal peptide and the heptad repeat sequences were disrupted. Saga and colleagues inserted a lacZ-neo construct just in front of the translational initiation codon in exon 2 of the tenascin-C gene, deleting parts of the exon 2 and intron 2 and keeping the regulatory unit of the tenascin-C gene for lacZ expression (Saga *et al.*, 1992). Since expression of a truncated tenascin-C in these mice was detected (Mitrovic and Schachner, 1995), a second independent tenascin-C knock out mouse was generated where a neomycin resistance cassette was inserted into exon 2 leading to two aberrant splice products of tenascin-C in homozygous mice inducing a frameshift and translation stop after 99 and 18 nucleotides (Forsberg *et al.*, 1996). It is now clear that tenascin-C expression is lost in most tissues. Surprisingly, in both cases tenascin-C knock out mice were alive and fertile and exhibited an apparently normal development. The apparently normal development and tissue organization of these mice has been attributed to compensation mechanisms (reviewed in Orend and Chiquet-Ehrismann, 2006). It was noticed that in the subventricular zone of the brain oligodendrocyte precursor cells respond differently to growth factors and proliferate less, but this appears to be compensated by a reduced apoptosis rate later on. Thus the number of oligodendrocytes ends up being similar in the tenascin-C knock out and wildtype mouse (Garcion *et al.*, 2001). Later studies showed that the absence of tenascin-C imposes problems for tissue homeostasis which is particularly evident during wound- or inflammation-associated tissue repair (reviewed in Orend and Chiquet-Ehrismann, 2006). Meanwhile tenascin-C knock out mice present valuable tools for addressing the roles of tenascin-C in development, angiogenesis, inflammation, heart failure and tumorigenesis.

By using a cardiac allograft model it was shown that tenascin-C is a mediator of postnatal cardiac angiogenic mechanisms in mice (Ballard *et al.*, 2006). Upon subdermal transplantation of wild-type cardiac tissue into a syngenic host, a fibrin clot forms around the allograft and both the clot and cardiac tissue become vascularized, resulting in engraftment of viable cardiac tissue. Clot formation is unaffected in tenascin-C-null mice; however, these mice fail to form any vessels and no engraftment of cardiac tissue is observed. In wildtype mice the donor endothelial cells engrafted at sites of tenascin-C expression, suggesting that tenascin-C acts to promote homing and incorporation of endothelial or progenitor cells. Indeed, cultured rat cardiac microvascular endothelial cells adhere to tenascin-C substrata, but spreading and monolayer formation are delayed compared to cells plated on fibronectin or collagen. Futhermore, migration of these cells into a collagen gel is enhanced when cultured on tenascin-C (Ballard *et al.*, 2006). These data support a role for tenascin-C in the early stages of angiogenesis by modulating endothelial cell adhesiveness, and thus promoting migration.

Tenascin-C also seems to play a role in vascularization associated with lung development. The tenascin-C knock out mouse does not show apparent defects in lung anatomy and function, presumably due to unknown compensatory mechanisms. This compensation seems not to apply when the embryonic lung is placed in culture since the lung explants from tenascin-C knock out embryos display reduced branching (defective cleft formation and enlarged terminal lung buds) and decreased vascularization (Roth-Kleiner *et al.*, 2004). Results from another report indicate that lung vascularization and branching morphogenesis are dependent on Wnt and fibronectin signaling. Wnt signaling is turned on between E10.5 and E12.5 in the developing lung. Later (E13.5) Wnt signaling is largely reduced by Dickkopf (DKK) 1–3, and this coincides with induction of the Wnt target gene, fibronectin. Moreover DKK1 and fibronectin are instrumental in promoting lung branching morphogenesis and angiogensis, since recombinant DKK1 and anti-fibronectin antibody both block cleft formation and angiogenesis. DKK1 treatment causes thinner blood vessels, reduced sprouting from existing vessels and impaired formation of large vessels with fewer interconnections (De Langhe *et al.*, 2005). Given that tenascin-C blocks fibronectin signaling, represses DKK1, and plays a role in lung branching morphogenesis, it is possible that a tight balance between fibronectin and tenascin-C regulates normal lung branching and vascularization. In this scenario DKK1 repression by tenascin-C would result in Wnt activation and induction of fibronectin.

The role of tenascin-C in tumorigenesis was also investigated in a mouse model that develops metastasizing mammary gland tumors (due to ectopic expression of the polyoma virus middle T-antigen in the mammary epithelium) in the presence of wildtype

tenascin-C or in a tenascin-C knock out setting (Talts *et al.*, 1999). There was no difference observed in tumor onset, angiogenesis or metastasis between the genotypes, but the authors observed an altered organization of the tumor tissue. In tenascin-C wildtype tumors ECM molecules such as fibronectin, collagen I, nidogen and fibulin-2 were arranged in continuous long tracks whereas they were assembled in shorter matrix patches in the tenascin-C knock out background. These structures might represent matrix channels that were subsequently identified by others in metastasizing melanomas (Kaariainen *et al.*, 2006, see below). In contrast to melanomas, where the tenascin-C matrix channels seem to promote metastasis, other mechanisms might exist to promote metastasis in mammary gland tumors, in the absence of tenascin-C. It was also noted that tenascin-C knock out breast carcinomas are significantly more infiltrated by activated macrophages (Talts *et al.*, 1999). Since M2 macrophages promote tumor metastasis (Mantovani *et al.*, 2008) it is possible that this species is increasingly attracted to the tissue that lacks tenascin-C. Previously it was shown that tenascin-C inhibits T lymphocyte adhesion to fibronectin (Hauzenberger *et al.*, 1999) and activation (Puente Navazo *et al.*, 2001). Thus, it is possible that in the tenascin-C knock out mammary gland carcinomas the inhibitory effect of tenascin-C is absent and this situation allows the attraction of macrophages. The reason why this would only affect a subset of macrophages needs to be addressed in the future.

In Balb/c-nude mice lacking tenascin-C, subcutaneously xenografted human melanoma cells made smaller tumors (Tanaka *et al.*, 2004). In this model blood vessels were visualized by immunofluorescence upon injection of rhodamine-labeled gelatin, which allows selective visualization of perfused vessels that arise through sprouting angiogenesis. Despite a lack of quantitative data, the authors showed in tissue stainings that the arising tumor vasculature is reduced in the absence of host tenascin-C. They link this to reduced VEGFA expression in the tumor tissue. Although the melanoma cells exhibit strong tenascin-C expression, this does not appear to have a significant impact on VEGFA levels in the tumor. These data suggest that tenascin-C made by stromal cells has a major impact on VEGFA expression and that this mechanism potentially accounts for the angiogenesis promoting effect of tenascin-C (Tanaka *et al.*, 2004).

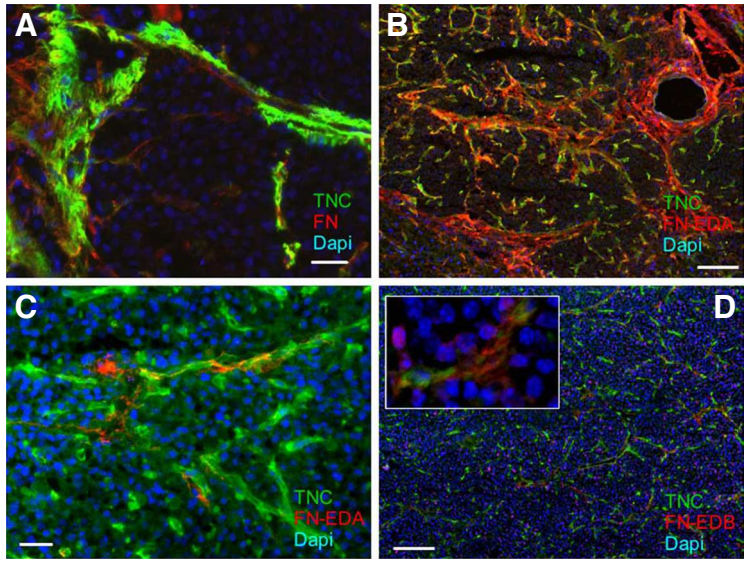

Fig. 3. Colocalization of fibronectin and tenascin-C in the tumor vasculature. (A-D) *Tenascin-C and fibronectin expression in tumors. Coexpression of total fibronectin* **(A)**, *FN-EDA* **(B,C)** *or FN-EDB* **(D)** *and tenascin-C in fibrils of an RT2 tumor (Gasser and Orend, unpublished). The anti FN-EDB antibody was kindly provided by Dr. A. K. Olsson (Uppsala University, Sweden). Scale bar 20 μm (A,C) and 100 μm (B,D). Note the fibrillar organization of both molecules and their close apposition in tube-like structures, presumably representing blood vessels and/or matrix tubes.*

Effects of fibronectin and tenascin-C on the vasculature in tumors and in other pathological tissues

Similar to fibronectin, tenascin-C is only weakly expressed, or undetectable, in the ECM of quiescent vasculature. However, following vessel injury, tenascin-C and fibronectin are highly upregulated. Tenascin-C expression is strongly associated with sites of vascular remodeling during dermal tissue repair (Betz *et al.*, 1993; Fassler *et al.*, 1996; Latijnhouwers *et al.*, 1996; Mackie *et al.*, 1988). Tenascin-C expression is also highly associated with angiogenesis in a wide range of disease states, including diabetes, aortic aneurysm (Castellon *et al.*, 2002; Jallo *et al.*, 1997; Paik *et al.*, 2004), artherosclerosis (Fischer, 2007), ulcerative colitis (Dueck *et al.*, 1999), inflammatory bowel disease (Geboes *et al.*, 2001), Crohn's disease (Riedl *et al.*, 2001), vasculitis (Gindre *et al.*, 1995) and cancer.

Recently, Berndt and collaborators reported the distribution of tenascin-C and fibronectin in several different carcinomas using antibodies specific for different splice variants (Berndt *et al.*, 2010). Both proteins were generally present in the vessel wall, with fibronectin being preferentially localized at the luminal side and tenascin-C at the extraluminal side of the vascular basement membrane. Interestingly, tumour vessels showed a heterogenous positivity for oncofetal fibronectin and tenascin-C variants, with some vessels lacking both proteins, some vessels exclusively positive for fibronectin or tenascin-C, and other vessels surrounded by both matrix proteins. As an example, expression and partial colocalization of c-fibronectin variants and tenascin-C in a murine RT2 insulinoma is shown (Fig. 3). This stratified pattern clearly suggests a temporally and spatially regulated expression of these ECM proteins in the tumor vasculature and may reflect different maturation states of the vessels. In the study by Berndt *et al.*, fibronectin was expressed by endothelial cells and carcinoma associated fibroblasts (CAFs) whereas tenascin-C was abundantly produced by carcinoma cells. It will be important to identify which cell types in various cancer tissues express tenascin-C and fibronectin with different domain structures. Further, it remains to be determined whether tenascin-C and c-fibronectin variants with different domain compositions fulfill distinct roles in tumor angiogenesis.

Some light was shed on these questions by RNA expression analysis in breast cancer tissue. Amongst the more than 500 theoretically possible splice variants only 2 or 3 are usually expressed in cancer tissue, and these differ between cancers of different organs (reviewed in Orend, 2005). In invasive breast cancer, the authors found a prominent expression of a tenascin-C molecule with extra repeats B and D that is derived from the tumor cells, whereas a tenascin-C molecule only expressing the D domain appears to be expressed by carcinoma associated fibroblasts (reviewed in

Guttery *et al.*, 2010).

During tissue neovascularization, endothelial cells undergo pro-angiogenic activation, and assume a migratory morphology (Carmeliet, 2000; Ingber, 2002). Tenascin-C may promote tumor angiogenesis through several mechanisms, such as by serving as a chemoattractant for endothelial cells by initiating endothelial cell differentiation, or by promoting survival and proliferation. *In vitro*, tenascin-C is specifically upregulated by sprouting and cord forming bovine aortic endothelial cells but not by non-sprouting (i.e., resting) cells (Canfield and Schor, 1995; Schenk *et al.*, 1999). This angiogenic phenotype is inhibited when cells are grown in the presence of anti–tenascin-C antibodies, suggesting that the transition from a resting to a sprouting phenotype may be promoted by tenascin-C (Canfield and Schor, 1995). Indeed, soluble tenascin-C reduces focal adhesions in endothelial cells (Chung *et al.*, 1996; Murphy-Ullrich *et al.*, 1991) and enhances endothelial cell migration (Chung *et al.*, 1996). These events appear to involve integrin $\alpha v\beta 3$, FAK and Prx1 amongst other, not yet identified, molecules (reviewed in Orend and Chiquet-Ehrismann, 2006).

Counter-adhesive activities of fibronectin and tenascin-C

Shortly after its discovery in the early 1980s as myotendinous antigen (Chiquet and Fambrough, 1984), as glioma-mesenchymal extracellular matrix molecule (GMEM) (Bourdon *et al.*, 1983) and as neuronal protein janusin J1 (Faissner *et al.*, 1988) it was noted that tenascin-C can bind to fibronectin (Chung *et al.*, 1995; Lightner and Erickson, 1990). Since then, several reports have extended this finding although some controversy exists whether the long and/or the short form of tenascin-C (i.e. including or lacking the alternatively spliced fibronectin type III repeats, respectively) (Chiquet-Ehrismann *et al.*, 1991; Chung *et al.*, 1995; Huang *et al.*, 2001) have different affinities for fibronectin. All three heparin binding domains seem to bind tenascin-C, with Hep-I being cryptic and exhibiting low affinity (Ingham *et al.*, 2004). Tenascin-C binds to the Hep-III domain in fibronectin, but it is not known whether this interaction competes with binding of cell adhesion receptors. Binding of tenascin-C to the fibronectin-Hep-II domain blocks cell spreading (Chiquet-Ehrismann *et al.*, 1991; Huang *et al.*, 2001; Midwood *et al.*, 2004a; Orend *et al.*, 2003) and fibronectin fibrillogenesis (To and Midwood, 2010) through competition with syndecan-4. The Hep-II domain serves as coreceptor for the major fibronectin binding integrin $\alpha 5\beta 1$ (Fig. 4 A,B). The exact binding site in fibronectin has been mapped to the 13th fibronectin type III repeat within the Hep-II domain, and a peptide representing 10 amino acids of the cationic craddle rescued tenascin-C induced cell rounding (Huang *et al.*, 2001; Orend *et al.*, 2003). Activation of syndecan-4 signaling induced upon ectopic expression of syn-

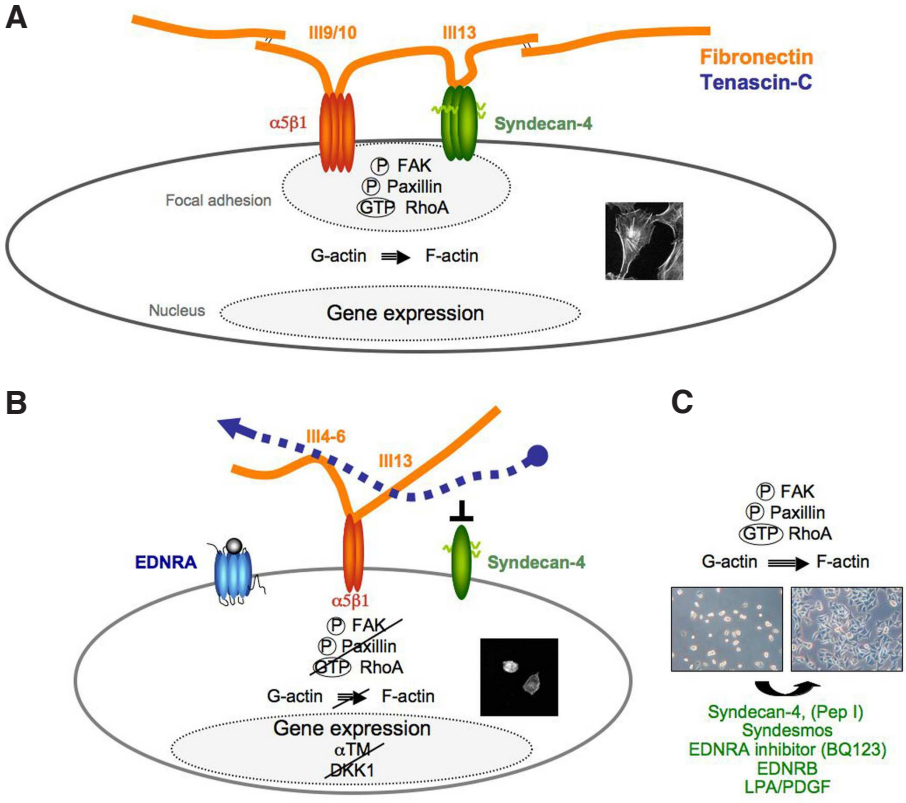

Fig. 4. Inhibition of syndecan-4 by tenascin-C. (A) *Cells activate integrin $\alpha 5\beta 1$ and syndecan-4 upon adhesion to their respective binding sites in fibronectin (FN type III repeats 9 and 10, and 13, respectively). This induces formation of focal adhesions. Crucial steps in cell spreading are phorphorylation of focal adhesion kinase (FAK) and paxillin and GTP loading of RhoA. Consequently, G-actin is polymerized into F-actin and cells spread on fibronectin.* **(B)** *Tenascin-C binds to the 13th FN type III repeat in fibronectin thus competing for cell binding to this domain. This mechanism applies to tumor cells and fibroblasts, but has yet to be addressed in endothelial cells. In the presence of tenascin-C, FAK and paxillin stay unphosphorylated and RhoA remains inactive (Huang et al., 2001, Midwood and Schwarzbauer, 2002). No focal adhesions or actin stress fibers are formed. The rounded cell shape translates into altered gene expression and causes repression of alpha tropomyosin (αTM) and Dickkopf-1 (DKK1) as well as induction of endothelin receptor type A (EDNRA) amongst changes in expression of several other genes (Ruiz et al., 2004).* **(C)** *The rounded cell shape can be reverted on a fibronectin/tenascin-C substratum upon activation of syndecan-4 with a peptide (pep I) that mimics the cationic craddle in syndecan-4 or upon overexpression of syndesmos, a molecule that binds to the cytoplasmic tail of syndecan-4 and provides a molecular bridge in the focal adhesions to proteins binding to integrins (Baciu et al., 2000; Lange et al., 2008; Orend et al., 2003). Inhibition of EDNRA with BQ123 also induces cell spreading (Lange et al., 2007). Combined signaling from platelet derived growth factor (PDGF) and the lysophosphatidic acid (LPA) and by endothelin receptor type B (EDNRB) involving the EGFR induce cell spreading on the mixed fibronectin/tenascin-C substratum. Signaling by these molecules induces focal adhesion and actin stress fiber formation although with a cell shape that is particular for each treatment. Nevertheless, repression of αTM is ablated and tropomyosins 1-3 are expressed to stabilize actin stress fibers (Lange et al., 2007; Lange et al., 2008). Regulation of αTM is crucial for cell spreading on fibronectin since its knock down inhibits cell spreading on fibronectin and interferes with restored cell spreading on the fibronectin/tenascin-C substratum upon treatment with pep I and activation of LPA receptors and PDGF receptors or EDNRB (Lange et al., 2007; Lange et al., 2008).*

decan-4 (but not of syndecan-1 or –2) rescued tenascin-C-inhibited cell spreading on fibronectin (Huang *et al.*, 2001; Midwood *et al.*, 2004b; Orend *et al.*, 2003) as did overexpression of syndesmos, a molecule that binds to the cytoplasmic tail of syndecan-4 and triggers downstream signaling (Lange *et al.*, 2008, Fig. 4C). The major binding site for fibronectin-Hep-II may reside in the 6-8 fibronectin type III repeats of tenascin-C as was deduced from antibody blocking experiments (Chiquet-Ehrismann *et al.*, 1988; Riou *et al.*, 1990). This is now supported by a recent report demonstrating that meprinβ-cleaved tenascin-C loses its anti-adhesive properties in a fibronectin context (Ambort *et al.*, 2010). The authors showed that meprinβ cleaves within the 7th fibronectin type III repeat of tenascin-C thus destroying this interaction site, and that meprinβ-cleaved tenascin-C does not interfere with cell spreading on fibronectin (Ambort *et al.*, 2010). Inhibition of syndecan-4 by tenascin-C prevents focal adhesion formation, blocks activation of FAK and paxillin and has a strong negative impact on expression and protein stability of RhoA and tropomyosin 1–3 (Lange *et al.*, 2007; Lange *et al.*, 2008), and Rho activation (Midwood *et al.*, 2006). The effect on the cytoskeleton appears to be instrumental in cell rounding by tenascin-C since ectopic expression of tropomyosin-1, an actin stress fiber stabilizing molecule with tumor suppressor activity, restores cell spreading which is linked to FAK and paxillin phosphorylation (Lange *et al.*, 2007).

Binding of tenascin-C to the Hep-II domain of fibronectin can also have implications for angiogenic growth factor signaling. Indeed, it has been shown using molecular and biochemical approaches that several growth factors (up to 25, including VEGF, HGF, FGF-2, PDGF-BB and TGF-β1) bind to this domain (see (Hynes, 2009; Martino and Hubbell, 2010). Moreover, fibronectin-Hep-II-bound growth factors are even more potent than their un-bound counterparts in triggering capillary morphogenesis of endothelial cells in fibrin gels (Martino and Hubbell, 2010). Although not shown in endothelial cells, cellular responses to tenascin-C can be modulated by growth factors. Thus, in fibroblasts and tumor cells growth factor signaling can override the necessity of syndecan-4 in fibronectin-induced cell spreading. Combined signaling from LPA and PDGF-BB (but not from each factor alone) restores cell spreading on a fibronectin/tenascin-C substratum even in cells that lack syndecan-4 (knock out) in a PI3K- and MEK-dependent manner, and this is linked to restored high expression of tropomyosins 1-3 and RhoA (Lange *et al.*, 2008, Fig. 4C). Again, high levels of tropomyosin 1-3 are essential since sh-mediated knock down of the tropomyosins 1, 2 and 3 counteracts LPA/PDGF-BB-induced cell spreading on the fibronectin/tenascin-C substratum (Lange *et al.*, 2008).

Adhesion to a fibronectin/tenascin-C substratum also has long term consequences as revealed by RNA profiling (Ruiz *et al.*, 2004). In particular, 12h after plating, endothelin receptor type A (EDNRA) is induced 5-fold, and, signaling through this receptor maintains cell rounding by tenascin-C since it is blocked by a specific EDNRA inhibitor. EDNRA associated cell rounding occurs in a MEK-dependent manner and EDNRA inhibition causes cell spreading with activation of FAK and restoration of tropomyosin and RhoA levels (Fig. 4 B,C). These studies also reveal that, depending on the receptors present on the membrane, interactions with tenascin-C can be interpreted very differently. In particular, in contrast to EDNRA signaling that induces tenascin-C cell rounding, activation of EDNRB restores cell spreading through a different pathway that does not involve MEK but does involve EGFR, PLCγ, PI3K and JNK (Lange *et al.*, 2007, Fig. 4C). Thus, whether cells respond to a fibronectin/tenascin-C matrix by rounding or spreading appears to be highly regulated and may have an impact on cell function, tissue stiffness and vessel diameter. Both endothelin receptors play an important role in modulating blood pressure and are linked to high blood pressure in heart disease and artherosclerosis (Nguyen *et al.*, 2010). Since tenascin-C is expressed in diseased heart tissue and artherosclerosis, it remains to be determined whether tenascin-C-associated EDNRA signaling plays a role in blood pressure regulation that has an impact in heart diseases.

Tenascin-C potentially plays a role in EDNRA-associated events involving angiogenesis, e.g., in ovarian cancer progression. Primary and metastatic ovarian cancer cells not only overexpress tenascin-C (Wilson *et al.*, 1999; Wilson *et al.*, 1996) but also EDNRA and its ligand endothelin-1 (ET1) (Rosano *et al.*, 2001). EDNRA signaling contributes to tumor angiogenesis presumably through stabilization of HIF-1α, induction of VEGFA (Grimshaw, 2007) and β-arrestin-linked Wnt signaling (Rosano *et al.*, 2001).

A tenascin-C – EDNRA axis might also be relevant in tumor cell migration and tumor lymphangiogenesis (Cueni *et al.*, 2010). Tumors derived from xenografted breast adenocarcinoma cells that ectopically express the orphan receptor podoplanin induce lymphatic vessels, whereas this was not observed in tumors of control cells with low or no podoplanin expression. RNA profiling of microdissected areas of the invading tumor front revealed overexpression of tenascin-C, ET1 and the ERM member villin. Previously it was shown that binding of the ERM family member ezrin to the cytoplasmic tail of podoplanin induces filopodia which was linked to collective tumor cell migration (Wicki *et al.*, 2006). These results suggest that ET1 signaling may induce migration on a tenascin-C substratum by podoplanin through its link to the actin cytoskeleton.

In addition to EDNRA, Wnt signaling is also induced in glioblastoma cells on a fibronectin/tenascin-C substratum. In particular, DKK1 is repressed, β-catenin stabilized and Wnt targets such as Id2 are induced (Ruiz *et al.*, 2004). This observation could be relevant in glioblastomas where a high expression of Id2 and tenascin-C correlated with malignancy (Ruiz *et al.*, 2004). Given that Wnt signaling is instrumental in angiogenesis, by triggering endothelial cell proliferation and sprouting (reviewed in Franco *et al.*, 2009), it remains to be determined whether tenascin-C promotes angiogenesis through Wnt signaling. Since EDNRA and Wnt signaling are linked through β-arrestin (Rosano *et al.*, 2009) and through ET1-induced DKK1 repression (Clines *et al.*, 2007) it is possible that tenascin-C enhances this cross-talk by activating both pathways.

Organization of fibronectin and tenascin-C into matrices

Fibronectin assembly and angiogenesis

Fibrillar organization is a key feature of the ECM. Many of the functions of fibronectin depend not only on its linear sequence but on the 3-dimensional structure of the protein and its assembly into a functional fibrillar matrix (see Mao and Schwarzbauer, 2005). Due to its compact conformation, fibronectin does not form fibrils in solution. Rather, fibril assembly is a cell-driven process in which α5β1 integrin plays a major role (recently reviewed in Singh *et al.*, 2010) and shown diagrammatically in Fig. 5). Importantly, soluble fibronectin selectively binds to α5β1 integrin, and not other RGD-binding

integrins (Huveneers *et al.*, 2008). Hence, bloodborne p-fibronectin in quiescent vessels is segregated from $\alpha5\beta1$ integrins, located on the abluminal surface of endothelial cells. Studies to elucidate the mechanisms of fibronectin fibrillogenesis in endothelial cells have revealed a determinant role for ILK in this process (Vouret-Craviari *et al.*, 2004). ILK, an integrin beta subunit adaptor, regulates actin dynamics and fibronectin fibrillogenesis by recruiting actin-binding regulatory proteins such as α-parvins and tensin (Legate *et al.*, 2006; Stanchi *et al.*, 2009) involved in generating acto-myosin contractility for fibril growth. More recently, loss of function studies have revealed that fibronectin fibrillogenesis in endothelial cells is a cell autonomous process, wherein basally directed secretion of autocrine fibronectin is tightly coupled to fibronectin assembly and cadherin-based junction formation (Cseh *et al.*, 2010). These results highlight the importance of spatial and temporal regulation of c-fibronectin expression and they support a model in which the induction of cellular c-fibronectin expression by angiogenic factors triggers the deposition of a perivascular fibrillar matrix.

One example of how transient c-fibronectin expression participates in a "pro-angiogenic switch" comes from elegant studies on vascular patterning in the developing retinal vasculature (Gerhardt *et al.*, 2003; Jiang *et al.*, 1994; Uemura *et al.*, 2006). During this process, blood vessels use the existing astrocyte network as a template, and fibronectin is the principal component of the astrocyte-derived extracellular scaffold. Upon contact with the growing blood vessels, fibronectin expression becomes dramatically down regulated in the astrocytes and turned on in the endothelial cells that deposit fibronectin matrices. It should be interesting to examine the expression and localization of tenascin-C in this model.

Once assembled, fibronectin fibrils provide a scaffold for the assembly of a growing list of matrix proteins, including fibrillar collagens, thrombospondin-1, fibulin-1, fibrinogen, fibrillins and tenascin-C (reviewed in Dallas *et al.*, 2006). Further, fibronectin interactions can impact higher order fibrils and matrix rigidity by bringing together cross-linking enzymes such as tissue transglutaminase (Mosher *et al.*, 1980) and lysyl oxidase (Fogelgren *et al.*, 2005) as well as their activators (e.g., Bone Morphogenetic Protein-1) and substrates (e.g., procollagen, biglycan and chordin, Huang *et al.*, 2009).

Fibronectin and tenascin-C co-assemble into a matrix

Apart from the $\alpha5\beta1$ integrin, other fibronectin-binding integrins have been reported to promote fibrillar assembly, albeit less efficiently (see Leiss *et al.*, 2008). Fibronectin matrix is also regulated by molecules that affect integrin expression or function, including transmembrane molecules (e.g., syndecans 2 and 4, the receptor for urokinase-type plasminogen activator, CD98hc, VEGFR1 and neuropillin), intracellular proteins (e.g., the tumor suppressor von Hippel-Lindau protein) or extracellular components (e.g., extracellular Alix ALG-2-interacting protein X). With regard to functional interactions between fibronectin and tenascin-C that impact matrix formation, they are likely to involve effects on the fibronectin matrix mediated by syndecans 2 and 4, and regulation of intracellular signaling events that accompany fibronectin binding to integrins, as mentioned above. Proteoglycans, such as decorin and periostin, known to modulate fibronectin matrix assembly (Kii *et al.*, 2010; Kinsella *et al.*, 2000) are essential for matrix incorporation of tenascin-C (Chung and Erickson, 1997; Kii *et al.*, 2010). It is known that tenascin-C can bind to purified fibronectin and co-localize with fibronectin fibrils on the surface of cultured cells (e.g., Ramos *et al.*, 1998). A recent study in fibroblasts involving the use of recombinant tenascin-C domains demonstrated an inhibitory effect of tenascin-C domain III 1-8 (fibronectin type III domains 1-8) on the formation of an insoluble fibronectin matrix, whereas the full length protein was without effect (To and Midwood, 2010). These data

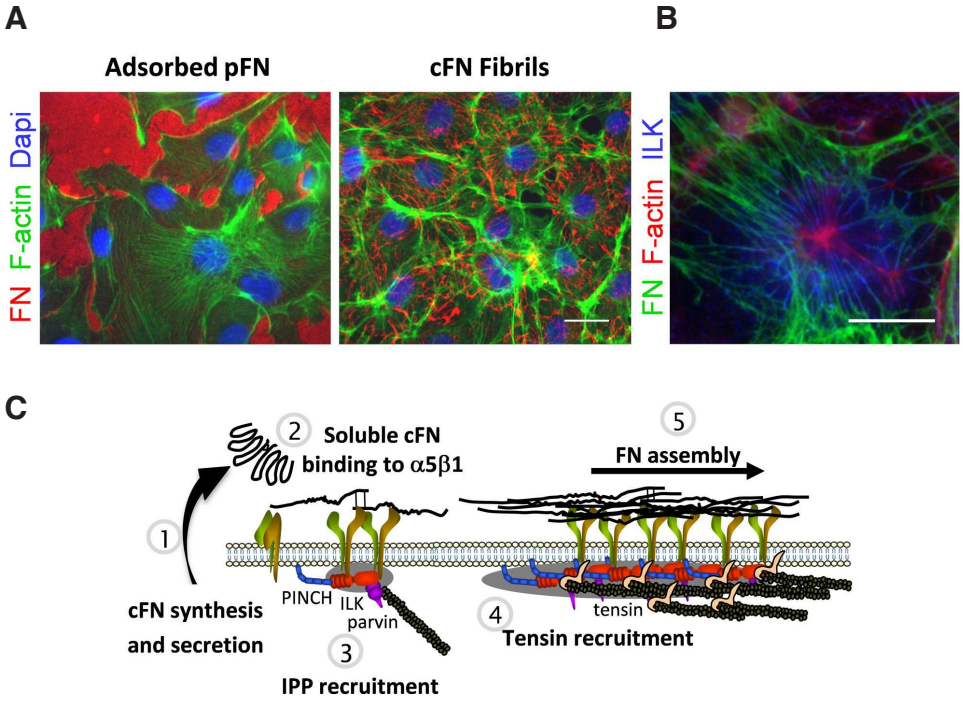

Fig. 5. Fibrillar organization of c-fibronection in endothelial cells and mechanisms of assembly. **(A,B)** *Immunostaining of fibronectin in bovine aortic endothelial cells plated on adsorbed p-fibronectin (left) or non-coated (right) coverslips. Upon adsorption, fibronectin undergoes conformational changes (stretch-induced "activation") that modify its interaction with other proteins (e.g. cellular receptors, ECM components) and affect its biological activity. Note the increase in stress fiber formation in cells plated on a dense carpet of p-fibronectin. Scale bars 20μm.* **(C)** *Sequence of events involved in fibronectin assembly. Work from numerous laboratories have contributed to the understanding of fibrillogenesis that can be summarized as follows (for a detailed review see Singh et al., 2010. Binding of secreted c-fibronectin to inactive α5β1 integrins (bent conformation) leads to integrin activation, clustering, and recruitment of integrin effectors, such as ILK, PINCH, parvin (IPP complex, (Legate et al., 2006)) and tensin that mediate cytoskeletal linkage and actin crosslinking. Acto-myosin-generated contractility "streches" the integrin-bound fibronectin, thereby exposing cryptic self-assembly sites and fibrillogenesis proceeds as integrins translocate along paths of growing fibrils.*

suggest that conformational changes may expose fibronectin-tenascin-C interaction sites that are important for regulation of matrix assembly *in vivo*.

Tenascin-C and fibronectin in tumor matrix tubes

In breast cancer tissue tenascin-C causes remodeling of the matrix. This effect, apparent at first glance by disruption of the basement membrane, can be seen in tumors and in cultured mammary epithelial cells. Using a 3-dimensional model of breast tumor cells, Taraseviciute and colleagues showed that tenascin-C interferes with basement membrane assembly in a c-Met dependent manner. In presence of tenascin-C the mammary epithelial cells proliferate and fill the acini lumen (Taraseviciute, 2009). In cancer tissue, the expression of tenascin-C is frequently not homogenous. Rather, it accumulates in matrix tracks as seen in the tissue of malignant melanomas (Kaariainen *et al.*, 2006), breast (Degen *et al.*, 2007) and colorectal carcinomas (Degen *et al.*, 2008). In the case of melanomas, the combined high expression of tenascin-C and fibronectin, amongst other factors, was found to discriminate between metastatic and non-metastatic malignancies. The switch to an invasive phenotype was associated with the presence of tenascin-C and fibronectin, colocalized with laminin and procollagen in tubular channels containing tumor cells, but not blood endothelial or lymph endothelial cells (Kaariainen *et al.*, 2006). In another study gene profiling revealed a panel of ECM molecules, including tenascin-C, several laminins, and collagens that were highly expressed in metastatic breast cancers from MMTV-VEGF/c-myc transgenic mice, whereas their expression was largely reduced or undetectable in non-metastatic c-myc-induced tumors (Calvo *et al.*, 2008). These studies suggest that a combined high expression of distinct ECM molecules, including tenascin-C and fibronectin, and their assembly in matrix channels, is somehow linked to metastasis.

The existence of vessel-like structures that are distinct from blood and lymphatic vessels has been known for a long time and was described as vasculogenic mimicry (VM) (Hendrix *et al.*, 2003). VM is characterized by the large absence of endothelial cells and by staining with PAS (Periodic Acid Schiff reagent), which identifies proteoglycans with glycosaminoglycan residues present in the ECM without further information on the molecular nature of these proteoglycans. It is likely that the matrix tubes that contain tenascin-C and fibronectin described in melanomas (Kaariainen *et al.*, 2006) are part of the PAS-positive structures that are characteristic of VM. In a large number of different cancers including melanoma, uveal melanomas, colorectal carcinoma, ovarian carcinoma (summarized in Kucera and Lammert, 2009) and astrocytoma (El Hallani *et al.*, 2010), VM is frequently associated with metastasis and bad prognosis. It is claimed that several forms of VM exist, which are classified according to the degree and nature of cells that associate with the ECM: no endothelial cells, patchy distribution of endothelial cells, tumor cells only, or a combination of both cell types. By comparing *in vitro* cultures of cancer cells that do or do not exhibit VM *in vivo*, several VM-associated molecules have been identified. These include γ2 chain containing laminins, several metalloproteases (MMPs 1, 2, 9 and 14), Cox2, PI3K, EphA2, nodal and pigment epithelial derived factor, amongst a list of growing candidates (reviewed in Dome *et al.*, 2007; Paulis *et al.*, 2010). Eventually, cells are found associated with matrix structures: melanoma cells, and erythrocytes in tenascin-C matrix channels (Kaariainen *et al.*, 2006), and macrophages along collagen-rich tracks found in so called co-opted vessels (Pollard, 2008). Although matrix structures had been identified that appear to be different, more work is needed to clarify whether they are potentially part of the same matrix network.

Currently there is little known about the functional significance of these matrix structures in respect to tumor angiogenesis and progression. However, there is experimental evidence that cancer cells can use the tenascin-C-containing matrix tubes to disseminate. In a coculture experiment of fibroblasts together with squamous carcinoma cells, the fibroblasts scouted their way through collagen-enriched matrigel by degrading the ECM at the front. Tubes were left behind that were filled with fibronectin and tenascin-C. The squamous carcinoma cells invaded the matrigel by using these matrix tubes (Gaggioli *et al.*, 2007). It was previously shown that carcinoma-associated fibroblasts or TGFβ1 treated fibroblasts (differentiating into myofibroblasts) secrete tenascin-C into the collagen gels preparing a path for colorectal carcinoma cells to invade in a c-MET- and EGFR-dependent manner, involving activation of Rac and inhibition of RhoA (De Wever *et al.*, 2004). They proved a crucial role of tenascin-C in these events since invasion was inhibited with an anti-tenascin-C antibody. Whether fibronectin plays a role in these structures is unknown, but likely.

Evolutionary development of endothelium-lined blood vessels in vertebrates seems to have followed laminin-based matrix tracks in invertebrates (Kucera *et al.*, 2009) (Fig. 2). In amphioxus, laminin-filled tubes are laid down as a scaffold in which a hole is drilled by cells of unknown origin to generate a coelom that allows blood to circulate (Kucera *et al.*, 2009). As mentioned above the tenascin-C gene is present in amphioxus and it remains to be seen whether tenascin-C is part of this matrix circulation network. In co-cultures of endothelial cells with a macrophage cell line, where the endothelial cells deposit laminin, macrophages create a coelom-like cavity by partially digesting and clearing the ECM to generate space. Thus, it is possible that this ancient vessel program is turned on in tumors to establish the observed matrix-based networks. More information about the composition of the matrix blood vessels in chordata and in human cancers is necessary to elucidate this possibility further. The observed tenascin-C matrix tubes in melanomas and other cancers may offer a route for dissemination of tumor and other cells through their continuum with blood vessels. They also potentially provide a scaffold to support growth of blood vessels. This possibility is interesting, considering that anti-angiogenic therapeutic approaches, despite efficient killing of the endothelial cells, fail in the long-run, and even promote tumor progression and earlier tumor metastasis (Paez-Ribes *et al.*, 2009; Stockmann *et al.*, 2008). Tenascin-C matrix tubes would not be affected by anti-angiogenic drugs. Indeed, Fusenig and coworkers (Vosseler *et al.*, 2005) demonstrated that expression of tenascin-C in xenografts of squamous carcinoma cells is unchanged upon elimination of the endothelial cells with a VEGFA-targeting antibody.

Matrix tubes containing tenascin-C are also present in a normal setting in mammals in so called reticular fibers of secondary lymphoid tissues such as lymph nodes, thymus and spleen (Lokmic *et al.*, 2008). They combine characteristics of basement membranes and fibrillar matrices, resulting in scaffolds that are strong and flexible, and in certain organs, such as the spleen and the thymus, form conduit networks for rapid fluid transport and cells (Lokmic *et al.*, 2008). In the thymus, the conduits exhibit a collagen core, a laminin wrapping and an outer lining of tenascin-C (Drumea-Mirancea *et*

al., 2006). Fibronectin is also part of the reticular fiber network (Sobocinski *et al.*, 2010). Whether tenascin-C and or fibronectin are required for the formation and function of the conduits is not known.

We speculate that a program may exist for the establishment of structured matrix that is potentially turned on inappropriately in cancer resulting in the described tenascin-C/fibronectin-containing matrix tubes. It is also tempting to consider that tubular matrix structures containing fibronectin and tenascin-C had developed once during evolution and were potentially further developed to fulfill other needs such as a transport system for maturing macrophages in reticular fibers, as scaffold for endothelial cell lined vessels and as an instructive matrix for branching morphogenesis. It will be important to understand how these matrix networks are created, and which signals induce their emergence.

Lysyl oxidase, transglutaminase and other enzymes modifying fibronectin may be relevant in modulating interactions of fibronectin with tenascin-C and other matrix molecules. It is likely that monomeric rather than bulky hexameric tenascin-C is part of a dense tubular matrix network. Monomeric tenascin-C can be generated upon cleavage by several proteases that are abundant and active in cancer tissue. In particular, separation of the N-terminal part from the remainder of the molecule seems to result in the release of monomeric tenascin-C from the hexamer (Mackie, 1997). The N-terminal oligomerizing part of tenascin-C can be cleaved off by meprinα and β (Ambort *et al.*, 2010), pepsin (Chiquet *et al.*, 1991), trypsin (Fischer *et al.*, 1995) and MMP7 (Siri *et al.*, 1995).

It will be necessary to determine what exact role tenascin-C plays in the matrix tubes in cancer. Recently, it was found that cancers are able to trick the immune system by using a chemokine signaling program that would mischievously tell the body that the tumor is a lymphoid tissue (Shields *et al.*, 2010) and thus trigger tumor evasion. Given that lymphocytes use the reticular fiber system to translocate within the lymphoid tissue and that tenascin-C and fibronectin are structural components of the reticular fibers it will be interesting to see whether these matrix molecules play a role in immune evasion in reticular fibers and in cancer. Assuming that ancient programs developed in evolution and are potentially involved in the creation of tubular matrix structures in mammals, it is intriguing to speculate that laminins and integrins may play an initial role followed by tenascin-C, fibronectin and other ECM molecules that were developed later during evolution.

Potential applications and outlook

Together, these data demonstrate that tenascin-C and fibronectin are key players in tumor angiogenesis and metastasis, and they represent attractive anti-cancer targets. Drugs targeting tenascin-C and c-fibronectin, or interactions with their cellular receptors are currently being developed, or have already reached clinical trials (reviewed in Desgrosellier and Cheresh, 2010; Midwood and Orend, 2009; Pedretti *et al.*, 2009; Schliemann and Neri, 2010). Novel approaches involving immunization against the EDB domain of c-fibronectin also may provide interesting alternative strategies for interfering with tumor angiogenesis and cancer growth (Huijbers *et al.*, 2010). To optimize potential treatments, several questions related to the biology of these relatively new (evolutionarily speaking) ECM proteins remain to be further addressed. Many secrets appear to be hidden in their topographical organization, some of which may be revealed by comparing cancer tissue with embryonic tissue, and the ECM of different types of cancer. Beyond circumstantial evidence, do these molecules collaborate or counteract each other in induction of pro-angiogenic signaling and blood vessel remodeling? Does this occur through a receptor-mediated mechanism or indirectly e.g. by modulating signaling of proangiogenic growth factors? What are the mechano-regulatory mechanisms involved? How is their spatial regulation (different cells) and temporal regulation in tumors controlled? Do both molecules serve as chemoattractants for endothelial cells or their precursors? How are they involved in the recruitment of mural cells or cells of the hematopoetic system? Finally, do fibronectin and tenascin-C-containing matrix channels support regrowth of vessels in residual tumor tissue upon an anti-angiogenic therapy? Finding answers to these questions will require the complicity of many researchers. The answers should clarify the function of ECM in the evolution and development of vasculature, and should lead to the discovery of more effective therapies for fighting tumor growth and metastasis.

Acknowledgements

We apologize to all authors whose work we did not have space to mention. The laboratories of EVOS and GO are financially supported by INSERM, the Agence National de la Recherche, the Association pour la Recherche sur le Cancer and the Institut National du Cancer. EVOS was additionally supported by the University of Nice-Sophia Antipolis, CNRS and the Centre A. Lacassagne; and GO by Oncosuisse, the University Hospital Hautepierre and the University Strasbourg. I.G. was supported by Inserm Region Alsace. Anti-FN-EDB antibody was generously provided by A.K. Olsson, Uppsala University, Sweden.

References

AMBORT, D., BRELLIER, F., BECKER-PAULY, C., STOCKER, W., ANDREJEVIC-BLANT, S., CHIQUET, M. and STERCHI, E.E. (2010). Specific processing of tenascin-C by the metalloprotease meprinbeta neutralizes its inhibition of cell spreading. *Matrix Biol* 29: 31-42.

ASTROF, S., CROWLEY, D. and HYNES, R.O. (2007a). Multiple cardiovascular defects caused by the absence of alternatively spliced segments of fibronectin. *Dev Biol* 311: 11-24.

ASTROF, S. and HYNES, R.O. (2009). Fibronectins in vascular morphogenesis. *Angiogenesis* 12: 165-175.

ASTROF, S., KIRBY, A., LINDBLAD-TOH, K., DALY, M. and HYNES, R.O. (2007b). Heart development in fibronectin-null mice is governed by a genetic modifier on chromosome four. *Mech Dev* 124: 551-558.

AVRAAMIDES, C.J., GARMY-SUSINI, B. and VARNER, J.A. (2008). Integrins in angiogenesis and lymphangiogenesis. *Nat Rev Cancer* 8: 604-617.

BACIU, P.C., SAONCELLA, S., LEE, S.H., DENHEZ, F., LEUTHARDT, D. and GOETINCK, P.F. (2000). Syndesmos, a protein that interacts with the cytoplasmic domain of syndecan-4, mediates cell spreading and actin cytoskeletal organization. *J Cell Sci* 113: 315-324.

BAJOGHLI, B., AGHAALLAEI, N., HESS, I., RODE, I., NETUSCHIL, N., TAY, B.H., VENKATESH, B., YU, J.K., KALTENBACH, S.L., HOLLAND, N.D. *et al.* (2009). Evolution of genetic networks underlying the emergence of thymopoiesis in vertebrates. *Cell* 138: 186-197.

BALLARD, V.L., SHARMA, A., DUIGNAN, I., HOLM, J.M., CHIN, A., CHOI, R., HAJJAR, K.A., WONG, S.C. and EDELBERG, J.M. (2006). Vascular tenascin-C regulates cardiac endothelial phenotype and neovascularization. *FASEB J* 20: 717-719.

BALZA, E., SASSI, F., VENTURA, E., PARODI, A., FOSSATI, S., BLALOCK, W., CARNEMOLLA, B., CASTELLANI, P., ZARDI, L. and BORSI, L. (2009). A novel human fibronectin cryptic sequence unmasked by the insertion of the angiogenesis-associated extra type III domain B. *Int J Cancer* 125: 751-758.

BAZIGOU, E., XIE, S., CHEN, C., WESTON, A., MIURA, N., SOROKIN, L., ADAMS, R., MURO, A.F., SHEPPARD, D. and MAKINEN, T. (2009). Integrin-alpha9 is required for fibronectin matrix assembly during lymphatic valve morphogenesis. *Dev Cell* 17: 175-186.

BENCHARIT, S., CUI, C.B., SIDDIQUI, A., HOWARD-WILLIAMS, E.L., SONDEK, J., ZUOBI-HASONA, K. and AUKHIL, I. (2007). Structural insights into fibronectin type III domain-mediated signaling. *J Mol Biol* 367: 303-309.

BENTLEY, A.A. and ADAMS, J.C. (2010). The evolution of thrombospondins and their ligand-binding activities. *Mol Biol Evol* 27: 2187-2197.

BENTLEY, K., GERHARDT, H. and BATES, P.A. (2008). Agent-based simulation of notch-mediated tip cell selection in angiogenic sprout initialisation. *J Theor Biol* 250: 25-36.

BERNDT, A., KOLLNER, R., RICHTER, P., FRANZ, M., VOIGT, A., BORSI, L., GIAVAZZI, R., NERI, D. and KOSMEHL, H. (2010). A comparative analysis of oncofetal fibronectin and tenascin-C incorporation in tumour vessels using human recombinant SIP format antibodies. *Histochem Cell Biol* 133: 467-475.

BETZ, P., NERLICH, A., TUBEL, J., PENNING, R. and EISENMENGER, W. (1993). Localization of tenascin in human skin wounds—an immunohistochemical study. *Int J Legal Med* 105: 325-328.

BOURDON, M.A., WIKSTRAND, C.J., FURTHMAYR, H., MATTHEWS, T.J. and BIGNER, D.D. (1983). Human glioma-mesenchymal extracellular matrix antigen defined by monoclonal antibody. *Cancer Res* 43: 2796-2805.

CALVO, A., CATENA, R., NOBLE, M.S., CARBOTT, D., GIL-BAZO, I., GONZALEZ-MORENO, O., HUH, J.I., SHARP, R., QIU, T.H., ANVER, M.R. *et al.* (2008). Identification of VEGF-regulated genes associated with increased lung metastatic potential: functional involvement of tenascin-C in tumor growth and lung metastasis. *Oncogene* 27: 5373-5384.

CANFIELD, A.E. and SCHOR, A.M. (1995). Evidence that tenascin and thrombospondin-1 modulate sprouting of endothelial cells. *J Cell Sci* 108 (Pt 2): 797-809.

CARMELIET, P. (2000). Mechanisms of angiogenesis and arteriogenesis. *Nat Med* 6: 389-395.

CARNEMOLLA, B., LEPRINI, A., ALLEMANNI, G., SAGINATI, M. and ZARDI, L. (1992). The inclusion of the type III repeat ED-B in the fibronectin molecule generates conformational modifications that unmask a cryptic sequence. *J Biol Chem* 267: 24689-24692.

CASTELLETTI, F., DONADELLI, R., BANTERLA, F., HILDEBRANDT, F., ZIPFEL, P.F., BRESIN, E., OTTO, E., SKERKA, C., RENIERI, A., TODESCHINI, M. *et al.* (2008). Mutations in FN1 cause glomerulopathy with fibronectin deposits. *Proc Natl Acad Sci USA* 105: 2538-2543.

CASTELLON, R., CABALLERO, S., HAMDI, H.K., ATILANO, S.R., AOKI, A.M., TARNUZZER, R.W., KENNEY, M.C., GRANT, M.B. and LJUBIMOV, A.V. (2002). Effects of tenascin-C on normal and diabetic retinal endothelial cells in culture. *Invest Ophthalmol Vis Sci* 43: 2758-2766.

CASTILLEJO-LOPEZ, C., ARIAS, W.M. and BAUMGARTNER, S. (2004). The fat-like gene of *Drosophila* is the true orthologue of vertebrate fat cadherins and is involved in the formation of tubular organs. *J Biol Chem* 279: 24034-24043.

CHAKRAVARTI, R. and ADAMS, J.C. (2006). Comparative genomics of the syndecans defines an ancestral genomic context associated with matrilins in vertebrates. *BMC Genomics* 7: 83.

CHIQUET-EHRISMANN, R. and CHIQUET, M. (2003). Tenascins: regulation and putative functions during pathological stress. *J Pathol* 200: 488-499.

CHIQUET-EHRISMANN, R., KALLA, P., PEARSON, C.A., BECK, K. and CHIQUET, M. (1988). Tenascin interferes with fibronectin action. *Cell* 53: 383-390.

CHIQUET-EHRISMANN, R., MATSUOKA, Y., HOFER, U., SPRING, J., BERNASCONI, C. and CHIQUET, M. (1991). Tenascin variants: differential binding to fibronectin and distinct distribution in cell cultures and tissues. *Cell Regul* 2: 927-938.

CHIQUET, M. and FAMBROUGH, D.M. (1984). Chick myotendinous antigen. II. A novel extracellular glycoprotein complex consisting of large disulfide-linked subunits. *J Cell Biol* 98: 1937-1946.

CHIQUET, M., VRUCINIC-FILIPI, N., SCHENK, S., BECK, K. and CHIQUET-EHRISMANN, R. (1991). Isolation of chick tenascin variants and fragments. A C-terminal heparin-binding fragment produced by cleavage of the extra domain from the largest subunit splicing variant. *Eur J Biochem* 199: 379-388.

CHUNG, C.Y. and ERICKSON, H.P. (1997). Glycosaminoglycans modulate fibronectin matrix assembly and are essential for matrix incorporation of tenascin-C. *J Cell Sci* 110 (Pt 12): 1413-1419.

CHUNG, C.Y., MURPHY-ULLRICH, J.E. and ERICKSON, H.P. (1996). Mitogenesis, cell migration, and loss of focal adhesions induced by tenascin-C interacting with its cell surface receptor, annexin II. *Mol Biol Cell* 7: 883-892.

CHUNG, C.Y., ZARDI, L. and ERICKSON, H.P. (1995). Binding of tenascin-C to soluble fibronectin and matrix fibrils. *J Biol Chem* 270: 29012-29017.

CIMA, F., PERIN, A., BURIGHEL, P. and BALLARIN, L. (2001). Morpho-functional characterization of haemocytes of the compound ascidian Botrylloides leachi (Tunicata, Ascidiacea). *Acta Zool.* 82: 261-274.

CLINES, G.A., MOHAMMAD, K.S., BAO, Y., STEPHENS, O.W., SUVA, L.J., SHAUGHNESSY, J.D., JR., FOX, J.W., CHIRGWIN, J.M. and GUISE, T.A. (2007). Dickkopf homolog 1 mediates endothelin-1-stimulated new bone formation. *Mol Endocrinol* 21: 486-498.

CSEH, B., FERNANDEZ-SAUZE, S., GRALL, D., SCHAUB, S., DOMA, E. and VAN OBBERGHEN-SCHILLING, E. (2010). Autocrine fibronectin directs matrix assembly and crosstalk between cell-matrix and cell-cell adhesion in vascular endothelial cells. *J Cell Sci* 123: 3989-3999.

CUENI, L.N., HEGYI, I., SHIN, J.W., ALBINGER-HEGYI, A., GRUBER, S., KUNSTFELD, R., MOCH, H. and DETMAR, M. (2010). Tumor lymphangiogenesis and metastasis to lymph nodes induced by cancer cell expression of podoplanin. *Am J Pathol* 177: 1004-1016.

DALLAS, S.L., CHEN, Q. and SIVAKUMAR, P. (2006). Dynamics of assembly and reorganization of extracellular matrix proteins. *Curr Top Dev Biol* 75: 1-24.

DANEN, E.H., AOTA, S., VAN KRAATS, A.A., YAMADA, K.M., RUITER, D.J. and VAN MUIJEN, G.N. (1995). Requirement for the synergy site for cell adhesion to fibronectin depends on the activation state of integrin alpha 5 beta 1. *J Biol Chem* 270: 21612-21618.

DAVIDSON, B. (2007). Ciona intestinalis as a model for cardiac development. *Semin Cell Dev Biol* 18: 16-26.

DE LANGHE, S.P., SALA, F.G., DEL MORAL, P.M., FAIRBANKS, T.J., YAMADA, K.M., WARBURTON, D., BURNS, R.C. and BELLUSCI, S. (2005). Dickkopf-1 (DKK1) reveals that fibronectin is a major target of Wnt signaling in branching morphogenesis of the mouse embryonic lung. *Dev Biol* 277: 316-331.

DE WEVER, O., NGUYEN, Q.D., VAN HOORDE, L., BRACKE, M., BRUYNEEL, E., GESPACH, C. and MAREEL, M. (2004). Tenascin-C and SF/HGF produced by myofibroblasts *in vitro* provide convergent pro-invasive signals to human colon cancer cells through RhoA and Rac. *FASEB J* 18: 1016-1018.

DEGEN, M., BRELLIER, F., KAIN, R., RUIZ, C., TERRACCIANO, L., OREND, G. and CHIQUET-EHRISMANN, R. (2007). Tenascin-W is a novel marker for activated tumor stroma in low-grade human breast cancer and influences cell behavior. *Cancer Res* 67: 9169-9179.

DEGEN, M., BRELLIER, F., SCHENK, S., DRISCOLL, R., ZAMAN, K., STUPP, R., TORNILLO, L., TERRACCIANO, L., CHIQUET-EHRISMANN, R., RUEGG, C. *et al.* (2008). Tenascin-W, a new marker of cancer stroma, is elevated in sera of colon and breast cancer patients. *Int J Cancer* 122: 2454-2461.

DESGROSELLIER, J.S. and CHERESH, D.A. (2010). Integrins in cancer: biological implications and therapeutic opportunities. *Nat Rev Cancer* 10: 9-22.

DOME, B., HENDRIX, M.J., PAKU, S., TOVARI, J. and TIMAR, J. (2007). Alternative vascularization mechanisms in cancer: Pathology and therapeutic implications. *Am J Pathol* 170: 1-15.

DOOLITTLE, R.F. (2009). Step-by-step evolution of vertebrate blood coagulation. *Cold Spring Harb Symp Quant Biol* 74: 35-40.

DRUMEA-MIRANCEA, M., WESSELS, J.T., MULLER, C.A., ESSL, M., EBLE, J.A., TOLOSA, E., KOCH, M., REINHARDT, D.P., SIXT, M., SOROKIN, L. *et al.* (2006). Characterization of a conduit system containing laminin-5 in the human thymus: a potential transport system for small molecules. *J Cell Sci* 119: 1396-1405.

DUECK, M., RIEDL, S., HINZ, U., TANDARA, A., MOLLER, P., HERFARTH, C. and FAISSNER, A. (1999). Detection of tenascin-C isoforms in colorectal mucosa, ulcerative colitis, carcinomas and liver metastases. *Int J Cancer* 82: 477-483.

EBNER, B., BURMESTER, T. and HANKELN, T. (2003). Globin genes are present in Ciona intestinalis. *Mol Biol Evol* 20: 1521-1525.

EGEBLAD, M., NAKASONE, E.S. and WERB, Z. (2010). Tumors as organs: complex tissues that interface with the entire organism. *Dev Cell* 18: 884-901.

EL HALLANI, S., BOISSELIER, B., PEGLION, F., ROUSSEAU, A., COLIN, C., IDBAIH, A., MARIE, Y., MOKHTARI, K., THOMAS, J.L., EICHMANN, A. *et al.*"(2010). A new alternative mechanism in glioblastoma vascularization: tubular vasculogenic mimicry. *Brain* 133: 973-982.

ERLER, J.T. and WEAVER, V.M. (2009). Three-dimensional context regulation of metastasis. *Clin Exp Metastasis* 26: 35-49.

EXPOSITO, J.Y., LARROUX, C., CLUZEL, C., VALCOURT, U., LETHIAS, C. and DEGNAN, B.M. (2008). Demosponge and sea anemone fibrillar collagen di-

versity reveals the early emergence of A/C clades and the maintenance of the modular structure of type V/XI collagens from sponge to human. *J Biol Chem* 283: 28226-28235.

FAISSNER, A., KRUSE, J., CHIQUET-EHRISMANN, R. and MACKIE, E. (1988). The high-molecular-weight J1 glycoproteins are immunochemically related to tenascin. *Differentiation* 37: 104-114.

FASSLER, R., SASAKI, T., TIMPL, R., CHU, M.L. and WERNER, S. (1996). Differential regulation of fibulin, tenascin-C, and nidogen expression during wound healing of normal and glucocorticoid-treated mice. *Exp Cell Res* 222: 111-116.

FFRENCH-CONSTANT, C. and HYNES, R.O. (1989). Alternative splicing of fibronectin is temporally and spatially regulated in the chicken embryo. *Development* 106: 375-388.

FISCHER, D., CHIQUET-EHRISMANN, R., BERNASCONI, C. and CHIQUET, M. (1995). A single heparin binding region within the fibrinogen-like domain is functional in chick tenascin-C. *J Biol Chem* 270: 3378-3384.

FISCHER, J.W. (2007). Tenascin-C: a key molecule in graft stenosis. *Cardiovasc Res* 74: 335-336.

FOGELGREN, B., POLGAR, N., SZAUTER, K.M., UJFALUDI, Z., LACZKO, R., FONG, K.S. and CSISZAR, K. (2005). Cellular fibronectin binds to lysyl oxidase with high affinity and is critical for its proteolytic activation. *J Biol Chem* 280: 24690-24697.

FORSBERG, E., HIRSCH, E., FROHLICH, L., MEYER, M., EKBLOM, P., ASZODI, A., WERNER, S. and FASSLER, R. (1996). Skin wounds and severed nerves heal normally in mice lacking tenascin-C. *Proc Natl Acad Sci USA* 93: 6594-6599.

FRANCIS, S.E., GOH, K.L., HODIVALA-DILKE, K., BADER, B.L., STARK, M., DAVIDSON, D. and HYNES, R.O. (2002). Central roles of alpha5beta1 integrin and fibronectin in vascular development in mouse embryos and embryoid bodies. *Arterioscler Thromb Vasc Biol* 22: 927-933.

FRANCO, C.A., LIEBNER, S. and GERHARDT, H. (2009). Vascular morphogenesis: a Wnt for every vessel? *Curr Opin Genet Dev* 19: 476-483.

GAGGIOLI, C., HOOPER, S., HIDALGO-CARCEDO, C., GROSSE, R., MARSHALL, J.F., HARRINGTON, K. and SAHAI, E. (2007). Fibroblast-led collective invasion of carcinoma cells with differing roles for RhoGTPases in leading and following cells. *Nat Cell Biol* 9: 1392-1400.

GARCION, E., FAISSNER, A. and FFRENCH-CONSTANT, C. (2001). Knockout mice reveal a contribution of the extracellular matrix molecule tenascin-C to neural precursor proliferation and migration. *Development* 128: 2485-2496.

GARMY-SUSINI, B., AVRAAMIDES, C.J., SCHMID, M.C., FOUBERT, P., ELLIES, L.G., BARNES, L., FERAL, C., PAPAYANNOPOULOU, T., LOWY, A., BLAIR, S.L. *et al.* (2010). Integrin alpha4beta1 signaling is required for lymphangiogenesis and tumor metastasis. *Cancer Res* 70: 3042-3051.

GEBOES, K., EL-ZINE, M.Y., DALLE, I., EL-HADDAD, S., RUTGEERTS, P. and VAN EYKEN, P. (2001). Tenascin and strictures in inflammatory bowel disease: an immunohistochemical study. *Int J Surg Pathol* 9: 281-286.

GEORGE, E.L., BALDWIN, H.S. and HYNES, R.O. (1997). Fibronectins are essential for heart and blood vessel morphogenesis but are dispensable for initial specification of precursor cells. *Blood* 90: 3073-3081.

GEORGE, E.L., GEORGES-LABOUESSE, E.N., PATEL-KING, R.S., RAYBURN, H. and HYNES, R.O. (1993). Defects in mesoderm, neural tube and vascular development in mouse embryos lacking fibronectin. *Development* 119: 1079-1091.

GERHARDT, H., GOLDING, M., FRUTTIGER, M., RUHRBERG, C., LUNDKVIST, A., ABRAMSSON, A., JELTSCH, M., MITCHELL, C., ALITALO, K., SHIMA, D. *et al.* (2003). VEGF guides angiogenic sprouting utilizing endothelial tip cell filopodia. *J Cell Biol* 161: 1163-1177.

GINDRE, D., PEYROL, S., RACCURT, M., SOMMER, P., LOIRE, R., GRIMAUD, J.A. and CORDIER, J.F. (1995). Fibrosing vasculitis in Wegener's granulomatosis: ultrastructural and immunohistochemical analysis of the vascular lesions. *Virchows Arch* 427: 385-393.

GRIMSHAW, M.J. (2007). Endothelins and hypoxia-inducible factor in cancer. *Endocr Relat Cancer* 14: 233-244.

GUTTERY, D.S., SHAW, J.A., LLOYD, K., PRINGLE, J.H. and WALKER, R.A. (2010). Expression of tenascin-C and its isoforms in the breast. *Cancer Metastasis Rev* 29: 595-606.

HASHIMOTO-UOSHIMA, M., YAN, Y.Z., SCHNEIDER, G. and AUKHIL, I. (1997). The alternatively spliced domains EIIIB and EIIIA of human fibronectin affect cell adhesion and spreading. *J Cell Sci* 110: 2271-2280.

HAUZENBERGER, D., OLIVIER, P., GUNDERSEN, D. and RUEGG, C. (1999). Tenascin-C inhibits beta1 integrin-dependent T lymphocyte adhesion to fibronectin through the binding of its fnIII 1-5 repeats to fibronectin. *Eur J Immunol* 29: 1435-1447.

HELLEMAN, J., JANSEN, M.P., RUIGROK-RITSTIER, K., VAN STAVEREN, I.L., LOOK, M.P., MEIJER-VAN GELDER, M.E., SIEUWERTS, A.M., KLIJN, J.G., SLEIJFER, S., FOEKENS, J.A. *et al.* (2008). Association of an extracellular matrix gene cluster with breast cancer prognosis and endocrine therapy response. *Clin Cancer Res* 14: 5555-5564.

HENDRIX, M.J., SEFTOR, E.A., HESS, A.R. and SEFTOR, R.E. (2003). Vasculogenic mimicry and tumour-cell plasticity: lessons from melanoma. *Nat Rev Cancer* 3: 411-421.

HILLEN, F. and GRIFFIOEN, A.W. (2007). Tumour vascularization: sprouting angiogenesis and beyond. *Cancer Metastasis Rev* 26: 489-502.

HODIVALA-DILKE, K. (2008). alphavbeta3 integrin and angiogenesis: a moody integrin in a changing environment. *Curr Opin Cell Biol* 20: 514-519.

HUANG, G., XIE, X., HAN, Y., FAN, L., CHEN, J., MOU, C., GUO, L., LIU, H., ZHANG, Q., CHEN, S. *et al.* (2007). The identification of lymphocyte-like cells and lymphoid-related genes in amphioxus indicates the twilight for the emergence of adaptive immune system. *PLoS One* 2: e206.

HUANG, G., ZHANG, Y., KIM, B., GE, G., ANNIS, D.S., MOSHER, D.F. and GREENSPAN, D.S. (2009). Fibronectin binds and enhances the activity of bone morphogenetic protein 1. *J Biol Chem* 284: 25879-25888.

HUANG, W., CHIQUET-EHRISMANN, R., MOYANO, J.V., GARCIA-PARDO, A. and OREND, G. (2001). Interference of tenascin-C with syndecan-4 binding to fibronectin blocks cell adhesion and stimulates tumor cell proliferation. *Cancer Res* 61: 8586-8594.

HUANG, X.Z., WU, J.F., FERRANDO, R., LEE, J.H., WANG, Y.L., FARESE, R.V., JR. and SHEPPARD, D. (2000). Fatal bilateral chylothorax in mice lacking the integrin alpha9beta1. *Mol Cell Biol* 20: 5208-5215.

HUIJBERS, E.J., RINGVALL, M., FEMEL, J., KALAMAJSKI, S., LUKINIUS, A., ABRINK, M., HELLMAN, L. and OLSSON, A.K. (2010). Vaccination against the extra domain-B of fibronectin as a novel tumor therapy. *FASEB J.* 24: 4535-4544

HUMPHRIES, J.D., BYRON, A. and HUMPHRIES, M.J. (2006). Integrin ligands at a glance. *J Cell Sci* 119: 3901-3903.

HUVENEERS, S., TRUONG, H., FASSLER, R., SONNENBERG, A. and DANEN, E.H. (2008). Binding of soluble fibronectin to integrin alpha5 beta1 - link to focal adhesion redistribution and contractile shape. *J Cell Sci* 121: 2452-2462.

HYNES, R.O. (2007). Cell-matrix adhesion in vascular development. *J Thromb Haemost* 5 Suppl 1: 32-40.

HYNES, R.O. (2009). The extracellular matrix: not just pretty fibrils. *Science* 326: 1216-1219.

INGBER, D.E. (2002). Mechanical signaling and the cellular response to extracellular matrix in angiogenesis and cardiovascular physiology. *Circ Res* 91: 877-887.

INGHAM, K.C., BREW, S.A. and ERICKSON, H.P. (2004). Localization of a cryptic binding site for tenascin on fibronectin. *J Biol Chem* 279: 28132-28135.

JALLO, G.I., FRIEDLANDER, D.R., KELLY, P.J., WISOFF, J.H., GRUMET, M. and ZAGZAG, D. (1997). Tenascin-C expression in the cyst wall and fluid of human brain tumors correlates with angiogenesis. *Neurosurgery* 41: 1052-1059.

JIANG, B., LIOU, G.I., BEHZADIAN, M.A. and CALDWELL, R.B. (1994). Astrocytes modulate retinal vasculogenesis: effects on fibronectin expression. *J Cell Sci* 107: 2499-2508.

KAARIAINEN, E., NUMMELA, P., SOIKKELI, J., YIN, M., LUKK, M., JAHKOLA, T., VIROLAINEN, S., ORA, A., UKKONEN, E., SAKSELA, O. *et al.* (2006). Switch to an invasive growth phase in melanoma is associated with tenascin-C, fibronectin, and procollagen-I forming specific channel structures for invasion. *J Pathol* 210: 181-191.

KASPAR, M., ZARDI, L. and NERI, D. (2006). Fibronectin as target for tumor therapy. *Int J Cancer* 118: 1331-1339.

KAWASHIMA, T., KAWASHIMA, S., TANAKA, C., MURAI, M., YONEDA, M., PUTNAM, N.H., ROKHSAR, D.S., KANEHISA, M., SATOH, N. and WADA, H. (2009). Domain shuffling and the evolution of vertebrates. *Genome Res* 19: 1393-1403.

KII, I., NISHIYAMA, T., LI, M., MATSUMOTO, K., SAITO, M., AMIZUKA, N. and KUDO, A. (2010). Incorporation of tenascin-C into the extracellular matrix by periostin underlies an extracellular meshwork architecture. *J Biol Chem* 285: 2028-2039.

KINSELLA, M.G., FISCHER, J.W., MASON, D.P. and WIGHT, T.N. (2000). Retrovirally

mediated expression of decorin by macrovascular endothelial cells. Effects on cellular migration and fibronectin fibrillogenesis *in vitro*. *J Biol Chem* 275: 13924-13932.

KOHAN, M., MURO, A.F., WHITE, E.S. and BERKMAN, N. (2010). EDA-containing cellular fibronectin induces fibroblast differentiation through binding to {alpha}4{beta}7 integrin receptor and MAPK/Erk 1/2-dependent signaling. *FASEB J* 24:4503-4512.

KUCERA, T. and LAMMERT, E. (2009). Ancestral vascular tube formation and its adoption by tumors. *Biol Chem* 390: 985-994.

KUCERA, T., STRILIC, B., REGENER, K., SCHUBERT, M., LAUDET, V. and LAMMERT, E. (2009). Ancestral vascular lumen formation via basal cell surfaces. *PLoS ONE* 4: e4132.

LANGE, K., KAMMERER, M., HEGI, M.E., GROTEGUT, S., DITTMANN, A., HUANG, W., FLURI, E., YIP, G.W., GOTTE, M., RUIZ, C. *et al.* (2007). Endothelin receptor type B counteracts tenascin-C-induced endothelin receptor type A-dependent focal adhesion and actin stress fiber disorganization. *Cancer Res* 67: 6163-6173.

LANGE, K., KAMMERER, M., SAUPE, F., HEGI, M.E., GROTEGUT, S., FLURI, E. and OREND, G. (2008). Combined lysophosphatidic acid/platelet-derived growth factor signaling triggers glioma cell migration in a tenascin-C microenvironment. *Cancer Res* 68: 6942-6952.

LATIJNHOUWERS, M.A., BERGERS, M., VAN BERGEN, B.H., SPRUIJT, K.I., ANDRIESSEN, M.P. and SCHALKWIJK, J. (1996). Tenascin expression during wound healing in human skin. *J Pathol* 178: 30-35.

LEGATE, K.R., MONTANEZ, E., KUDLACEK, O. and FASSLER, R. (2006). ILK, PINCH and parvin: the tIPP of integrin signalling. *Nat Rev Mol Cell Biol* 7: 20-31.

LEISS, M., BECKMANN, K., GIROS, A., COSTELL, M. and FASSLER, R. (2008). The role of integrin binding sites in fibronectin matrix assembly *in vivo*. *Curr Opin Cell Biol* 20: 502-507.

LIAO, Y.F., GOTWALS, P.J., KOTELIANSKY, V.E., SHEPPARD, D. and VAN DE WATER, L. (2002). The EIIIA segment of fibronectin is a ligand for integrins alpha 9beta 1 and alpha 4beta 1 providing a novel mechanism for regulating cell adhesion by alternative splicing. *J Biol Chem* 277: 14467-14474.

LIGHTNER, V.A. and ERICKSON, H.P. (1990). Binding of hexabrachion (tenascin) to the extracellular matrix and substratum and its effect on cell adhesion. *J Cell Sci* 95: 263-277.

LINDER, E., VAHERI, A., RUOSLAHTI, E. and WARTIOVAARA, J. (1975). Distribution of fibroblast surface antigen in the developing chick embryo. *J Exp Med* 142: 41-9.

LOKMIC, Z., LAMMERMANN, T., SIXT, M., CARDELL, S., HALLMANN, R. and SOROKIN, L. (2008). The extracellular matrix of the spleen as a potential organizer of immune cell compartments. *Semin Immunol* 20: 4-13.

MACKIE, E.J. (1997). Molecules in focus: tenascin-C. *Int J Biochem Cell Biol* 29: 1133-1137.

MACKIE, E.J., HALFTER, W. and LIVERANI, D. (1988). Induction of tenascin in healing wounds. *J Cell Biol* 107: 2757-2767.

MANTOVANI, A., ROMERO, P., PALUCKA, A.K. and MARINCOLA, F.M. (2008). Tumour immunity: effector response to tumour and role of the microenvironment. *Lancet* 371: 771-783.

MAO, Y. and SCHWARZBAUER, J.E. (2005). Fibronectin fibrillogenesis, a cell-mediated matrix assembly process. *Matrix Biol* 24: 389-399.

MARTINO, M.M. and HUBBELL, J.A. (2010). The 12th-14th type III repeats of fibronectin function as a highly promiscuous growth factor-binding domain. *FASEB J* 24:4711-4721.

MIDWOOD, K.S., MAO, Y., HSIA, H.C., VALENICK, L.V. and SCHWARZBAUER, J.E. (2006). Modulation of cell-fibronectin matrix interactions during tissue repair. *J Investig Dermatol Symp Proc* 11: 73-78.

MIDWOOD, K.S. and OREND, G. (2009). The role of tenascin-C in tissue injury and tumorigenesis. *J Cell Commun Signal* 3: 287-310.

MIDWOOD, K.S. and SCHWARZBAUER, J.E. (2002). Tenascin-C modulates matrix contraction via focal adhesion kinase- and Rho-mediated signaling pathways. *Mol Biol Cell* 13: 3601-3613.

MIDWOOD, K.S., VALENICK, L.V., HSIA, H.C. and SCHWARZBAUER, J.E. (2004a). Coregulation of fibronectin signaling and matrix contraction by tenascin-C and syndecan-4. *Mol Biol Cell* 15: 5670-5677.

MIDWOOD, K.S., WILLIAMS, L.V. and SCHWARZBAUER, J.E. (2004b). Tissue repair and the dynamics of the extracellular matrix. *Int J Biochem Cell Biol* 36: 1031-1037.

MINN, A.J., GUPTA, G.P., SIEGEL, P.M., BOS, P.D., SHU, W., GIRI, D.D., VIALE, A., OLSHEN, A.B., GERALD, W.L. and MASSAGUE, J. (2005). Genes that mediate breast cancer metastasis to lung. *Nature* 436: 518-524.

MITROVIC, N. and SCHACHNER, M. (1995). Detection of tenascin-C in the nervous system of the tenascin-C mutant mouse. *J Neurosci Res* 42: 710-717.

MIYAMOTO, S., TERAMOTO, H., GUTKIND, J.S. and YAMADA, K.M. (1996). Integrins can collaborate with growth factors for phosphorylation of receptor tyrosine kinases and MAP kinase activation: roles of integrin aggregation and occupancy of receptors. *J Cell Biol* 135: 1633-1642.

MOSHER, D.F., SCHAD, P.E. and VANN, J.M. (1980). Cross-linking of collagen and fibronectin by factor XIIIa. Localization of participating glutaminyl residues to a tryptic fragment of fibronectin. *J Biol Chem* 255: 1181-1188.

MURPHY-ULLRICH, J.E., LIGHTNER, V.A., AUKHIL, I., YAN, Y.Z., ERICKSON, H.P. and HOOK, M. (1991). Focal adhesion integrity is downregulated by the alternatively spliced domain of human tenascin. *J Cell Biol* 115: 1127-1136.

NERI, D. and BICKNELL, R. (2005). Tumour vascular targeting. *Nat Rev Cancer* 5: 436-446.

NGUYEN, A., THORIN-TRESCASES, N. and THORIN, E. (2010). Working under pressure: coronary arteries and the endothelin system. *Am J Physiol Regul Integr Comp Physiol* 298: R1188-1194.

OREND, G. (2005). Potential oncogenic action of tenascin-C in tumorigenesis. *Int J Biochem Cell Biol* 37: 1066-1083.

OREND, G. and CHIQUET-EHRISMANN, R. (2006). Tenascin-C induced signaling in cancer. *Cancer Lett* 244: 143-163.

OREND, G., HUANG, W., OLAYIOYE, M.A., HYNES, N.E. and CHIQUET-EHRISMANN, R. (2003). Tenascin-C blocks cell-cycle progression of anchorage-dependent fibroblasts on fibronectin through inhibition of syndecan-4. *Oncogene* 22: 3917-3926.

PAEZ-RIBES, M., ALLEN, E., HUDOCK, J., TAKEDA, T., OKUYAMA, H., VINALS, F., INOUE, M., BERGERS, G., HANAHAN, D. and CASANOVAS, O. (2009). Antiangiogenic therapy elicits malignant progression of tumors to increased local invasion and distant metastasis. *Cancer Cell* 15: 220-231.

PAIK, D.C., FU, C., BHATTACHARYA, J. and TILSON, M.D. (2004). Ongoing angiogenesis in blood vessels of the abdominal aortic aneurysm. *Exp Mol Med* 36: 524-533.

PANKOV, R. and YAMADA, K.M. (2002). Fibronectin at a glance. *J Cell Sci* 115: 3861-3863.

PAULIS, Y.W., SOETEKOUW, P.M., VERHEUL, H.M., TJAN-HEIJNEN, V.C. and GRIFFIOEN, A.W. (2010). Signalling pathways in vasculogenic mimicry. *Biochim Biophys Acta* 1806: 18-28.

PEDRETTI, M., RANCIC, Z., SOLTERMANN, A., HERZOG, B.A., SCHLIEMANN, C., LACHAT, M., NERI, D. and KAUFMANN, P.A. (2010). Comparative immunohistochemical staining of atherosclerotic plaques using F16, F8 and L19: Three clinical-grade fully human antibodies. *Atherosclerosis* 208: 382-389.

PEDRETTI, M., SOLTERMANN, A., ARNI, S., WEDER, W., NERI, D. and HILLINGER, S. (2009). Comparative immunohistochemistry of L19 and F16 in non-small cell lung cancer and mesothelioma: two human antibodies investigated in clinical trials in patients with cancer. *Lung Cancer* 64: 28-33.

PETERS, J.H., CHEN, G.E. and HYNES, R.O. (1996). Fibronectin isoform distribution in the mouse. II. Differential distribution of the alternatively spliced EIIIB, EIIIA, and V segments in the adult mouse. *Cell Adhes Commun* 4: 127-148.

PETERS, J.H. and HYNES, R.O. (1996). Fibronectin isoform distribution in the mouse. I. The alternatively spliced EIIIB, EIIIA, and V segments show widespread codistribution in the developing mouse embryo. *Cell Adhes Commun* 4: 103-125.

POLLARD, J.W. (2008). Macrophages define the invasive microenvironment in breast cancer. *J Leukoc Biol* 84: 623-630.

PUENTE NAVAZO, M.D., VALMORI, D. and RUEGG, C. (2001). The alternatively spliced domain TnFnIII A1A2 of the extracellular matrix protein tenascin-C suppresses activation-induced T lymphocyte proliferation and cytokine production. *J Immunol* 167: 6431-6440.

PUTNAM, N.H., BUTTS, T., FERRIER, D.E., FURLONG, R.F., HELLSTEN, U., KAWASHIMA, T., ROBINSON-RECHAVI, M., SHOGUCHI, E., TERRY, A., YU, J.K. *et al.* (2008). The amphioxus genome and the evolution of the chordate karyotype. *Nature* 453: 1064-1071.

RAMOS, D.M., CHEN, B., REGEZI, J., ZARDI, L. and PYTELA, R. (1998). Tenascin-C matrix assembly in oral squamous cell carcinoma. *Int J Cancer* 75: 680-687.

RICHARDS, G.S. and DEGNAN, B.M. (2009). The dawn of developmental signaling in the metazoa. *Cold Spring Harb Symp Quant Biol* 74: 81-90.

RIEDL, S., TANDARA, A., REINSHAGEN, M., HINZ, U., FAISSNER, A., BODEN-

MULLER, H., BUHR, H.J., HERFARTH, C. and MOLLER, P. (2001). Serum tenascin-C is an indicator of inflammatory bowel disease activity. *Int J Colorectal Dis* 16: 285-291.

RINKEVICH, Y., ROSNER, A., RABINOWITZ, C., LAPIDOT, Z., MOISEEVA, E. and RINKEVICH, B. (2010). Piwi positive cells that line the vasculature epithelium, underlie whole body regeneration in a basal chordate. *Dev Biol* 345: 94-104.

RIOU, J.F., SHI, D.L., CHIQUET, M. and BOUCAUT, J.C. (1990). Exogenous tenascin inhibits mesodermal cell migration during amphibian gastrulation. *Dev Biol* 137: 305-317.

RISAU, W. (1997). Mechanisms of angiogenesis. *Nature* 386: 671-674.

ROSANO, L., CIANFROCCA, R., MASI, S., SPINELLA, F., DI CASTRO, V., BIROCCIO, A., SALVATI, E., NICOTRA, M.R., NATALI, P.G. and BAGNATO, A. (2009). Beta-arrestin links endothelin A receptor to beta-catenin signaling to induce ovarian cancer cell invasion and metastasis. *Proc Natl Acad Sci USA* 106: 2806-2811.

ROSANO, L., VARMI, M., SALANI, D., DI CASTRO, V., SPINELLA, F., NATALI, P.G. and BAGNATO, A. (2001). Endothelin-1 induces tumor proteinase activation and invasiveness of ovarian carcinoma cells. *Cancer Res* 61: 8340-8346.

ROTH-KLEINER, M., HIRSCH, E. and SCHITTNY, J.C. (2004). Fetal lungs of tenascin-C-deficient mice grow well, but branch poorly in organ culture. *Am J Respir Cell Mol Biol* 30: 360-366.

ROY, S., CAGLIERO, E. and LORENZI, M. (1996). Fibronectin overexpression in retinal microvessels of patients with diabetes. *Invest Ophthalmol Vis Sci* 37: 258-266.

RUIZ, C., HUANG, W., HEGI, M.E., LANGE, K., HAMOU, M.F., FLURI, E., OAKELEY, E.J., CHIQUET-EHRISMANN, R. and OREND, G. (2004). Growth promoting signaling by tenascin-C [corrected]. *Cancer Res* 64: 7377-7385.

RUPERT, E.E. and CARLE, K.J. (1983). Morphology of metazoan circulatory systems. *Zoomorphology* 103: 193-208.

SAGA, Y., YAGI, T., IKAWA, Y., SAKAKURA, T. and AIZAWA, S. (1992). Mice develop normally without tenascin. *Genes Dev* 6: 1821-1831.

SCHENK, S., CHIQUET-EHRISMANN, R. and BATTEGAY, E.J. (1999). The fibrinogen globe of tenascin-C promotes basic fibroblast growth factor-induced endothelial cell elongation. *Mol Biol Cell* 10: 2933-2943.

SCHLIEMANN, C. and NERI, D. (2010). Antibody-based vascular tumor targeting. *Recent Results Cancer Res* 180: 201-216.

SEBE-PEDROS, A., ROGER, A.J., LANG, F.B., KING, N. and RUIZ-TRILLO, I. (2010). Ancient origin of the integrin-mediated adhesion and signaling machinery. *Proc Natl Acad Sci USA* 107: 10142-10147.

SHIELDS, J.D., KOURTIS, I.C., TOMEI, A.A., ROBERTS, J.M. and SWARTZ, M.A. (2010). Induction of lymphoidlike stroma and immune escape by tumors that express the chemokine CCL21. *Science* 328: 749-752.

SINGH, P., CARRAHER, C. and SCHWARZBAUER, J.E. (2010). Assembly of Fibronectin Extracellular Matrix. *Annu Rev Cell Dev Biol* 26: 397-419.

SIRI, A., KNAUPER, V., VEIRANA, N., CAOCCI, F., MURPHY, G. and ZARDI, L. (1995). Different susceptibility of small and large human tenascin-C isoforms to degradation by matrix metalloproteinases. *J Biol Chem* 270: 8650-8654.

SOBOCINSKI, G.P., TOY, K., BOBROWSKI, W.F., SHAW, S., ANDERSON, A.O. and KALDJIAN, E.P. (2010). Ultrastructural localization of extracellular matrix proteins of the lymph node cortex: evidence supporting the reticular network as a pathway for lymphocyte migration. *BMC Immunol* 11: 42.

STANCHI, F., GRASHOFF, C., NGUEMENI YONGA, C.F., GRALL, D., FASSLER, R. and VAN OBBERGHEN-SCHILLING, E. (2009). Molecular dissection of the ILK-PINCH-parvin triad reveals a fundamental role for the ILK kinase domain in the late stages of focal-adhesion maturation. *J Cell Sci* 122: 1800-1811.

STOCKMANN, C., DOEDENS, A., WEIDEMANN, A., ZHANG, N., TAKEDA, N., GREENBERG, J.I., CHERESH, D.A. and JOHNSON, R.S. (2008). Deletion of vascular endothelial growth factor in myeloid cells accelerates tumorigenesis. *Nature* 456: 814-818.

TAKAHASHI, S., LEISS, M., MOSER, M., OHASHI, T., KITAO, T., HECKMANN, D., PFEIFER, A., KESSLER, H., TAKAGI, J., ERICKSON, H.P. *et al.* (2007). The RGD motif in fibronectin is essential for development but dispensable for fibril assembly. *J Cell Biol* 178: 167-178.

TALTS, J.F., WIRL, G., DICTOR, M., MULLER, W.J. and FASSLER, R. (1999). Tenascin-C modulates tumor stroma and monocyte/macrophage recruitment but not tumor growth or metastasis in a mouse strain with spontaneous mammary cancer. *J Cell Sci* 112: 1855-1864.

TANAKA, K., HIRAIWA, N., HASHIMOTO, H., YAMAZAKI, Y. and KUSAKABE, M. (2004). Tenascin-C regulates angiogenesis in tumor through the regulation of vascular endothelial growth factor expression. *Int J Cancer* 108: 31-40.

TARASEVICIUTE, A., VINCENT, B.T., SCHEDIN, P. and JONES, P.L. Quantitative analysis of three-dimensional human mammary epithelial tissue architecture reveals a role for tenascin-C in regulating c-met function. *Am J Pathol* 176: 827-38.

TO, W.S. and MIDWOOD, K.S. (2010). Cryptic domains of tenascin-C differentially control fibronectin fibrillogenesis. *Matrix Biol* 29: 573-585.

TUCKER, R.P. (1993). The *in situ* localization of tenascin splice variants and thrombospondin 2 mRNA in the avian embryo. *Development* 117: 347-358.

TUCKER, R.P. and CHIQUET-EHRISMANN, R. (2009). Evidence for the evolution of tenascin and fibronectin early in the chordate lineage. *Int J Biochem Cell Biol* 41: 424-434.

TUCKER, R.P., DRABIKOWSKI, K., HESS, J.F., FERRALLI, J., CHIQUET-EHRISMANN, R. and ADAMS, J.C. (2006). Phylogenetic analysis of the tenascin gene family: evidence of origin early in the chordate lineage. *BMC Evol Biol* 6: 60.

UEMURA, A., KUSUHARA, S., WIEGAND, S.J., YU, R.T. and NISHIKAWA, S. (2006). Tlx acts as a proangiogenic switch by regulating extracellular assembly of fibronectin matrices in retinal astrocytes. *J Clin Invest* 116: 369-377.

VENTURA, E., SASSI, F., PARODI, A., BALZA, E., BORSI, L., CASTELLANI, P., CARNEMOLLA, B. and ZARDI, L. (2010). Alternative splicing of the angiogenesis associated extra-domain B of fibronectin regulates the accessibility of the B-C loop of the type III repeat 8. *PLoS One* 5: e9145.

VOSSELER, S., MIRANCEA, N., BOHLEN, P., MUELLER, M.M. and FUSENIG, N.E. (2005). Angiogenesis inhibition by vascular endothelial growth factor receptor-2 blockade reduces stromal matrix metalloproteinase expression, normalizes stromal tissue, and reverts epithelial tumor phenotype in surface heterotransplants. *Cancer Res* 65: 1294-1305.

VOURET-CRAVIARI, V., BOULTER, E., GRALL, D., MATTHEWS, C. and VAN OBBERGHEN-SCHILLING, E. (2004). ILK is required for the assembly of matrix-forming adhesions and capillary morphogenesis in endothelial cells. *J Cell Sci* 117: 4559-4569.

WHITE, E.S., BARALLE, F.E. and MURO, A.F. (2008). New insights into form and function of fibronectin splice variants. *J Pathol* 216: 1-14.

WICKI, A., LEHEMBRE, F., WICK, N., HANTUSCH, B., KERJASCHKI, D. and CHRISTOFORI, G. (2006). Tumor invasion in the absence of epithelial-mesenchymal transition: podoplanin-mediated remodeling of the actin cytoskeleton. *Cancer Cell* 9: 261-272.

WILSON, K.E., BARTLETT, J.M., MILLER, E.P., SMYTH, J.F., MULLEN, P., MILLER, W.R. and LANGDON, S.P. (1999). Regulation and function of the extracellular matrix protein tenascin-C in ovarian cancer cell lines. *Br J Cancer* 80: 685-692.

WILSON, K.E., LANGDON, S.P., LESSELLS, A.M. and MILLER, W.R. (1996). Expression of the extracellular matrix protein tenascin in malignant and benign ovarian tumours. *Br J Cancer* 74: 999-1004.

YANG, J.T., RAYBURN, H. and HYNES, R.O. (1993). Embryonic mesodermal defects in alpha 5 integrin-deficient mice. *Development* 119: 1093-1105.

YOKOSAKI, Y., MATSUURA, N., HIGASHIYAMA, S., MURAKAMI, I., OBARA, M., YAMAKIDO, M., SHIGETO, N., CHEN, J. and SHEPPARD, D. (1998). Identification of the ligand binding site for the integrin alpha9 beta1 in the third fibronectin type III repeat of tenascin-C. *J Biol Chem* 273: 11423-11428.

Annex3:
« OpenLAB »: A 2h PCR- based practical for high school students

BIOCHEMISTRY AND MOLECULAR BIOLOGY EDUCATION
Vol. 38, No. 5, pp. 296–302, 2010

Laboratory Exercises

"OpenLAB": A 2-Hour PCR-Based Practical for High School Students

Received for publication, February 7, 2010, and in revised form, March 18, 2010

Caroline Bouakaze†‡§, Judith Eschbach†‡§, Elise Fouquerel†‡¶, Isabelle Gasser†‡‖, Emmanuelle Kieffer†‡‡‡, Sophie Krieger†‡§§, Sara Milosevic†‡‡‡, Thoueiba Saandi†‡‖, Catherine Florentz#‡¶¶, Laurence Maréchal-Drouard#‡‖‖, and Michel Labouesse#‡‡‡

From the ‡Ecole Doctorale des Sciences de la Vie et de la Santé (ED414), Université de Strasbourg, 12 rue de l'Université, F-67000 Strasbourg, §Faculté de Médecine, 11 rue Humann, F-67000 STRASBOURG, ¶ESBS, IGL-UMR 7175, Boulevard Sébastien Brant, F-67400 Illkirch, ‖Unité 682 INSERM, 3 avenue Molière, F-67200 Strasbourg, ‡‡IGBMC, 1 rue Laurent Fries, BP10142, F-67400 Illkirch, §§U748 INSERM, Institut de Virologie, 3 rue Koeberlé, F-67000 Strasbourg, ¶¶IBMC, UPR 9022 CNRS, 15 rue R. Descartes, F-67000 Strasbourg, ‖‖IBMP, UPR 2357 CNRS, 12 rue du général Zimmer, F-67000 Strasbourg

The Strasbourg University PhD school in Life and Health Sciences launched an initiative called "OpenLAB." This project was developed in an effort to help high school teenagers understand theoretical and abstract concepts in genetics. A second objective of this program is to help students in defining their future orientation and to attract them to biology. The general idea is a 2-hour PCR-based practical that is developed around a fictitious criminal investigation. The practical is taught by PhD graduate students who bring all the required reagents and modern equipment into the classroom. Running the PCR provides free time dedicated to discussions with students about their future plans after the high school diploma. A specific website and a powerpoint presentation were developed to provide appropriate scientific information. Starting on a modest scale in Strasbourg in December 2008, "OpenLAB" was rapidly and well received all around, visiting 53 classes spread over a 200 km area in Alsace until May 2009. It permitted interactions with almost one thousand students in their last year of high school, with the prospect to visit 20% more classes this school year. Our experience, along with feedback from students and their teachers, suggests that it is possible to reach out to many students and have a strong impact with a rather limited budget.

Keywords: hands-on experiments, in-school learning, molecular biology education, PCR, genetics.

Although research careers were once very attractive in Europe, they have become less so in several countries, including France, particularly in Biology. Multiple reasons might explain this partial disaffection. Scientific careers are less prestigious, less glamorous, and offer lower salaries than jobs in finance and business. Science has become very specialized, and young people often fail to see the broader picture. Hence, only a few students are attracted to the rare aspects of biology that they do hear about in the news. Finally, recent affairs have perhaps made Biology slightly frightening, such as when the general public hears about mad cow, tainted blood [1], Genetically Modified Organisms (GMO; see debate at http://www.gmo-safety.eu/en/debate/) and stem cells [2].

In parallel to those general concerns, teaching molecular concepts in Genetics and Biology is challenging, because DNA and proteins are invisible entities that can thus remain abstract notions. Helping those teenagers who dislike abstractness understand what DNA actually is and how genes and characteristics can be transmitted is important to raise general awareness in biology among the population. Indeed, teenagers will become adults, and it might help them in their life, as they may face (directly or through their relatives) issues related to DNA (for instance genetic counseling, cancer diagnosis [3, 4]) or it might help them grasp the complexity of news concerning hot issues such as GMO. Last, because modern biology has made huge and rapid progress during the last decades, even teachers have a hard time keeping up with new concepts, which, as a result, are often rapidly skimmed over during high school courses. A strategy often useful to help understand abstract notions is to practice "hands-on" experiments. Its power has been demonstrated by the French physicists Georges Charpak,

†The first eight authors contributed equally to this work.

*This work is supported by - Région Alsace, Université de Strasbourg, local CNRS Administration, IBMP, IGBMC, Comités départementaux du Haut-Rhin et du Bas-Rhin de la Ligue Nationale contre le Cancer, Company Roche Diagnostics, Company Dominique Dutscher, Company FranceSystèmes.

To whom correspondence should be addressed. E-mail: c.florentz@unistra.fr, laurence.drouard@ibmp-cnrs.unistra.fr, lmichel@igbmc.fr

Pierre Léna and Yves Quéré, with their project "La Main à la Pâte" (http://www.lamap.fr/) for teaching science to children under 10. However, demonstrating that DNA or proteins can be visualized requires specific equipment, often beyond the reach of high school budgets.

With these issues in mind, the Strasbourg PhD School in Life and Health Sciences decided to launch an initiative that might: (i) help teenagers understand the concept of DNA and heredity; (ii) modify the perhaps negative view of research in biology; (iii) show that science can be fun; (iv) provide information about careers in biology and the many job opportunities in this area.

Below, we describe the strategy used for that initiative, exploring both its organizational and practical aspects.

MATERIALS AND METHODS

DNA Preparation

For technical and ethical reasons, the DNA samples provided to the students was not of human origin. Although we did not openly inform the classroom of the true nature of the DNA used, we clearly mentioned during the presentation that DNA-based forensic police investigations rely on noncoding DNA, which frequently prompted questions about the real origin of the DNA. We always provided details when asked such a question by teachers and students. They correspond to two mouse β-actin cDNA fragments of 155 bp and 298 bp, respectively, which were amplified by RT-PCR from mouse embryonic stem cells and cloned with a TOPO TA Cloning® Kit into the pCR®2.1-TOPO® vector (Invitrogen) according to the manufacturer's recommendations, using the primers 5′-GACGGCCAGGTCATCACTAT-3′ (forward primer) and 5′-CCACCGATCCACACAGAGTA-3′ (1st reverse primer for the 298 bp cDNA clone) or 5′-GGCATAGAGGTCTTTACGGA-3′ (2nd reverse primer for the 155 bp cDNA clone). Plasmids are available upon request.

PCR Amplification

Students were paired together and each pair received six 1.5-mL microtubes containing the different solutions necessary for running the PCR:

- Two tubes containing 10 μL of forward (5′-GAGCTCGGATCCACTAGTAA-3′) and reverse (5′- GTGTGATGGATATCTGCAGAA-3′) primers at 10 μM. The complementary sequence of these two primers flank the insert on the pCR®2.1-TOPO® vector.
- One tube containing 80 μL PCR mix (1× Taq polymerase buffer (Roche)/0.2 mM of each desoxyribonucleotide (Promega) / 1.5 mM $MgCl_2$).
- One tube with 10 μL water (used as negative control).Two tubes annotated "victim," "suspect 1" or "suspect 2" containing 2 ng/μL of plasmids.

The classroom was divided in two halves, each of which received a different "DNA sample from a suspect's car". The tubes "victim" and "suspect 1" contained plasmids with the 155 bp cDNA clone corresponding to the "deleted gene fragment", whereas the tube "suspect 2" contained plasmid with the 298 bp cDNA clone corresponding to "the gene fragment of a non-diseased person." After adding 2 μL of each primer and 1 μL of Taq DNA Polymerase to the PCR mix tube, each team of students divided the mixture in three 0.2 mL PCR microtubes (24 μL per tube). In the first one, they added 1 μL of "victim DNA"; in the second, 1 μL of DNA from "suspect 1" or DNA from "suspect 2"; in the third, 1 μL of water. PCR was performed in a thermocycler (Applied Biosystems) with conditions set at 96°C for 15 seconds followed by 25 cycles of 94°C for 3 seconds, 56°C for 3 seconds and 72°C for 5 seconds. Based on the positions of the primers used for PCR, the expected sizes of the PCR products are 236 bp and 379 bp for suspect 1 and suspect 2, respectively (Fig. 1).

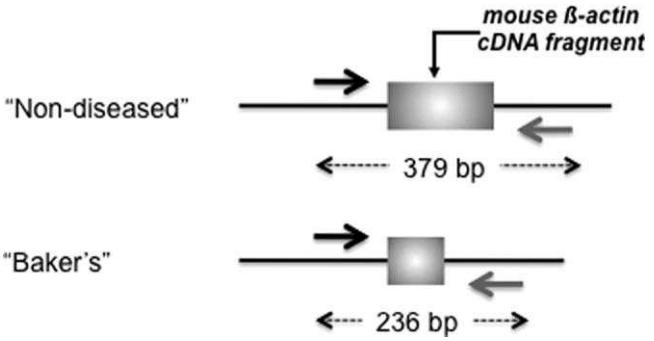

FIG. 1. **Structure of the plasmid used as a template for PCR.** Two fragments of mouse β-actin cDNA were cloned in the pCRII®TOPO® vector. Their PCR amplification with a unique set of primers (arrows) generated fragments of 379 bp and 236 bp, which were considered as representative of "non-diseased" and "baker's," respectively.

Gel Electrophoresis

Three microliters of loading buffer 6× (Fermentas, France) was added to each PCR product and 12 μL of each mixture ("victim"/"suspect 1 or 2"/"negative control") were subjected to electrophoresis on a 1.5% agarose gel containing SYBR-Green dye (1:10,000-fold dilution of the stock solution; Invitrogen). To estimate the size of the DNA fragments, a DNA ladder (Fermentas, France) was run in parallel. Electrophoresis was performed at 100 V in 0.5× TAE buffer. A minigel electrophoretic system was used (RunOne electrophoresis system, Embi Tec) and a short time of migration (about 15 minutes) was sufficient. The agarose gel was rapidly cooled down by a 2–3 minutes immersion in water. The DNA fragments were then visualized under a Dark Reader transilluminator (Clare Chemical Research). The advantage of this transilluminator is that it emits in visible blue light, and therefore does not raise the typical safety issues encountered with traditional UV transilluminators. An amber screen that fits over the glass surface and the agarose gel permits visualization of fluorescent light through DNA fragments in the dark. Results of the electrophoresis were captured with a standard commercial digital camera, or in some instances with the camera device present in students' cell phones.

Companion Website

A specific website (http://www-ed-sdvs.u-strasbg.fr/openlab/accueil/index.php) was designed, which provides information about genes, the flow of information from DNA to protein, and heredity. It also features a glossary of technical terms, useful links to other websites. Pictures of the practical are also available. Registration and evaluation forms can be downloaded and teachers can obtain further information via email (contact-openlab@unistra.fr).

Miscellaneous

A powerpoint presentation was prepared to help introduce the practical as well as understand the different scientific notions. This slideshow also provides explanations on the use of micropipettes (P-20 and P-200). As most students have never used such material before, explanations were important to ensure accurate pipetting of small volumes during the practical.

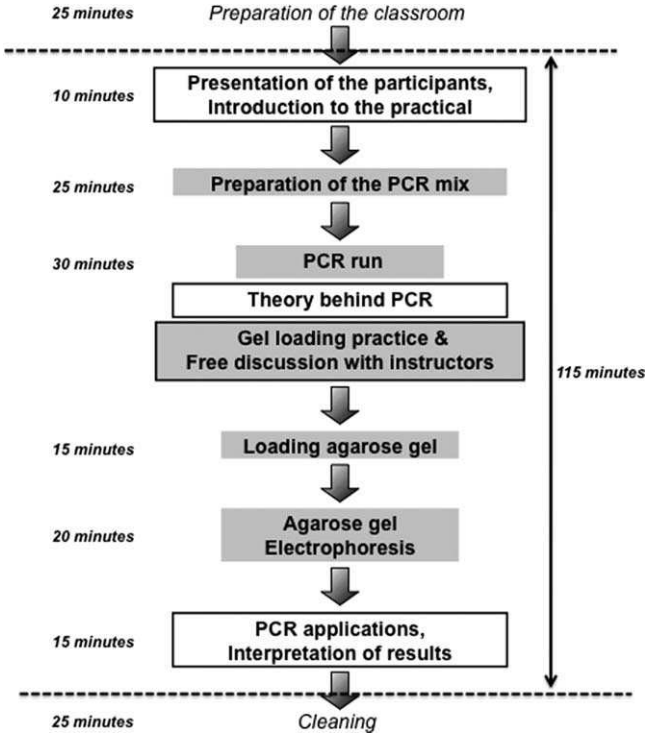

FIG. 2. **Description of the 2-hour OpenLAB session.** Schedule of a typical OpenLAB session. White boxes, steps run by OpenLAB instructors; grey boxes, steps performed by high school students. As the PCR runs, instructors provide background information about the PCR, then teach students how to load a gel and at the same time freely discuss with them about Biology curriculum and careers. Above and below the dashed lines are represented the time required for instructors before and after the practical. For further details, see text.

RESULTS AND DISCUSSION

General Scheme of the Project

French high schools offer students who embark in a theoretical, rather than practical, curriculum, to specialize in humanities, economics, math/physics, or biology. We initially targeted high school students who specialize in biology, and only those in their final high school year, which is when they study DNA and heredity. This is also the year they have to determine their future orientation. The general scheme was to offer these students the possibility to perform a PCR reaction [5] using modern laboratory equipment and reagents brought by PhD graduate students involved in the project.

High schools are under the supervision of the local government (Region) and of the local representative of the Ministere de l'Education Nationale (Rectorat). Both entities expressed their high interest and approval for the project. The higher authorities of Strasbourg University also enthusiastically offered support for this new activity, which nicely fits with one of the official missions of the university, namely transmission of advanced knowledge gained in laboratories to the public. The three entities signed an agreement endorsing the project, which we nicknamed "OpenLAB" (standing for "Ouverture PÈdagogique Et Novatrice des LABoratoires," or "educational and innovative opening of laboratories"). Two PhD graduate students (EK and SK) initially designed and tested the protocol, and subsequently six additional graduate students were recruited to run the project (CB, JE, EF, IG, SM, TS). Graduate students will hereafter be referred to as instructors. Each instructor had a fellowship for his or her PhD. In addition to their regular salary, they signed a specific contract and also received a supplementary stipend for their involvement in the project, which was paid by the University and the local government (their official denomination was "doctorant–conseil" last year, now "doctorant missionné"). Funds for reagents, equipment, and gas were entirely provided by external sponsors (see Title page footnote). High schools are thus free of charge for this 2-hours PCR-based practical.

Problem to be Solved

To add interest for the students, "OpenLAB" was presented as a fictitious criminal investigation along the following line: "The baker (a young lady) had disappeared. Two eyewitnesses saw her being abducted and forced into a car, but as it was dark they could not identify the kidnapper. The police could rapidly identify two individuals as the potential perpetrator of the kidnapping. Which one is the real culprit?" To solve this question the students had a clue: "The baker, who is fair haired, has a genetic disorder caused by a very rare deletion of $\sim$ 150 bp in a well-characterized gene. Hairs of the same color were found in the car of each suspect." Thus to identify the culprit amongst the two suspects, the students had to determine whether or not the hairs found in each car belonged to the baker. For this purpose, the students had to compare the DNA samples extracted from the hairs found in the two cars (suspect 1 and suspect 2) with a reference sample (DNA extracted from hairs found on a baker's hairbrush) after amplifying a gene fragment spanning the region mutated in the baker's genome. We chose to portray the victim as having a genetic disorder on purpose, to be subsequently able to introduce the concept of genetic disease and genetic mutation.

Organization of the Practical

The practical took place during a session of 2 hours corresponding to the time slot normally devoted for biology practical in the high school curriculum. Nothing is required from the high school except a video-projector, water and either a microwave or an electrical plate. The instructors worked in pairs to present the project, teach high school students how to perform and interpret the experiment, assisting them at each step. High school students worked in teams of two (exceptionally three).

The organization of a typical session in terms of timing and steps is described in Fig. 2. At the beginning of each session, the goal of the practical and the problem to be solved were introduced with the help of an appropriate powerpoint presentation. A two-page hand-out describing the protocol was distributed, and the use of P-20 and P-200 micropipettes for manipulating small volumes

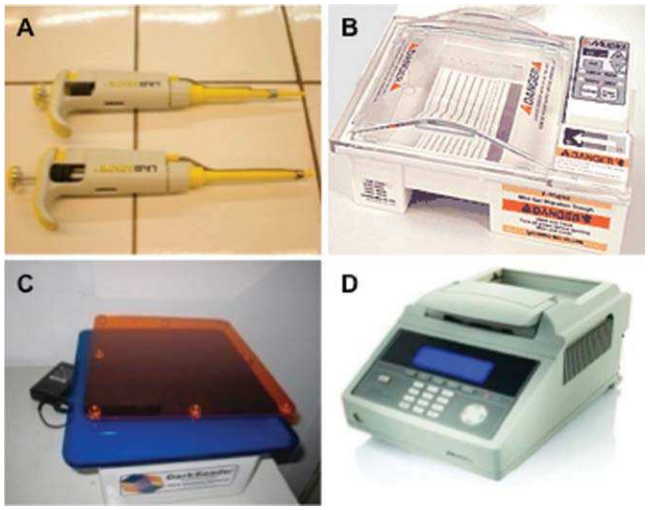

FIG. 3. **Material used during OpenLab operation.** (*a*) Micropipettes (Labmate). (*b*) Gel electrophoresis chamber (Embi Tec). (*c*) Dark reader Transilluminator (Clare Chemical Research). (*d*) Thermocycler (Roche).

was explained (10 minutes). Thereafter, the students prepared the PCR tubes according to the protocol and placed them into the thermocycler (25 minutes). While the PCR program was running (30 minutes), the principles of this amplification technique and of gel electrophoresis were explained (15 minutes). Subsequently, each student practiced loading samples into agarose gel slots (15 minutes). This time period was also dedicated to discussions with students about their orientation after the high school diploma. The small generation gap between high school students and instructors made this discussion very lively; instructors could share their experience, and high school students could collect useful information from young adults who had been in their position only 5 or 6 years before.

Once the PCR program was over, each group added loading buffer to their PCR products and loaded their amplification products on a SYBR-Green stained agarose gel (15 minutes). While electrophoresis was taking place (20 minutes), various applications of PCR were reviewed and illustrated with concrete examples. At the end of the practical, students were invited to discuss the results of the electrophoresis easily visualized on a Dark Reader transilluminator (10 minutes). The main equipment used for the practical is shown in Fig. 3. Tips, microtube racks, and gloves are also provided. Altogether, three plastic boxes of appropriate size are sufficient to carry the material in the classroom.

Typical Results and Interpretation

A typical result is available on Fig. 4. We explain that the smaller PCR product of 236 bp migrates further and faster than the larger PCR product of 379 bp on a gel. As the baker supposedly has a deletion in a gene, students know that the "victim" PCR product will migrate further than one from a non-diseased person. According to the difference of migration of the PCR products, students can easily find the culprit, which is "suspect 1."

On average, 7–8 groups within a class of 10 groups could obtain the expected results, indicating both that the protocol is robust enough to be handled by newcomers and that we could train them adequately to perform PCR. Students who failed generally experienced difficulties in dealing with the micropipettes. The following problems were encountered: (i) no PCR product, which is probably due to the omission of either the Taq DNA polymerase or the DNA template, or to mis-pipetting (too little or too much), (ii) PCR products in negative control well, probably due to DNA contamination. Successful pipetting helps students understand why it is important to concentrate and be meticulous when working in life science. The final discovery of the results under the blue light brings a climax to the practical, and making the appropriate deductions generally brings a large smile among students.

Concepts Illustrated

While the PCR is running, a certain number of biological concepts with direct relevance to PCR are explained to the students using the PowerPoint presentation. Although the biology teacher has generally introduced several issues prior to the practical, these should be pre-

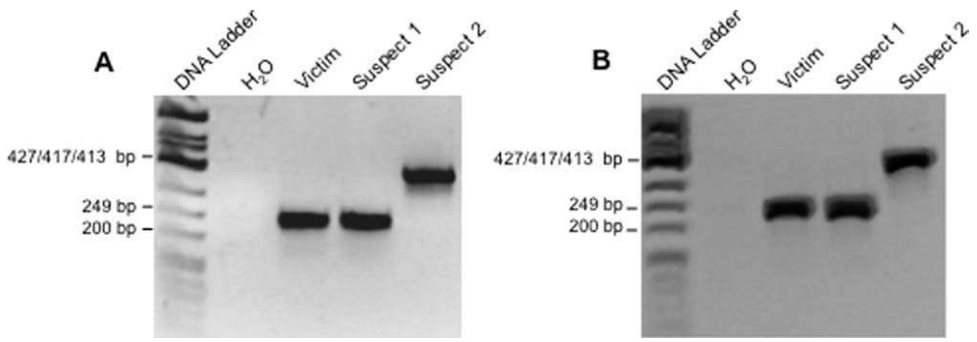

FIG. 4. **PCR result.** Typical PCR results using the protocol performed by high school students. Comparison between an agarose gel stained with Ethidium bromide and viewed with a UV transilluminator (*a*) and a similar gel stained with SYBR Green I and viewed with the Dark Reader Transilluminator (*b*). The latter solution, which was chosen for the practical, provides good pictures and is safe to use.

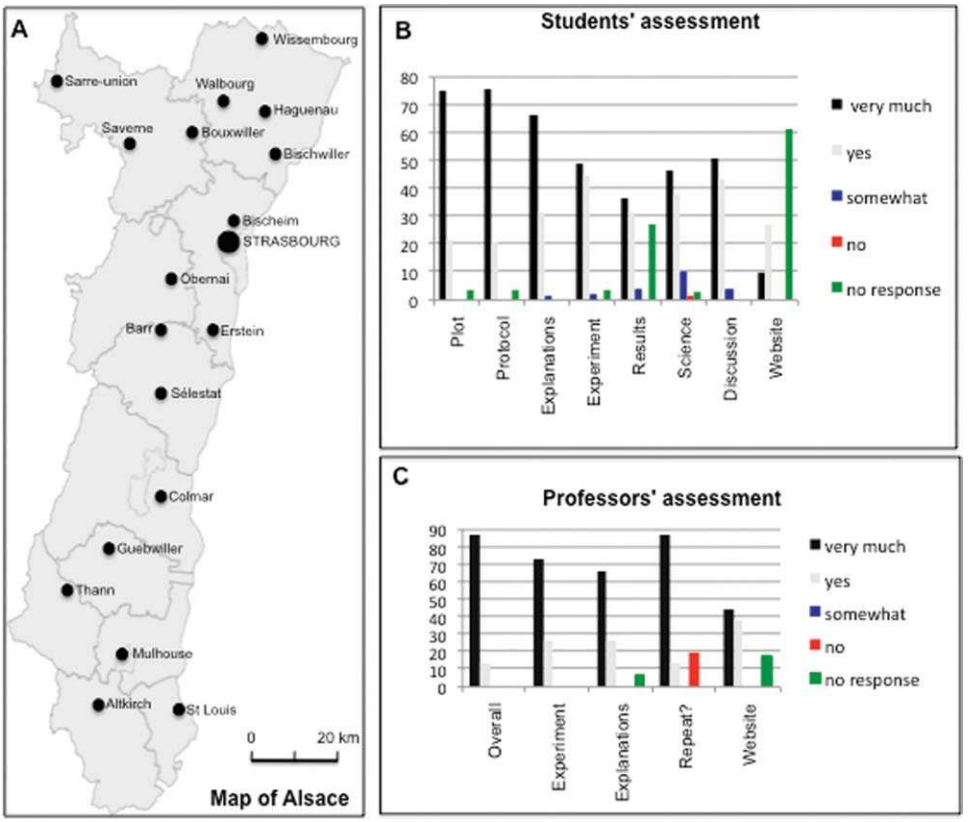

FIG. 5. **Achievements and assessment**. (*a*) Map of the Alsace region with the positions of towns in which at least one high school received an OpenLAB visit. A larger black circle is associated to Strasbourg's town where 21 classes were visited. (*b*) High school students' assessment. Results are given in percentage. The questions were: Plot, "Did you like the background of the experiment?"; Protocol, "Did you understand the protocol?"; Explanations, "Did you understand the explanations provided by instructors?"; Experiment, "Did you understand what you did?"; Results, "Did you understand the interpretation of results?"; Science, "How attractive is the world of Science to you?"; Discussion, "Were free discussions with instructors positive and useful?"; Website, "Did you visit and like our website?" A total of 321 student pairs provided an answer, thus 642 students (about 2/3 of all students); although not all students provided an answer, we do not think there was any significant bias. (*c*) High school biology professors' assessment. The questions were: Overall, "Do you feel that the practical was overall a benefit for your class?"; Experiment, "Do you think that the experiment was interesting and manageable by your students?"; Explanations, "Do you think that the explanations that were provided were understandable by your students?"; Repeat, "Would you ask us to come back next year?"; Website, "Did you visit and like our website?" 15 professors provided an answer.

sented again as they are important for its understanding. In particular, the PCR can serve to explain the constitution of DNA as a double-stranded structure, its replication and the different mutational changes such as insertion, deletion, and point mutation. The electrophoresis part helps students understand that DNA is a negatively charged molecule, and that it has a defined size that affects its migration behavior. As the plot supposedly involves a victim with a genetic disease, the PCR helps to highlight one of the most striking achievements in biology, namely that the human genome has been fully sequenced. Explaining how PCR primers are designed, certainly the most difficult part to convey, helps students think about the genome [6–9]. Finally, as we explain that the French legislation forbids the use of coding sequences for human genotyping, which must thus rely on polymorphisms located in noncoding regions, the students learn how each individual is likely to be different from his/her neighbor. All the information used for the PowerPoint presentation is available on a dedicated website (http://www-ed-sdvs.u-strasbg.fr/openlab/accueil/index.php). Teachers are invited to encourage their students to visit the website prior to our visit. It is perhaps useful to point out what we did not attempt to do. We did not quiz students after our visit to assess whether they actually understood the practical; we leave it to teachers. We also by no means planned to cover the whole curriculum of the students; our purpose is to bring a snapshot of modern techniques and the world of biological research.

The PCR technique offers several highly remarkable features for a classroom practical. It is a fairly robust and rapid technique, which has revolutionized biology and is commonly applied in many fields of science. We illustrate some of them with examples in medicine with both clinical (e.g., diagnosis of infectious and genetic diseases) and fundamental research aspects, food industry (e.g., GMO), forensic genetics (e.g., paternity test, scientific police investigation) and ancient DNA with historical examples (e.g., identification of the members of the Romanov family) [10, 11], and population migration history such as the origin of Icelanders [12].

Achievements and Assessment

The project started on a modest scale, yet between December 2008 and May 2009 we visited 53 classes in 30 different high schools spread over 200 km area of the Alsace Region of France (Fig. 5*a*). It allowed us to interact with ~950 high school students aged between 17 and 19 at a time when they decide on their next step in life. Applications for the 2009–2010 school year, with 67 prospective classes (i.e., corresponding to about 80% of the high schools in Alsace) to visit, give a rather positive measure of our impact.

As we were eager to improve the quality of each session, we asked high school students and their teachers how they appreciated the practical using a questionnaire containing three parts. The first part dealt with the proposed experiment and its understanding, the second part enquired about how students appreciate the world of Science and whether they enjoyed the discussion with PhD graduate students, and the last one concerned our website. Figure 5 presents the responses.

High school students overall enjoyed the practical a lot (78%; not shown). Specifically, ~70% of them enjoyed the plot a lot, had a good understanding of the protocol and of the explanations provided by the instructors (Fig. 5*b*, first 3 sections). Satisfaction was lower for the experimental part itself, and the analysis of the results (Fig. 5*b*, sections 4, 5). Understanding how to use micropipettes and how to be very precise when pipetting and loading gels, a real surprise and in our experience a significant hurdle for many, might explain why several students rated the experimental part lower. Devoting more time to the interpretation of results is necessary, yet difficult, because it comes late in the session when students are preparing for their next class. To address this issue, we have recently created an animation within the website, which is structured as a game, and should help them understand what they have done. Clearly, this practical exposes high school students to novel information and new tools, which is a challenge for them, even though they like this challenge, as it is a welcome departure from their routine. We also noticed that student groups who had visited our website prior to the practical or who had been prepared by their professor did much better.

Discussion with the students indicated that, while 55% have a very positive view of science (Fig. 5*b*, section 6), few actually choose to embark in a scientific curriculum. Students generally (55%; Fig. 5*b* section 7) very much appreciated the interactions with PhD graduate students and being able to ask information about their curriculum, their work environment and research project. The questionnaire finally revealed that few students had visited the website, and that those who did it thought it could be improved (Fig. 5*b*, last section). We have refurbished it for the 2009–2010 school year trying to make it more interactive.

Biology professors had in general a very positive view of our practical (Fig. 5*c*), with more than 70% giving the highest rating for all categories, except the website. Indeed, professors for all 53 classes (but two) requested us to come back this year. A few professors mentioned in written remarks that our visit had prompted some of their students to consider entering Biology University after high school. Discussing with some of them, they also encouraged us in creating new modules in the future that might help students to understand other abstract notions, such as protein folding and 3D-structure.

Finally, it is worth pointing out that the instructors also enjoyed their experience. At a stage when graduate students are still training and hesitating between research in private industries or in academia, whether or not to seek a teaching position or to become a manager, the "OpenLAB" experience provides an opportunity to test other skills and reflect on which one they may prefer. It helps instructors to address a nonspecialist public with the appropriate words while remaining precise. It provides confidence when speaking in public. It helps organizational skills and teaches efficient management of two projects (PhD experiments and the practicals). A gratifying aspect is that graduate students realize they had most of those skills but did not know about it. Overall, the "OpenLAB" project was exciting for those who had been running it (even for the three PIs) as it was a team effort with a social purpose.

CONCLUSIONS

We feel that the practical is overall well understood and has reached its main goals, although there is room for some technical improvements. Similar initiatives have been recently proposed in Europe to address the very same issues outlined at the beginning. To name a few, the University of Utrecht PhD program in Development and Cancer Biology has pioneered a similar project named "DNAlabs" (http://www.dnalabs.eu/); the INMED in Marseille has launched a program for hosting classes and even patient with genetic diseases (http://www.touschercheurs.fr); six high schools located at the German/Swiss/French border have launched a related project, the Biovalley College Network (http://www.biovalley-college.net/). We hope that our experience and that in Utrecht can inspire others.

Acknowledgments— The authors are extremely grateful to the late Adrien Zeller, former Président de la Région Alsace, to Mme Claire Lovisi, Recteur de l'Académie de Strasbourg, and to M. Alain Beretz, Président de l'Université de Strasbourg, for their enthusiastic support. The OpenLAB project would not have been possible without the generous support from the companies Roche Diagnostics and Dominique Dutscher, which provided the equipment used for the project, to the *IBMP* and the local CNRS Administration, which allowed us to use the IBMP car to reach high schools, as well as to the company FranceSystèmes for additional support. They are also very thankful to Michel Dreyer and Christophe Laville, Inspecteurs d'Académie, Rectorat de Strasbourg for their support and for organizing the contacts with high school professors. The authors thank Fanny Hummel, Pascal Mathelin, Arnaud de la Hogue, and Sylviane Bronner for their practical help.

REFERENCES

[1] J.J. Lefrere and P. Hewitt (2009) From mad cows to sensible blood transfusion: the risk of prion transmission by labile blood components in the United Kingdom and in France, *Transfusion* **49**, 797–812.

[2] M. A. Majumder and C. B. Cohen (2009) Research ethics. The NIH draft guidelines on human stem cell research, *Science* **324**, 1648–1649.
[3] C. Gonzalo and A. R. Quesada (2000) PCR as a specific, sensitive and simple method suitable for diagnostics. *Biochem. Mol. Biol. Educ.* **28**, 223–226.
[4] U. Bacher, S. Schnittger, C. Haferlach, and T. Haferlach (2009). Review: Molecular diagnostics in acute leukemias, *Clin. Chem. Lab. Med*. **47**, 1333–1341.
[5] K. Mullis, F. Faloona, S. Scharf, R. Saiki, G. Horn, and H. Erlich (1986) Specific enzymatic amplification of DNA in vitro: The polymerase chain reaction. *Cold Spring Harb. Symp. Quant. Biol.* **51**(Part 1), 263–273.
[6] S. Deepak, K. Kottapalli, R. Rakwal, G. Oros, K. Rangappa, H. Iwahashi, Y. Masuo, and G. Agrawal (2007) Real-time PCR: Revolutionizing detection and expression analysis of genes. *Curr. Genomics* **8**, 234–251.
[7] J. C. Venter, M. D. Adams, E. W. Myers, P. W. Li, R. J. Mural, G. G. Sutton, H. O. Smith, M. Yandell, C. A. Evans, R. A. Holt, J. D. Gocayne, P. Amanatides, R. M. Ballew, D. H. Huson, J. R. Wortman, Q. Zhang, C. D. Kodira, X. H. Zheng, L. Chen, M. Skupski, G. Subramanian, P. D. Thomas, J. Zhang, G. L. Gabor Miklos, C. Nelson, S. Broder, A. G. Clark, J. Nadeau, V. A. McKusick, N. Zinder, A. J. Levine, R. J. Roberts, M. Simon, C. Slayman, M. Hunkapiller, R. Bolanos, A. Delcher, I. Dew, D. Fasulo, M. Flanigan, L. Florea, A. Halpern, S. Hannenhalli, S. Kravitz, S. Levy, C. Mobarry, K. Reinert, K. Remington, J. Abu-Threideh, E. Beasley, K. Biddick, V. Bonazzi, R. Brandon, M. Cargill, I. Chandramouliswaran, R. Charlab, K. Chaturvedi, Z. Deng, V. Di Francesco, P. Dunn, K. Eilbeck, C. Evangelista, A. E. Gabrielian, W. Gan, W. Ge, F. Gong, Z. Gu, P. Guan, T. J. Heiman, M. E. Higgins, R. R. Ji, Z. Ke, K. A. Ketchum, Z. Lai, Y. Lei, Z. Li, J. Li, Y. Liang, X. Lin, F. Lu, G. V. Merkulov, N. Milshina, H. M. Moore, A. K. Naik, V. A. Narayan, B. Neelam, D. Nusskern, D. B. Rusch, S. Salzberg, W. Shao, B. Shue, J. Sun, Z. Wang, A. Wang, X. Wang, J. Wang, M. Wei, R. Wides, C. Xiao, C. Yan, A. Yao, J. Ye, M. Zhan, W. Zhang, H. Zhang, Q. Zhao, L. Zheng, F. Zhong, W. Zhong, S. Zhu, S. Zhao, D. Gilbert, S. Baumhueter, G. Spier, C. Carter, A. Cravchik, T. Woodage, F. Ali, H. An, A. Awe, D. Baldwin, H. Baden, M. Barnstead, I. Barrow, K. Beeson, D. Busam, A. Carver, A. Center, M. L. Cheng, L. Curry, S. Danaher, L. Davenport, R. Desilets, S. Dietz, K. Dodson, L. Doup, S. Ferriera, N. Garg, A. Gluecksmann, B. Hart, J. Haynes, C. Haynes, C. Heiner, S. Hladun, D. Hostin, J. Houck, T. Howland, C. Ibegwam, J. Johnson, F. Kalush, L. Kline, S. Koduru, A. Love, F. Mann, D. May, S. McCawley, T. McIntosh, I. McMullen, M. Moy, L. Moy, B. Murphy, K. Nelson, C. Pfannkoch, E. Pratts, V. Puri, H. Qureshi, M. Reardon, R. Rodriguez, Y. H. Rogers, D. Romblad, B. Ruhfel, R. Scott, C. Sitter, M. Smallwood, E. Stewart, R. Strong, E. Suh, R. Thomas, N. N. Tint, S. Tse, C. Vech, G. Wang, J. Wetter, S. Williams, M. Williams, S. Windsor, E. Winn-Deen, K. Wolfe, J. Zaveri, K. Zaveri, J. F. Abril, R. Guigo, M. J. Campbell, K. V. Sjolander, B. Karlak, A. Kejariwal, H. Mi, B. Lazareva, T. Hatton, A. Narechania, K. Diemer, A. Muruganujan, N. Guo, S. Sato, V. Bafna, S. Istrail, R. Lippert, R. Schwartz, B. Walenz, S. Yooseph, D. Allen, A. Basu, J. Baxendale, L. Blick, M. Caminha, J. Carnes-Stine, P. Caulk, Y. H. Chiang, M. Coyne, C. Dahlke, A. Mays, M. Dombroski, M. Donnelly, D. Ely, S. Esparham, C. Fosler, H. Gire, S. Glanowski, K. Glasser, A. Glodek, M. Gorokhov, K. Graham, B. Gropman, M. Harris, J. Heil, S. Henderson, J. Hoover, D. Jennings, C. Jordan, J. Jordan, J. Kasha, L. Kagan, C. Kraft, A. Levitsky, M. Lewis, X. Liu, J. Lopez, D. Ma, W. Majoros, J. McDaniel, S. Murphy, M. Newman, T. Nguyen, N. Nguyen, M. Nodell, S. Pan, J. Peck, M. Peterson, W. Rowe, R. Sanders, J. Scott, M. Simpson, T. Smith, A. Sprague, T. Stockwell, R. Turner, E. Venter, M. Wang, M. Wen, D. Wu, M. Wu, A. Xia, A. Zandieh, and X. Zhu (2001) The sequence of the human genome. *Science* **291**, 1304–1351.
[8] E. S. Lander, L. M. Linton, B. Birren, C. Nusbaum, M. C. Zody, J. Baldwin, K. Devon, K. Dewar, M. Doyle, W. FitzHugh, R. Funke, D. Gage, K. Harris, A. Heaford, J. Howland, L. Kann, J. Lehoczky, R. LeVine, P. McEwan, K. McKernan, J. Meldrim, J. P. Mesirov, C. Miranda, W. Morris, J. Naylor, C. Raymond, M. Rosetti, R. Santos, A. Sheridan, C. Sougnez, N. Stange-Thomann, N. Stojanovic, A. Subramanian, D. Wyman, J. Rogers, J. Sulston, R. Ainscough, S. Beck, D. Bentley, J. Burton, C. Clee, N. Carter, A. Coulson, R. Deadman, P. Deloukas, A. Dunham, I. Dunham, R. Durbin, L. French, D. Grafham, S. Gregory, T. Hubbard, S. Humphray, A. Hunt, M. Jones, C. Lloyd, A. McMurray, L. Matthews, S. Mercer, S. Milne, J. C. Mullikin, A. Mungall, R. Plumb, M. Ross, R. Shownkeen, S. Sims, R. H. Waterston, R. K. Wilson, L. W. Hillier, J. D. McPherson, M. A. Marra, E. R. Mardis, L. A. Fulton, A. T. Chinwalla, K. H. Pepin, W. R. Gish, S. L. Chissoe, M. C. Wendl, K. D. Delehaunty, T. L. Miner, A. Delehaunty, J. B. Kramer, L. L. Cook, R. S. Fulton, D. L. Johnson, P. J. Minx, S. W. Clifton, T. Hawkins, E. Branscomb, P. Predki, P. Richardson, S. Wenning, T. Slezak, N. Doggett, J. F. Cheng, A. Olsen, S. Lucas, C. Elkin, E. Uberbacher, M. Frazier, R. A. Gibbs, D. M. Muzny, S. E. Scherer, J. B. Bouck, E. J. Sodergren, K. C. Worley, C. M. Rives, J. H. Gorrell, M. L. Metzker, S. L. Naylor, R. S. Kucherlapati, D. L. Nelson, G. M. Weinstock, Y. Sakaki, A. Fujiyama, M. Hattori, T. Yada, A. Toyoda, T. Itoh, C. Kawagoe, H. Watanabe, Y. Totoki, T. Taylor, J. Weissenbach, R. Heilig, W. Saurin, F. Artiguenave, P. Brottier, T. Bruls, E. Pelletier, C. Robert, P. Wincker, D. R. Smith, L. Doucette-Stamm, M. Rubenfield, K. Weinstock, H. M. Lee, J. Dubois, A. Rosenthal, M. Platzer, G. Nyakatura, S. Taudien, A. Rump, H. Yang, J. Yu, J. Wang, G. Huang, J. Gu, L. Hood, L. Rowen, A. Madan, S. Qin, R. W. Davis, N. A. Federspiel, A. P. Abola, M. J. Proctor, R. M. Myers, J. Schmutz, M. Dickson, J. Grimwood, D. R. Cox, M. V. Olson, R. Kaul, N. Shimizu, K. Kawasaki, S. Minoshima, G. A. Evans, M. Athanasiou, R. Schultz, B. A. Roe, F. Chen, H. Pan, J. Ramser, H. Lehrach, R. Reinhardt, W. R. McCombie, M. de la Bastide, N. Dedhia, H. Blocker, K. Hornischer, G. Nordsiek, R. Agarwala, L. Aravind, J. A. Bailey, A. Bateman, S. Batzoglou, E. Birney, P. Bork, D. G. Brown, C. B. Burge, L. Cerutti, H. C. Chen, D. Church, M. Clamp, R. R. Copley, T. Doerks, S. R. Eddy, E. E. Eichler, T. S. Furey, J. Galagan, J. G. Gilbert, C. Harmon, Y. Hayashizaki, D. Haussler, H. Hermjakob, K. Hokamp, W. Jang, L. S. Johnson, T. A. Jones, S. Kasif, A. Kaspryzk, S. Kennedy, W. J. Kent, P. Kitts, E. V. Koonin, I. Korf, D. Kulp, D. Lancet, T. M. Lowe, A. McLysaght, T. Mikkelsen, J. V. Moran, N. Mulder, V. J. Pollara, C. P. Ponting, G. Schuler, J. Schultz, G. Slater, A. F. Smit, E. Stupka, J. Szustakowski, D. Thierry-Mieg, J. Thierry-Mieg, L. Wagner, J. Wallis, R. Wheeler, A. Williams, Y. I. Wolf, K. H. Wolfe, S. P. Yang, R. F. Yeh, F. Collins, M. S. Guyer, J. Peterson, A. Felsenfeld, K. A. Wetterstrand, A. Patrinos, M. J. Morgan, P. de Jong, J. J. Catanese, K. Osoegawa, H. Shizuya, S. Choi, and Y. J. Chen (2001) Initial sequencing and analysis of the human genome. *Nature* **409**, 860–921.
[9] I. H. G. S. Consortium (2004) Finishing the euchromatic sequence of the human genome. *Nature* **431**, 931–945.
[10] M. D. Coble, O. M. Loreille, M. J. Wadhams, S. M. Edson, K. Maynard, C. E. Meyer, H. Niederstatter, C. Berger, B. Berger, A. B. Falsetti, et al. (2009) Mystery solved: the identification of the two missing Romanov children using DNA analysis. *PLoS One* **4**, e4838.
[11] P. Gill, P. L. Ivanov, C. Kimpton, R. Piercy, N. Benson, G. Tully, I. Evett, E. Hagelberg, and K. Sullivan (1994). Identification of the remains of the Romanov family by DNA analysis. *Nat. Genet.* **6**, 130–135.
[12] A. Helgason, S. Sigureth Ardottir, J. Nicholson, B. Sykes, E. W. Hill, D. G. Bradley, V. Bosnes, J. R. Gulcher, R. Ward, and K. Stefansson (2000) Estimating Scandinavian and Gaelic ancestry in the male settlers of Iceland. *Am. J. Hum. Genet.* **67**, 697–717.